The role of NK family receptor interactions with HLA-B27 in Ankylosing Spondylitis pathogenesis.



Joanna Giles

St-Anne's College

University of Oxford

Hilary Term 2011

The role of NK family receptor interactions with HLA-B27 in Ankylosing Spondylitis pathogenesis.

Contents

Abbreviations……. 6

Abstract…….. 9

Acknowledgements…….…… 10

Chapter 1: Introduction

1.1 Ankylosing Spondylitits ……12

1.2 HLA Class I molecule assembly ……..……..13

1.3 HLA-B27 structure ……15

1.4 HLA-B27 subtypes ……16

1.5 Natural Killer Cells ……19

1.6 Immune Receptors ……20

1.7 Killer-cell Immunoglobulin like Receptors ……...21

1.8 Leukocyte Immunoglobulin like Receptors ……...22

1.9 B27 Transgenic Animal models ……27

1.10 Theories of pathogenesis in Ankylosing Spondylitis ……..….28

1.11 Aims of the project ……..… 33

Chapter 2: Materials and Methods

2.1 Bacterial Culture ……... 35

2.2 Molecular Biology ……36

2.3 Protein Expression ……37

2.4 Protein Refolding and Purification ……40

2.5 Flow Cytometry ……41

2.6 Surface Plasmon Resonance ……..41

2.7 Functional Dendritic Cell Assay ……45

2.8 Epitope Mapping ……46

2.9 Protein purification for crystal trials……...……47

2.10 Crystal Trials ……..……..48

2.11 Mammalian cell expression of soluble B27…….…….50

Chapter 3: Immune cell and receptor interactions with HLA-B27 homodimers and heterotrimers

3.1 Introduction…….53

3.2 LILRB1/LILRB2 display different binding affinities and specificities for B*2705 heterotrimers and B*2705 homodimers…….…..……..54

3.3 LILRB2 can bind to B*2705 free heavy chains……..67

3.4 LILRB1 and LILRB2 bind to B*2705 heterotrimers, complexed to GAG variant peptides, with comparable affinities……71

3.5 B27 dimer interactions with myeolomonocytic cells……..76

3.6 CD8αα binding to B27 homodimers and B27 heterotrimers…….82

3.7 Discussion……...88

Chapter 4: HLA-B27 homodimer formation and LILR interactions – A comparison of two B27 subtypes *in vitro*

4.1 Introduction……98

4.2 B*2705 forms more homodimers *in vitro* compared to B*2709……....99

4.3 Fluorescently labelled tetrameric complexes of B*2705 and B*2709 heterotrimers stain LILRB2, KIR3DL1 and KIR3DL2 expressing Baf cells……..…..104

4.4 LILRB1 and LILRB2 bind to B*2705 and B*2709 heterotrimers with comparable affinities by SPR…….106

4.5 Fluorescently labelled tetrameric complexes of B*2705 and B*2709 homodimers both bind to LILRB2 and not LILRB1 expressing Baf cells……....…….117

4.6 LILRB2 binds to B*2705 and B*2709 homodimers by SPR equilibrium binding analysis……....119

4.7 Discussion…….122

Chapter 5: Properties of the B*2705 homodimer and biophysical investigation of candidate B27 homodimer-specific monoclonal antibodies

5.1 Introduction……..127

5.2 B*2705 homodimers do not contain peptide……128

5.3 HD5, HD6 and HD8 bind B27 homodimer but not B27 heterotrimer…….132

5.4 HD6 binds to B*2705 homodimers, but not to HLA-G homodimers-……..…..137

5.5 HD6 binds to B*2705 heavy chains, but not to HLA-A3 or HLA-G heavy chains…….138

5.6 HD5/ HD6 / HD8 do not compete with LILRB2 for B*2705 homodimer binding but HC-10 partially competes for binding……..140

5.7 Epitope mapping of B*2705 dimer : HD6 interaction…….145

5.8 Discussion……147

Chapter 6: B27 homodimer expression and purification for Crystal trials

6.1 Introduction……..154

6.2 B27 homodimer purification ……...155

6.3 B27 homodimer : Fab of HD8 complex purification……...159

6.4 Crystal screening, optimisation and additive screen ……...161

6.5 Discussion ……..……..167

Chapter 7: Discussion

7.1 Summary of results……..……..170

7.2 Discussion ……..……..170

7.3 Concluding remarks ……178

Chapter 8: Appendix

8.1 Calibration of the Superdex 75 and Superdex 200 columns……175

8.2 Confirming the purity of analytes before SPR experiments……178

8.3 Doublet formation in dendritic cells cultured with B27 homodimer…….…..179

8.4 Generation of candidate dimer specific antibodies by Phage Display Technology ……180

8.5 HC-10 antibody avidity for B27 homodimer …….…….181

8.6 Mammalian-cell Expression system…….182

References ……..……..……...189

Abbreviations

Amp – Ampicillin

ARTS1 /ERAP - ER aminopeptidase associated with antigen processing

AS – Ankylosing Spondylitis

B27 – Human Leukocyte Antigen-B27

β_2m – Beta – 2 – microglobulin

Bicine – 2-(Bis(2-hydroxyethyl)amino)acetic acid – an organic buffering agent

BiP – Binding Immunoglobulin Protein

CHOP – C/EBP homologous Protein

CTL – Cytotoxic T Lymphocytes

DC – Dendritic Cell

DMSO – Dimethyl Sulphoxide

DTT – Dithiothreitol

EA – Enteropathic Arthritis

***E.coli* –** Escherichia coli

ER – Endoplasmic Reticulum

ERAD – ER associated Degradation

Fab – Fragment Antigen Binding

FCS – Fetal Calf Serum

FPLC - Fast Performance Liquid Chromatography

GFP – Green Fluorescent Protein

GMCSF – Granulocyte Macrophage Colony Stimulating Factor

HBS-EP – Hepes Buffered Saline

HLA – Human Leukocyte Antigen

HPLC – High Pressure Liquid Chromatography

HT – Heterotrimer

Ig – Immunoglobulin

IL – Interleukin

ILT – Immunoglobulin Like Transcript

IPTG – Isopropyl β-D-1 thiogalactopyranoside

ITIM – Immunotyrosine based Inhibitory Motif

K_D - Equilibrium Dissociation Constant

KIR – Killer-cell Immunoglobulin like Receptor

LB – Luria Bertani

LILR – Leukocyte Immunoglobulin Like Receptor

MHC – Major Histocompatibility Complex

MWCO – Molecular Weight Cut Off

NK – Natural Killer

PBS – Phosphate Buffered Saline

PCR – Polymerase Chain Reaction

PCT – Pre-Crystallisation Test

PDI – Protein Disulphide Isomerase

PGE – Prostaglandin E

PIR – Paired Immunoglobulin-like Receptors

PMSF – Phenylmethanesulphonylfluoride

PsA – Psoriatic Arthritis

ReA – Reactive Arthritis

RL - the immobilisation level of a Surface Plasmon Resonance Chip

R_{max} - Maximum Binding Capacity of a Surface Plasmon Resonance chip surface

Sd – Superdex

SDS- PAGE - Sodium Dodecyl Sulphate Polyacrylamide Gel Electrophoresis

Sm - the stoichiometric ratio

SpA – Spondyloarthropathies

SPR – Surface Plasmon Resonance

TAP – Transporter associated with Antigen Processing

TCR – T Cell Receptor

TNF – Tumour Necrosis Factor

uSpA – Undifferentiated Spondyloarthritis

UPR – Unfolded Protein Response

XBP1 - X box Binding Protein 1

The role of NK family receptor interactions with HLA-B27 in Ankylosing Spondylitis pathogenesis.

Joanna Giles, St-Anne's College, DPhil thesis abstract, MT 2010

Possession of the Major Histocompatibility Complex (MHC) allele, HLA-B27 (B27), strongly predisposes to the development of spondyloarthritis. Furthermore, B27 exists as polymorphic variants, with some subtypes (such as B*2705) being more strongly associated with disease than others (B*2709). The immunological function of MHC molecules is to present peptides in a heterotrimeric complex with beta-2-microglobulin (β_2m); however, B27 has also been observed to form non-classical (β_2m –free) homodimers at the cell surface. It has been suggested that there may be a pathogenic role for cell surface B27 homodimer interactions with Natural Killer (NK) cell receptors, such as Leukocyte Immunoglobulin like Receptors (LILRs). In this thesis I characterise these interactions and investigate molecular differences between two B27 subtypes.

Here I show that the B*2705 subtype forms homodimers more readily than the B*2709 subtype, but once formed, B27 homodimers of the 2 different subtypes exhibit comparable binding specificities and affinities to the NK receptors. On the other hand, I show significant differences in the binding specificities and affinities of these receptors to B27 homodimers and heterotrimers. LILRB1 does not bind B27 homodimers, but does bind B27 heterotrimers. LILRB2 binds B27 heterotrimers with a K_D of 22μM, whereas LILRB2 binds B27 homodimers more strongly with a K_D of 2.5μM. In addition to these main findings, I have characterised the specificity and affinity of candidate B27 homodimer-specific antibodies. I have performed epitope-mapping experiments and developed a model for binding to the B27 homodimer. Finally, I have identified crystallisation conditions for the B27 homodimer in complex with a Fab, allowing for X-ray crystallography studies.

In this thesis, I have characterised for the first time the molecular interactions of the B27 homodimer with NK cell ligands and show that they are different from those with the B27 heterotrimer. This work supports a hypothesis of B27 homodimer induced pathology involving NK receptors.

Acknowledgements

I would firstly like to thank my supervisors, Dr Paul Bowness and Dr Simon Kollnberger for their support and encouragement throughout my research. I have had a really enjoyable time in the Bowness group, owing to the friendly and enthusiastic atmosphere in the lab. I would like to thank all members of the Bowness lab for this: Kirsty McHugh, Jackie Shaw, Anna Ridley, Liye Chen and Isabelle Wong.

I have been very lucky to receive such fantastic support and helpful discussions from many scientists at the University of Oxford, including Dr Ed Evans, Tom Walter and Abi Culshaw in particular. Also, I am thankful to Tica Pichulik for help with the isolation of the dendritic cells and Kati DiGleria for help with the Mass Spectroscopy and peptide synthesis. I am also grateful to Dr Katsumi Maenaka and Dr Kimiko Kuroki for hosting me in their lab in Fukuoka, Japan, and for their excellent tutorials using the Biacore. I would also like to thank Dr Michael Williams for his help in analysing my Biacore data and for his encouragement over the last year.

Arthritis Research UK have been a fantastic charity to work with and I am so very grateful for the funding they have provided to allow me to undertake this project.

Last, but not least, I would like to thank my family: My Mum, my Dad, Donna, Ben, my Nanna and my Grancha. I know that I would not have been able to work this hard without their constant love and support, and for this I am truly grateful.

Chapter 1 – Introduction

1.1 Ankylosing Spondylitits ……12

1.2 HLA Class I molecule assembly ……..……..13

1.3 HLA-B27 structure ……15

1.4 HLA-B27 subtypes ……16

1.5 Natural Killer Cells ……19

1.6 Immune Receptors ……20

1.7 Killer-cell Immunoglobulin like Receptors ……...21

1.8 Leukocyte Immunoglobulin like Receptors ……...22

1.9 B27 Transgenic Animal models ……27

1.10 Theories of pathogenesis in Ankylosing Spondylitis ……..….28

1.11 Aims of the project ……..… 33

1.1 Ankylosing Spondylitis

Ankylosing Spondylitis (AS) is the main member of a family of related rheumatic disorders known as the spondyloarthropathies (SpA) [1]. The SpA are chronic inflammatory diseases, sharing several clinical features including inflammation of the entheses, inflammatory back pain, and dactylitis. Other SpA include Psoriatic Arthritis (PsA), Reactive Arthritis (ReA), enteropathic arthritis (EA) and Undifferentiated Spondyloarthritis (uSpA). After Rheumatoid Arthritis, SpA are the most common form of inflammatory arthritis, where AS is estimated to affect between 0.1 and 1.4% of the Caucasian population [2-4]. AS is a chronic disease that affects young people; around 80% of patients develop symptoms of AS before the age of 30 with a strong male bias towards disease [5]. The main symptom of AS is inflammatory back pain caused by sacroilitis and inflammation of the axial spine. These initial inflammatory processes lead to structural changes in the spine by new bone formation, and in the most severe cases can lead to complete fusion of the vertebrae. This is commonly described as "bamboo spine" as patients suffer spinal stiffness, loss of spinal mobility and curvature of the spine [6]. AS is therefore a debilitating and painful condition requiring a clear understanding of disease pathogenesis to allow the development of successful treatments.

Although the mechanism of disease pathogenesis remains elusive, its association with Human Leukocye Antigen B27 (B27) is well established [7, 8]. This association is one of the strongest known genetic associations, where 96% of Caucasian AS patients possess the B27 allele compared with only 9% of healthy individuals [8]. A direct role for B27 in disease pathogenesis has emerged from B27 transgenic rat models that develop an inflammatory arthritis resembling AS [9]. However, family and twin studies have suggested that several

other genes are also likely to be involved. Such studies have suggested that the contribution of B27 attributes to only about 20-30% of the total genetic risk [10]. Furthermore, there are several cases of AS noted in B27 negative patients. Besides B27, other HLA molecules have been shown to be associated with AS with a high risk association attributed to the whole Major Histocompatibility Complex (MHC) region [11]. In addition to these associations, ARTS1 (ERAP), IL23R [12], IL-1 [13] and TNFα have been identified as genes involved in the disease, and probably several more remain to be identified. AS is therefore a polygenic disease, with the strongest risk factor being attributed to B27.

1.2 HLA Class I molecule assembly

B27 is an HLA class I protein, its classic immunological function is, therefore, to form a heterotrimeric complex (HT) with beta-2-microglobulin (β_2m) and antigenic peptide (normally between 8-11 amino acids in length) at the surface of most nucleated cells. The HT complex then presents peptides for recognition by CD8+ cytotoxic T lymphocytes (CTLs) [14]. Peptides are derived from an intracellular pool of proteins processed by components of the class I antigen presentation pathway, where endogenous proteins are degraded in the cytosol (by the proteasome) and then translocated into the Endoplasmic Reticulum (ER) by the Transporter associated with Antigen Processing (TAP) heterodimer for loading onto MHC class I molecules.

MHC class I assembly and the acquisition of an optimal peptide is a multi-step process requiring two groups of chaperones (reviewed in [15]). These are (i) the assembly chaperones and (ii) the chaperones of the multi-molecular Peptide-Loading Complex (PLC). The process

of MHC I assembly begins with the initial insertion of nascent MHC class I heavy chains into the ER. Following insertion, the MHC class I assembly chaperone, calnexin binds to, and assists with the initial folding and stabilisation of the heavy chain to allow for the subsequent binding of β_2m. This heterodimer formation causes a conformational change to the MHC protein, resulting in the rapid release of calnexin and its subsequent replacement with the chaperones of the PLC. Specifically, calnexin is replaced by its orthologue chaperone, calreticulin. Two chaperones, ERp57 and tapasin then assist in the recruitment of partially folded complexes to the PLC [16]. ERp57 is a cellular thiol oxidoreductase and functions to ensure correct disulphide bond formation [17]. Therefore, calreticulin and ERp57 work in tandem to ensure correct folding and maturation of the molecule. In addition to these chaperones, tapasin has a central role in the PLC, where it forms the scaffold of the whole complex and is disulphide bonded to ERp57. Tapasin functions to recruit the MHC class I proteins by forming direct contacts with TAP and facilitates the editing and optimisation of the peptide cargo. Tapasin is also thought to stabilise the open peptide-receptive conformation of the MHC class I complex to encourage peptide binding. Loading of peptide into the MHC class I binding groove has recently been suggested to be assisted by Protein Disulphide Isomerase (PDI) [18], where peptide binding is initially suboptimal, and later editing processes optimise the cargo. ERAP (which also shows genetic associations with AS [12]) has been shown to participate in peptide optimisation by the final trimming of longer peptides into shorter ones (around nine to ten amino acids in length). This MHC class I assembly pathway is complex, but central to CD8+ T cell recognition and effective immune responses (reviewed in [15,19, 20]).

1.3 HLA-B27 structure

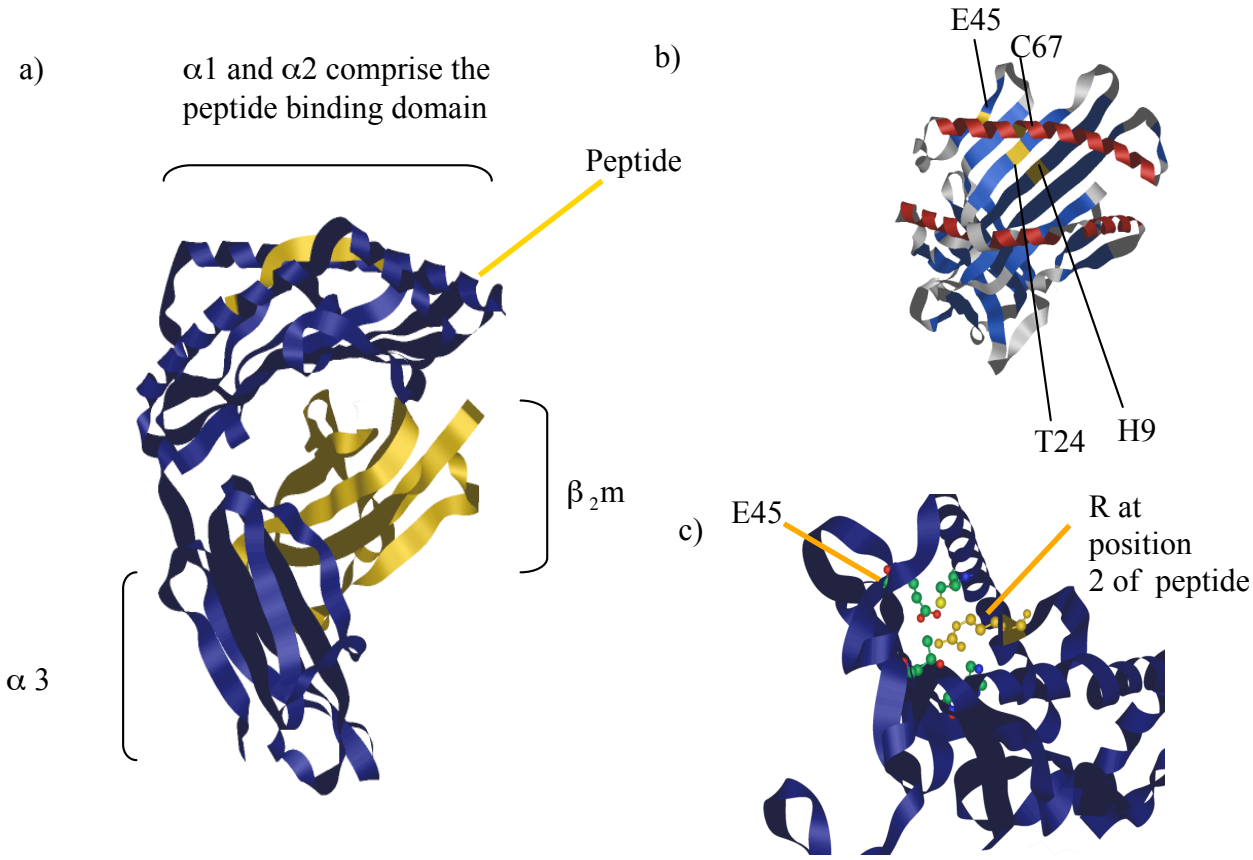
Due to the strong disease association, the B27 heterotrimer crystal structure was among the first MHC molecules to be solved [21]. The B27 structure is characteristic of all MHC class I molecules with a B27 heavy chain consisting of three α domains. The α3 domain and β_2m domains show immunoglobulin (Ig)- like folds and the peptide sits in an extended conformation in the binding groove formed by two α helices, and a β sheet base formed by the α1 and α2 domains. This binding groove has been shown to hold peptides by their side chains accommodated in binding pockets (pockets denoted A-F). B27, in particular, contains a deep B pocket that is observed to contain a Glutamic acid (E45) at its base and an unpaired Cysteine (C67) at its mouth (fig 1.1). This combination of residues confers a strong specificity for particular peptide sequences, particularly an Arginine residue at position 2 [22, 23] (fig 1.1, table 1).

B27 has 5 Cysteine residues in the extracellular domain: C101, C164, C203, C259 and, more unusually, a cysteine at position 67 (C67). It is this C67 that has been shown to be important in the formation of an additional non-classical form of B27, the B27 homodimer [24]. As such, B27 is said to be an unusual HLA molecule. The B27 homodimer is a di-sulphide bonded dimer, lacking β_2m. Whether there is a peptide present in this structure is still under debate. "Empty" B27 on the surface of cells has been shown to be peptide-receptive [25]. B27 homodimers have been observed to be expressed on the cell surface [26, 27] and are thought to play a role in the inflammatory process of Ankylosing Spondylitis. The two heavy chains are bonded through their unpaired C67 residues, which are suggested to have heightened reactivity on account of the nearby Lysine 70 (K70) residue (fig. 1.2) [28]. One

other HLA molecule that has been shown to form β_2m-free homodimers is the HLA-G molecule. HLA-G has restricted expression, where it plays a role in maternal-fetal tolerance. It has been shown to form several isoforms including a di-sulphide bonded β_2m-free isoform named HLA-G5, which forms di-sulphide bonds through free cysteine residues at position 42 [29]. A second isoform of HLA-G is an HLA-G dimer that contains β_2m, and this crystal structure has been solved [30].

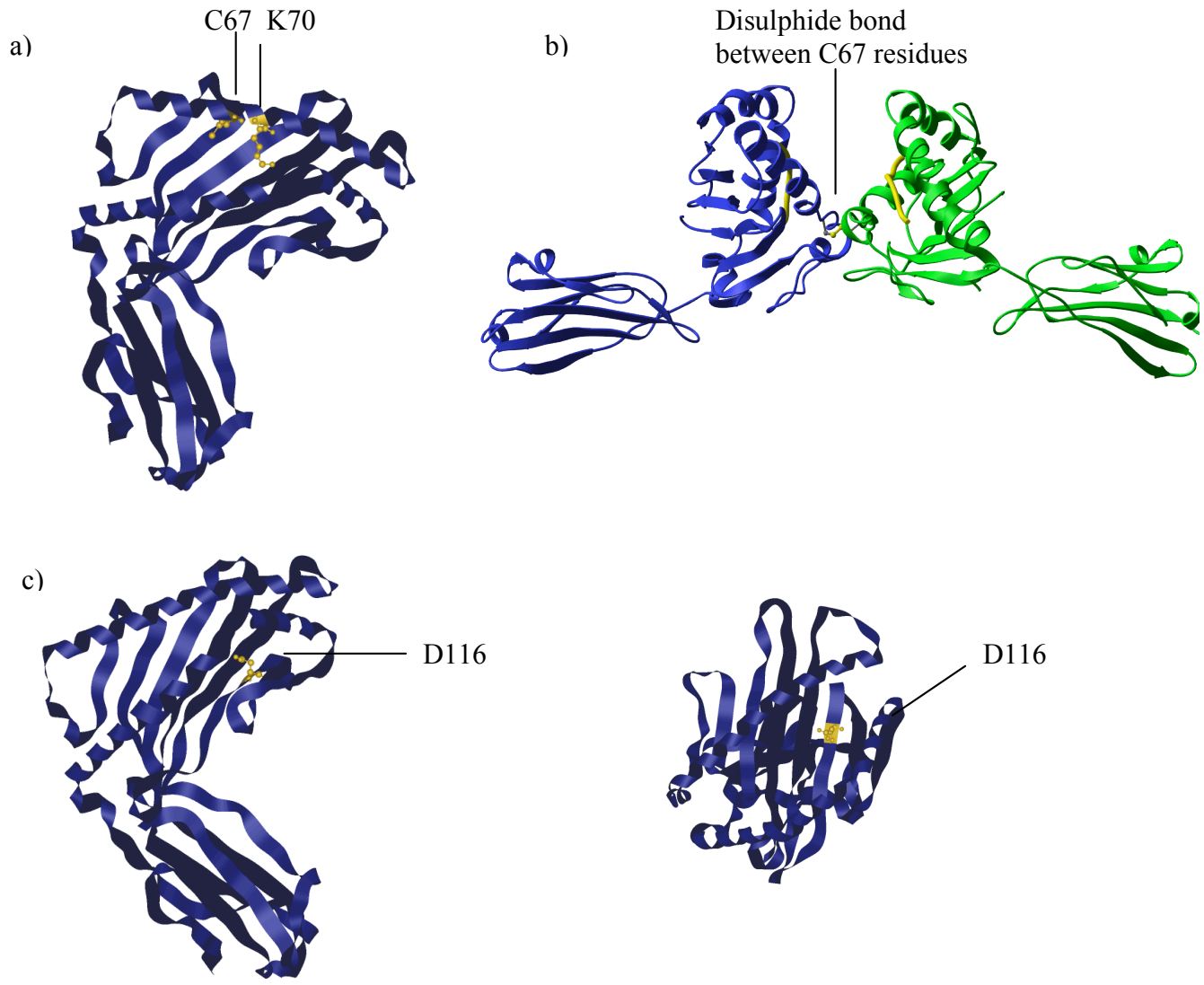
1.4 HLA-B27 subtypes

An added layer of complexity in the B27 conundrum is that B27 exists as a family of different alleles. To date, 75 different subtypes of B27 have been identified, with 62 subtypes found to be translated into protein [31, 32]. The different subtypes are thought to have evolved from the most common subtype, B*2705 [33]. The subtypes differ from each other by one or a few amino acids, predominantly in the α2 and α3 domains making up the peptide binding groove [34]. Population studies have shown that HLA-B*2705 (B*2705) is strongly associated with AS around the world and so is thought to be the ancestral subtype. Other subtypes shown to be strongly associated with AS include HLA-B*2702 (B*2702), HLA-B*2704 (B*2704) and HLA-B*2707 (B*2707). By contrast, HLA-B*2709 (B*2709) and HLA-B*2706 (B*2706) have been shown to lack such associations where B*2709 is found predominantly in the Sardinian population [35]. Strikingly, B*2709 differs from B*2705 by only one amino acid substitution. Aspartic acid (in B*2705) at position 116, within the α1 domain, is substituted by a Histidine (in B*2709) (D116H) [36] (fig. 1.2). B*2706 differs from B*2705 at positions 77, 114, 116 and 152 [37].



Models modified from PDB entry 2BSR using imol

Figure 1.1 Structural features of B27. *a) B27 structure comprises a heavy chain (blue), β_2m (yellow) and a small peptide fragment sitting in the peptide-binding groove. b) The peptide binding groove comprises 2 α helices (red) and a β sheet base. It incorporates a combination of key residues (H9, T24, E45 and C67) that confer a strong preference for particular peptide sequences. c) B27 has a strong preference for R at position 2 of the peptide due to the amino acids surrounding this region. E45 of B27 can make contacts with R at position 2 of the peptide.*



Models modified from PDB entry 2BSR using imol, except homodimer model, by P Bowness.

Figure 1.2 Key residues of HLA-B*2705. *a) B27 homodimers form through an unpaired C residue at position 67 (C67). The nearby K70 enhances the reactivity of C67. b) Model of the B27 homodimer. c) B*2705 has an aspartic acid residue at position 116 (D116) in the peptide-binding groove, where B*2709 has a histidine (H) residue at this position.*

1.5 Natural Killer Cells

Natural Killer (NK) cells are CD56 positive, CD3 negative cells that have an important role in the innate immune response. Specifically, NK cells in humans and mice have been shown to participate in the initial defence against viral infection and tumours (reviewed in [38, 39]). Furthermore, NK cells have been shown to play a key role in several autoimmune diseases [40, 41]. The response of the NK cell is rapid, and diverse. Prior to activation, NK cells become primed by various signals including IL-15 and IL-12 (from DCs or macrophages) (reviewed in [42]). In addition a "licensing" interaction between an NK cell inhibitory receptor (to be discussed later) and a self-MHC has been suggested to be vital for functional competence in mice (reviewed in [43]).

The licensing model remains be shown in humans and the molecular mechanisms are unclear, but the process is thought to require signalling through NK cell inhibitory receptors, meaning that only cells expressing inhibitory receptors can become active. This activation of NK cells then leads to the release of cytokines (including IFN-γ, TNF-α and IL-10) and chemokines (XCL1) for the activation and recruitment of other immune cells. Furthermore, NK cells are cytotoxic and so can lyse selected cells. The exact mechanism by which NK cells are activated and controlled is still unclear, although the "missing self" hypothesis is widely accepted as the principle for understanding target cell recognition by NK cells [38]. This model proposes that NK cells circulate in an inactive form and subsequently become primed to attack any target cells that fail to express sufficient MHC class I molecules on their cell surface. This hypothesis became widely accepted when it was shown that NK cells have the capacity to attack normal cell types (as opposed to tumour cells) that lack MHC molecules

through targeted mutagenesis [44]. This model was then further supported through the identification of MHC class I (and MHC class I related) binding inhibitory receptors such as Ly49 (in mice), KIRs (in humans) and NKG2A (in both humans and mice) (reviewed in [45]). Over the years a wide range of activatory, inhibitory, adhesion and chemotactic receptors have been identified on the surface of NK cells, all of which have a role in shaping the NK cell response and localisation (reviewed in [46, 47]). The direct recognition and subsequent activation of NK cells is currently thought to be achieved by the scanning of cells for the absence or incomplete expression of MHC molecules using these activatory and inhibitory receptors. NK cell activation is then triggered when MHC expression is reduced and the balance of activatory and inhibitory interactions favours activation (fig 1.5a).

Although NK cells are classically considered as central players of the innate system, recent findings have suggested that at least some mature NK cells can be long lived, possessing "immunological memory". For example studies have shown that activated NK cells transferred into naive recipients can persist for at least a month (reviewed in [42]).

1.6 Immune Receptors

Aside from the T-Cell Receptor (TCR), HLA molecules (including B27) have been shown to bind to a range of immune receptors, including the Killer-cell Immunoglobulin Like Receptors (KIRs) [48, 49] and the Leukocyte Immunoglobulin Like Receptors (LILRs) [50, 51]. Both the KIR and LILR families are encoded within the leukocyte receptor complex on chromosome 19 and have a role in immune modulation (reviewed in [52]). These receptors are expressed on many immune cells including NK cells, monocytes, macrophages and T

cells [53]. Both the LILRs and KIRs are members of the Ig superfamily and exist in both inhibitory and activating forms. Activatory isoforms have short cytoplasmic tails harbouring a specific amino acid sequence termed the Immuno-Tyrosine based Activatory Motif (ITAM sequence, $YxxL/Ix_{(6–12)}YxxL/I$, where x denotes any amino acid). The intracellular domains of these receptors associate with adaptor proteins in the cytosol to trigger an activatory response. An activatory signal may trigger differentiation, proliferation or cytokine production. On the other hand, inhibitory isoforms are characterised by a long cytoplasmic tail containing an Immuno-Tyrosine-based Inhibitory Motif (ITIM sequence, I/V/L/SxYxxV/L), which functions to trigger an inhibitory signal by recruiting phosphatases such as SHP-1 or SHIP (fig. 1.3). The phosphatases function to dephosphorylate the activatory molecules and thus suppress the signal (reviewed in [52], [54]). However, the exact workings of ITIM-bearing receptors are not fully understood and it has been suggested that some ITIM-bearing receptors may recruit other molecules to affect cell signalling and cell function [55].

1.7 Killer-cell Immunoglobulin Like Receptors

A major group of receptors used by NK cells (and some T cells) are the Killer-cell Immunoglobulin-like Receptors (KIRs). After the HLA family, the KIR family is considered the second most polymorphic family of genes (reviewed in [56]). As a result, they vary in certain structural features and ligand specificity. KIRs are generally cell surface receptors comprising 2-3 extracellular Ig-like domains, a transmembrane region and an intracellular domain. However, some cDNA sequences have been observed to harbour early stop codons, suggesting that some KIRs may be released as secretory proteins [57]. The nomenclature of

the KIR molecule serves to describe its structure and function. The acronym KIR is followed by a suffix to describe the number of Ig-like domains (2 domains (2D) or 3 domains (3D)); then the letter S or L describes whether they have long (L) and inhibitory cytoplasmic tails, or short (S) and activatory domains. Finally a code number determines the gene/molecule [58].

The crystal structures of several unbound KIRs and KIR/HLA complexes have been reported [48, 59, 60]. The structures of the KIRs that have been resolved show that the tandem Ig-like domains have almost identical topologies with one β-sheet packed against a second. The domains are connected by a three-residue linker, with the orientation of the domains observed to be quite variable. This suggests high interdomain flexibility. The binding of some (but not all) KIRs to their HLA ligands has been shown to be peptide-dependent; a crystal structure of B27 in complex with KIR3DL1 demonstrates the presence of a binding site between B27 and KIR3DL1 in the peptide-binding region [54]. For KIR3DL1 the HLA bound peptide has been shown to influence the specificity of its interaction, with some peptides showing higher binding avidities than others.

The KIR proteins studied in this thesis are KIR3DL1 and KIR3DL2 (fig. 1.3). **KIR3DL1** is the most polymorphic of the KIR genes, expressed by NK and T cells [61]. The inhibitory KIR3DL1 allotypes have been shown to recognise a subgroup of HLA-B (and some HLA-A) molecules expressing the Bw4 epitope [49]. The Bw4 epitope is defined by positions 77-83 of α1 helix of the class I heavy chain (this includes B27). Binding of KIR3DL1 to ligand at the immunological synapse results in phosphorylation of the internal ITIM motifs and triggering of a signalling cascade leading to inhibition of cell activation. **KIR3DL2** is considered to be one of the framework KIR genes and is also found to be expressed on NK

and T cells. KIR3DL2 is structurally very similar to KIR3DL1. The previously characterised immunological ligands for KIR3DL2 have been shown to be HLA-A3 and HLA-A11 with binding observed to be highly peptide dependent [62]. Additionally, KIR3DL2 has been shown to bind to the B27 homodimer [63] where enhanced binding of the B27 homodimer to KIR3DL2 has been shown to promote the survival of Natural Killer Cells [64].

1.8 Leukocyte Immunoglobulin Like Receptors

Like the KIRs, the Leukocyte Immunoglobulin Like Receptors (LILRs (previously termed ILTs)) are a group of activatory and inhibitory receptors of the Ig superfamily (reviewed in [51]). By contrast with the KIRs, LILRs have been shown to be a lot less polymorphic, with some slight polymorphisms observed with LILRB1, LILRB2, LILRB4 and LILRA3 [65]. Several members of the LILR family have been found to recognise HLA class I molecules [54, 66-68]. The exracellular Ig-like domains of the LILRs are responsible for their recognition properties, while their transmembrane and cytoplasmic domains define their activatory or inhibitory properties. Interestingly, LILRB2 has been shown to bind to HLA molecules both in trans (between different cells) and in cis (on the surface of the same cell) [69]. In addition to the cell surface membrane bound LILR molecules, it has also been suggested that alternative splice variants of the LILRs can lead to the secretion of soluble forms of these proteins [70].

The crystal structures of several LILR molecules have been solved. In contrast to the KIR recognition properties, the structural data for LILRB1 and LILRB2 in complex with their HLA ligands show that their interactions are distant from the peptide binding region of the

HLA, and so the interactions are peptide-independent [50, 71, 72]. The LILR proteins studied in this thesis are LILRB1 and LILRB2. **LILRB1** (formerly ILT-2) is a widely expressed inhibitory receptor found on the surface of NK cells, B cells, T cells and myelomonocytic cells [73-75]. It is composed of four separate Ig extracellular domains (designated D1 – D4), a transmembrane domain and four ITIM motifs (fig.1.3). LILRB1 has been shown to bind to a broad range of HLA-class I molecules and cytomegalovirus UL18 through the two distal Ig domains (D1 and D2) [67, 76]. The binding site of the D1 and D2 domain has been mapped to the $\alpha 3$ and β_2m domains of the HLA molecules (fig 1.4), where β_2m plays a major role in the interaction between LILRB1 and its ligands. This explains why LILRB1 has been shown to bind B27 HT but not the β_2m-free B27 homodimers [27].

LILRB2 (formerly ILT-4) has very high sequence homology to LILRB1. It is less widely expressed than LILRB1, mainly being restricted to cells of the myelomonocytic lineage such as dendritic cells and macrophages [77]. LILRB2 has been shown to also bind a broad range of classical and non-classical HLA-class I molecules, including B27 and B27 homodimers [78]. Despite high sequence homology LILRB2 has been shown to adopt a distinct mode of binding compared to LILRB1. Whilst there is overlap in the binding interface, LILRB2 predominantly recognises ligand through the $\alpha 3$ domain (binding site 2), rather than the β_2m domain (binding site 1) to form more intimate associations. This was shown to result in a higher binding affinity of LILRB2 for a non-classical HLA molecule, the β_2m-associated HLA-G dimer [79]. The interactions at site 2 have been shown to be predominantly hydrophobic at residues 195 – 197 (hydrophobic pocket of the AB loop) (fig. 1.4) whereas LILRB1 predominantly interacts through the C strand at this site. Also, the LILRB1 structure

showed interdomain angle changes upon complex formation, whereas LILRB2 maintains the same interdomain angle.

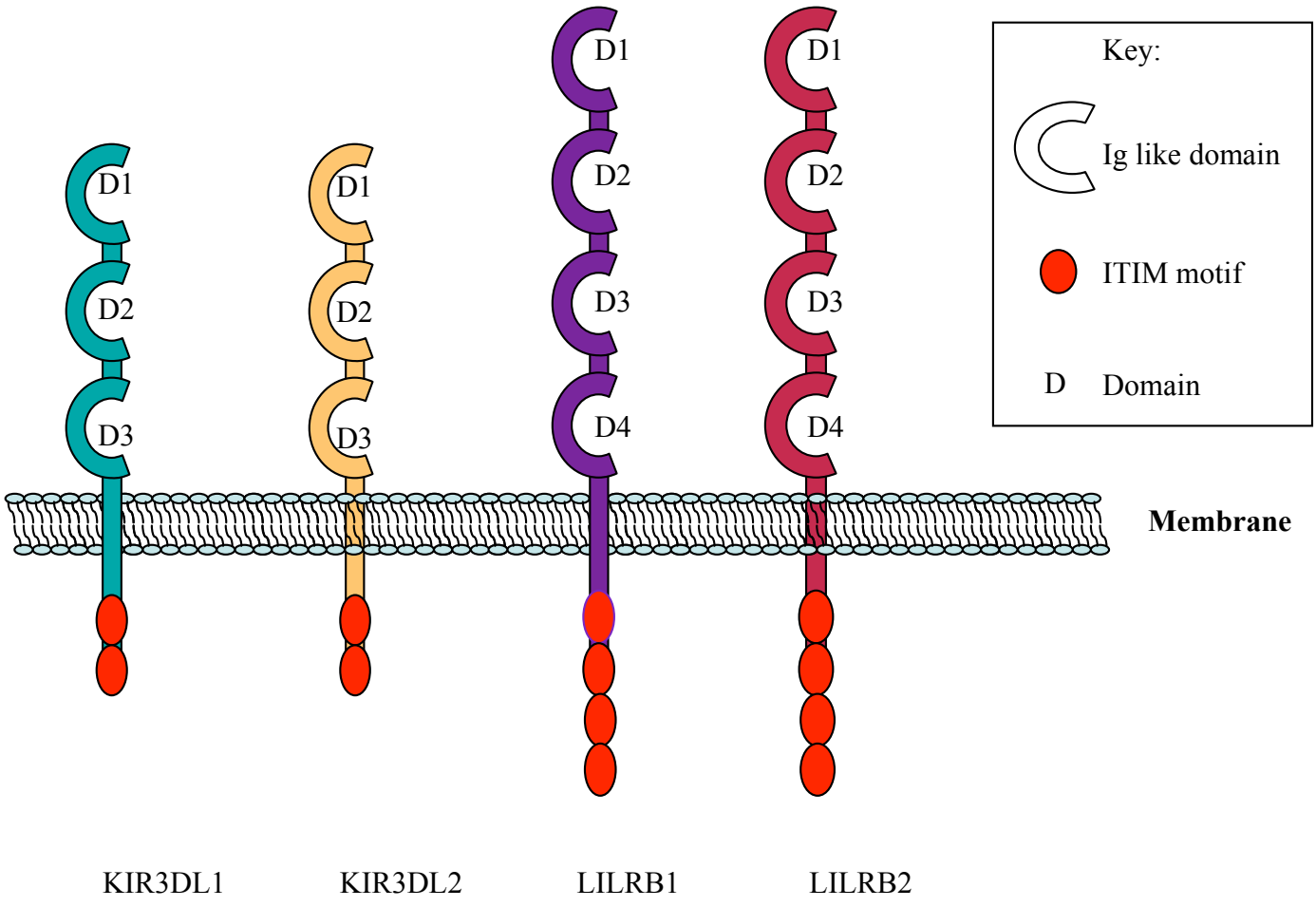
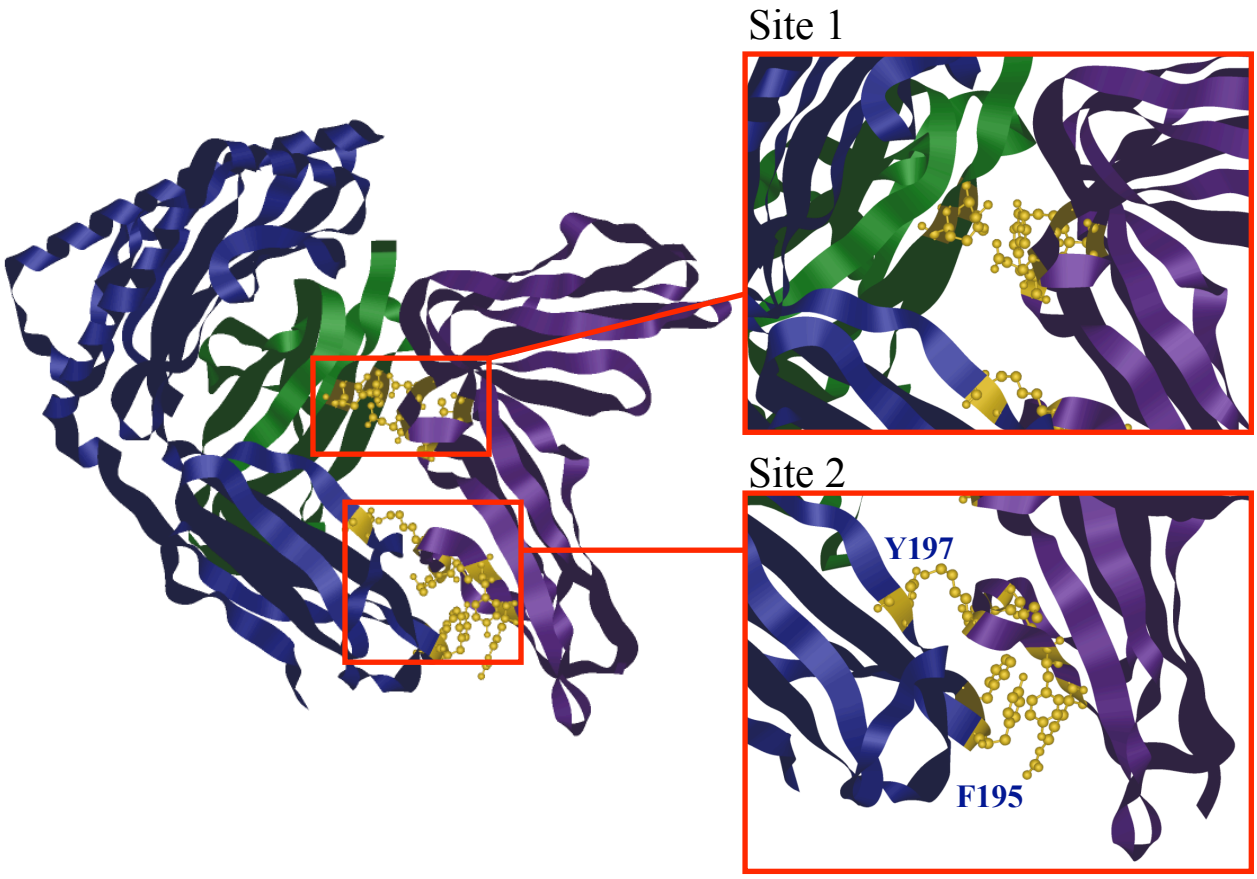


Figure 1.3. Schematic illustration of the KIR and LILR receptors studied in this thesis. *These inhibitory receptors have a long cytoplasmic tail with two or four ITIM domains and varying sequences.*



Model modified from PDB entry 2DYP using imol

Figure 1.4 Binding sites between HLA-G and LILRB2. *LILRB2 adopts a different mode of binding from LILRB1. The majority of contacts are formed at binding site 2 between the α3 domain of HLA-G and D1 (residues F195 and Y197) of LILRB2.*

1.9 B27 Transgenic animal models

B27 transgenic animals which develop arthritis resembling the human disease strongly support a central role for B27 in pathogenesis, rather than a closely linked gene (reviewed in [80]). B27 transgenic rats expressing B*2705 and human β_2m [9], and transgenic mice expressing B*2705 or B*2705/human β_2m in the absence of endogenous β_2m have been shown to develop inflammatory disease and nail disease resembling that in humans [81-83]. B*2705 transgenic rats from Taurog's group have been observed to develop an inflammatory disease resembling SpA. It became more severe with age and also depended upon B27 copy number [84].

In order to confirm that the disease observed in the animal models was B27 specific, other HLA alleles have been used and shown not to cause inflammatory disease, including HLA-Cw6 transgenic rats (reviewed in [85]). Furthermore, Taurog et al have reported that transgenic rats expressing a C67S-mutated B27 develop a less severe form of arthritis than the wild type B27-transgenic rats [85]. Most recently Taurog et al have shown that CD8α negative, B27/human β_2m transgenic rat lines still displayed the disease phenotype. This result shows that the rat inflammatory arthritis can occur in the absence of CD8+ T cells [83]. The transgenic B27 mouse models have also been revealing, where Khare has shown that inflammatory disease onset is more common in the males (as in the patients) and that the mice only developed disease on a β_2m-deficient background [81]. This observation has supported suggestions that the disease requires neither cell surface expression of "classical" heterotrimeric B27 complexes nor CD8+ T-cells to recognise them. Furthermore, this spontaneous arthritis has been shown in β_2m or TAP-deficient mice with mixed genetic

background [86]. Interestingly, *in vivo* treatment of the B*2705/β_2m -/- transgenic mice with a heavy chain-specific antibody (HC-10) led to a delay in disease progression. What actually triggers disease development in these transgenic animals remains unclear, although there is thought to be an ubiquitous environmental trigger such as microbial infection or stress [87].

1.10 Theories of pathogenesis in AS

Although the exact role of B27 in disease remains elusive, many theories have been put forward to explain the role of B27 in SpA (reviewed in [88, 89]). The current theories derive from the immunological functions of B27 and its unusual biochemical features as an HLA molecule.

The **Arthritogenic Peptide Hypothesis** is one of the original and popular theories for the involvement of B27 in SpA [80]. This hypothesis stemmed from findings that ReA has a strong correlation with certain microbial infections [90-92] and the observations that B27 has the ability to bind a unique set of peptides, including unusually long peptides up to 33 amino acids in length [93]. The arthritogenic peptide hypothesis suggests that B27 is able to present a joint-specific peptide to the T-cell receptor. It suggests that there are certain immunodominant arthritis-causing B27-specific antigenic peptides that are shared among the arthritis-causing pathogens, and that these peptides are also cross-reactive with auto-antigens. Thus, residues unique to disease-associated B27 alleles have the ability to bind arthritogenic peptides, which are recognised by auto-reactive T-cells. When an individual is infected with an organism producing an arthritis-causing peptide, a B27-specific, cytotoxic, T-cell-mediated response is triggered in the joints. This theory has been supported indirectly

through studies which demonstrate the presence of autoimmune and bacteria-cross-reactive, B27-restricted CD8+ T-cells in patients with ReA and AS [94]. In addition, B27-restricted CD8+ T cells reacting with collagen-derived self peptides in a B27 dependent way were detected in the synovial fluid of AS patients [95]. This theory is also attractive as it explains why some B27 individuals remain healthy. In spite of this evidence, several problems challenge the arthritogenic peptide hypothesis, especially the identification of such arthritogenic peptide candidates, which has been attempted but has not been fruitful for AS [96]. In addition, the transgenic rat studies have shown that, although the disease demonstrates some T-cell-dependency, the disease model does not require CD8+ T-cells [97]. Thus, although some lines of evidence have supported the arthritogenic peptide hypothesis, the lack of conclusive evidence means that it is important to consider other possible mechanisms of disease.

Several theories concerning the biochemistry of B27 have also been put forward. The transgenic mouse models showed that spontaneous arthritis develops in the absence of β_2m, and that treatment of the mice with HC-10 leads to a delay in disease progression [82]. Such observations suggest a direct role for the B27 heavy chain. Due to the unusual unpaired C67 residue of B27 (fig. 1.2), the molecule has a tendency to form β_2m-free, disulphide-linked B27 homodimers [26]. The importance of C67 was confirmed when B27 homodimer formation was found to be diminished in C67S mutants [63]. It has also been observed that C164 has an important role in B27 homodimer formation, since B*2705 C164S mutants also influenced B27 homodimer formation [98]. B27 has also been observed to have much slower folding kinetics than other HLAs. Mutagenesis of the entire B pocket of B27 to that of HLA-A2 has been shown to result in a dramatically increased folding kinetics and assembly of the

hybrid (HLA-B27.A2B) [99]. This slow folding assembly exhibited by B27 also contributes to its tendency to misfold.

Two theories surrounding the biochemistry of B27 misfolding are currently being considered: the intracellular stress response hypothesis and the B27 homodimer theory.

As a consequence of its slower folding kinetics and the unusual biochemistry, B27 has been observed to misfold prior to its transport to the cell surface. Misfolding was shown to take place in the ER, demonstrated by the observations that newly synthesised B27 heavy chains were undergoing ER associated degradation (ERAD) [100], and the aberrant disulphide-linked heavy chain accumulated in the ER [101]. A build-up of these heavy chains can then signal a **stress response**, leading to the **Unfolded Protein Response** (UPR). The stress response serves to firstly ensure that any misfolded protein is removed, and secondly, if proper function of the cell is not restored, apoptosis is induced. The UPR is a cascade of events that, when triggered, leads to the induction of ER-associated chaperones to assist protein folding and upregulate protein degradation. The consequences of the UPR include activation of the transcription factor NFκB, which then stimulates the synthesis of pro-inflammatory cytokines such as TNFα and Interleukins, including IL-23 [102]. Evidence for the UPR in the synovial fluid of AS patients has been reported [103], and the UPR has been shown to occur in B27/ human β_2m transgenic rats [104]. Moreover, misfolded B27 was later shown to be more prone to bind to ER chaperone proteins, including BiP [105]. Further examination of gene expression in these transgenic rats by microarray analysis has confirmed UPR target genes to be BiP, CHOP and XBP1 and also showed a strong interferon response gene signature [106]. The overall effect of the UPR in SpA is still unclear, but it is possible

that the misfolding of B27 provides one of the signals necessary for the inflammatory response.

The final theory that I will introduce, **the B27 homodimer theory**, is the main focus of this thesis. This theory focuses on the aberrant folding of B27, which leads to the unusual conformation of B27 as disulphide-bridged, β_2m-free homodimers (fig. 1.2). B27 homodimer formation has been observed both in *in vitro* refolding experiments [26] as well as at the cell surface [27].

Cell surface expression of B27 homodimers has been shown to occur during endosomal recycling, rather than egression from the ER [24]. Here, unstable B27 HT complexes at the surface undergo cargo (peptide cargo) recycling, particularly if the loaded peptide is "sub-optimal". Pulsing these cells with strongly binding peptides diminished B27 homodimer expression at the cell surface. This evidence of B27 homodimer expression at the cell surface has led to the proposal that it may be a ligand for immunoreceptors [107]. B27 homodimers have been shown to bind to a number of immune receptors, including some KIRs and LILRs (section 1.5-1.7) [64]. Specifically, fluorescently labelled tetrameric complexes of B27 homodimer have been used to stain transfected cell lines to show that KIR3DL1, KIR3DL2 and LILRB2 are all receptors for the B27 homodimers [78, 108]. Although the functional outcome of this interaction remains unclear, given the importance of the immune receptor interactions in activation of innate immune responses, it is likely that an upset to the balance of homeostasis by B27 homodimer interactions may lead to an autoimmune inflammatory response (fig. 1.5).

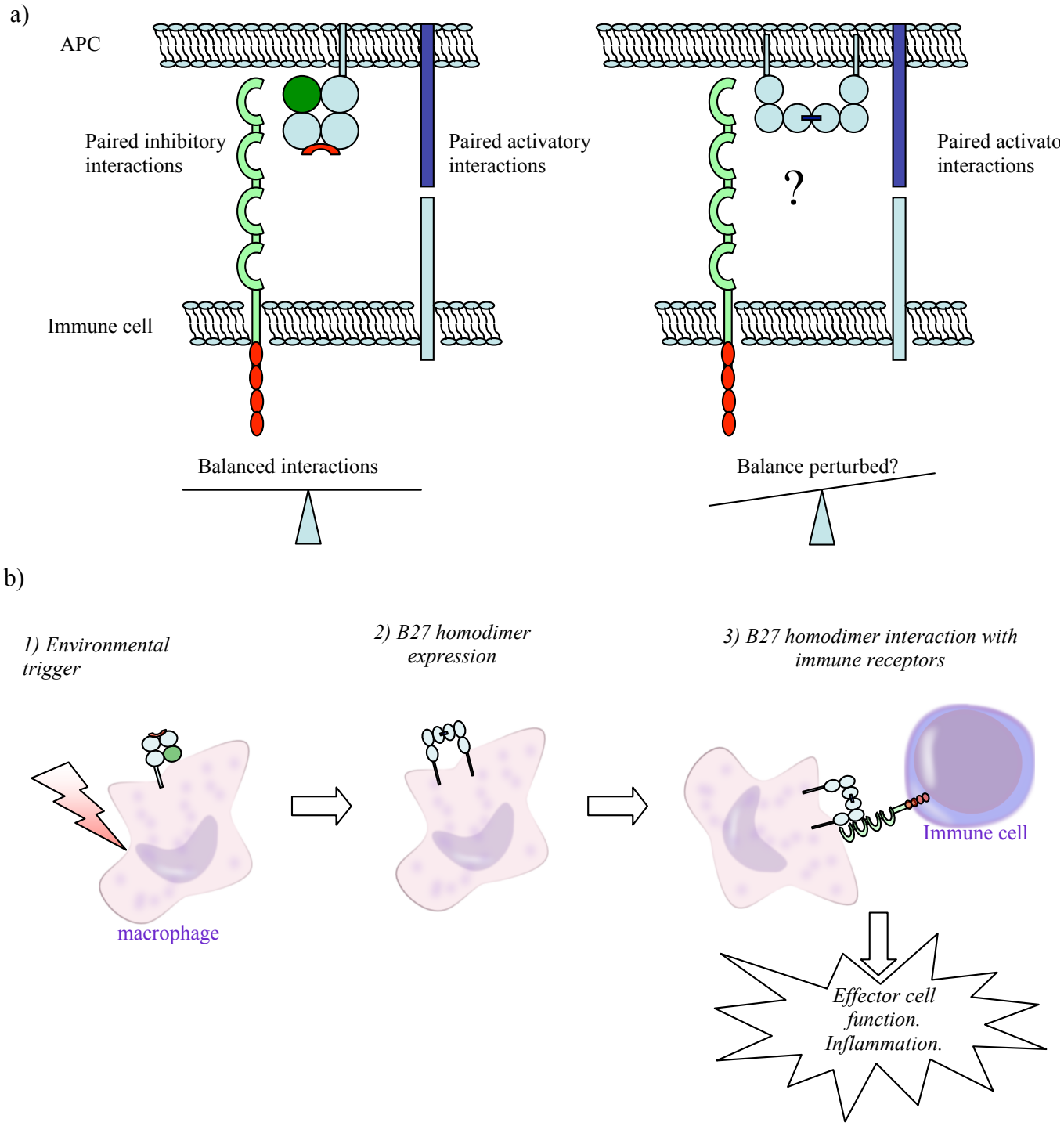


Figure 1.5 Model for the role of B27 in disease *a) The balance of inhibitory and activatory interactions maintains immune cell function. B27 homodimers may perturb this delicate balance to promote inflammation. b) B27 homodimer hypothesis suggests that an environmental trigger induces B27 homodimer formation that can alter subsequent immune cell interactions.*

1.11 Aims of this project

The aims of the work undertaken in this thesis are based on the B27 homodimer theory. Firstly, I compare the binding specificities and affinities of B27 homodimers and heterotrimers for their KIR and LILR ligands. Secondly, I investigate the abilities of B*2705 and B*2709 subtypes to form homodimeric and hetrotrimeric molecules *in vitro*. Thirdly, I compare the binding specificities and avidities of the B27 subtype homodimers and heterotrimers to the immune receptors: KIR3DL1, KIR3DL2, LILRB1 and LILRB2. I then investigate the binding properties of a novel B27 homodimer specific antibody, HD-6 and compare its specificity with the more widely used antibody HC-10. Finally, I begin crystal trials experiments by expressing, purifying and crystal screening for the B27 homodimer. Overall, this thesis aims to elucidate the molecular details of B27 homodimer immune receptor recognition in order to further develop our understanding of the role of B27 homodimer immune receptor interactions in the development of inflammation in AS.

Chapter 2. Materials and Methods

2.1 Bacterial Culture ……... 35

2.2 Molecular Biology ……36

2.3 Protein Expression ……37

2.4 Protein Refolding and Purification ……40

2.5 Flow Cytometry ……41

2.6 Surface Plasmon Resonance ……..41

2.7 Functional Dendritic Cell Assay ……45

2.8 Epitope Mapping ……46

2.9 Protein purification for crystal trials……...……47

2.10 Crystal Trials ……..……..48

2.11 Mammalian cell expression of soluble B27…….…….50

2.1 Bacterial Culture

2.1.1 Bacterial broths

Bacterial nutrient broth was made with de-ionised water and autoclaved. All media reagents were purchased from BD Biosciences.

Recipe for low salt Luria-Bertani (LB) broth (1 Litre)

10.0g Bacto® - tryptone

5.0g Bacto® - yeast extract

5.0g sodium chloride

(standard LB media contains 10.0g sodium chloride/litre)

Agar plates were made by adding 15.0g Bacto® agar per litre of media before autoclaving.

2.1.2 Antibiotic selection

Bacteria were cultured under antibiotic selection, using the following concentrations; ampicillin 100μg/ml and Chloramphenicol 50μg/ml. The stock solutions of antibiotics were filter sterilised and added to media before use.

Antibiotics were added to liquid agar solutions after cooling to 60°C, before pouring the plates.

2.2 Molecular Biology

*2.2.1 Mutagenesis of B*2705*

B*2709 (his tagged with biotinylation site) was generated by mutagenesis of Plasmid pLM1-HLA-B*2705 using the QuickChange® Site-directed mutagenesis kit (Invitrogen). The B*2709 single mutation reaction (D116H) was performed using the forward and reverse primers, 5' GGG TAC CAC CAG CAC GCC TAC GAC G 3' and 5' CGT CGT AGG CGT GCT GCT GGT GGT ACC 3' respectively. The PCR cycle used for each of these reactions was:

Segment	Cycles	Temp (°C)	Time (s)
1	1	95	30
2	18	95 55 68	60 60 360
3	1	5	∞

The PCR product was Dpn1-treated (to eliminate the template plasmid) as described in the kit and then amplified in XL-I blue super-competent bacterial cells (Invitrogen) plated onto ampicillin-(amp), Isopropyl β-D-1-thiogalactopyranoside-(1mM) and X-gal- treated plates and incubated at 37°C for 16 hours. White colonies were selected and amplified in 10ml ampicillin-supplemented Luria Bertani (LB) broth overnight. pDNA was extracted using a Qiagen Miniprep kit and then verified by sequencing.

2.3 Protein Expression

2.3.1 Recombinant HLA class I protein expression and inclusion body purification

100µl of BL-21 (DE3) pLys competent *E.coli* cells (Novagen) were transformed with 50ng of pDNA of either B*2705 or B*2709 (modified by removal of the leader sequence, transmembrane region and cytosolic tail, but including a C terminal biotinylation site and C terminal 6 his tag) or β2m expression plasmids. These bacteria utilize the inducible expression depending on IPTG addition. 100µl of transformation mix was plated onto LB-amp agar plates and incubated at 37°C for 16hr. An isolated colony was picked and inoculated into 250ml of amp- and chloramphenicol- supplemented LB broth. The culture was then left shaking overnight at 37°C. This culture was inoculated into 3 litres of LB broth supplemented with 0.4% D glucose and amp. This was incubated at 37°C for 4 hours and then induced to express recombinant protein by addition of IPTG (1mM). Cell pellets were harvested by centrifugation once an $O.D_{650}$ of 2.0 was reached. Cell pellets were re-suspended in 40ml ice-cold PBS and stored overnight at -80°C in order to lyse cells by freeze-thaw. Cells were sonicated to lyse cells in bursts of 40 seconds, ten times on ice and then centrifuged (15,000 x*g*) for 25 min. The inclusion body-containing pellet was then washed three times in Triton wash buffer (0.5% Triton X100, 50mM Tris pH 8.0, 100mM NaCl) using a hand-held homogeniser, and then washed once in the buffer without Triton. The pellet was then resuspended in 15ml denaturing solution (8M Urea, 0.025M NaCl, 0.005M Na_2HPO_4) and left over-night at 4°C to allow the pellet to re-dissolve. The recombinant protein was then centrifuged to remove undissolved material before being aliquotted and frozen at -80°C for subsequent use in refolding.

2.4 Protein refolding and purification

2.4.1 HLA protein Refolding by limiting dilution

300ml of refolding buffer consisting of 100mM Tris-HCl, pH 8.0/ 400mM L arginine / 2mM EDTA / 0.5mM reduced Glutatione/ 0.5mM oxidised glutathione / 0.5 mM phenylmethanesulphonylfluoride (PMSF) was set up, stirring at 4°C. 3mg of synthetic-peptide (as described in section 4.2, synthesised in the in house facility on an automated peptide synthesiser (396 MPS, Advanced Chemtech) by conventional solid phase Fmoc chemistry, then analysed for purity by reverse phase HPLC) was dissolved in 1ml of DMSO and then added directly to the refold. Refolding of heterotrimeric complexes was performed by solubilisation of 10mg B27 heavy chain and 20mg β2m into 2ml of 10M urea and 50μM Dithiothreitol (DTT). Once prepared, the dissolved β2m was added slowly to the refold buffer. 10mg of B27 heavy chain was then added slowly (pulsed) to the refold. The refold was then pulsed on 3 more occasions with 10mg B27 heavy chain at intervals of at least 4 hours. This refold was left stirring for 48hr at 4°C. The 300ml was centrifuged to remove any insoluble precipitates, and the protein concentrated to 10ml in an amicon stirrer (Millipore) (cut off 10kDa). B27 homodimer refolds were performed as described above, with peptide, but without any β2m included in the refold mix.

2.4.2 Protein purification and analysis

The 10ml refold was then filtered (0.22μm) prior to purification using a Fast Pressure Liquid Chromatography system (FPLC) using a superdex 75 (Sd75) size exclusion column (GE Healthcare) (for heterotrimeric complex) or superdex 200 (Sd200) size exclusion column (GE Healthcare) (for homodimers) using the AKTA purification system. The buffer used was

20mM Tris pH 8.0, 150mM NaCl (filtered) buffer. The peak corresponding to the heterotrimeric complex (45Kd elution volume 160-175ml on sd75) or homodimeric complex (66kD elution volume 185-200ml on sd200) was harvested and concentrated to <1ml. Protease inhibitors were added. Purity of refold was confirmed by 12% SDS-PAGE gel electrophoresis (NuPAGE, Invitrogen) running for 150V for 1h 30m. For comparison of refold yields the areas under the relevant peak were quantified using the Unicorn software.

2.4.3 LILR expression, refolding and purification

Truncated LILRB1 and LILRB2 expression plasmids containing only two Ig like domains, D1 and D2, were provided by K Maenaka, Medical Institute of Bioregulation, Japan. Inclusion bodies were produced as described for B27 above. Refolding was performed by limiting dilution as described above, pulsing only once with 40mg of solubilised protein and refolding in 500ml of buffer for 48hr. Purification was performed on an sd75 gel filtration column. The peaks corresponding to recombinant LILRB1 and LILRB2 (20-22kD) were harvested (185ml and 220ml respectively) and concentrated to <1ml.

2.4.4 CD8 alpha expression, refolding and purification

A plasmid containing the expression sequence for the ectodomain of human CD8 alpha (CD8α), with six silent mutations (to increase expression) were provided by K Maenaka, Medical Institute of Bioregulation, Japan. Inclusion bodies were prepared, as described above, and refolded by pulsing 3 times with 10mg of solubilised and reduced CD8α inclusion body preparation in 250ml of refolding buffer for 48hr. The refolds were concentrated and purified on a pre-calibrated Sd 75 gel filtration column, where the peak corresponding to CD8 alpha homodimer (CD8αα) (26kDa) was harvested (180ml).

2.4.6 Site-specific biotinylation of refolded protein and generation of tetrameric complexes

B27 heterotrimer tetramers were generated by expression and refolding of B27 with a 6-histidine tag and a C-terminal biotinylation recognition sequence, as described previously. Prior to purification, the concentrated refolded protein solution was then buffer-exchanged into 10mM Tris pH 8.0 using disposable PD10 columns (Pharmacia, Biotech) following the manufacturer's instructions. Briefly, columns were equilibrated with 25mls of 10mM Tris (pH 8.0), then 2.5mls of refolded complex was added and eluted with 3.5mls 10mM Tris pH 8.0. Recombinant BirA enzyme (10μM final concentration,) was added with Biomixes A & B (containing 100mM ATP (pH 7.0)) and 0.5mM biotin (all Avidity) for the specific addition of bioin and catalysis of the biotinylation reaction. Protease inhibitors were also added: 1μg/ml pepstatin and 1μg/ml leupeptin. The reaction was left overnight at room temperature. Homodimer complexes were first purified by gel filtration, and then biotinylated as described. Residual biotin was removed by nickel purification using nickel beads (GE Healthcare). The purified biotinylated protein was then made into tetramers by addition of phycoerythrin-labelled extravidin (Sigma) at a 4:1 molar ratio of biotinylated refolded protein : extravidin. Tetramers were then stored at 4°C and in the dark.

2.5 Flow Cytometry

2.5.1 Cell culture

All tissue culture was carried out in a containment class 2 cabinet. Cell lines were incubated at 37°C in 5.5% CO_2. All cell lines were cultured in RPMI 1640 medium (Gibco or Sigma) supplemented with 10% fetal calf serum (FCS) (Sigma) and 2mM L-Glutamine (Sigma)

(R10) unless otherwise stated. All disposable tissue culture material was supplied by Falcon (Becton Dickinson, USA).

2.5.2 Staining using fluorescently labelled tetrameric HLA complexes and Flow cytometry

Tetrameric complexes were used to stain Baf cells (murine derived pro-B-cell line derived by L.Lanier) transfected with KIR3DL1, KIR3DL2, LILRB1 or LILRB2 receptor. Stains were carried out on $2x10^5$ cells per well, in the dark for 30 min at 37°C. Cells were then washed three times with PBS supplemented with 10% FCS, then fixed with 0.5% formaldehyde and analysed with a CyAn flow cytometer and FlowJo software (Dako, Denmark). For blocking of tetrameric staining, B27 tetrameric complexes were pre-incubated with increasing concentrations of competing ligand (CD8αα or HD6/8 Fab) at 37°C for 60 min. These complexes were then used to stain LILR-transfected BAF cell lines, as described above.

2.6 Surface Plasmon Resonance

2.6.1 Sample Preparation

Biacore ligands and analytes were purified using an sd75 column the day before the Biacore was conducted, and then concentrated to a suitable concentration (≥ 1mg/ml). All analytes were then buffer exchanged into HBS-EP running buffer (Biacore, GE healthcare) to match the running buffer of the Biacore system. This was done using centrifugal spin concentrators (Amicon Ultra Centrifugal filters (10,000 MWCO)) at 4000g and 4°C until a volume of 500µl was reached, whereupon the volume was increased to 15ml by addition of HBS-EP and the process repeated. Buffer exchange of the analyte was conducted using 50ml HBS-EP

per sample. Samples were concentrated to a suitable concentration for binding analysis and purity was confirmed by SDS-PAGE prior to each experiment.

2.6.2 Sample Immobilisation

Surface Plasmon Resonance (SPR) ligands were diluted to 1μM. A streptavidin-coated gold-coated SPR chip (Biacore, GE Healthcare) was docked onto the SPR machine. The correct flow cell was selected and an injection of ligand was initiated until the Response Difference of that flow cell had reached the desired Response level for the specific experiment (1,000 RU for equilibrium binding). B27 heterotrimers, B27 dimers and HLA-A3 heterotrimers were immobilised in this way. For immobilisation of β_2m-free heavy chains, B27 heterotrimers were immobilised and then the β_2m was washed off using Glycine pH 2.5 (Biacore). This removed the β_2m and peptide but maintained the B27 heavy chain of the protein. The β_2m was shown to be removed by injecting 10μl of an anti-β_2m antibody (BBM1 – made in-house) over the surface of the chip and no binding to the surface was observed.

2.6.3 Regeneration of the chip surface

Regeneration of the chip was needed for kinetic binding experiments where the bound analyte was not removed completely from the surface. The activity of the surface then remained unaffected for the subsequent injection of analyte. Optimal conditions were selected for each ligand : analyte configuration. Low pH was selected for removing the analyte. In order to select the mildest conditions possible, an injection of analyte was flown over the ligand. Bound ligand was then removed by an injection of Glycine-HCl pH 3.0 (Biacore, GE healthcare). It was then observed whether the analyte was completely removed from the ligand by comparing the before and after Response value for the flow cell. If the

analyte was not completely removed, more analyte and then injections of decreasing pH solutions were added until the analyte was completely removed. The Glycine-HCl buffer with the highest pH at which all the analyte was removed whilst maintaining ligand activity was chosen. This was then selected as the regeneration solution to be included in the Kinetic experiments.

2.6.4 Equilibrium binding experiments

Equilibrium binding SPR experiments were performed using a Biacore 3000 (Biacore) in HBS-EP running buffer (Biacore, GE Healthcare). Biotinylated soluble HLA (ligand) was immobilized on streptavidin-coated chip (Biacore, GE Healthcare) at 1,000 RU (response units) per flow cell. Equilibrium binding of LILRs was measured at the flow rate of 10 µl/min, starting from the lowest LILR concentration. Biotinylated BSA or/and an empty flow cell was used as a negative control. Biotinylated HLA-A3 was used as a positive control (a kind gift from Yanchun Peng). Experiments were performed at 25°C and 37°C. Classically, SPR experiments are conducted at 25°C in order to compare results to ELISA data. Here, I also conducted the experiments at 37°C as a more physiological measurement. Data collected at each temperature gave comparable results. The data points were plotted using Origin software. *KD* values were obtained using the standard hyperbolic model fitting kinetics software.

2.6.5 Kinetic binding analysis

Kinetic binding analysis using SPR was performed using a Biacore 3000 (Biacore, GE healthcare). The amount of ligand to be immobilised onto a chip should be calculated depending on the molecular masses of both the ligand and analyte. An R_{max} value describes

the optimal binding capacity of the surface. Biotinylated soluble ligand (HLA) was immobilised on a streptavidin-coated chip (Biacore, GE Healthcare) at 100 R_{max} Units (where 50 – 150 units gives a binding capacity that limits mass transport effects). This value was calculated using the equation below:

$$R_{max} = \frac{\text{Analyte MW}}{\text{Ligand MW}} \times RL \times Sm$$

RL = the immobilization level

Sm = the stoichiometric ratio

For HLA-B27 dimer binding LILRB2, this was

100 = 22000 / 66000 x RL X 1

RL = 300 RU

For HLA-B27 dimer binding Fab, this was

100 = 22000 / 50000 x RL X 1

RL = 227 RU

The kinetic experiments were then conducted using the "Kinetics of Binding" program on the Biacore 3000 software, whereby increasing concentrations of analyte are injected over the ligand surface and an empty flow cell, with an extra regeneration step between each injection, to ensure all of the analyte is removed from the ligand. The response for each concentration of analyte was calculated by subtracting the response achieved for injection over the empty flow cell from the response observed over the immobilised ligand. Relevant Mass Transfer

Control experiments and Linked Reaction Control experiments were also conducted at this stage, and the Baseline stabilities of the flow cells were also analysed, to ensure stability of the ligand. The results are then analysed using the Biaevaluate software (Biacore). Experiments were conducted at 25°C and later repeated at 37°C to check for any discrepancies.

2.6.6 Competition experiments

In order to test whether different ligands were able to compete for binding to the B27 homodimer, the biotinylated B27 homodimer was immobilised to the streptavidin chip. Injection of analyte (analyte A) was then conducted using volumes of 20µl per injection. When Antibody or Fab was injected as analyte, a larger volume was injected (up to 300µl) to ensure binding had saturated. The next analyte (analyte B) was then injected to see whether analyte A blocked binding of analyte B. The blocking capacity of analyte A was reflected in the change in response units for the binding of analyte B; e.g. if full blocking occurred, then analyte B would be represented as no change in response from the control flow cell.

2.6.7 Free Heavy Chain binding experiments

In order to assess whether free heavy chains of B27, HLA-G or HLA-A3 were able to bind to candidate antibodies and LILR molecules, the biotinylated heterotrimeric complexes were immobilised onto a streptavidin-coated SPR chip. Next, a Glycine-HCl buffer of pH 3.0 was flowed over the complexes in order to remove peptide and β_2m. The absence of β_2m was confirmed by ensuring that no binding was observed to an anti-β_2m antibody (BB-M1). For B27 0.1M DTT was also flowed over the chip to prevent the formation of any B27 homodimers.

2.7 Functional Dendritic cell assay

Immature dendritic cells (DCs) were derived from healthy donors by positive selection using a standard protocol for CD14 beads (MACs kit). The immature DC were cultured in 50μg/ml of GMCSF and 10ng/ml of IL-4. The cells were cultured for 5 days and then plated into a six well plate at 1 million cells per well in R10. Plated cells were photographed using the Openlab software to monitor dendrite formation and cell clumping. Cells were then cultured with 10μg per well of sterile filtered, unlabelled HLA tetramer for 4 hours at 37°C. After 4 hours a cytokine cocktail was added (IL1-β (5ng/ml), TNFα (5ng/ml), PGE-2 (1μg/ml), IL-6 (150ng/ml) (all Sigma)) to stimulate cell differentiation and cells were incubated for a further 16 hours. After 16 hours cells were photographed again, and then stained using fluorescently conjugated antibodies to the DC maturation markers: CD86, CD83, HLA-DR and CD80. These were analysed by flow cytometry.

2.8 Epitope Mapping by Mass Spectroscopy

2.8.1 Trypsin Digestion of B27 homodimer complex

Trypsin Digestion of recombinant B27 homodimer complex (section 2.4) was performed by Kati DiGleria following the standard protocol in the Trypsin digestion kit (Thermo Scientific). The digestion was then analysed by Mass Spectroscopy to ensure there were no other peptide contaminants.

2.8.2 HD6 binding to B27 peptide fragments

Trypsin Digested B27 homodimer was incubated with HD6 antibody for 2 hours at 4°C, then this mixture was incubated with Protein A beads for an hour at 4°C. The beads were then washed with Tris Buffered Saline (pH 8.0) 6 times to remove any unbound peptide. The resultant Protein A, HD6 and peptide complex was washed with Glycine-HCl (pH 2.0) to wash off any bound peptide. The isolated peptide(s) were then analysed by Mass Spectroscopy. The peptide products were identified using the Mascot Search engine (http://www.matrixscience.com/).

2.9 Protein Purification for Crystal Trial experiments

2.9.1 Purification of B27 dimer

For crystal trials, inclusion bodies of 6-histidine tagged free heavy chains (section 2.3.1) were purified prior to refolding by Nickel affinity purification using the Ni Sepharose High Performance 5ml HisTrap column (GE Healthcare) and the standard included protocol on the AKTA system. These purified inclusion bodies were then refolded with High Pressure Liquid Chromatography (HPLC)-purified GAG peptide (synthesised in the in-house facility on an automated peptide synthesiser) as described above (section 2.4). After 48hr the refold was concentrated, and purified by FPLC using a sd200 column as described previously. Iodoacetamide was added to the purified dimer and purity was then confirmed by non-reducing SDS PAGE gel electrophoresis.

In the initial crystal trials the dimer described above was concentrated to 100μM and then used to set up trials.

*2.9.2 Purification of B*2705 dimer and Fab complex.*

Once the HD6 and HD8 Fabs became more readily available, purification of the B27 dimer and Fab complex was undertaken for crystal trial screening. B27 dimer was prepared as described and was then incubated in a 1:1 molar ratio with the Fab at 4°C for 1 hour. This complex was then run on a calibrated Sd200 column for purification of the B27 dimer : Fab complex. An aliquot of purified sample was retained for SDS-PAGE electrophoresis and the remaining complex was used in crystal trial experiments.

2.10 Crystal Trials

2.10.1 Pre Crystallisation Test (PCT)

A PCT was performed on the purified protein complex to ensure the correct concentration of complex was used for crystal screening. The PCT kit was obtained from Hampton Research and was used according to the manufacturer's instructions. Briefly, 2µl of the protein was mixed with buffers known to induce high or low protein precipitation and this precipitation was monitored over a range of protein concentrations. A concentration of 2mg/ml was seen to be appropriate for the B*2705 Fab complex as mild precipitation of protein was observed using the buffers supplied.

2.10.2 Crystal screens

The purified protein complex was concentrated to 2mg/ml in 20mM Tris pH 8.0, 150mM NaCl (filtered) buffer. The initial crystallisation conditions were screened in 8 separate 96-well crystallisation plates using the following 96-deep-well screening buffer blocks (all Hampton Research): Block 1, Block 2, Block 3, Block 4, Block 5, Salt RX, Index screen.

Crystal conditions were screened in sitting drops containing 100nl of protein complex solution, and 100nl of crystallisation buffer using the sitting-drop vapour-diffusion method with a reservoir containing 500µl of reagent. Reservoir solutions were transferred from 96-deep-well blocks to crystallization plates (Greiner plates) in a single step with a Robbins-Hydra pipettor, Nanolitre droplets of protein as well as reservoir solution were dispensed by a Cartesian pipetting instrument. Plates were barcoded and imaged by an automated storage system. Plates were incubated at 21°C and later moved to 4°C.

2.10.3 Optimisation of crystal screens

Both Ammonium Sulphate, Bicine (2-Bis(2-hydroxyethyl)amino)acetic acid) pH 9.0 (block 3) and Polyethylene Glycol 30%, Sodium Acetate 0.2M and Sodium Cacodylate pH 6.5 (Limited Protein) screening conditions yielded low quality crystals for the B27-Fab complex. These conditions were then used as the basis for crystal screening optimisation. The conditions optimised were the pH, the protein concentration and the ratio of protein to screening reagent. Optimisation plates were set up as shown in the grid below, using only rows F,G and H of the Greiner plates. The pH of the solutions were modified by hand (by addition of HCl or NaOH). These solutions were pipetted as dilution series (using a programmed protocol on an MWG RoboGo, MWG Biotech (UK) Ltd) into the appropriate Greiner plate reservoirs. Nanolitre-scale sitting drops with a range of protein to reservoir solution ratios, to vary the protein concentration in the final drop, were then set up using a programmed protocol on the Cartesian Technologies Microsys MIC4000. Plates were incubated at 21°C and later moved to 4°C.

Well:					Protein: Reagent ratio
F					1:1
G					2:1
H					3:1
pH – (alkali)	100%	90%	80%	70%	pH + (acid)
		Dilution of buffer			

2.10.4 Additive Crystal Screens

Additive screens were performed using the Ammonium Sulphate, Bicine pH 9.0 and Ammonium Sulphate, Citrate pH 3.5 buffer conditions in order to promote crystal growth. The additive screen buffers (Hampton Research) contained 96 different reagents to promote solute-protein interactions for crystal growth. The screening buffer and additive solutions were combined using an automated pipetting instrument (programmed protocol on an MWG RoboGo, MWG Biotech (UK) Ltd), then 96-well-crystal plates were set up as described in 2.10.2.

2.11 Mammalian cell Expression of soluble B27

The pLM1-HLA-B*2705 construct was amplified by PCR to incorporate a six-his tag and to remove the transmembrane domain using the forward primer: 5’ TT ATG GAT CCGCCA CCA TGC GGG TCA CG 3’ and the reverse primer: 5’ ATT ATC TCG AGT CAA TGG TGA TGG TGA TGC TCC CAT CTC 3’. Pfu enzyme was used for this reaction and the PCR cycle used for this reaction is shown:

Segment	Cycles	Temp (°C)	Time (s)
1	1	94	180
2	25	94 55 72	30 60 120
3	1	4	∞

The resulting PCR product was then treated to remove excess primers using a Primer Clean up kit (Qiagen). The product and the pHR-BX-IRES-Em (pIRES) vector were then incubated separately with restriction enzymes Xho I and Bam HI for 2 hrs at 37°C to cut out the B27 soluble sequence and vector (respectively) leaving "sticky ends". The PCR product (insert) and the vector were then ligated using DNA ligase (Invitrogen) for 1 hour at room temperature before amplification by transformation of DH5α competent cells (Invitrogen). This construct was sequenced by the in house sequencing facility.

In order to prepare lentivirus, 1μg of GAG pol and 1μg of VSV-G (envelope vector) in pMO.G were incubated with 1μg of the pIRES vector. This was then used to transfect HEK-293T cells using the Fugene© 6 transfection reagent (Promega) following the manufacturer's instructions. This was incubated at 37°C for 3 days before harvesting the virus. The virus was then used to infect U937 cells and .220 cells by addition of 200μl to the cell cultures. After 3 days cells were analysed by Flow Cytometry to identify a GFP signal. Cells were also lysed using Krebs HEPES buffer (Invitrogen) for Western Blot analysis using HRP conjugated anti-penta his antibody (Invitrogen).

Chapter 3

Immune cell interactions with HLA-B*2705 homodimers and heterotrimers

3.1 Introduction…….53

3.2 LILRB1/LILRB2 display different binding affinities and specificities for B*2705 heterotrimers and B*2705 homodimers……..……..54

3.3 LILRB2 can bind to B*2705 free heavy chains……..67

3.4 LILRB1 and LILRB2 bind to B*2705 heterotrimers, complexed to GAG variant peptides, with comparable affinities…….71

3.5 B27 dimer interactions with myelomonocytic cells……..……..76

3.6 CD8αα binding to B27 homodimers and B27 heterotrimers…….82

3.7 Discussion……...88

3.1 Introduction

Immune cell activation depends upon a delicate balance of interactions between cell surface inhibitory and activatory receptors with their ligands. These ligands include HLA molecules. This activation is strictly regulated to ensure that healthy cells are not destroyed; this function is met by expression of both inhibitory and activatory receptors as discussed in section 1.5. The immune receptors discussed in this chapter include the LILR molecules – LILRB1 and LILRB2; and the KIR receptors – KIR3DL1 and KIR3DL2. All four of these receptors function to monitor expression of HLA class I on healthy cells.

This chapter compares the interactions between these immune receptors and B*2705 heterotrimers, B*2705 homodimers and B*2705 free heavy chains. I use FACS analysis (fig. 3.1) to study B27 homodimer and heterotrimer binding to LILR and KIR transfected cell lines. I then extend these studies by using SPR (fig.s 3.4, 3.5 and 3.8) to assess the affinity and specificity of the interactions. Further to this I evaluate whether a peptide "HIV escape mutation" in the B27 heterotrimer has an effect on the strength of interaction with LILRB1 and LILRB2 (fig. 3.12).

The experiments reported in this chapter test whether there are any biophysical differences between the interactions of different forms of B27 with the discussed inhibitory receptors. I then further these studies to assess how differences in binding specificity and affinity may translate to differences in DC cell function. Here, I incubate recombinant B27 with maturing DCs and monitor changes in DC phenotype (fig. 3.13).

3.2 LILRB1 and LILRB2 display different binding affinities and specificities for B*2705 heterotrimers and B*2705 homodimers

In this section I compare the binding of the LILRB1 and LILRB2 receptors to B*2705 heterotrimers and B*2705 homodimers. I assess whether the binding of receptors (such as the the LILRs) differs between B*2705 heterotrimers and homodimers to elucidate whether a difference in recognition could lead to a difference in function of B27 homodimer-expressing cells. I assess the interactions at the cell surface (by FACS analysis) and I look more intricately at the biophysical properties of the interactions by using SPR.

Recombinant B*2705 homodimer and heterotrimer complexes were refolded in the presence of synthetic GAG peptide (KRWIILGLNK), purified, biotinylated then fluorescently labelled and tetramerised using Extravidin PE. Using FACS analysis I tested the binding of the recombinant proteins and compared B*2705 homodimer and heterotrimer binding to LILRB2 and KIR3DL2. My data confirm previous reports that both B*2705 homodimers and heterotrimers bound LILRB2-expressing cells [103]. B*2705 heterotrimers, but not B*2705 homodimers, are observed to bind LILRB1-expressing cells (fig. 3.1).

*FACS staining of LILRB2- and KIR3DL2- expressing Baf cells by B*2705 homodimer tetramers and B*2705 heterotrimer tetramers*

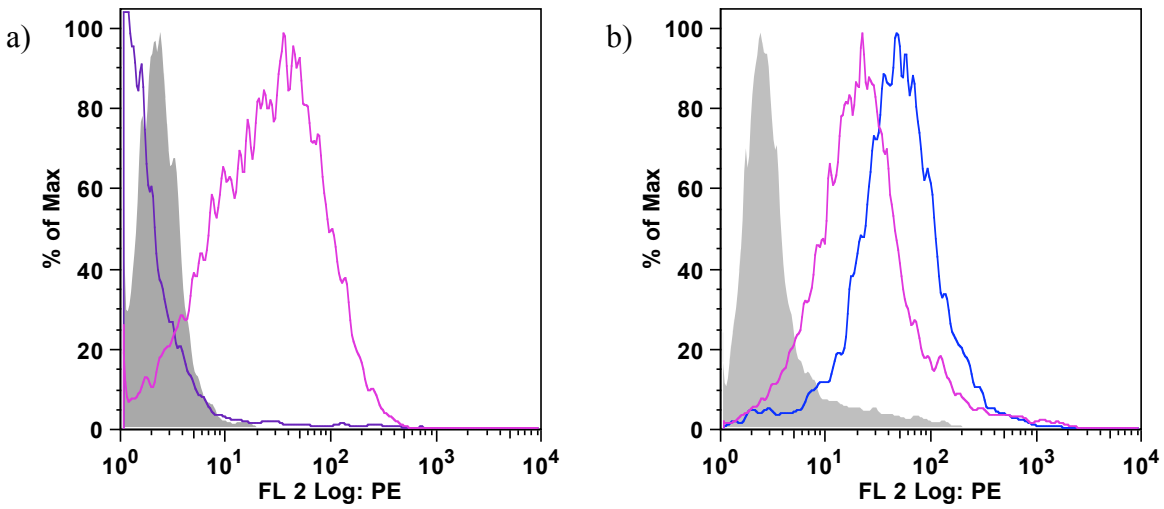


Figure 3.1 B*2705 homodimers and heterotrimers have different specificities for LILRB1 and LILRB2-expressing Baf cells. *a) B*2705 homodimers refolded with a GAG peptide (blue) do not stain LILRB1 transfected Baf cells compared to B*2705 heterotrimers complexed with a GAG peptide (pink), Extravidin-PE only control (shaded grey) or untransfected cells (not shown); b) B*2705 homodimers and B*2705 heterotrimers both stain LILRB2 expressing Baf cells.*

Biophysical measurement of the interactions between LILRB1/2 and B27 heterotrimers and homodimers

Biotinylated B*2705 heterotrimer complexes and B*2705 homodimer complexes were immobilised in separate flow cells of a streptavidin-coated gold chip. Increasing concentrations of LILRs were flowed over the chip. LILR proteins were expressed as described in section 2.4.3 (fig. 3.2) and the purity of the analytes was confirmed prior to each SPR experiment (see appendix, section 8.2). Figures 3.5 and 3.6 show that B*2705 heterotrimers and homodimers (refolded with a GAG peptide KRWIILGLNK) have different binding specificities and affinities for LILRB1 and LILRB2. Results were repeated 4 times with the GAG peptide and 3 times with an EBV peptide (RRIYDLIEL) with consistent results. The mean K_D value for LILRB1 binding to B*2705 heterotrimer was 5.3 ± 0.9 μM, whereas LILRB1 did not bind B*2705 homodimers by SPR (fig. 3.4). This K_D value is consistent with previously reported K_D values for binding of LILRB1 to other classical class I molecules [43]. Using SPR equilibrium binding analysis, a mean K_D value of 22.0 ± 0.5 μM was obtained for LILRB2 binding to B*2705 heterotrimer (fig. 3.5). It was not possible to obtain reliable affinity constants using this method for the B27 homodimer, as the binding did not reach equilibrium at the LILRB2 concentrations used. At the higher concentrations used in subsequent experiments in an attempt to attain equilibrium, the proteins tended to aggregate. Analysis of the data revealed non-linear (bi-phasic) binding over the indicated concentration ranges (fig. 3.6) in six experiments. This observation may be explained by aggregation of protein at the sensor surface. Using an SPR kinetic approach, a K_D value of 2.5μM was obtained for the LILRB2 : B27 homodimer interaction (fig. 3.8).

Expression and purification of LILRB1/LILRB2 proteins

LILRB1 and LILRB2 proteins were expressed and purified as described in section 2.4.3. The refolding condition for these proteins were established (K.Maenaka) and the proteins purified by size exclusion chromatography on a calibrated gel filtration column (fig 3.2). The purity of the LILRs was confirmed by SDS-PAGE (fig 3.3). Refolded and purified proteins were significantly more pure than inclusion body preparation, and so were used for subsequent SPR experiments.

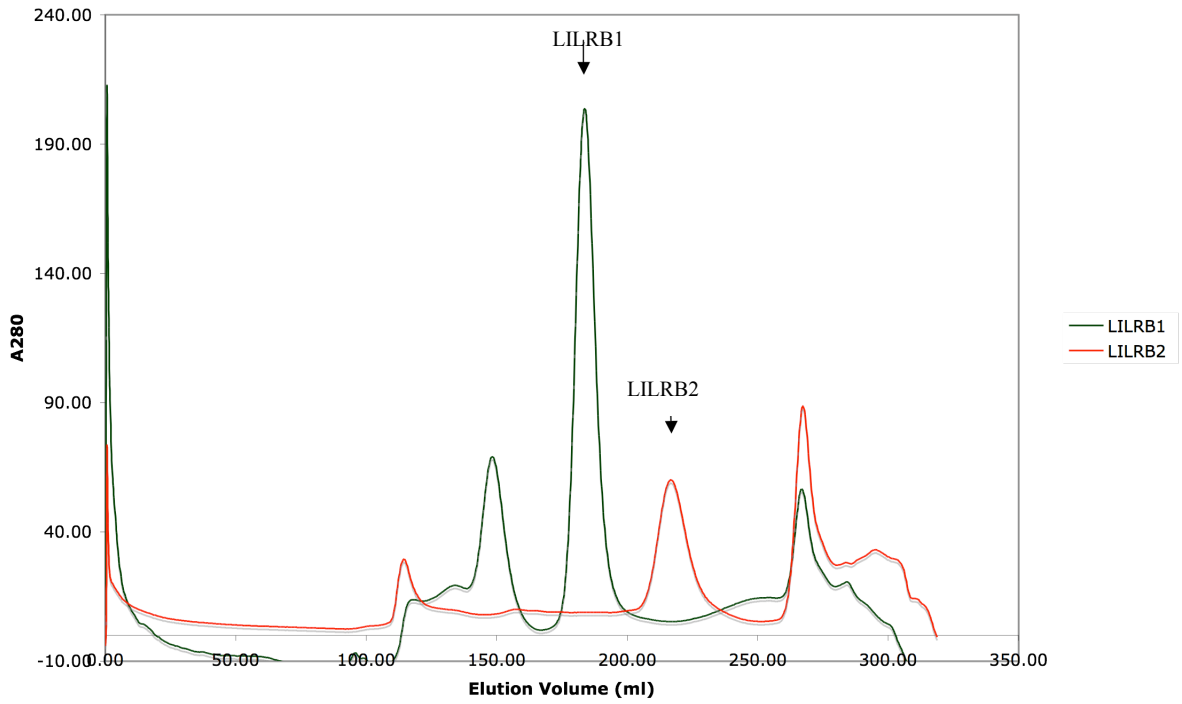


Figure 3.2 FPLC of refolded recombinant LILRB1 and LILRB2. *Labelled peaks were collected and the identities and purity of isolated fractions were confirmed by SDS PAGE.*

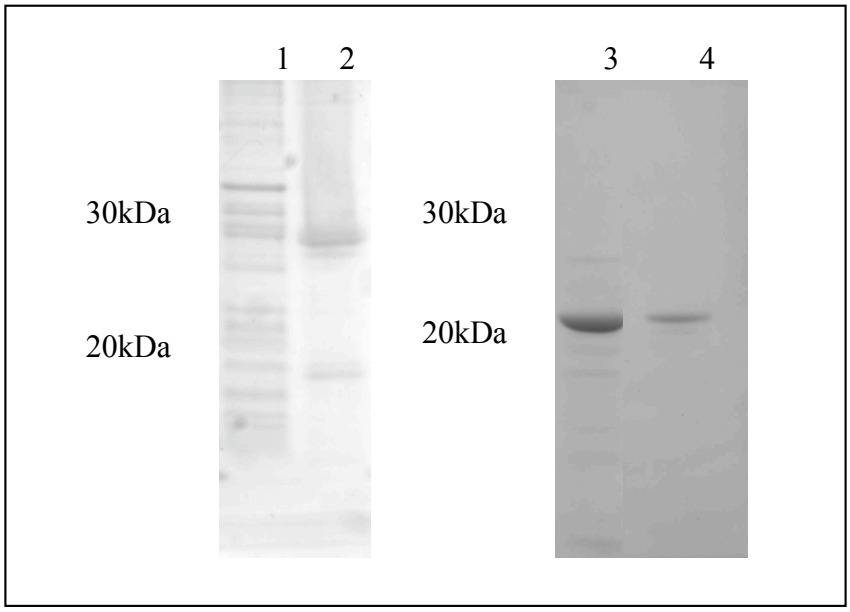
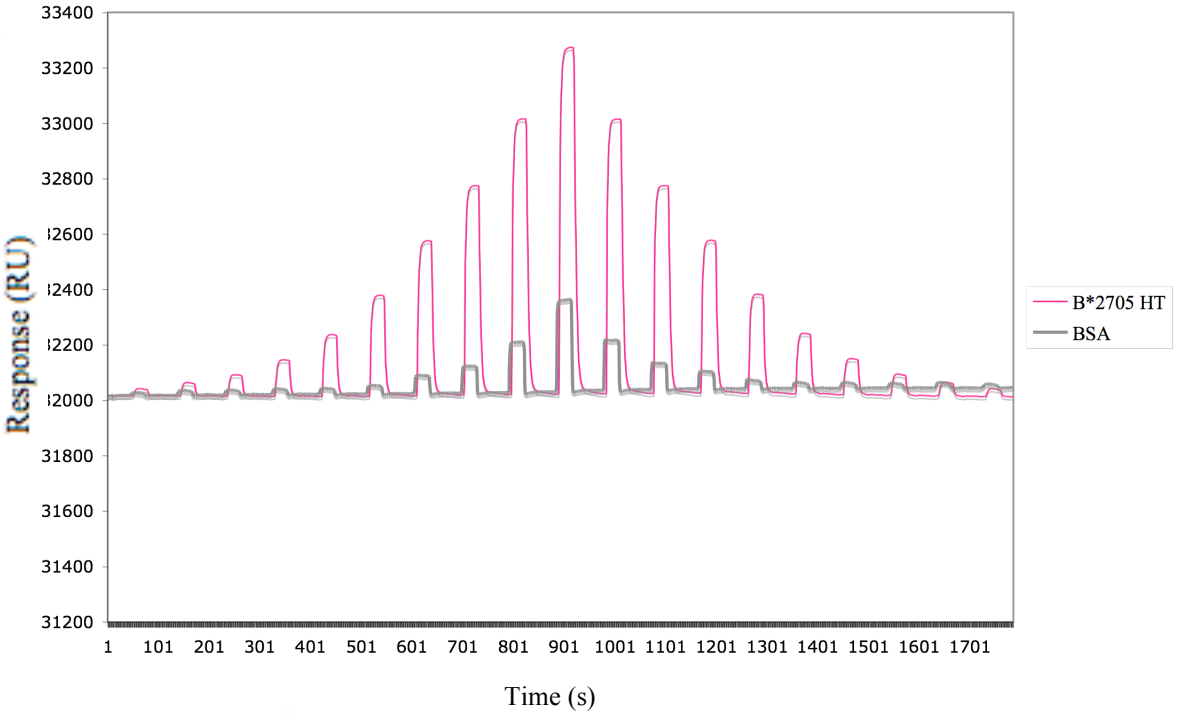


Figure 3.3 Non-reducing SDS PAGE analysis of LILRB1 and LILRB2 proteins. *Lane 1 is the LILRB1 inclusion body preparation, Lane 2 is the LILRB2 inclusion body preparation. Lane 3 is refolded LILRB1 protein and lane 4 is refolded LILRB2 protein.*

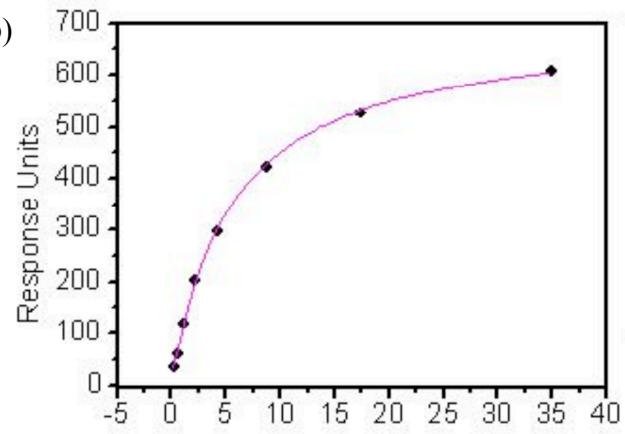
*LILRB1 equilibrium binding to B*2705 heterotrimer*

a)



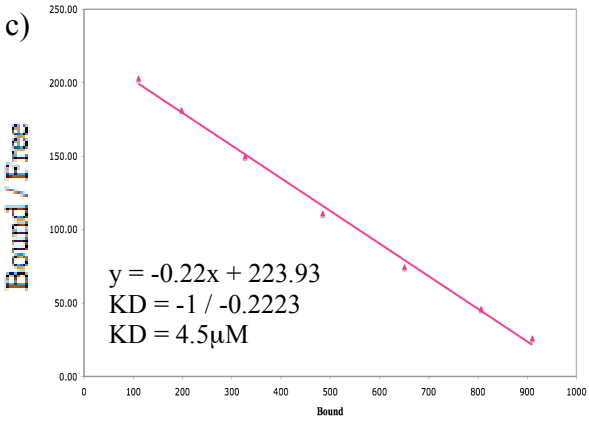
Time (s)

b)



LILRB1 Concentration (μM)

c)



Bound (RU)

*LILRB1 equilibrium binding to B*2705 homodimer*

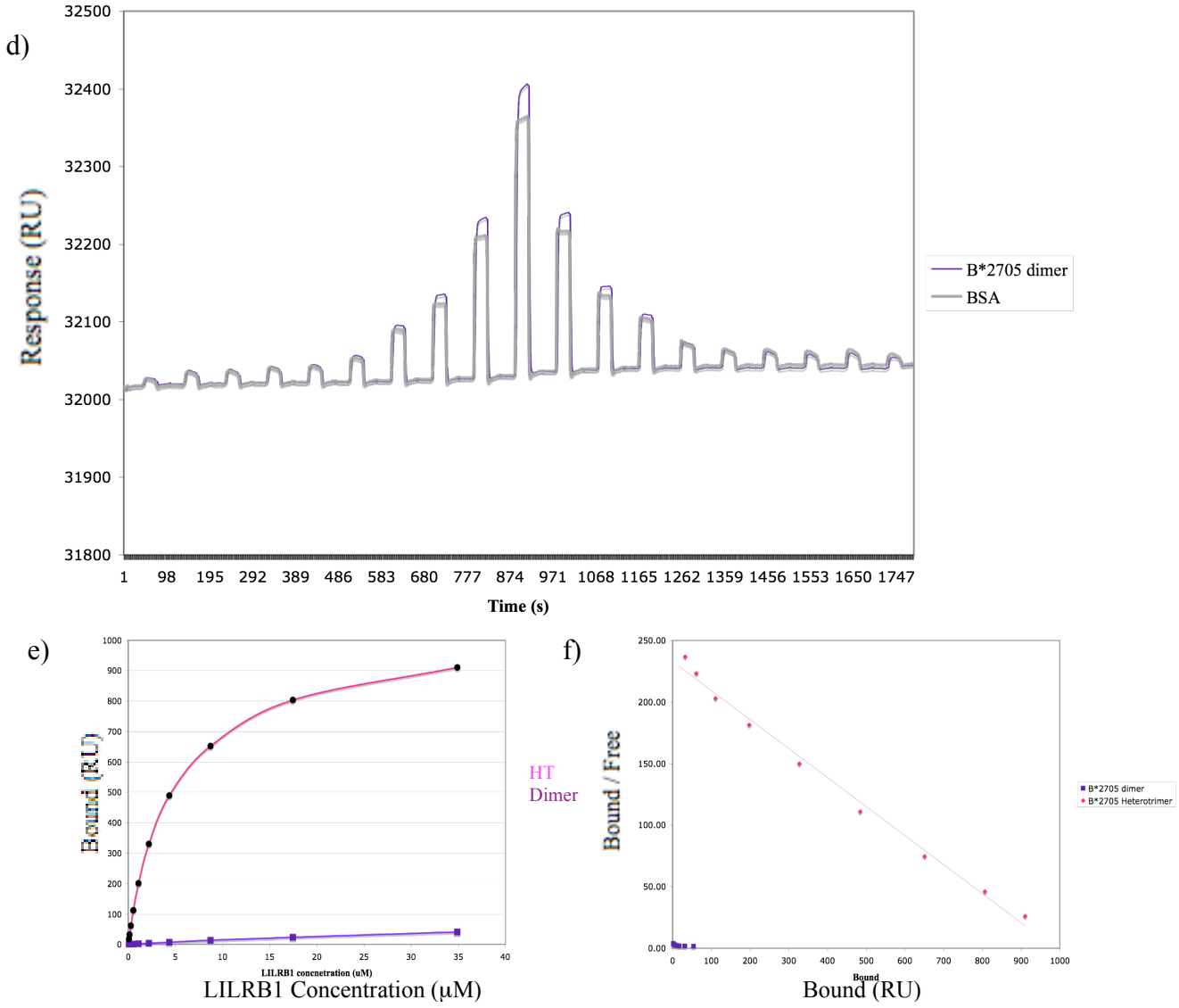
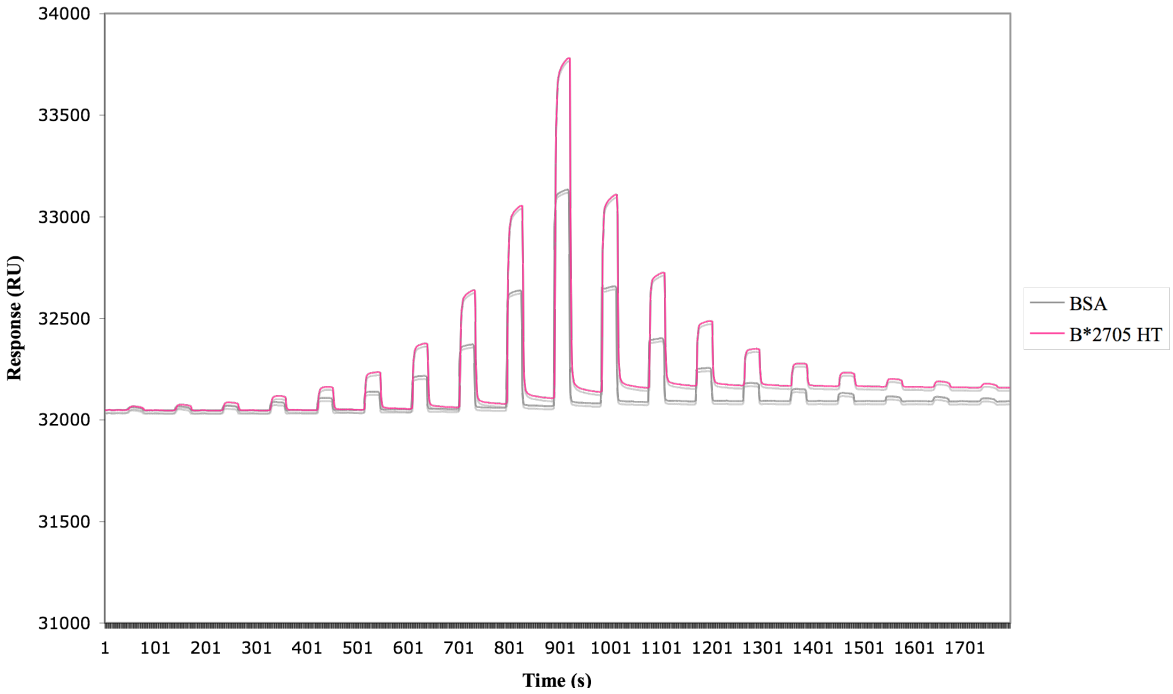


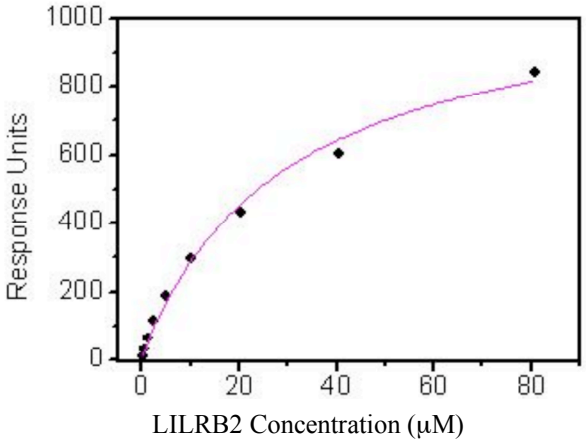
Figure 3.4 LILRB1 binding to B*2705 heterotrimer and homodimer measured by SPR. *Figures a and d are sensograms for binding of LILRB1 to B*2705 heterotrimer and B*2705 homodimer respectively. b and e are non-linear fits of the Langmuir binding isotherm for LILRB1 binding, where e shows a comparison of B*2705 homodimer (purple) and heterotrimer (pink). B*2705 homodimer was shown not to bind LILRB1 compared to the B*2705 heterotrimer; c and f are Scatchard plots for LILRB1 binding to B*2705 heterotrimer (pink) and f shows that no Scatchard curve could be derived for LILRB1 binding to homodimer (purple).*

*LILRB2 equilibrium binding to B*2705 heterotrimers*

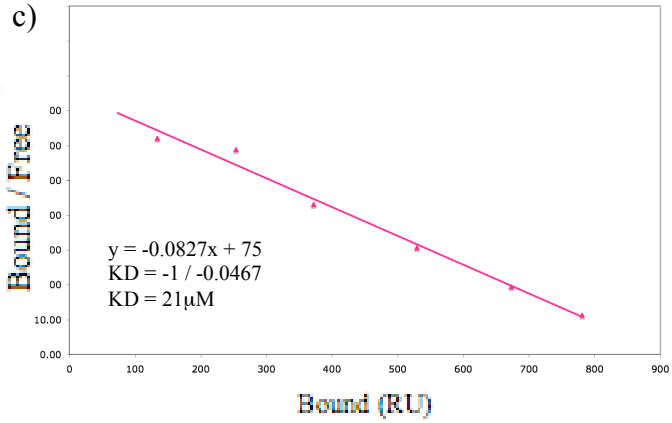
a)



b)



c)



*LILRB2 equilibrium binding to B*2705 homodimers*

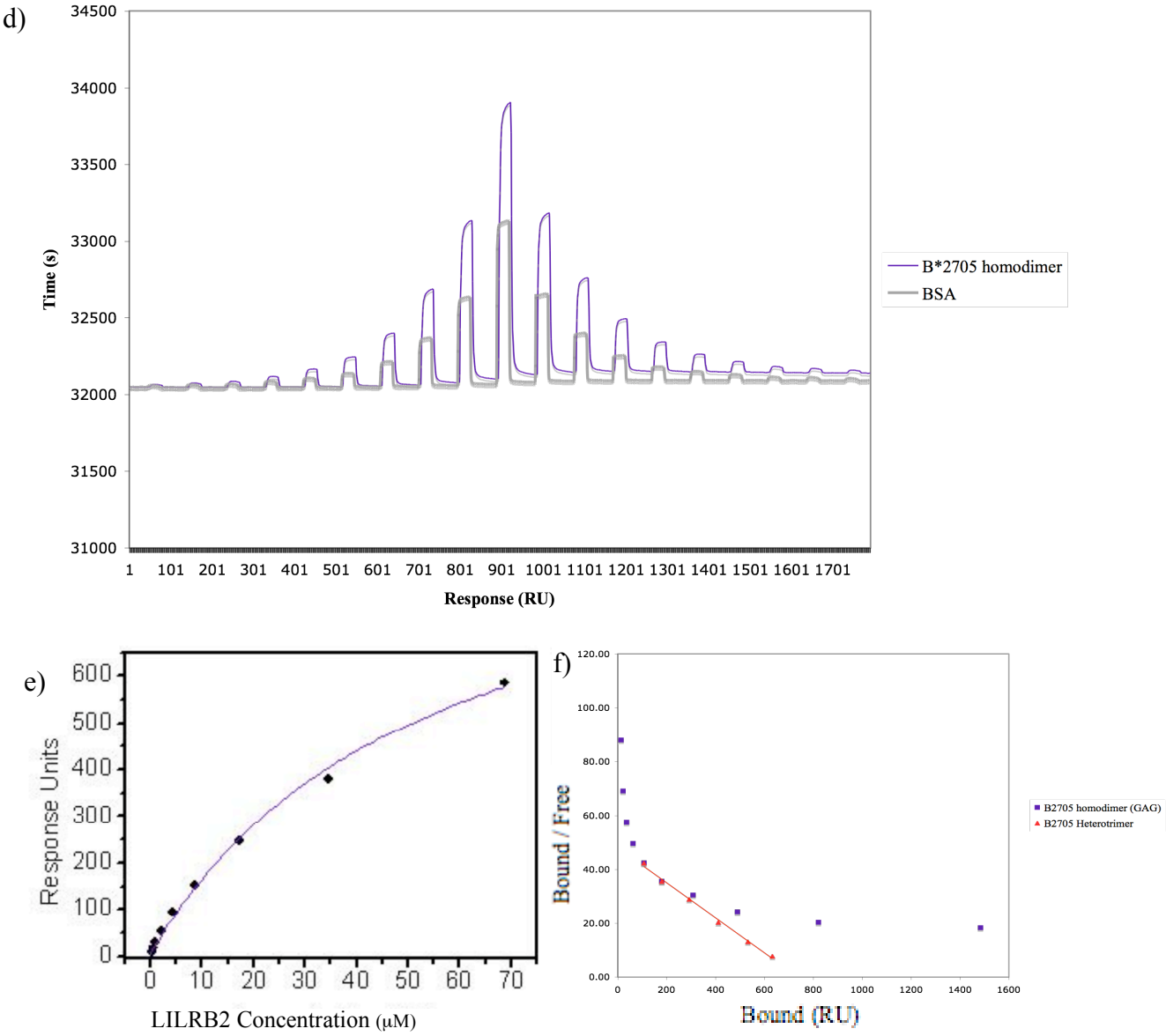


Figure 3.5 Characterisation of LILRB2 binding to B*2705 heterotrimer and homodimer by SPR. *Figures a and d are sensograms for binding of LILRB2 to B*2705 heterotrimer (pink) and B*2705 homodimer (purple) respectively. b and e are non-linear fits of the Langmuir binding isotherm for LILRB2 binding, c and f are Scatchard plots for LILRB2 binding to B*2705 heterotrimer and f shows that the Scatchard plot was curved for B*2705 homodimer binding (purple) compared to a straight line for B*2705 heterotrimer binding (pink). The curved Scatchard shows that no reliable binding data can be attained for LILRB2 binding to B*2705 homodimer by equilibrium binding analysis.*

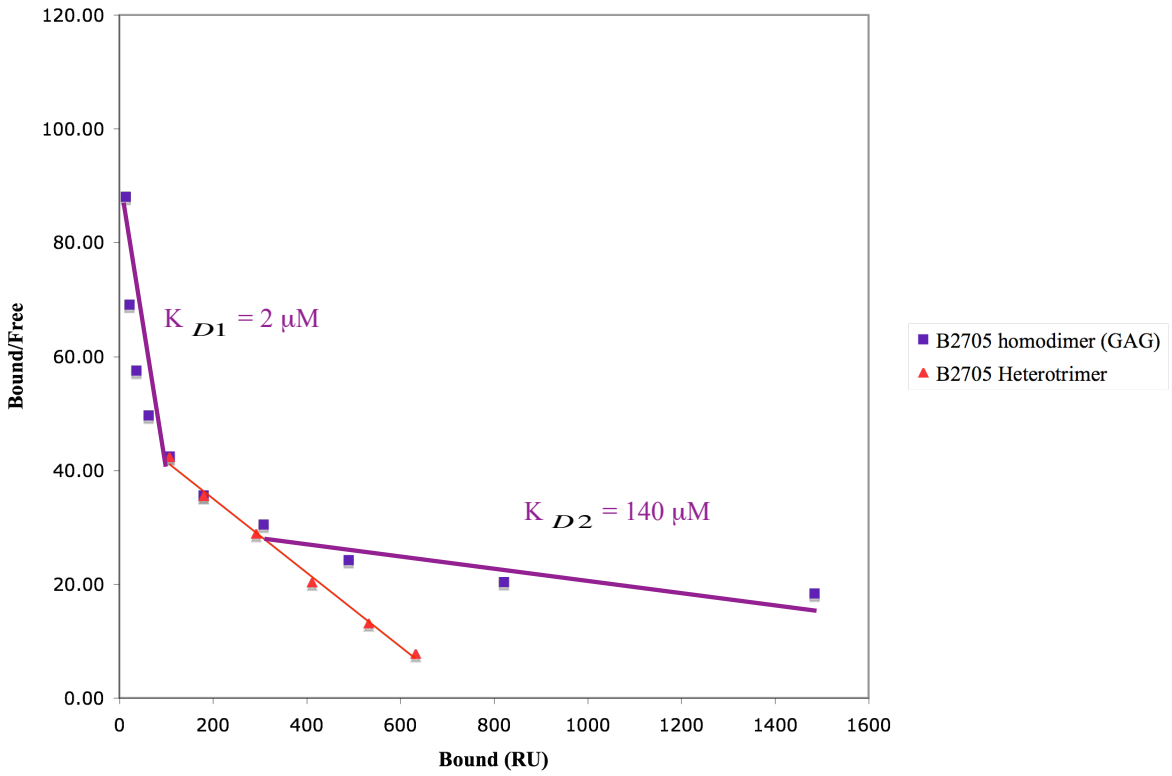


Figure 3.6 B*2705 homodimers do not demonstrate linear 1:1 binding to LILRB2. *B*2705 homodimers demonstrate bi-phasic binding to LILRB2 as indicated by the curved Scatchard plot of the data. This curve could represent two separate binding events occurring on the dimer, since each dimer has two binding sites for the LILR molecule. As such, this curve could be split into two separate Scatchard lines, where two binding events may be occurring. At lower concentrations, the initial binding interaction is observed giving a low* K_D *value (high affinity). At higher concentrations the second binding event (possibly due to aggregation at the sensor surface) is also occurring, reflecting a second higher* K_D *(low affinity).*

*Kinetic analysis of LILRB2 binding to B*2705 homodimers*

LILRB2 was observed to bind to B*2705 homodimers using equilibrium analysis by SPR. However, in order to attain reliable K_D values for the B*2705 homodimer interaction with LILRB2, I developed a kinetic analysis approach using the Biacore 3000, incorporating a B*2705 homodimer regeneration step between each injection of LILRB2 analyte (pH of regeneration selected as shown in fig. 3.7). From these kinetic data (fig. 3.8) it can be seen that B*2705 homodimer binds to LILRB2 with an affinity of 2.5 μM, with a chi^2 value of 30, suggesting high confidence for the fitting analysis.

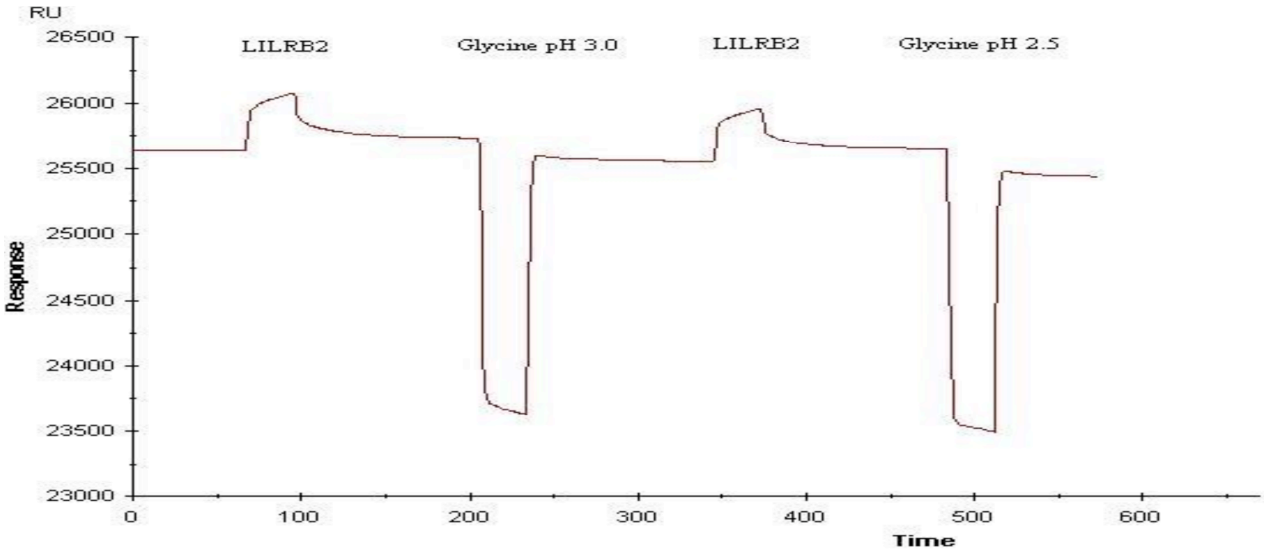
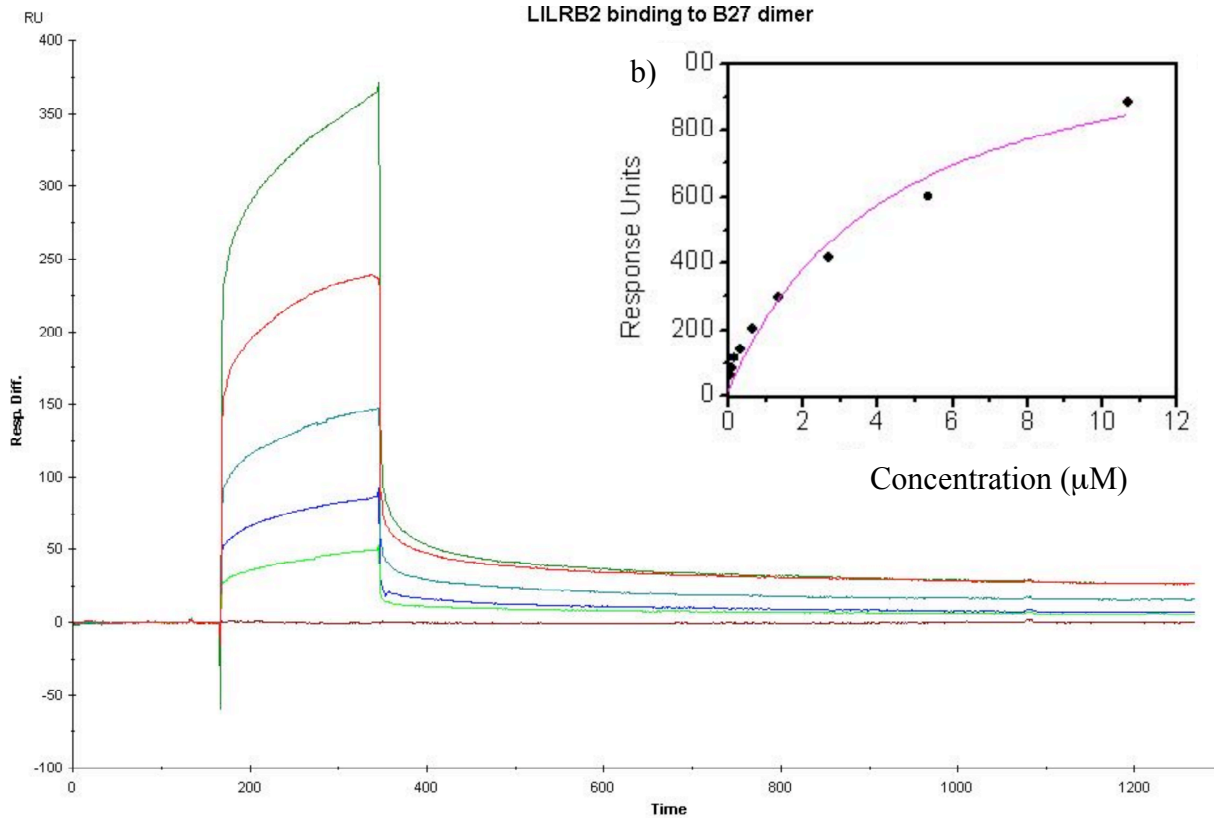


Figure 3.7 Selection of pH 3.0 glycine buffer as a suitable pH for removing excess LILRB2 from the immobilised B*2705 homodimer. *Glycine-HCl pH 3.0 removed excess LILRB2 from the B*2705 homodimer complex without disturbing the baseline response for B*2705 homodimer immobilised on the chip. Maintaining the baseline response suggests that the conformation and concentration of B*2705 immobilised onto the chip was not compromised by the regeneration step.*

*Kinetic analysis of LILRB2 binding to B*2705 homodimer*

a)



c)

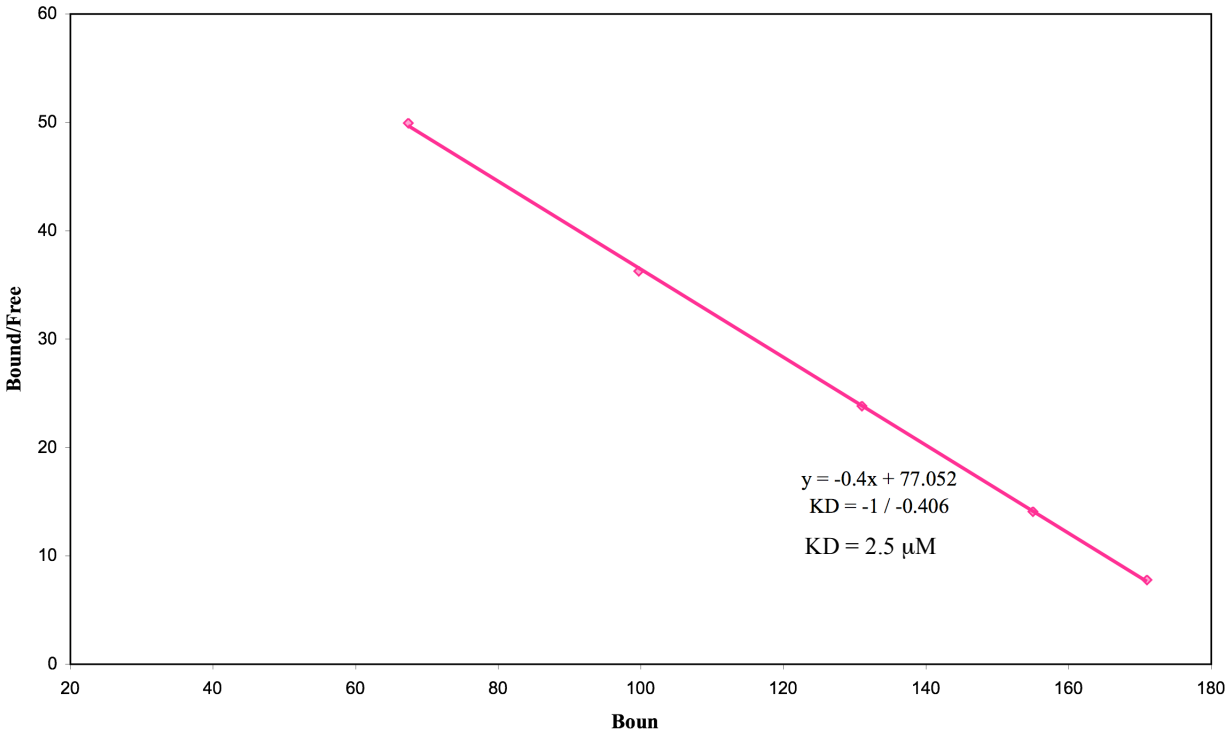


Figure 3.8 Kinetic analysis of B*2705 homodimer binding to LILRB2 *a) Increasing concentrations of 0μM, 0.56μM, 1.13μM, 2.25μM, 5.5μM, 11μM and 22μM LILRB2, were injected over immobilised B*2705 homodimer and the response at each concentration was measured. b) The* K_D *value was calculated using the Langmuir fit on the Biaevaluate software as well as being plotted and analysed using Origin 7.5 to give a* K_D *of 2.5μM. c) Scatchard analysis of this data gives a* K_D *value of 2.5μM.*

3.3 LILRB2 can bind to B*2705 free heavy chains

In order to assess whether B*2705 free heavy chains could interact with LILRB1 or LILRB2, B*2705 heterotrimers were immobilised onto a streptavidin-coated chip, and the β_2m and peptide were washed off using a low pH glycine wash. Glycine buffer at a pH of 2.5 was selected as it had previously been observed that pH 2.5 did not alter the binding of B*2705 homodimers (data not shown). To confirm the absence of β_2m on the chip, anti-β_2m antibody (BBM1) was injected over the flow cell to ensure there was no binding. Binding of BBM1 to recombinant B*2705 containing β_2m was tested previously using SPR (data not shown). LILRB1 and LILRB2 were injected before and after β_2m removal and the binding response before and after glycine buffer treatment was compared (Fig. 3.9). LILRB2 bound similarly to the B*2705 free heavy chains and to the B*2705 dimer, but LILRB1 binding was diminished. The SPR Kinetic analysis program was then used to calculate the affinity of the B*2705 heavy chain interaction with LILRB2. Figure 3.10 shows that a K_D value of 2.6μM was obtained from this kinetic analysis experiments. A chi^2 value of 11 was obtained in this experiment, showing high confidence for the K_D value obtained.

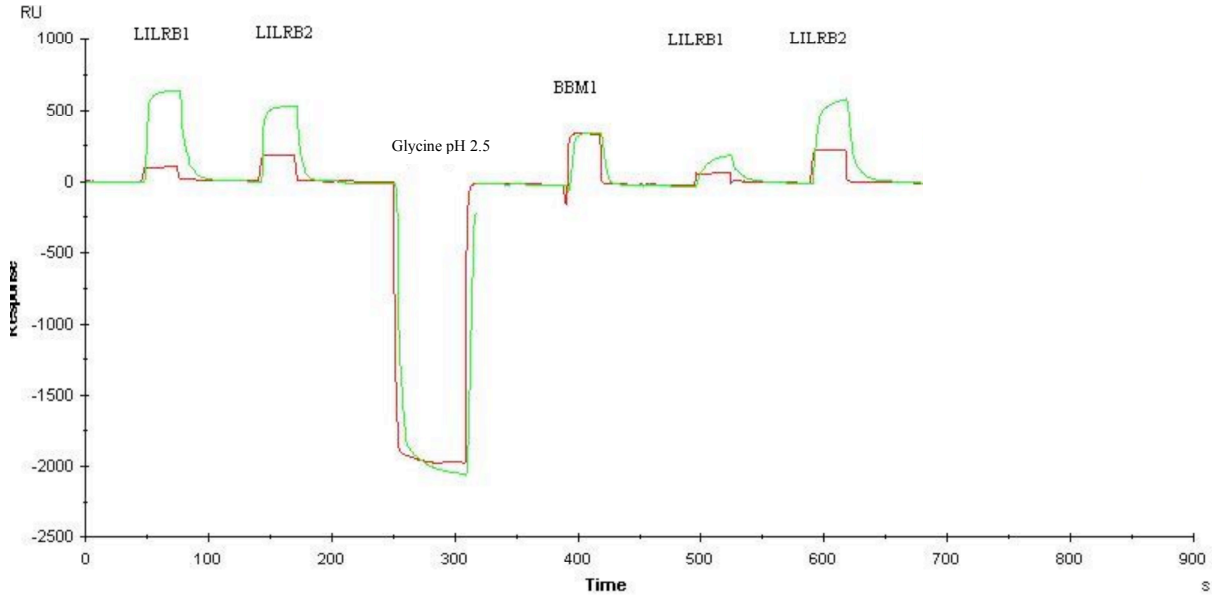
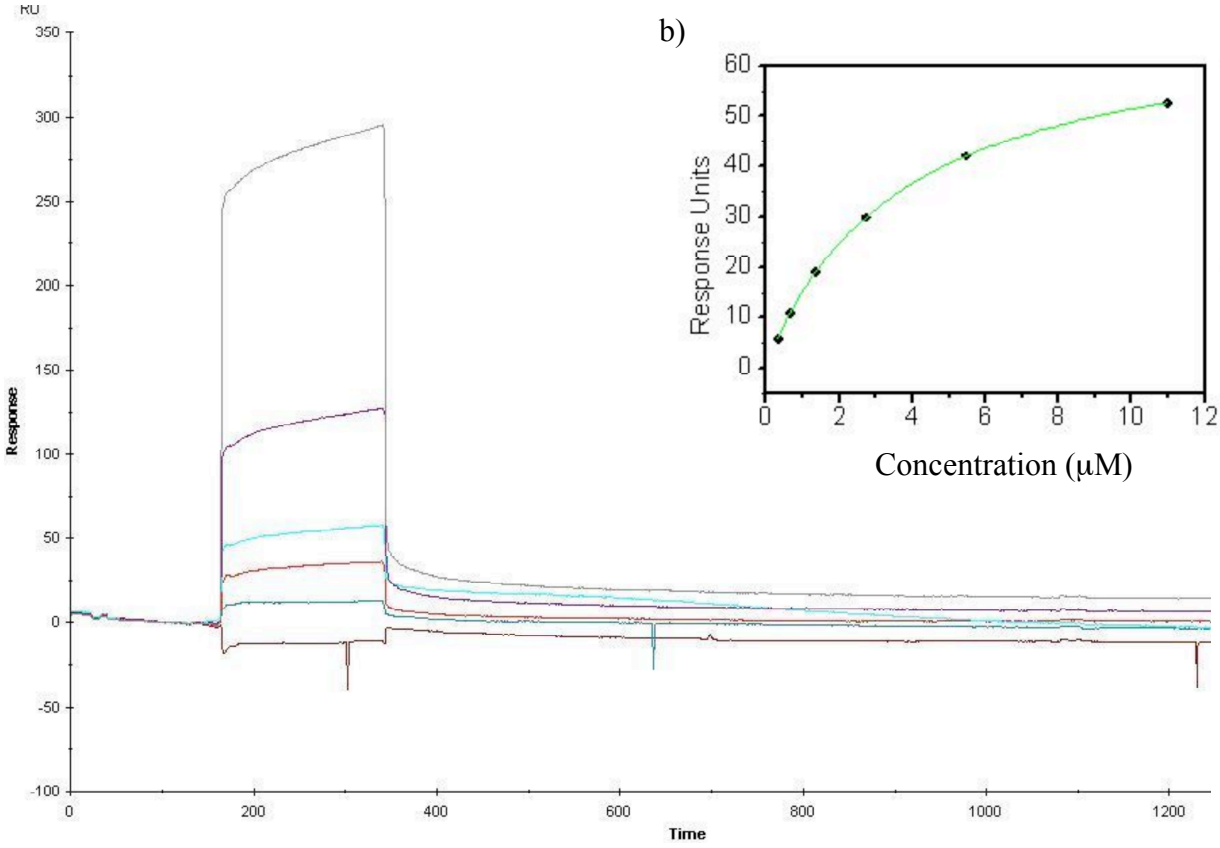


Figure 3.9 B*2705 free heavy chains are able to bind LILRB2 by SPR. *The green SPR trace shows the change in LILR binding to B*2705 heterotrimer (green) compared to the empty flow cell (red). The first two peaks correspond to injections of, and binding of LILRB1 and LILRB2. Subsequently a pH 2.5 glycine wash was injected (trough 3). This wash caused the β_2m and peptide to be removed. This was subsequently confirmed by an inability of anti-β_2m antibody (BBM1) to bind in the fourth injection (peak 4). LILRB1 and LILRB2 are then injected again. LILRB2 binding to the B*2705 is unchanged (peak 5), but LILRB1 binding is diminished.*

Kinetic analysis of B27 free heavy chains to LILRB2

a)



b)

c)

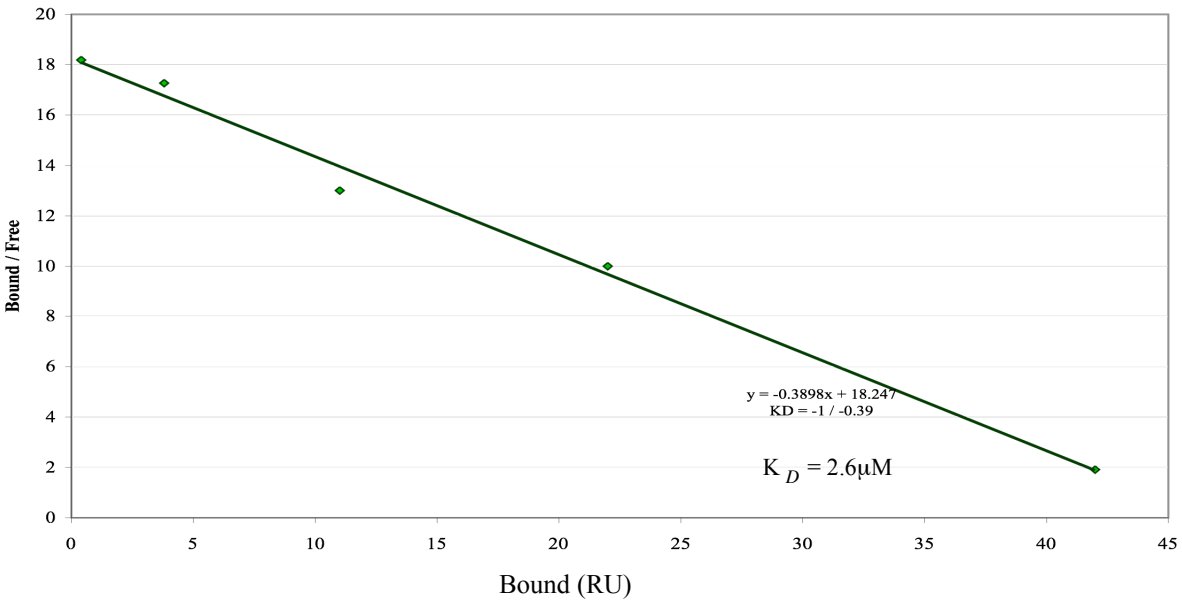


Figure 3.10 B*2705 free heavy chains bind to LILRB2 with an affinity of 2.6μM. *a) Increasing concentrations of 0μM, 0.28μM, 0.56μM, 1.13μM, 2.25μM, 5.5μM and 11μM soluble LILRB2, were injected over immobilised B*2705 free heavy chain and the response at each concentration was measured. The* K_D *value was calculated using the Langmuir fit on the Biaevaluate software as well as being plotted and analysed using Origin 7.5 (b). c) is a Scatchard Plot of the data, demonstrating that the* K_D *value is consistent over a range of analyte concentrations.*

3.4 LILRB1 and LILRB2 bind to B*2705 heterotrimers, complexed to GAG variant peptides, with comparable affinities

A common naturally occurring variant of the GAG peptide (GAG-M (KRWII**M**GLNK)), when complexed to B*2705 heterotrimer, has been reported to have different LILR binding properties from the more common GAG peptide (GAG-L (KRWII**L**GLNK) [109]. To test whether a single amino acid change in an MHC class I presented peptide could augment LILR binding, (B*2705) GAG-L and (B*2705) GAG-M complexes were refolded, biotinylated, purified and then fluorescently labelled and tetramerised. Tetramers were used to stain LILRB1-, LILRB2- and KIR3DL2- transfected cell lines. Figure 3.11 shows comparable staining of transfected-cells with B*2705 heterotrimers when complexed with either GAG-L or GAG-M. Binding of the B*2705 GAG variant heterotrimers was also studied by equilibrium binding using SPR. (B*2705) GAG-L, (B*2705) GAG-M were immobilised through the C terminal biotinylation tag onto a streptavidin chip and soluble LILRs at increasing then decreasing concentrations were flowed over. B*2705 homodimer was also immobilised as a negative control for LILRB1 binding. In these equilibrium experiments it was observed that (B*2705) GAG-L and (B*2705) GAG-M heterotrimers bound to both LILRB1 and LILRB2 with comparable affinity constants (fig. 3.12). Consistent results were obtained 5 times and representative data is presented.

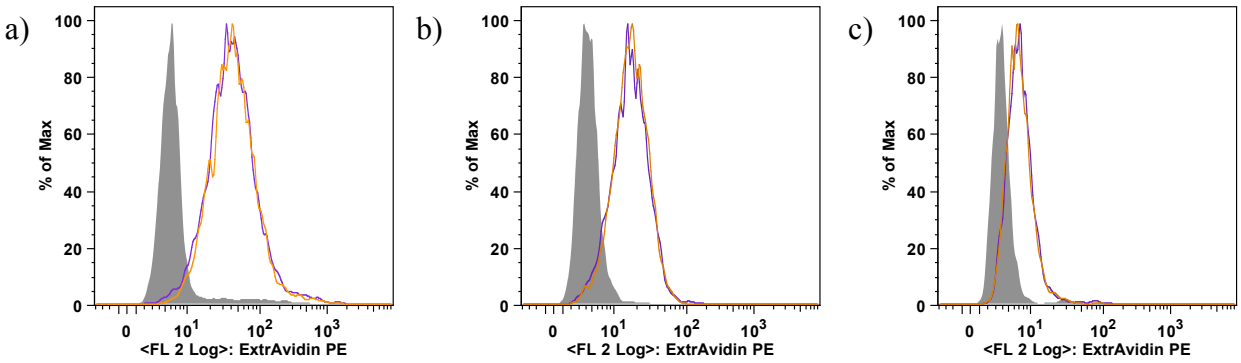
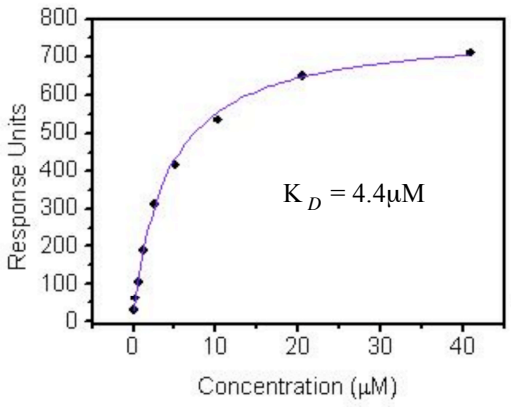
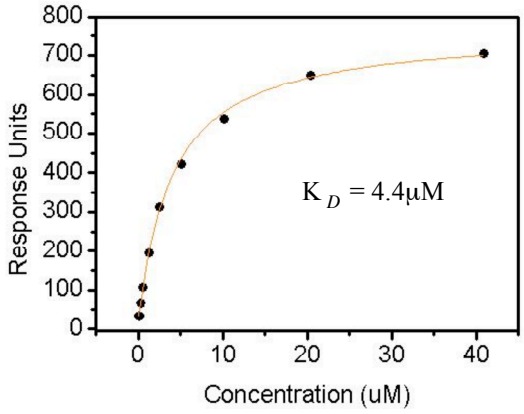


Figure 3.11 B*2705 GAG-L (purple) and B27 GAG-M (orange) tetramers demonstrate comparable staining pattern on a) LILRB1- b) LILRB2- and c) KIR3DL2- transfected cell lines by FACS analysis. *Grey plots show cells stained with extravidin PE only.*

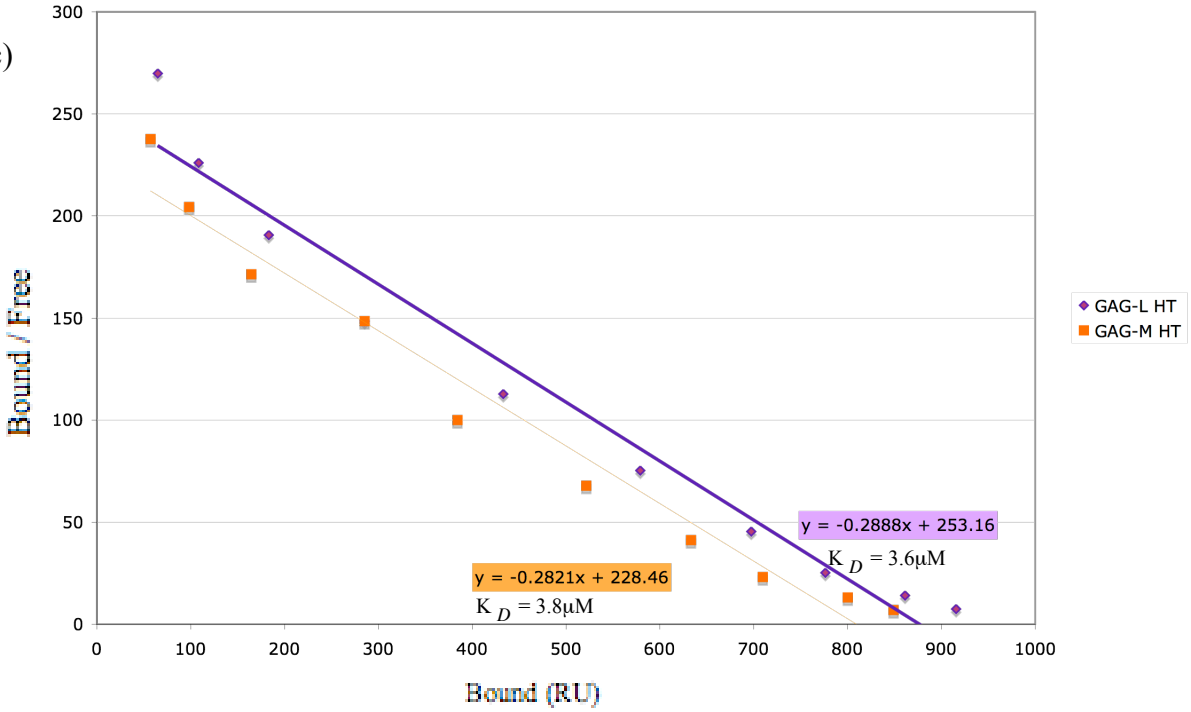
a)


LILRB1 binding to B27 heterotrimer GAG-L
Response Units
Concentration (μM)
K D = 4.4μM

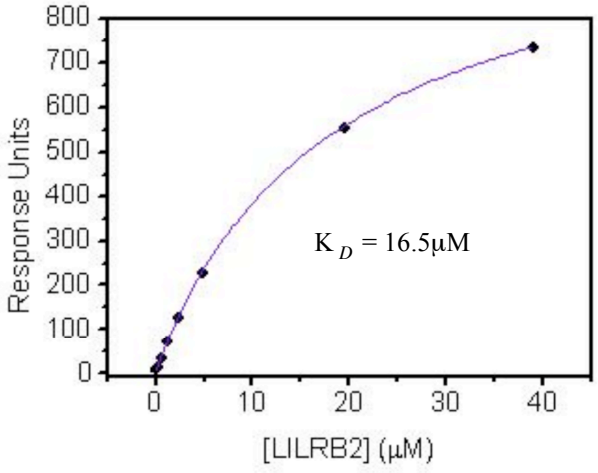
b)


LILRB1 binding to B27 heterotrimer GAG-M
Response Units
Concentration (uM)
K D = 4.4μM

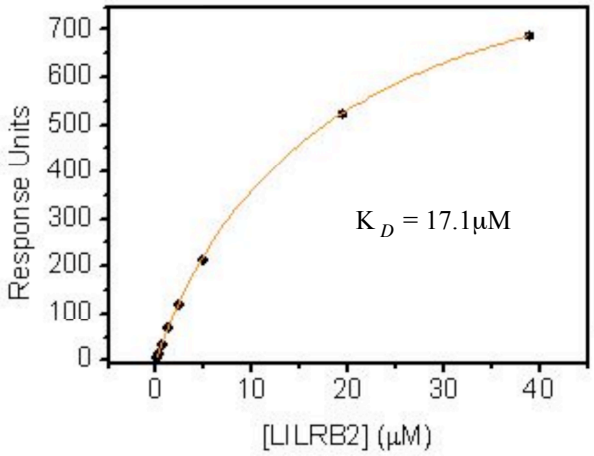
c)


Bound / Free
Bound (RU)
y = -0.2888x + 253.16
K D = 3.6μM
y = -0.2821x + 228.46
K D = 3.8μM
GAG-L HT
GAG-M HT

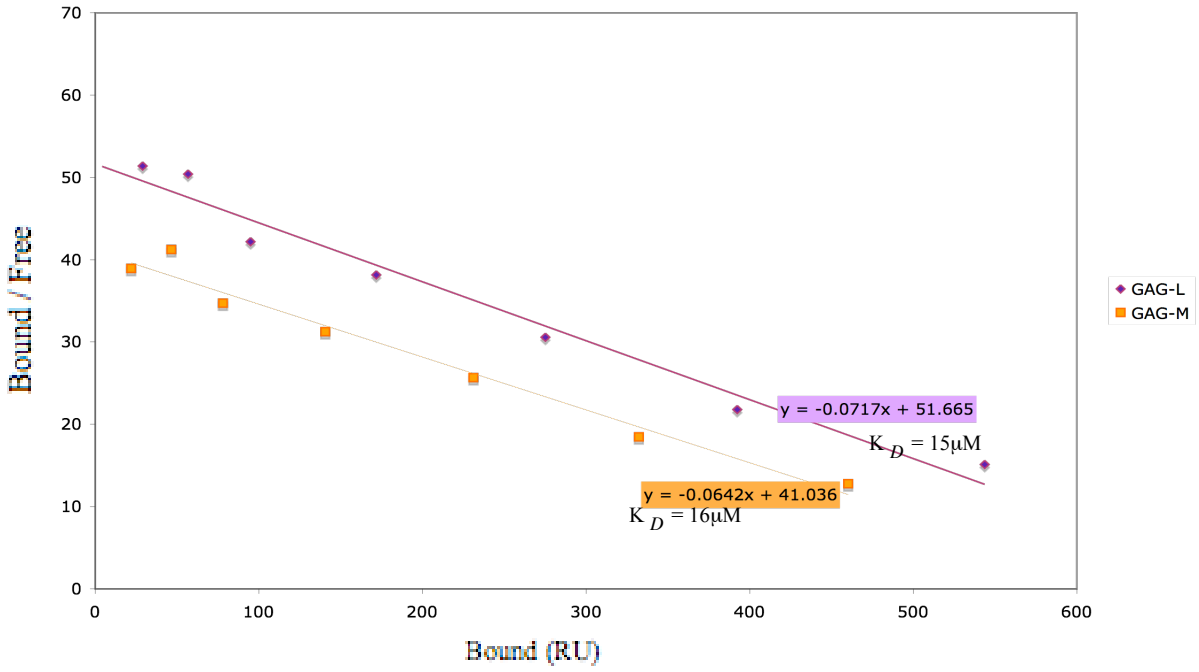
d) LILRB2 binding to B27 heterotrimers GAG-L



e) LILRB2 binding to B27 heterotrimers GAG-M



f)



K_D values obtained (μM)			
LILRB1 binding to:	K_D (μM)	LILRB2 binding to:	K_D (μM)
HLA-B*2705 heterotrimer (GAG-L)	3.90 ± 0.26	HLA-B*2705 heterotrimer (GAG-L)	15.0 ± 0.80
HLA-B*2705 heterotrimer (GAG-M)	3.93 ± 0.16	HLA-B*2705 heterotrimer (GAG-M)	16.0 ± 2.00

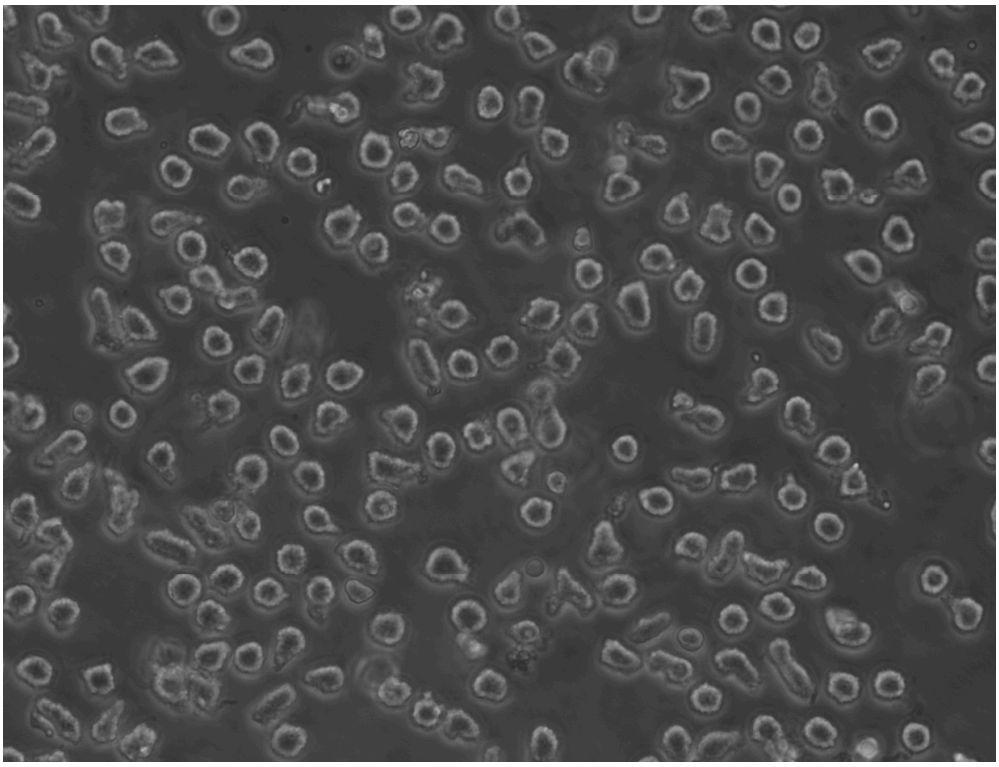
g) Table of K_D values for LILRB1 and LILRB2 binding to B*2705 HT complexes. *K_D values were obtained using Origin 7.5.*

Figure 3.12 SPR equilibrium binding results showing interactions of LILRB1 and LILRB2 with (GAG-L) and (GAG-M). *a and b are non-linear fits of the Langmuir binding isotherm for LILRB1 binding B*2705 GAG-L and B*2705 GAG-M respectively. c is a Scatchard plot for LILRB1 binding to B27 GAG-L and B27 GAG-M. d and e are equilibrium curves for LILRB2 binding B*2705 GAG-L and B*2705 GAG-M respectively. f is a Scatchard plot for LILRB2 binding. Table g shows the K_D values obtained by Origin 7.5 program in this experiment. Values obtained from Scatchard analysis were comparable.*

3.5 Effect of B27 homodimers on myelomonocytic cells

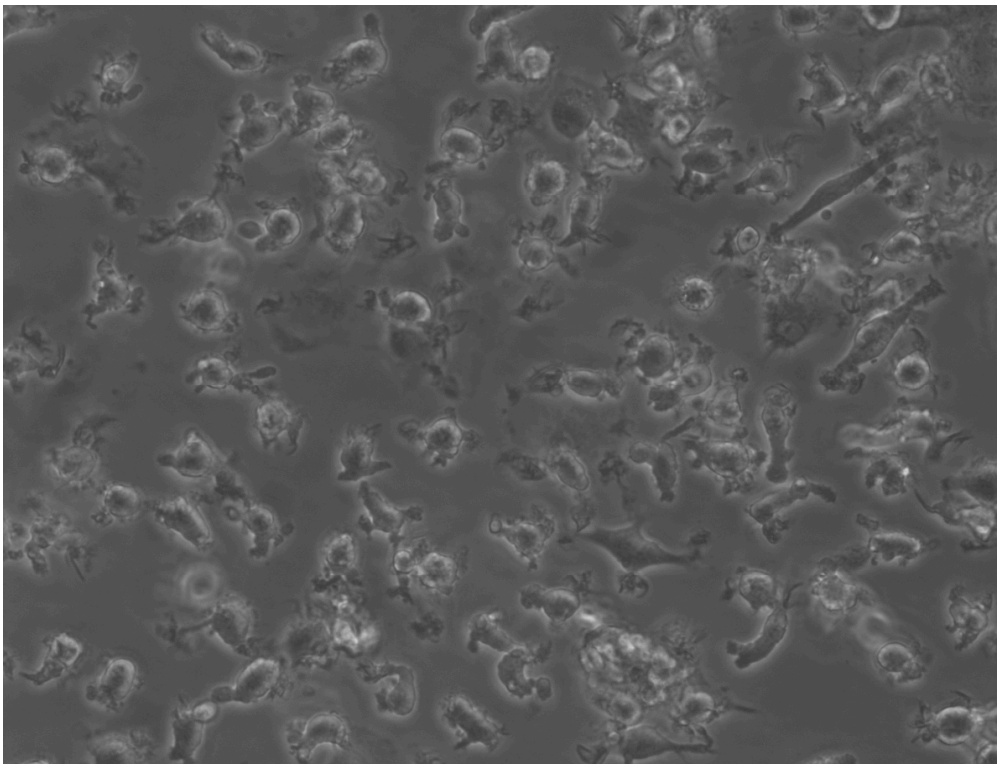
Having demonstrated differential interactions between B27 homodimers and B27 heterotrimers with LILRB2 using SPR, I then investigated how these molecular interactions translated into differences in functional effects on cells expressing LILRB2 [110]. LILRB2 is predominantly expressed on myelomonocytic cells, such as dendritic cells (DCs). Here I investigate the effect of B27 homodimer interactions on DC maturation. CD14 positive PBMCs were isolated, and then cultured in the presence or absence of sterile B27 homodimer, B27 heterotrimer or HLA-B8 heterotrimer. Maturation was stimulated after 4 hours using a cytokine cocktail as described in section 2.7. The appearance of the cells was monitored and the expression of DC phenotype markers was analysed after 20 hours by Flow Cytometry. The photographs showing DC maturation illustrate that the cells cultured in the presence of B27 homodimer (with, and without the maturation signals from the cytokine cocktail) had a tendency to form cell clumps. Such DC clumps are often found to be a sign of enhanced cell activation. This was not observed for the cells cultured in the absence of B27 (fig. 3.13). The size of the cells and the frequency of cell doublets was analysed by Flow Cytometry, and agreed with the photographic observations of more cell clumping in the presence of B27 homodimer (see appendix, section 8.3). The expression of cell surface markers was not significantly different between conditions (fig. 3.14). These observations were consistent in 4 separate experiments.

a)



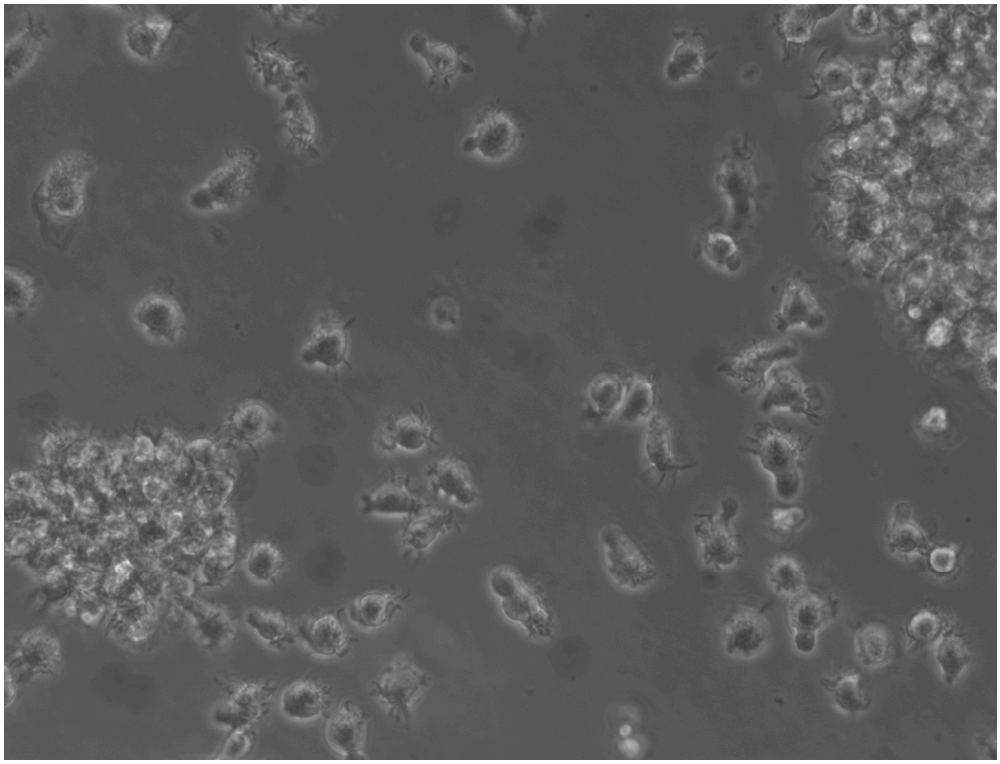
Immature cells t = 0 h

b)



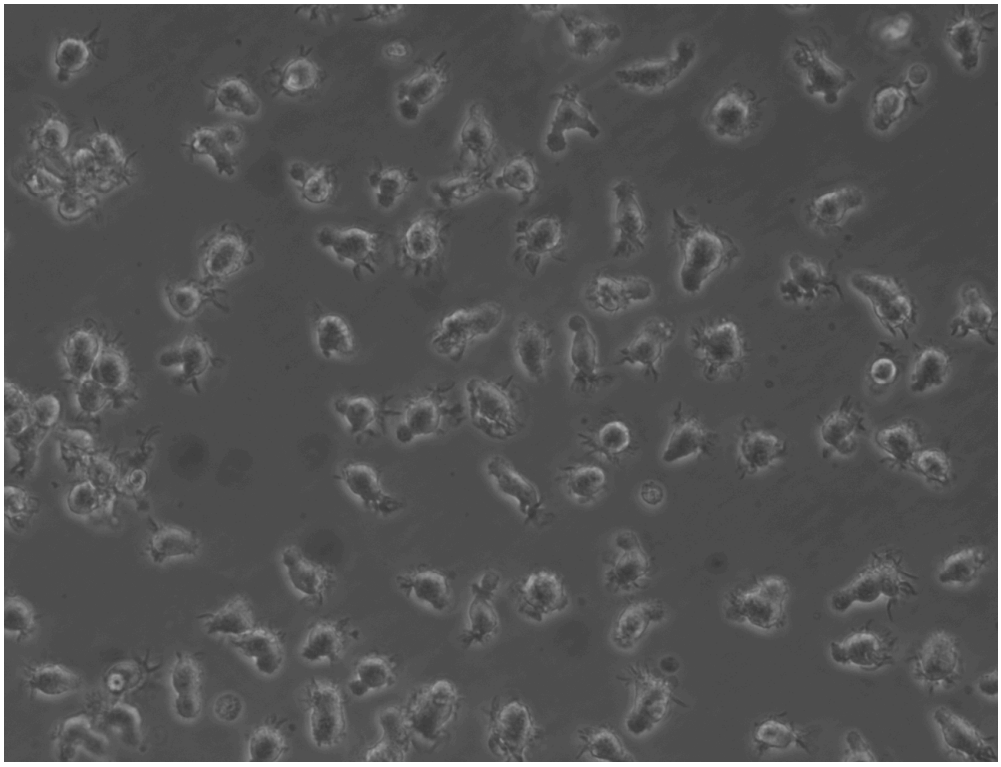
Unstimulated cells t =20 h

c)



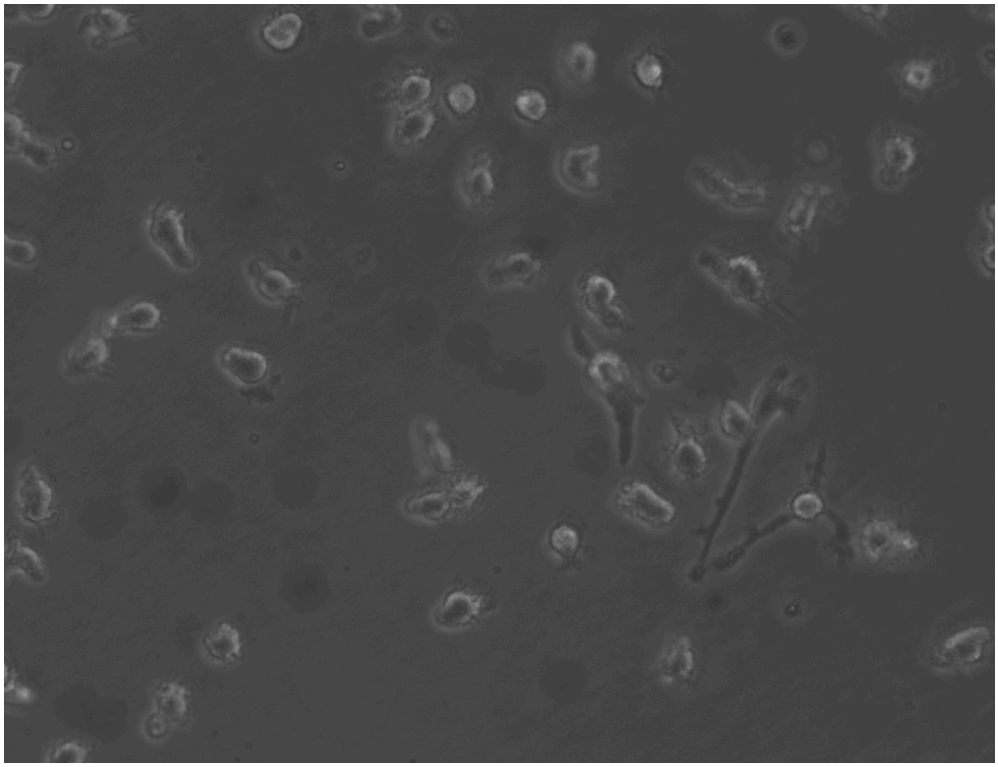
B27 homodimer and Cvtokines t = 20h

d)



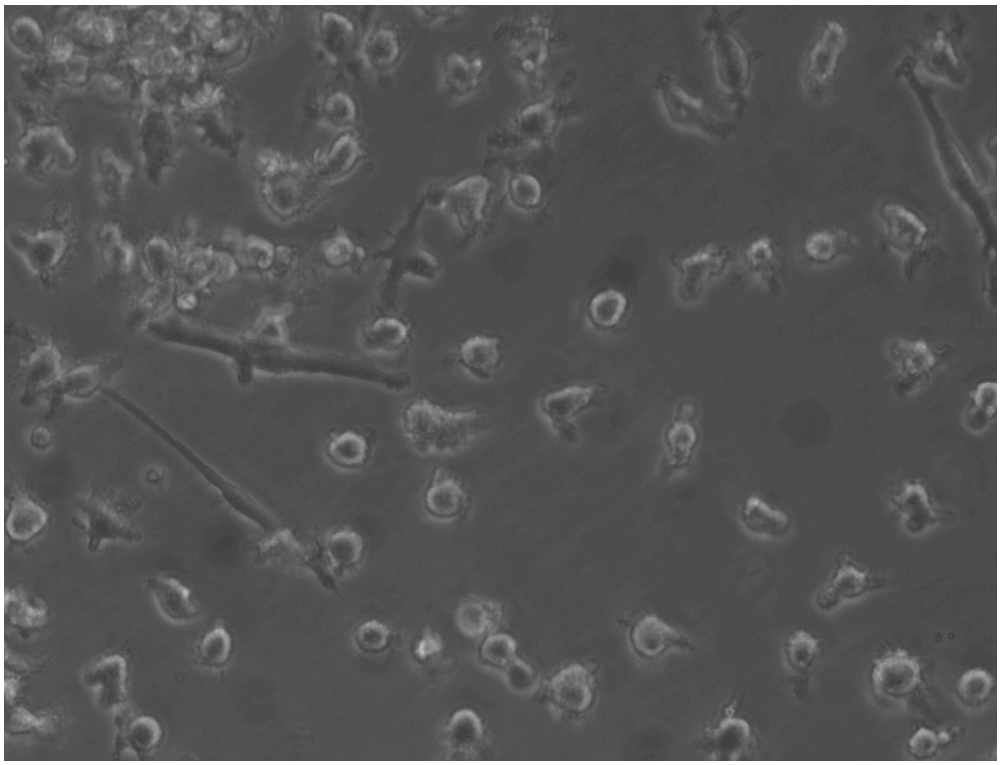
B27 heterotrimer and Cvtokines t = 20 h

e)



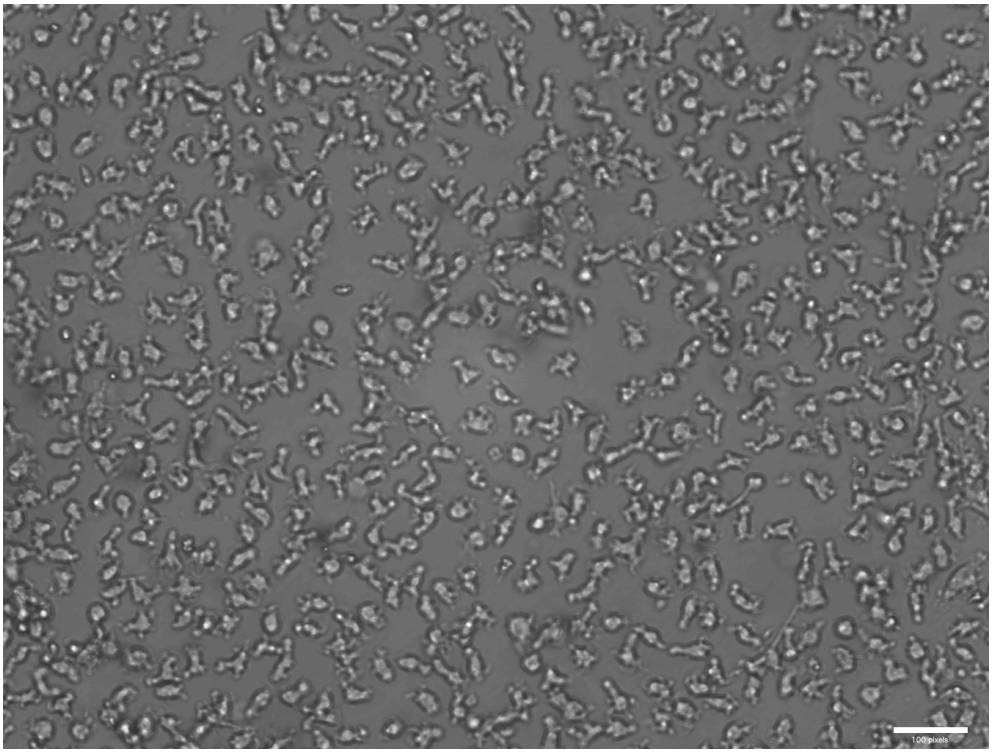
Cvtokines onlv t =20 h

f)



B27 homodimer alone t = 20 h

g)



HLA-B8 alone t = 20 hour

Figure 3.13 Dendritic cell clumping in the presence of B27 homodimer. *a) Immature DCs at 0hrs, before activation. b) Unstimulated cells cultured for 20 hours c) DCs stimulated with B27 homodimer tetramer and cytokines result in pronounced cell clumping d) DCs stimulated with B27 HT tetramer and cytokines e) DCs cultured with cytokine cocktail only f) DCs stimulated with B27 homodimer only g) DCs cultured with HLA-B8 tetramer only.*

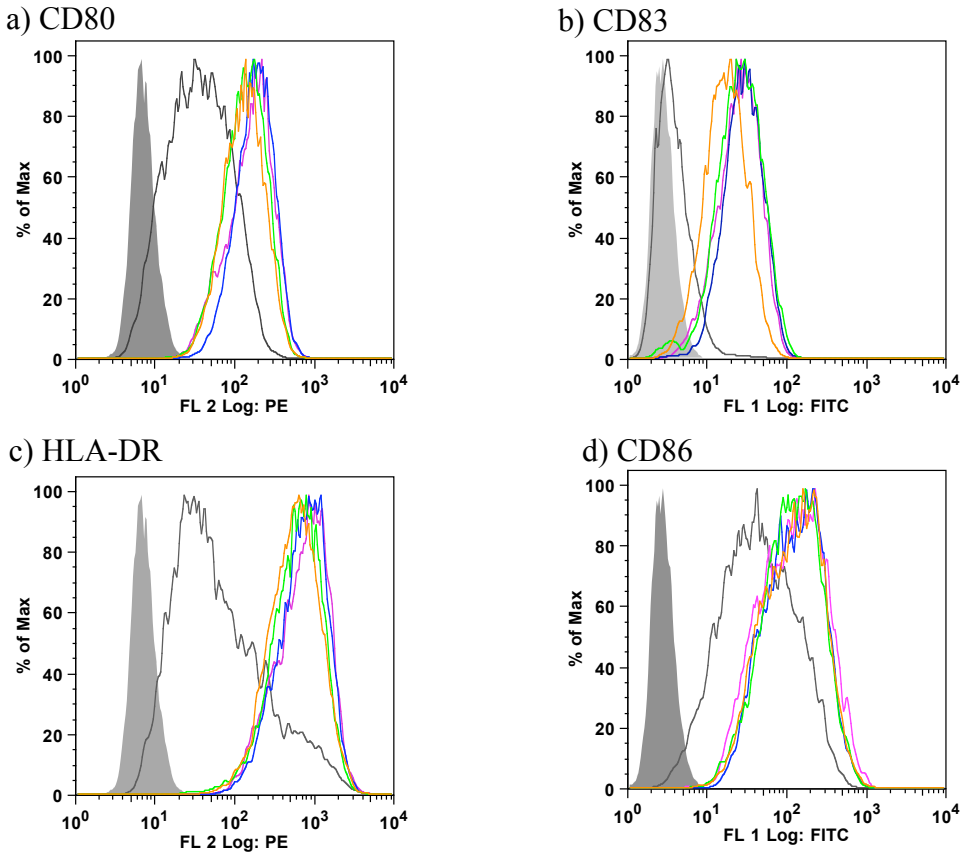


Figure 3.14 Flow Cytometry shows there is comparable expression of DC maturation markers under each condition. *a) CD80, b) CD83, c) HLA-DR and d) CD86 on cells stimulated with cytokine only (green), B27 dimer and cytokine (pink), B27 heterotrimer and cytokine (blue) and B27 dimer only (orange) compared to unstimulated cells (grey). Shaded cells are stained with Extravidin PE only.*

3.6 CD8αα binding to B27

HLA-B27 and HLA-G are both HLA class 1 molecules that display unusual folding properties (see section 1.2). Previous reports studying HLA-G interactions with the LILRs have shown that LILRB1 and LILRB2 are able to effectively compete with CD8 alpha homodimers (CD8αα) for MHC class I binding [111]. In this section I investigate the binding of B27 homodimers and heterotrimers with CD8αα using SPR to assess whether B27 homodimers display similar binding properties to that of the HLA-G homodimers. Soluble CD8α ectodomains were expressed in inclusion bodies and then refolded and purified by size exclusion chromatography (fig. 3.15). The purity and the size of the CD8αα was confirmed by SDS-PAGE and Mass Spectroscopy (fig. 3.15). The monomer was observed to have a molecular weight of 13.4kDa. CD8αα was then used in equilibrium based SPR experiments to assess the binding affinities to B*2705 homodimers and B*2705 heterotrimers (fig. 3.16). Finally, to test whether LILRB2 is able to compete with CD8αα for B27 homodimer binding, FACS competition experiments were performed by pre-incubating CD8αα with B27-homodimer tetramer before assessing its binding to LILRB2- expressing Baf cells.

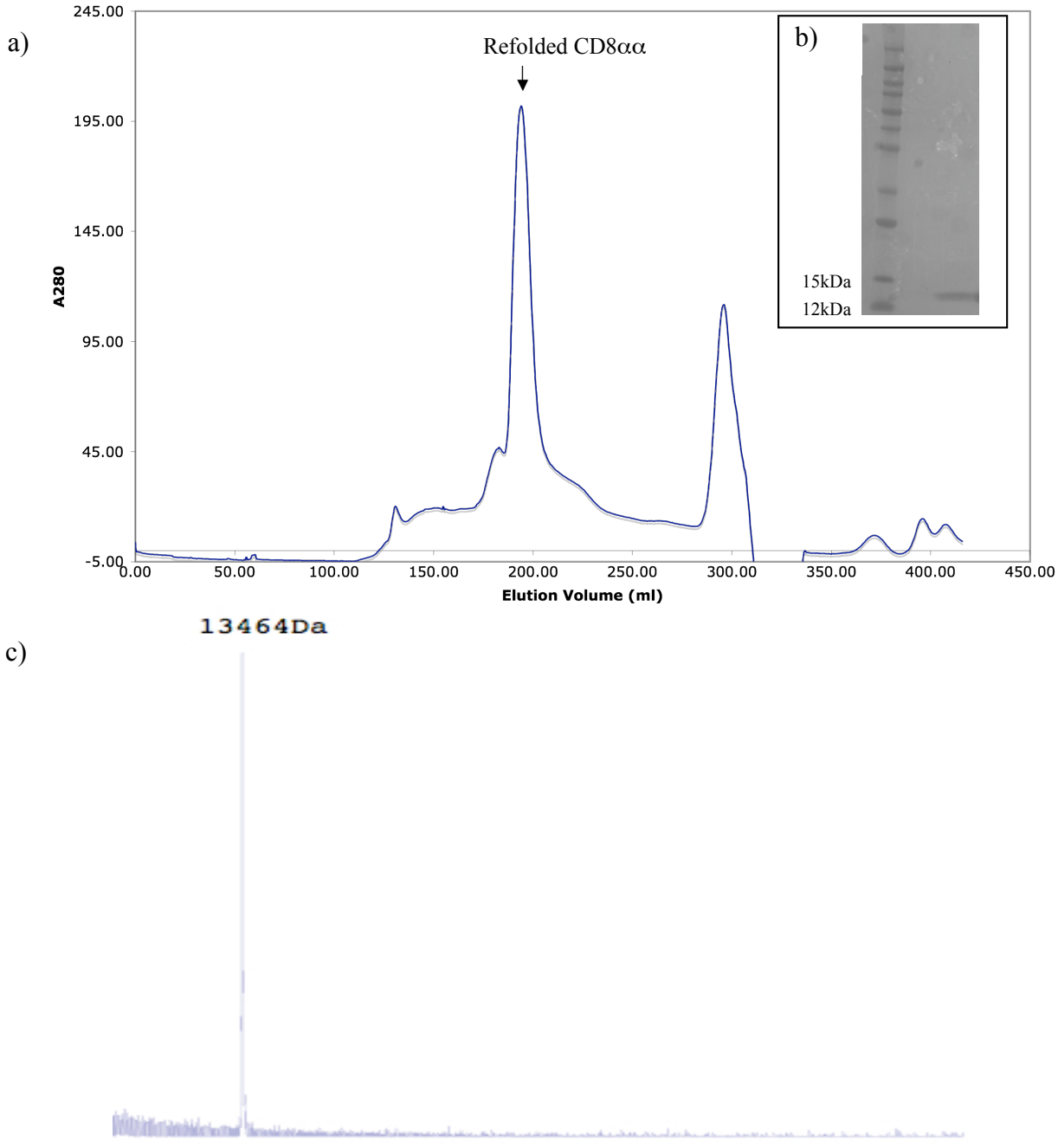
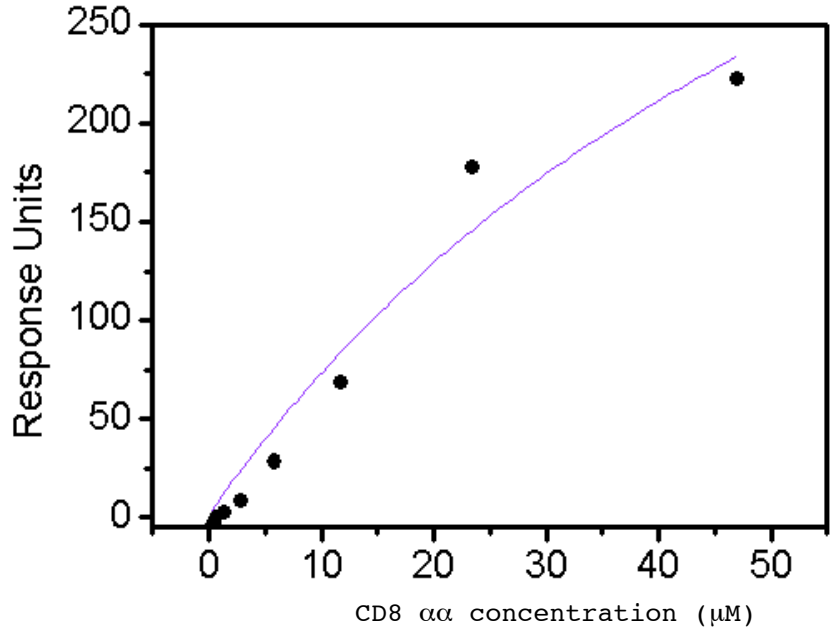


Figure 3.15 Expression and purification of CD8αα *a) FPLC elution profile of CD8αα and b) shows the SDS-PAGE gel of the sample peak. Figure c) Mass spectroscopy analysis of CD8αα sample showing a single peak corresponding to monomer of CD8α.*

CD8αα binding to B27 homodimer and heterotrimer

Biotinylated B*2705 heterotrimer and B*2705 homodimer complexes (both refolded with a GAG peptide KRWIILGLNK) were immobilised in separate flow cells of a streptavidin-coated gold chip. CD8αα was flowed over the chip at increasing concentrations. The CD8αα homodimer tended to stick to the streptavidin chip, and so, once the highest concentration was flowed over, it was unreliable to then again flow more protein over at decreasing concentrations. Figure 3.16 shows that B*2705 heterotrimers and homodimers demonstrate different binding specificities to CD8αα, with B*2705 homodimer binding with almost a 2 fold higher affinity (72μM) than the B*2705 heterotrimer (130μM). Consistent results were obtained in two separate experiments. K_D values are in agreement with those previously reported for the CD8αα : HLA-G heterotrimer interaction [111]. K_D values were obtained using equilibrium fitting using Origin 7.5. The kinetic approach was attempted for this interaction but the results were not interpretable, possibly due to the "sticky" nature of the CD8αα complex.

a)



b)

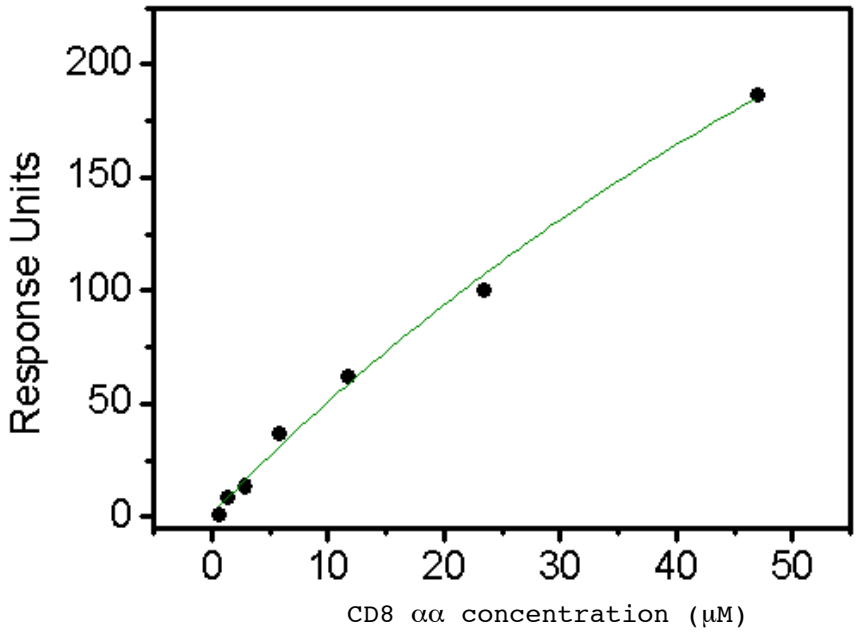


Figure 3.16 B*2705 homodimer (pink) binds to CD8αα with a 2 fold higher affinity than B*2705 heterotrimer (green). *Figure a is a hyperbolic binding fit for B*2705 homodimer binding to CD8αα, the* K_D *obtained in this experiment was 72μM. Figure b is a hyperbolic binding fit of B*2705 heterotrimer binding to CD8αα, the* K_D *obtained in this experiment was 131μM.*

*CD8αα does not compete with LILRB2 for binding to B*2705 homodimer*

The biophysical measurements in this chapter suggest that B*2705 homodimers bind to LILRB2 with a much higher affinity (2.5μM) than CD8αα (72μM). I therefore tested whether CD8αα could compete for binding of B*2705 homodimer tetramers to LILRB2-expressing cells. Figure 3.17 shows that increasing concentrations of CD8αα did not block homodimer binding to LILRB2-expressing Baf cells, supporting the previous data showing that LILRB2 binds to B*2705 homodimers with a higher affinity than CD8αα. Conversely, CD8αα was able to weakly compete with LILRB2 for B27 HT binding where some blocking of the B27 HT and LILRB2 interaction was observed at higher concentrations of CD8αα. This experiment was repeated twice with consistent results.

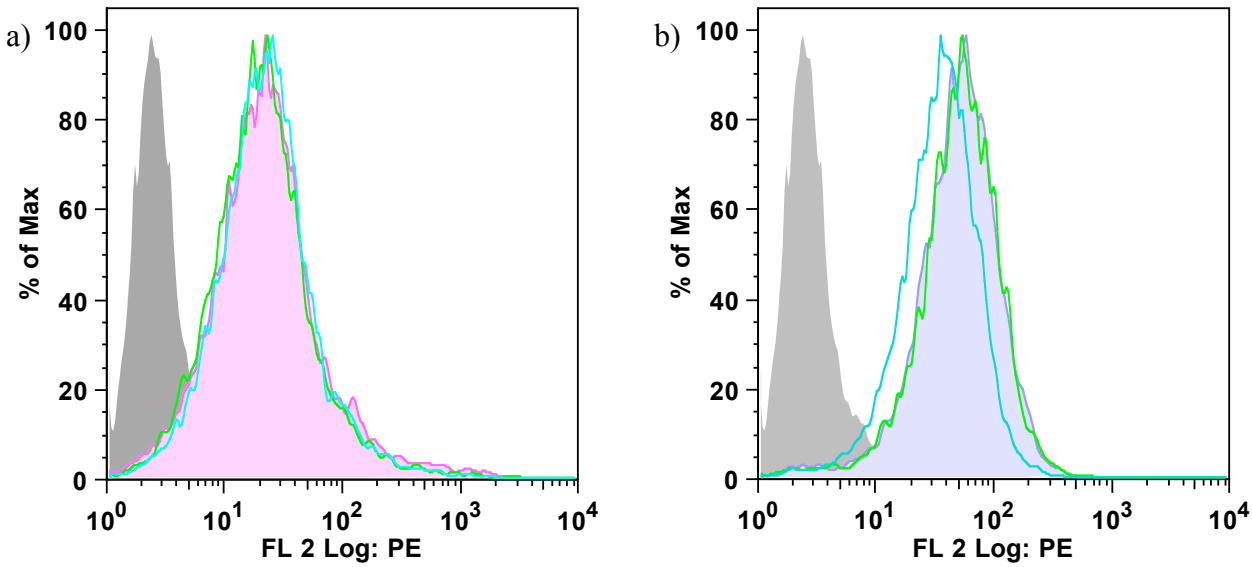


Figure 3.17 LILRB2 binds to B*2705 homodimer tetramers with a higher avidity than CD8αα. a) *FACS analysis shows that a 30 minute pre-incubation of B27 tetramers with (increasing concentrations of) CD8αα does not decrease B*2705 homodimer staining for LILRB2-expressing cells. Extravidin PE only staining is shown in shaded grey, B*2705 homodimer staining is shown in shaded pink, B*2705 homodimer tetramer plus 2μg CD8αα (in 200μl) is shown in green, B*2705 homodimer tetramer plus 10μg of CD8αα is shown in cyan. b) FACS analysis shows that increasing CD8αα concentration can diminish B*2705 HT staining of LILRB2-expressing cells. Extravidin PE only staining is shown in shaded grey, B*2705 heterotrimer staining is shown in shaded blue, B*2705 HT tetramer plus 2μg CD8αα is shown in green, B*2705 HT tetramer plus 10μg CD8αα is shown in cyan.*

3.7 Discussion

The key findings of this chapter are that B*2705 homodimers and heterotrimers differ in their binding specificity and affinity for LILRB1 and LILRB2 receptors. This supports our previous observations and hypothesis that augmented B27 interactions with the innate immune receptors could play a role in inflammatory disease [58]. In addition, I have shown that B*2705 free heavy chains also interact with the LILRB2 receptor, which may also have a functional outcome *in vivo*. Furthermore I have shown that the LILRB2 interaction with B*2705 heterotrimers, complexed to GAG peptide, is independent of a naturally occurring "escape mutation", which has previously been suggested to increase the avidity of binding to LILRB2 and thus inhibit DC maturation [110]. I have also undertaken some preliminary experiments showing that B27 homodimers may stimulate DC function. Finally, I have investigated the interaction of B*2705 homodimers and heterotrimers with CD8αα and shown that LILRB2 binding to B*2705 homodimers is of higher affinity than CD8αα binding to B*2705 homodimers.

The findings described in this chapter demonstrate that LILRB2 binds to B*2705 homodimers with an eight fold higher affinity than B*2705 heterotrimers. The affinity measurements calculated for the LILRB1 and LILRB2 binding to B27 heterotrimer are consistent with previously reported K_D values for the binding of LILRs to HLA-G [74]. Using SPR, Shiroishi reports K_D values of 3.5μM and 15μM for LILRB1 and LILRB2 binding to HLA-G respectively. In addition, K_D values calculated using Origin 7.5 program were consistent with K_D values obtained by Scatchard analysis, demonstrating reliability of the data (fig. 3.5 and 3.6). Reliable K_D values for B*2705 homodimer binding to LILRB2 could not be obtained in

equilibrium binding experiments since the B*2705 homodimer did not obey classical Michaelis Menten linear binding kinetics (fig. 3.5). The binding of B*2705 homodimer to LILRB2 was not observed to reach equilibrium over a wide range of concentrations. In these SPR equilibrium binding experiments, the protein concentration of the LILRB2 analyte used was increased to 85μM, but at concentrations above 100μM LILRB2 was observed to aggregate out of solution (not shown).

Equilibrium binding studies showed the B*2705 homodimer binding to LILRB2 to be bi-phasic (fig. 3.6). That might result from (i) a conformational change when LILRB2 binds, or (ii) its aggregation if "nucleated" by the B*2705 homodimer- which had been immobilised at relatively high concentrations for this equilibrium based SPR approach. In this situation, the curved Scatchard plot (fig. 3.6) could be divided into two straight lines – one straight line at low LILRB2 concentrations and one straight line at higher LILRB2 concentrations. At the low LILRB2 concentrations, the Scatcard yields a K_D value of 2μM, and at high concentrations the Scatchard plot correlates to a K_D of 140μM.

In these equilibrium experiments the high concentration of analyte (and high level of immobilised protein) may have been causing aggregation due to avidity affects and non-specific charge interactions. Therefore, a kinetic analysis approach was adopted in order to calculate the affinity of the B*2705 dimer to LILRB2 interaction. The K_D value of 2.5μM obtained using this method is consistent with the K_D obtained using low LILRB2 concentrations in the equilibrium based approach. The value is also supported by the findings in section 3.3, showing that B*2705 free heavy chains are also able to interact with the LILRB2 receptor, with a comparable affinity of 2.6μM. This result could reflect that the

B*2705 homodimer has two LILRB2 binding sites that interact with LILRB2, each with the same affinity of 2.5μM.

The kinetic method used to quantify the binding interaction between the B*2705 homodimer and LILRB2 could not be applied to the B27 heterotrimer and LILR interactions as an acid wash regeneration step would result in removal of the β_2m and peptide from the heterotrimeric complex (as used in the free heavy chain analysis).

SPR experiments were performed at both 25°C and 37°C with consistent results. The LILR molecules are known have flexible interdomain loops [66], so temperature has been suggested to influence the binding between LILRs and its ligands. However, in these SPR experiments, I used the two domain (D1D2) LILRB1 and LILRB2 proteins and this may explain why no difference in binding was observed at the two different temperatures.

As an extension to these SPR studies, it will be interesting to measure the binding between the LILRs and other classically folded (and β_2m free heavy chain) HLA-Bs, including HLA-B14 which also has a cysteine residue at position 67.

The values for the affinity of B27 homodimer interaction with LILRB2 are within the physiological range and suggest that binding of B*2705 homodimer to LILRB2 may have a functional consequence in *vivo.* LILRB2 is classically considered to be an inhibitory receptor of myelomonocytic cells, and here I have shown that the binding of LILRB2 to B*2705 dimer is of higher affinity than to B*2705 heterotrimer. This higher affinity interaction may lead to an augmented immune response. One explanation for how an inhibitory interaction could lead

to inflammation might be that this interaction may not be occurring between two different cells (in trans) but could instead be occurring on the surface of the myelomonocytic cells (in cis). This would mean that the B27 expressed on the surface of an APC (e.g a dendritic cell) would be "hidden" from the receptors of the NK cell as their LILR binding site would be masked by the LILRB2 cis interaction. Therefore reduced effective HLA class I surface expression might be recognised by an NK cell and an inflammatory response may ensue (fig. 3.18 b). Alternatively, it may be possible that LILRB2 is being secreted as a soluble molecule [63]. In this case perhaps an enhanced interaction of B27 with a secreted form of LILRB2 could mask detection of the B*2705 homodimer in order to perturb the immune cell balance (fig. 3.19 c). Another possible explanation for the role of LILRB2 in inflammatory disease may be that NK cell receptors are not simply "Activatory" or "Inhibitory" but may have an additional role in recruiting molecules other than phosphorylases. For example, binding by the B27 homodimer (with two LILRB2 binding sites) may cause cross-linking of two LILRB2 domains. It has been previously reported that the cross-linking of receptors may have a role in cell activation and this may also attribute to disease [50].

In each SPR experiment conducted here, I immobilised the biotinylated HLA complexes to the Biacore chip surface and then flowed over the LILR molecules as the analytes. The reason for this was that the purity of the recombinant LILRs was observed to be much higher and it is standard practice to use the purest protein as the analyte in order to minimise any non-specific binding.

Having characterised the affinities for the B27 and LILR(B1/B2) interactions, it will be important to show whether these binding events are being translated into signalling events in

the cell. An experiment that would expand our understanding of this would have been to use the cell-based NFAT-reporter assay developed by the Maenaka lab. This system uses a LILRB1/B2 construct with an intracellular PILRβ domain. The cells were also transfected with an NFAT GFP reporter. In this cell system cells could be stimulated with recombinant HLA proteins and the measurement of GFP fluorescence correlated with a direct measure of LILR stimulation. During my project I planned to use these cells to compare the signalling of the B27 homodimer and B27 heterotrimer, but unfortunately these cells were not available.

In the future it will be interesting to extend the investigations of the effect of B27 homodimers on DC function. I have shown that they caused clumping of DCs, but did not affect their maturation. Future work will focus on the analysis of cytokine profiles in order to further assess whether the cell clumping observed is a reflection of cell activation. It will also be important to repeat these experiments in the presence of an LPS inhibitor (such as polymixin A). In theory, the observed effect might reflect LPS contamination, as the B27 was expressed in bacteria; however the B27 and HLA-B8 used to prepare heterotrimers were also expressed in bacteria, and these did not induce clumping. This was observed in several experiments, suggesting that the clumping was not a result of LPS stimulation. Nevertheless it is an important control to include.

I have also shown in this chapter that the sequence of the GAG peptide bound to B*2705 does not affect the affinity of the heterotrimer interaction with LILRB1 and LILRB2. This observation does not agree with results from a previous SPR publication that also studied these interactions [109] which reported that LILRB2 exhibited substantially higher binding to B*2705 (GAG-M) variant compared to the B*2705 (GAG-L) variant. The reason for this

discrepancy is unclear, but it may be due to the way in which the B*2705 was immobilised. In my experiments, I used the site-specific biotinylation tag at the C terminus of the HLA heavy chain, whereas Lichterfeld et al immobilised tetrameric B27 complexes onto a sensor chip. The immobilisation method used in this thesis allows all B*2705 complexes to be presented in the same orientation for optimal binding to ligand following a 1:1 binding mode, whereas the latter method would allow avidity effects and encourage aggregation. My findings agree with the published LILRB2 : HLA structure [43], where the structure of the HLA-G:LILRB2 complex shows that the peptide-binding region does not contribute to the binding site for this interaction (section 1, figure 1.4).

In addition to the LILRs, I attempted to express and purify an Fc tagged KIR3DL2 construct using PEI transfection of 293T cells for SPR studies. Recombinant KIRs are notoriously difficult to express and purify and as a result, I was not able to express sufficient quantities of pure protein required for SPR studies. KIR3DL2 and other KIR interactions with B27 homodimers and heterotrimers will be important to study in the future in order to determine whether these interactions also contribute to the perturbed immune cell balance.

Finally, I have demonstrated that the CD8αα and B*2705 homodimer interaction is of lower affinity than the LILRB2 and B*2705 homodimer interaction. The SPR data for this interaction were not easy to collect as the recombinant CD8αα tended to stick non-specifically to the streptavidin chip. I therefore analysed the increase in refractive index at each successive concentration as an imperfect measure of binding. An attempt to use the kinetic analysis method was made for this interaction (stepwise injections of analyte with an acid buffer regeneration step) but it did not provide interpretable results (possibly due to poor

quality or stability of the CD8αα protein). The observation that CD8αα did not interact as strongly with B*2705 homodimers as LILRB2 was supported by CD8αα flow-cytometry competition assays. The assay demonstrated that pre-incubation of CD8αα with B*2705 homodimer tetramers did not significantly decrease tetramer staining of LILRB2- expressing cells. This observation suggests a dominant role of LILR – HLA interactions in modulating immune recognition, particularly where CD8αα expressing cells predominate, such as in the intestine epithelial cells [112]. Interestingly, gut infection has been implicated as one of the possible triggers of SpA [84], suggesting that the CD8αα cells could have a physiological role in disease. Comparison of the crystal structure of the HLA-G : LILRB2 complex and the structure of HLA-A2 : CD8αα complex, shows that the binding sites for the two ligands appear to be in close proximity (fig. 3.19), supporting the notion that the two ligands may compete for binding to different HLA class I molecules *in vivo*. However, it is worth mentioning that although CD8αα is expressed on the intraepithelial lymphocytes of the small intestine [112], CD8αβ is more widely expressed *in vivo.* Furthermore, CD8αα and CD8αβ may have different binding properties, but this could not be studied directly here as CD8αβ expression and purification has been shown to be problematic.

Although this chapter provides novel insights and ideas as to what may be occurring at the cell surface, it is also important to remember that other B27 receptor interactions may also be perturbed at the surface of immune cells. Here I show that the B27 dimer has its own unique binding properties to LILRB1 and LILRB2, and it will be important to understand the molecular details of how it interacts with these and other immune cell ligands.

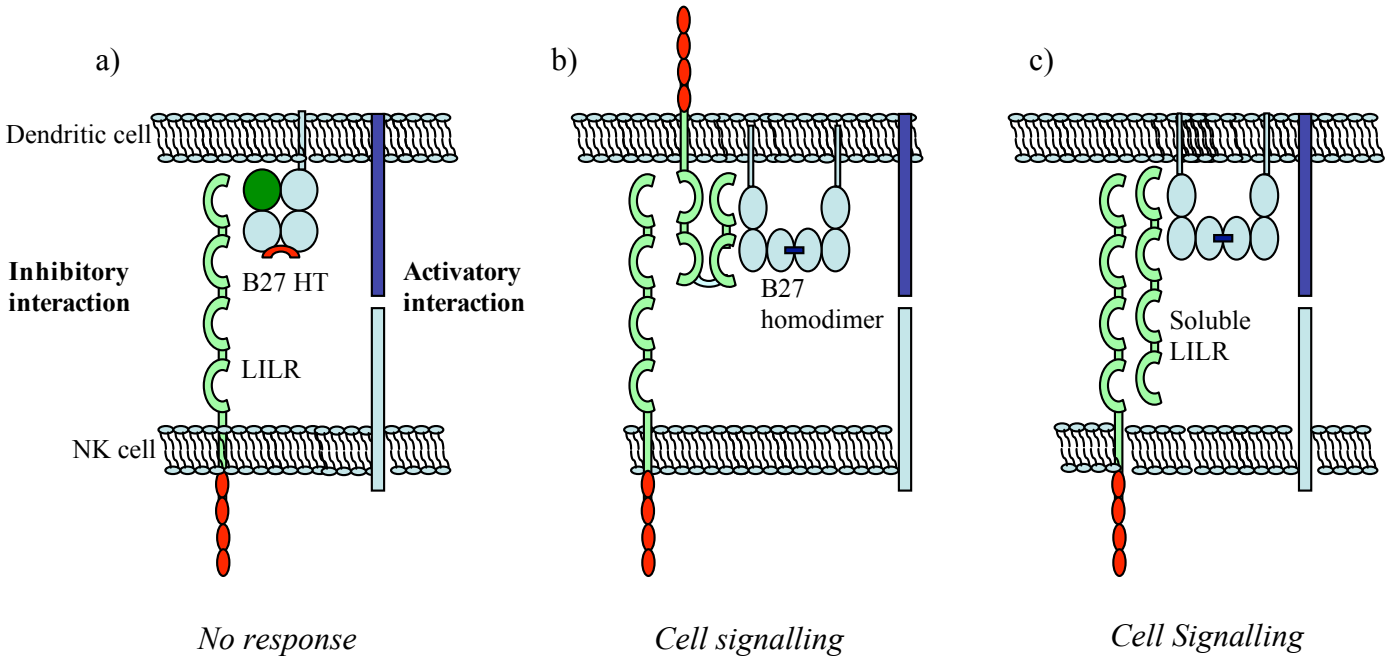
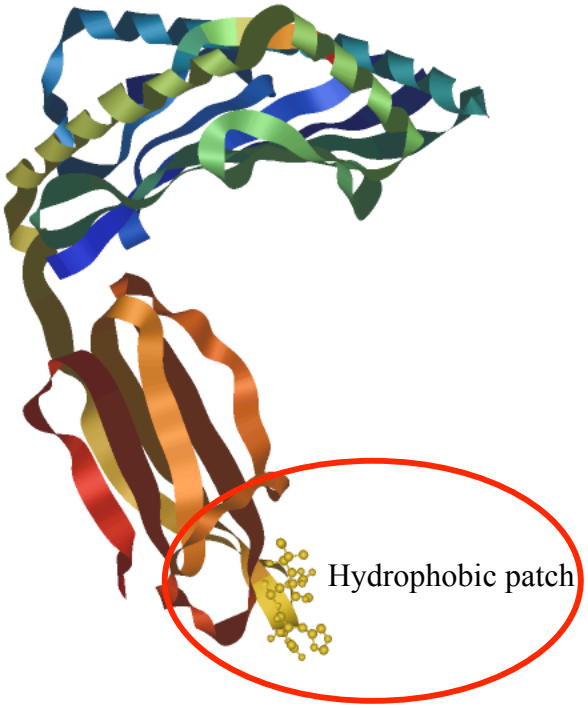
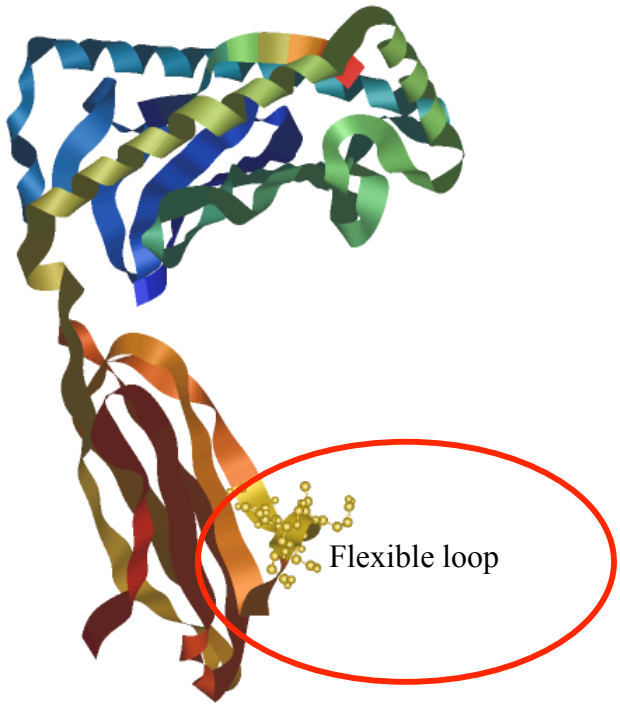


Figure 3.18 Cartoons showing how B*2705 homodimer interactions with LILRB2 might augment the balance of interactions on NK cell surface. *a) In healthy cells NK cells scan dendritic cells for HLA expression. Paired activatory and inhibitory interactions prevent NK cell licensing. b) B27 homodimer binding to LILRB2 in cis may perturb the balance of NK cell interactions to trigger NK cell licensing and propagate inflammation. c) Secreted forms of LILRB2 may mask the B27 LILRB2-binding site and tilt the NK cell balance, triggering inflammation.*

a)



b)



Figures modified from PDB entry 2BSR adapted using imol

Figure 3.19 Suggested binding regions of B27 to LILRB2 and CD8αα respectively. *a) Model of proposed binding region of B27 α3 domain for LILRB2 binding to HLA-B27. LILRB2 has been shown to bind HLA-G via the hydrophobic patch of the α3 domain (residues 195-197) b) Model of binding region for CD8αα binding to HLA-B27. CD8αα binds HLA-B27 by making contacts with the flexible loop region of α3 of B27. The two sites are in close proximity, supporting the suggestion that CD8αα and LILRB2 may compete for binding to this region.*

Chapter 4

HLA-B27 homodimer formation and LILR interactions – A comparison of two subtypes *in vitro*

4.1 Introduction……98

4.2 B*2705 forms more homodimers *in vitro* compared to B*2709……....99

4.3 Fluorescently labelled tetrameric complexes of B*2705 and B*2709 heterotrimers stain LILRB2, KIR3DL1 and KIR3DL2 expressing Baf cells……..…..104

4.4 LILRB1 and LILRB2 bind to B*2705 and B*2709 heterotrimers with comparable affinities by SPR…….106

4.5 Fluorescently labelled tetrameric complexes of B*2705 and B*2709 homodimers both bind to LILRB2 and not LILRB1 expressing Baf cells……....…….117

4.6 LILRB2 binds to B*2705 and B*2709 homodimers by SPR equilibrium binding analysis……119

4.7 Discussion…….122

4.1 Introduction

B27 has several polymorphic subtypes with differing degrees of disease association. B*2705 and B*2702 are the most common variants in Caucasian populations where B*2705 is thought to be the ancestral subtype. B*2705 and B*2702 are strongly associated with disease. B*2709 and B*2706 are not associated with disease, but it is still unclear whether these subtypes are "protective" against disease or are "neutral". B*2709 is found mainly in the Sardinian population (reviewed in [26, 28]). Strikingly, B*2705 and B*2709 differ by only one amino acid residue, Aspartic acid at position 116 in B*2705 and Histidine at position 116 in B*2709 and (D116H) [31].

Crystal structures of B*2705 and B*2709 reveal subtle structural differences surrounding position 116 [113]. One relevant difference includes the presence of an additional salt bridge at D77 in B*2709, which indirectly affects the position of K70. This K70 residue is known to affect the disulphide bonding capacity of C67 [23] (as discussed in section 1.3).

B*2705 has previously been shown to form homodimers, lacking β_2m *in vitro* and *in vivo*. The experiments in this chapter assess the abilities of the B*2705 and B*2709 subtypes to form homodimers in the presence of a variety of peptides and investigate whether the two subtypes display differing affinities and specificities for LILRB1, LILRB2, KIR3DL1 and KIR3DL2 receptors. The aim is to elucidate whether the D116H amino acid substitution has an effect on B27 folding and/or binding properties, and thus provides a possible explanation for the difference in their disease associations.

4.2 HLA-B*2705 forms more homodimers *in vitro* than to HLA-B*2709

One hypothesis for the differential association between B*2705 and B*2709 with disease is a possible difference in subtype abilities to form homodimeric molecules. This was investigated by performing *in vitro* refolds containing B27 heavy chain inclusion bodies, β_2m inclusion bodies and different synthetic peptides (as shown in table 4.1).

B*2705 and B*2709 were expressed in inclusion bodies and then refolded separately (but in parallel) in the presence of β_2m and peptide. The refolding conditions had previously been optimised (by S.Kollnberger) for the refolding of B*2705 heterotrimers, but were tested and shown to give comparable yields of B*2709 heterotrimers. After refolding, the solutions were concentrated and purified on a pre-calibrated size exclusion column. The gel filtration peaks corresponding to the heterotrimers and homodimers were identified and confirmed by SDS PAGE and mass spectroscopy. Refolds were performed for 7 different peptides and each refold repeated 1-5 times for each peptide. A representative purification is shown in figure 4.1. Figure 4.1 illustrates that B*2705 (blue) refold results in a higher yield of homodimer than B*2709 (pink) whereas they yielded similar amounts of heterotrimer. The peaks were quantified by size exclusion chromatography. Results were also expressed as ratios of homodimer to heterotrimers, where B*2705 consistently providing a higher homodimer to heterotrimer ratio, reflecting a higher yield of homodimer. A summary table and figure of results demonstrating the yields of refolds are shown in table 4.2 and figure 4.2.

Peptide selection

In vitro refolding of B*2705 and B*2709 free heavy chains in the presence of β_2m was performed in the presence of different B27-binding peptides. The peptide repertoire of B27 is known to be large and B27 has been shown to have a strong preference to bind peptides containing an Arginine anchor residue at position 2 as shown below. The peptide repertoires for B*2705 and B*2709 have been shown to be overlapping, with some different peptides identified for each subtype, although other peptides are still being identified. In these refolding assays, B*2705 eluted peptides, B*2709 eluted peptides and overlapping epitopes were used (table 4.1).

Anchors:

1	2	3	4	5	6	7	8	9
	R							L
								F

Other prevalent residues:

								Y
								R
								H
								K

Peptide sequence	Peptide number	Source of Peptide	Discovered by	Reference
RRRWRRLTY	1	EBV	Elution from B*2705	Lopez de Castro et al 2004
RRIYDLIEL	2	EBV	B*2705 epitope	Brooks et al. 1993
KRWIILGLNK	3	HIV	B*2705 epitope	Huet et al. 1990
TRIPKIQKL	4	Hsp 70	Elution from B*2709	Lopez de Castro et al. 2004
SRHHAFLFR	5	Aggrecan	Elution from B*2705	Kuon W et al, 2004
ARLQTALLV	6	Beta V spectrin	Elution from B*2705 and B*2709	Lopez de Castro et al. 2004
RRKWRRWHL	7	Self peptide pVIPR	Elution from B*2705	Fiorillo et al, 2000

Table 4.1 showing the peptides used for in vitro refolding studies of B*2705 and B*2709

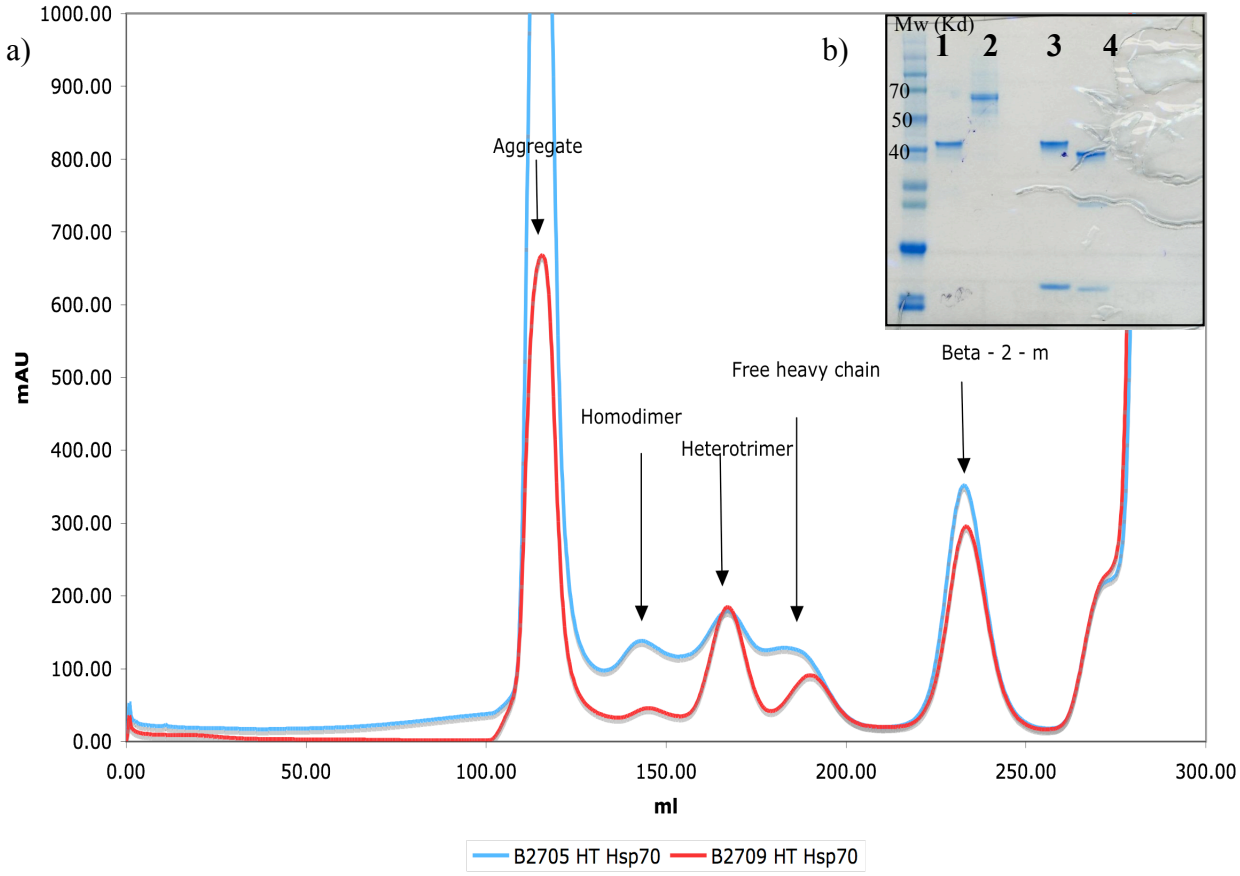


Figure 4.1 a) Representative FPLC result for B*2705 and B*2709 refolded with β_2m and an Hsp70 peptide (TRIPKIQKL). *Refolds were performed in parallel as discussed in section 2.1.3 for 48 hours at 4ºC. b) Homodimer and heterotrimer FPLC fractions were confirmed by SDS PAGE. Lane 1 is B*2705 homodimer peak, reduced. Lane 2 represents B*2705 homodimer non-reduced. Lane 3 is B27 heterotimer reduced. Lane 4 is B27 heterotrimer non-reduced.*

B27 Allele	Dimer (mAU*ml) Peak area	Heterotrimer (mAU*ml) Peak area	Ratio (mean) Dimer:Heterotrimer	Peptide Sequence	
*05	3139	1612	1.36	RRRWRRLTY	Peptide 1
*09	1631	1792	0.72	RRRWRRLTY	
*05	3155	1800	1.15	RRIYDLIEL	Peptide 2
*09	1541	3783	0.36	RRIYDLIEL	
*05	2601	2910	0.76	KRWIILGLNK	Peptide 3
*09	986	3137	0.24	KRWIILGLNK	
*05	2056	2980	0.75	TRIPKIQKL	Peptide 4
*09	216	1847	0.18	TRIPKIQKL	

Table 4.2. B*2705 forms more homodimer than B*2709 in vitro. *Summary of the mean ratios of dimer to heterotrimer yields from all experiments. B*2705 consistently yields more homodimer than B*2709.*

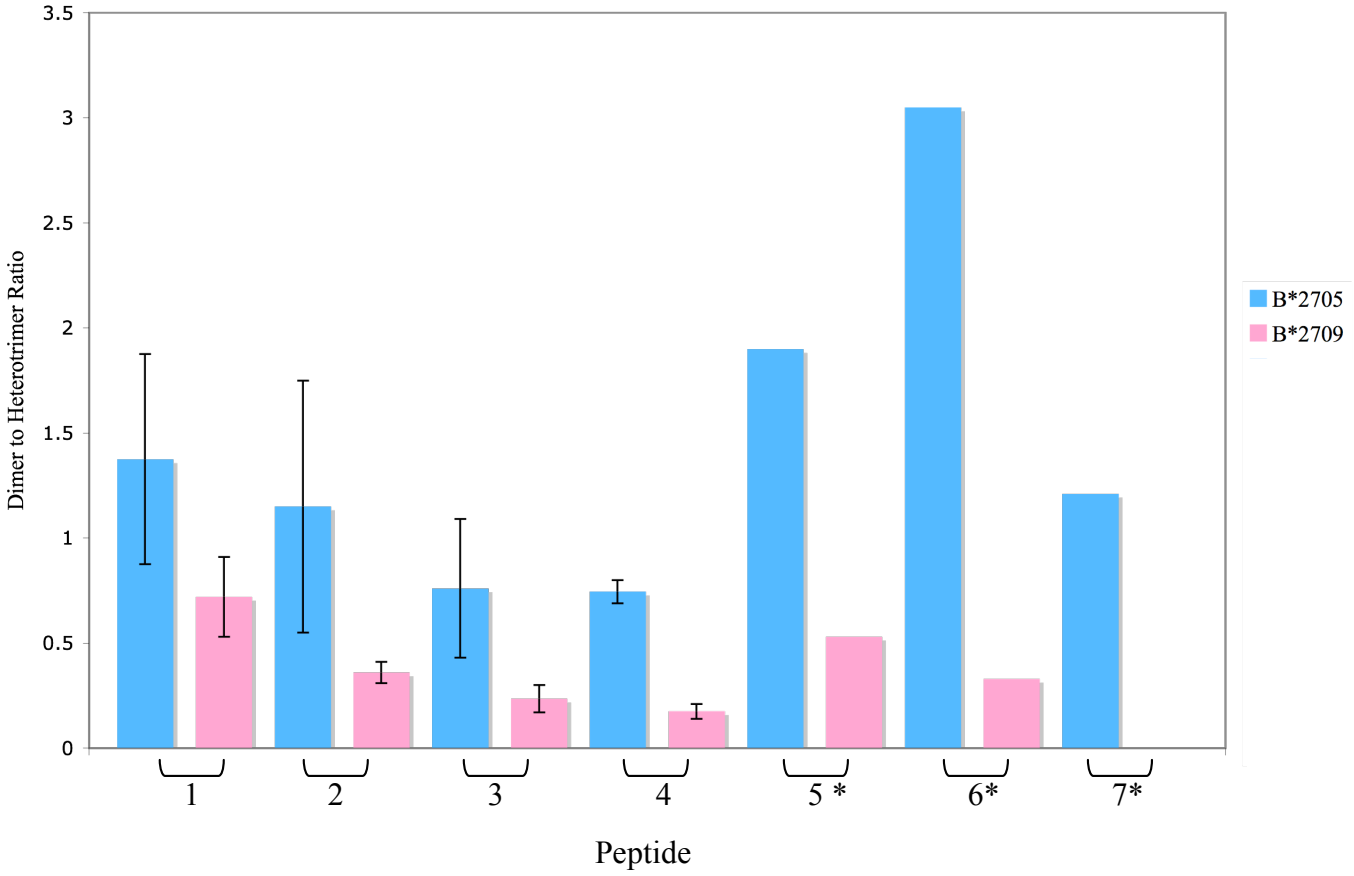


Figure 4.2 Dimer:heterotrimers ratios are higher for B*2705 refolds compared to B*2709 for 7 different B27 binding peptides. **Refolds using peptides 1-4 were performed by myself, refolds using peptides 5-7 were performed by Jackie Shaw and are included here for comparison.*

4.3 Fluorescently labelled tetrameric complexes of B*2705 and B*2709 heterotrimers stain LILRB2-expressing Baf cells

B*2705 heterotrimers have previously been shown to bind LILRB2-, KIR3DL1- and LILRB1- expressing cells. B27 heterotrimer complexes with VIPR peptide (RRKWRRWHL) were refolded, purified, biotinylated and tetramerised using extravidin PE. Using FACs analysis, I investigated whether fluorescently labelled B*2705 and B*2709 heterotrimer tetrameric complexes stained LILRB2- expressing cell lines.

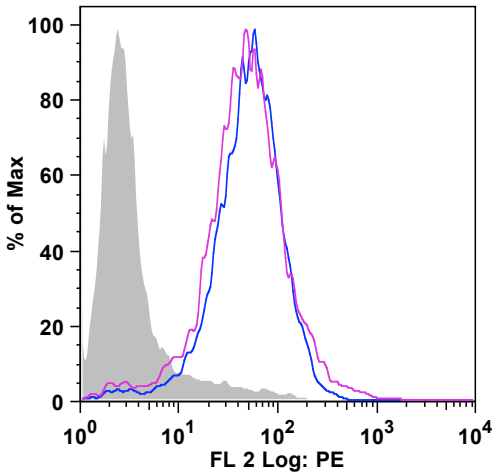


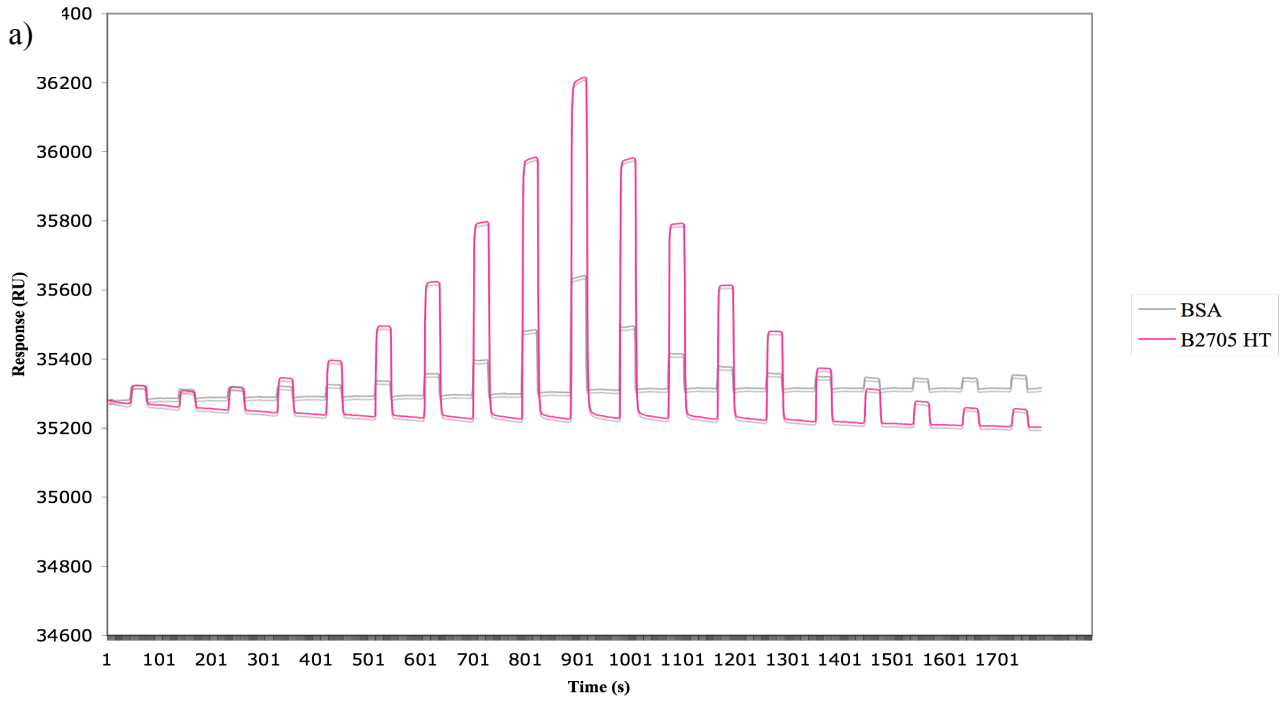
Figure 4.3 B*2705 and B*2709 heterotrimer tetramers binding to LILRB2- transfected cell lines. *FACS analysis shows similar staining of each of the cell lines by the B*2705 (blue) and B*2709 (pink) heterotrimer tetramers.*

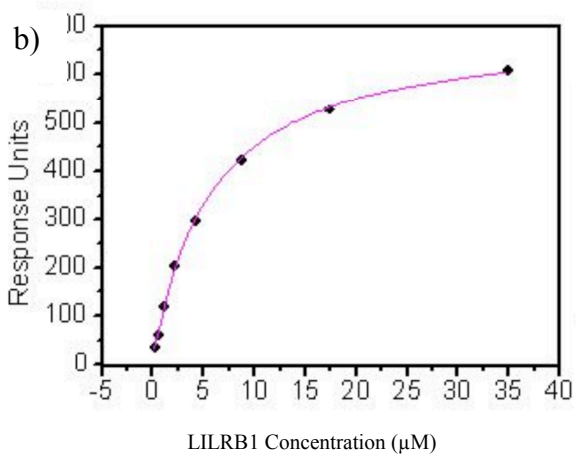
4.4 LILRB1 and LILRB2 bind to B*2705 and B*2709 heterotrimers with comparable affinities by SPR

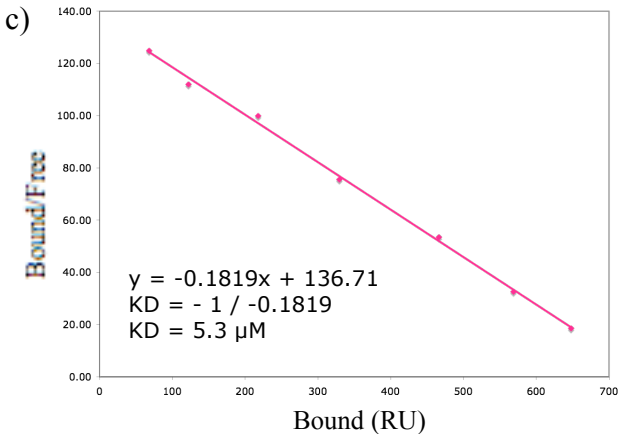
B*2705 heterotrimers have been shown previously to bind to both LILRB1 and LILRB2 receptors. Here I used Surface Plasmon Resonance (SPR) to ask whether the subtypes bound to LILRB1 and LILRB2 receptors with similar kinetics and specificities. The binding interaction between HLA class I and LILRB1/2 has previously been shown to be of low affinity by SPR. Therefore, equilibrium-binding experiments of LILRB1/2 binding to the B27 heterotrimer were conducted using SPR.

*LILRB1 binding to B*2705 and B*2709 heterotrimers*

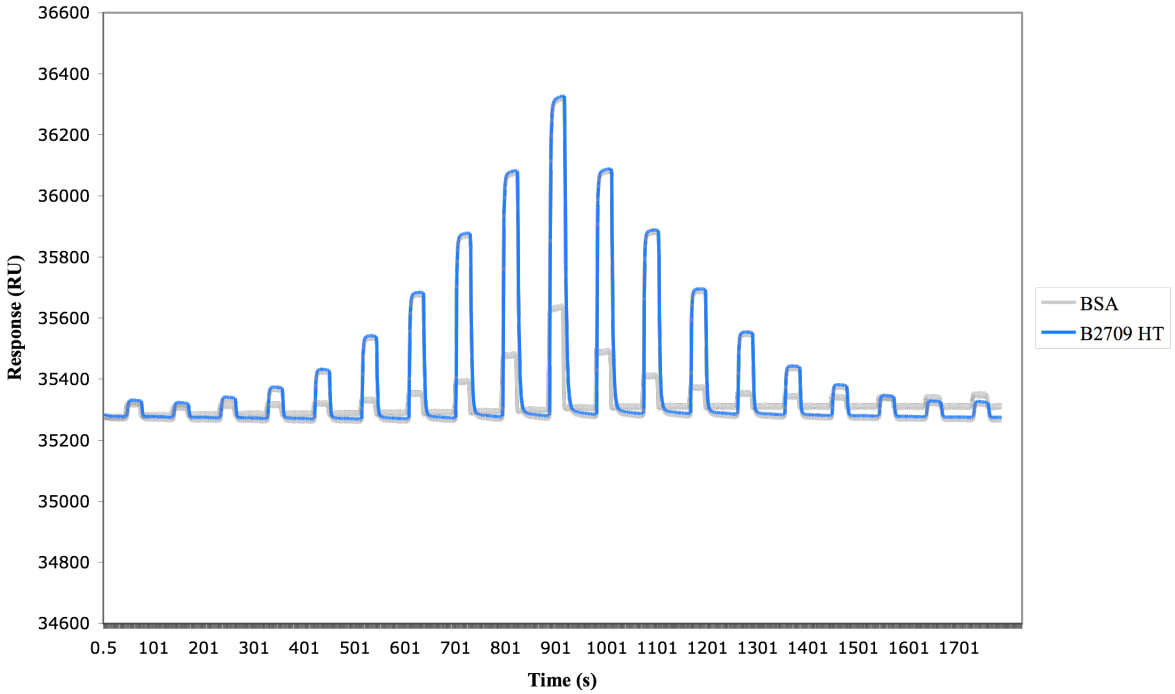
Biotinylated B*2705 and B*2709 heterotrimer complexes (refolded with a Hsp70 peptide, TRIPKIQKL) were immobilised on a streptavidin-coated gold chip. LILRB1 was flowed over the chip in increasing and then deceasing concentrations. Figure 4.4 shows that B*2705 and B*2709 demonstrate similar binding to LILRB1. Results were repeated 3 times with the Hsp70 peptide B27 complex, 3 times for a GAG peptide (KRWIILGLNK) B27 complex and once using an EBV peptide (RRIYDLIEL) B27 complex. Each experiment provided consistent results. Representative results are presented. The mean K_D values for LILRB1 binding to B*2705 heterotrimer and B*2709 were 5.10 μM and 5.46 μM respectively (fig. 4.4 a-f). K_D values obtained using Origin 7.5 were consistent with K_D values obtained from Scatchard plots. These results were comparable with values obtained for HLA-A3 (fig. 4.4 g,h,i).


a)
Response (RU)
Time (s)
BSA
B2705 HT

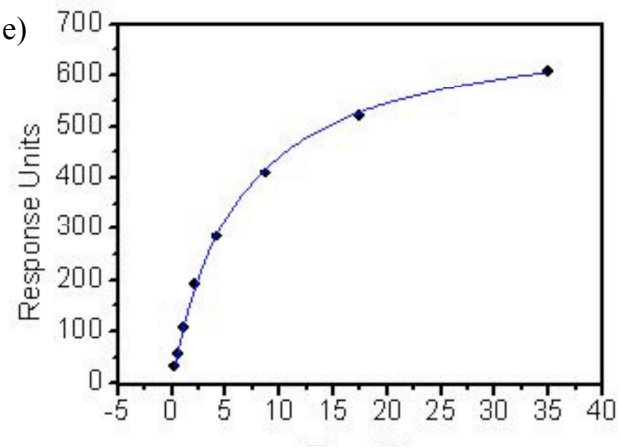

b)
Response Units
LILRB1 Concentration (µM)


c)
Bound/Free
y = -0.1819x + 136.71
KD = - 1 / -0.1819
KD = 5.3 µM
Bound (RU)

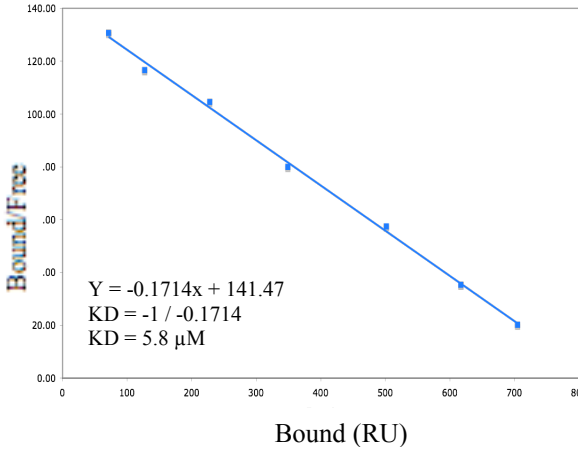
d)


Response (RU)
36600
36400
36200
36000
35800
35600
35400
35200
35000
34800
34600
0.5 101 201 301 401 501 601 701 801 901 1001 1101 1201 1301 1401 1501 1601 1701
Time (s)
BSA
B2709 HT

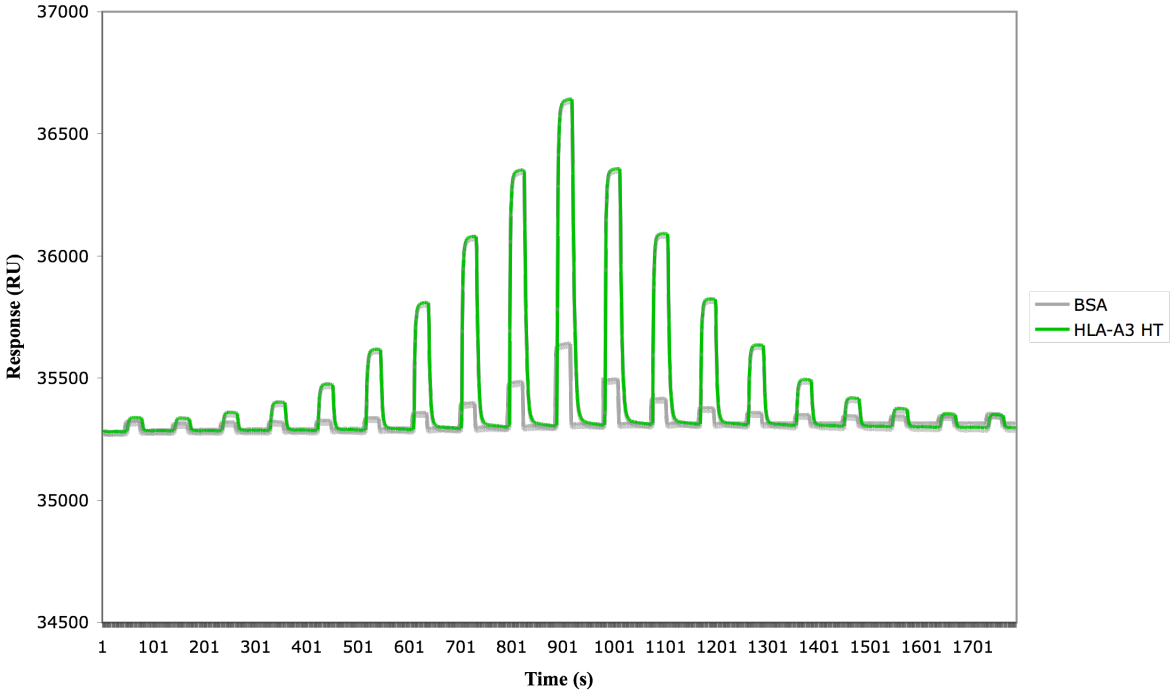
e)


Response Units
700
600
500
400
300
200
100
0
-5 0 5 10 15 20 25 30 35 40
LILRB1 Concentration (µM)

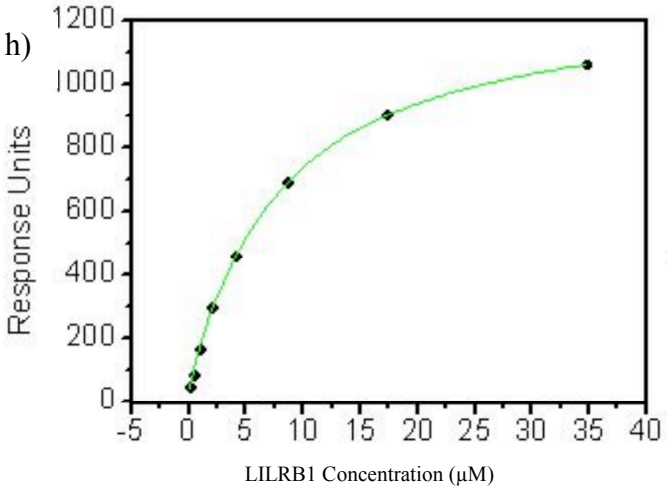
f)


Bound/Free
140.00
120.00
100.00
0 100 200 300 400 500 600 700
Y = -0.1714x + 141.47
KD = -1 / -0.1714
KD = 5.8 µM
Bound (RU)

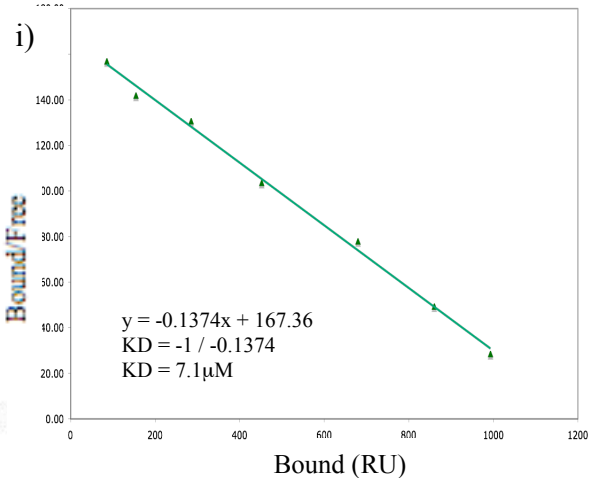
g)


37000
36500
36000
35500
35000
34500
Response (RU)
1 101 201 301 401 501 601 701 801 901 1001 1101 1201 1301 1401 1501 1601 1701
Time (s)
BSA
HLA-A3 HT

h)


1200
1000
800
600
400
200
0
Response Units
-5 0 5 10 15 20 25 30 35 40
LILRB1 Concentration (μM)

i)


Bound/Free
y = -0.1374x + 167.36
KD = -1 / -0.1374
KD = 7.1μM
0 200 400 600 800 1000 1200
Bound (RU)

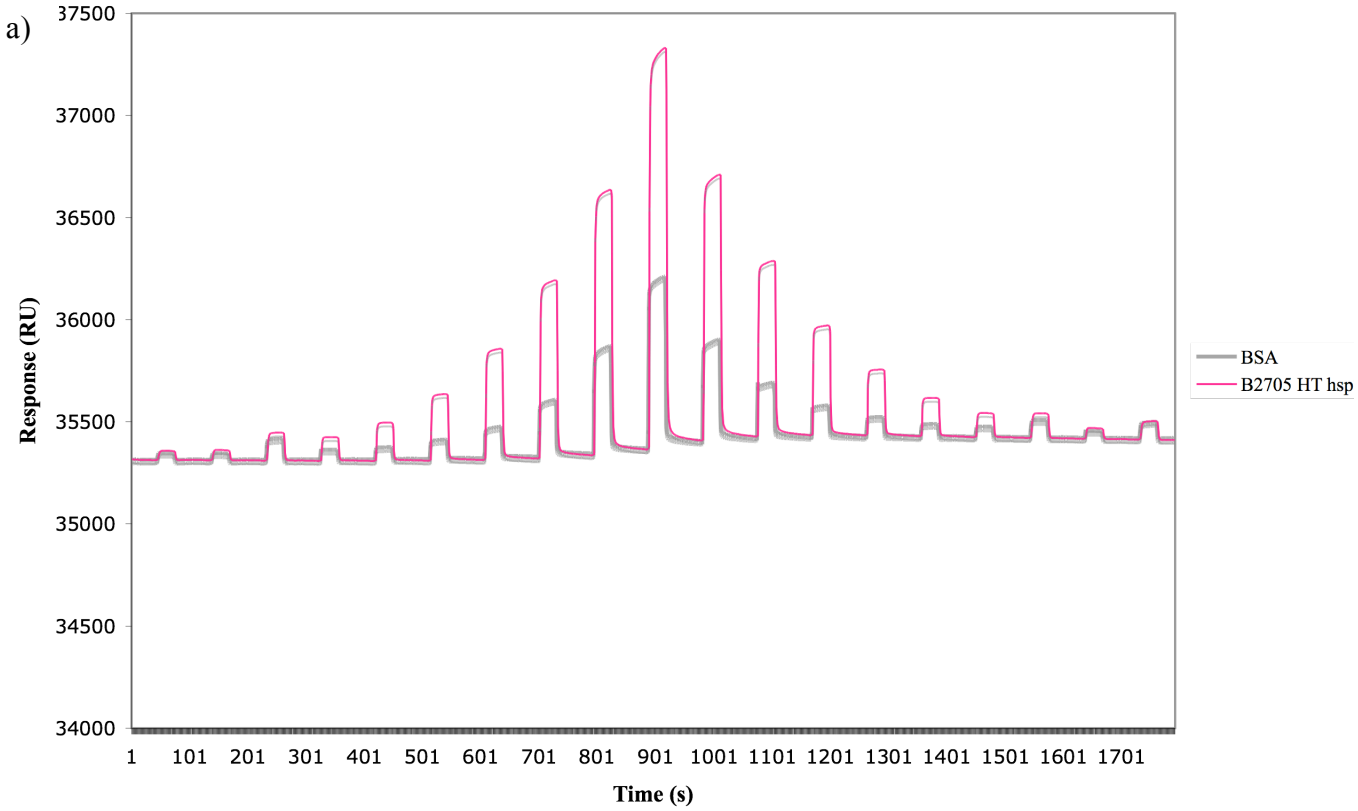
K_D **Values for binding to LILRB1 (μM)**	
HLA-B*2705 HT	**5.10 ± 0.80**
HLA-B*2709 HT	**5.46 ± 0.86**
HLA-A3 HT	**6.88 ± 1.30**

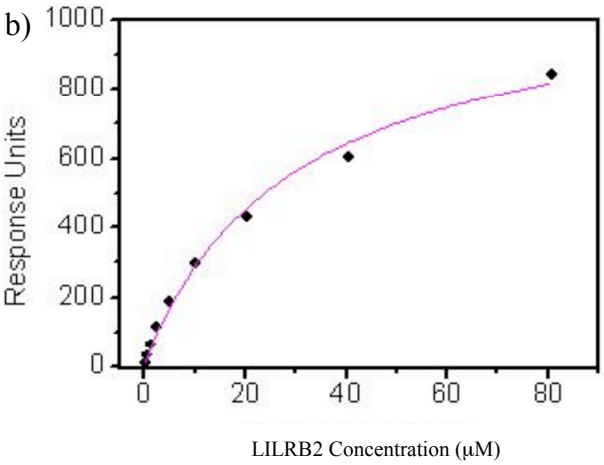
j) Table of K_D values for LILRB1 binding to B*2705 HT, B*2709 HT and HLA-A3 HT

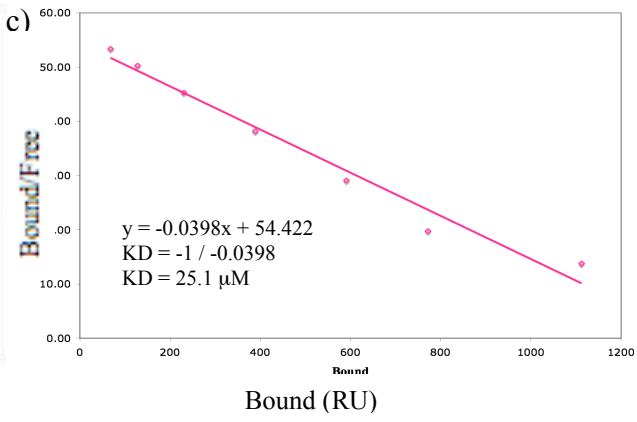
Figure 4.4 Calculation of dissociation constants for LILRB1 binding to B*2705 HT, B*2709 HT and HLA-A3 HT. *Figures a,d and g are the raw sensograms for LILRB1 equilibrium binding to B*2705 HT, B*2709 HT and HLA-A3 respectively. Figures b,e and h are hyperbolic-fit binding curves for LILRB1 binding to HLA complexes obtained using the Origin 7.5 program. The fits show that binding to the hetetrotrimeric molecule increases until binding is saturated and equilibrium is reached. Figures c,f and i are Scatchard plots, from the gradient of this line a K_D value for each interaction can be calculated. Scatchard analysis shows that the K_D is a constant value over a range of concentrations and that binding is homogeneous. Table j is a summary of mean K_D values obtained using SPR analysis.*

*LILRB2 binding to B*2705 and B*2709 heterotrimers*

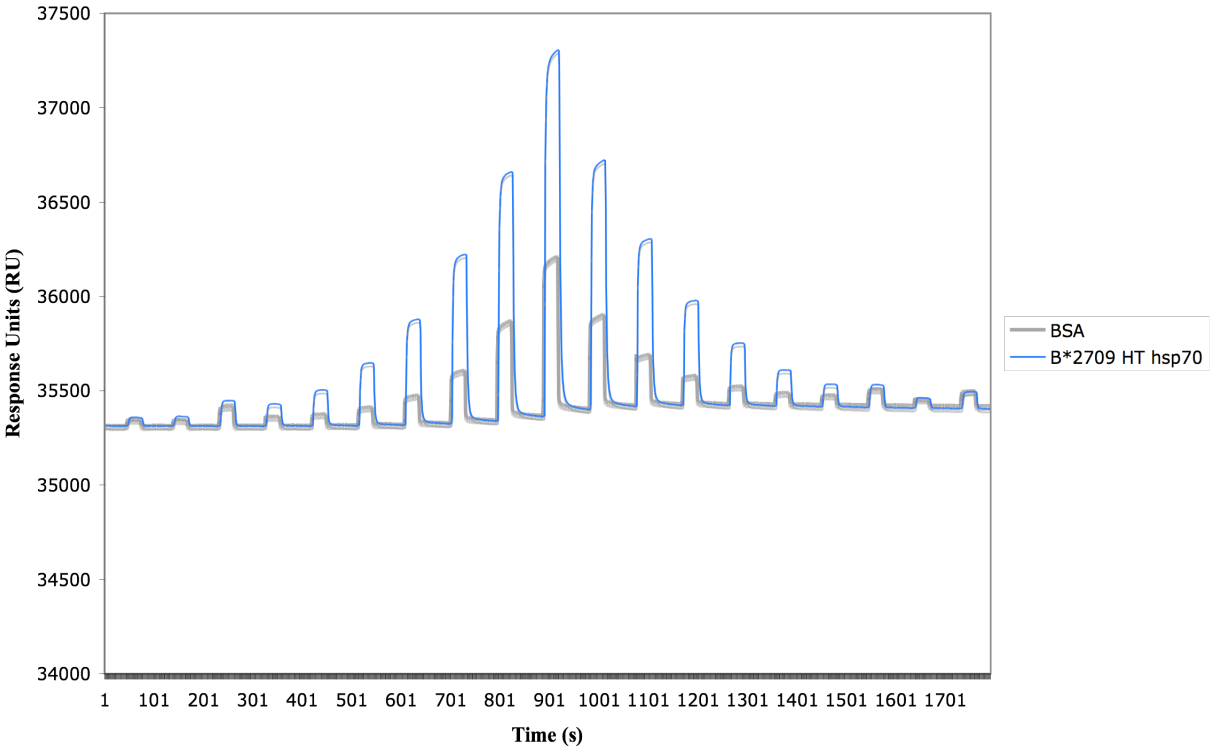
As described for Figure 4.4, biotinylated B*2705 and B*2709 heterotrimer complexes were immobilised on a streptavidin-coated gold chip and LILRB2 was flowed over the chip in increasing and then deceasing concentrations. Results were repeated 6 times with consistent results. Representative results are presented in figure 4.5. Mean K_D values for LILRB2 binding to B*2705 and B*2709 were 21.23 μM and 21.60 μM respectively. K_D values obtained using Origin 7.5 were consistent with K_D values obtained from Scatchard plots. These values were comparable with those obtained for HLA-A3 as shown in figure 4.5.


a)
Response (RU)
37500
37000
36500
36000
35500
35000
34500
34000
1 101 201 301 401 501 601 701 801 901 1001 1101 1201 1301 1401 1501 1601 1701
Time (s)
BSA
B2705 HT hsp

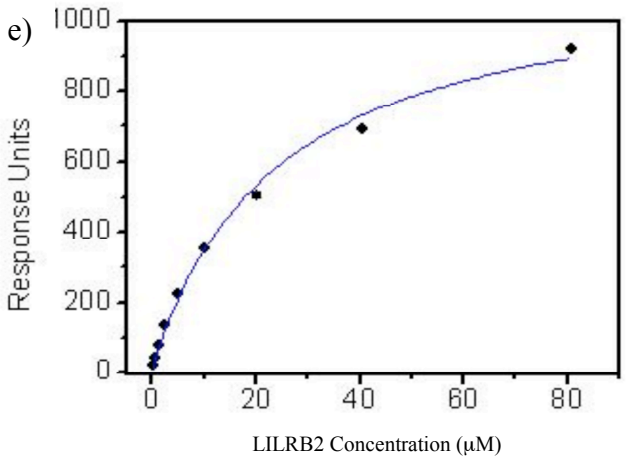

b)
Response Units
1000
800
600
400
200
0
0 20 40 60 80
LILRB2 Concentration (µM)


c)
Bound/Free
60.00
50.00
.00
.00
.00
10.00
0.00
y = -0.0398x + 54.422
KD = -1 / -0.0398
KD = 25.1 µM
0 200 400 600 800 1000 1200
Bound (RU)

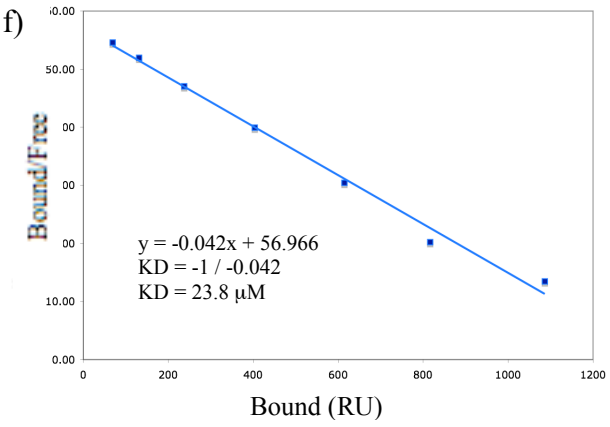
d)


Response Units (RU)
37500
37000
36500
36000
35500
35000
34500
34000
1 101 201 301 401 501 601 701 801 901 1001 1101 1201 1301 1401 1501 1601 1701
Time (s)
BSA
B*2709 HT hsp70

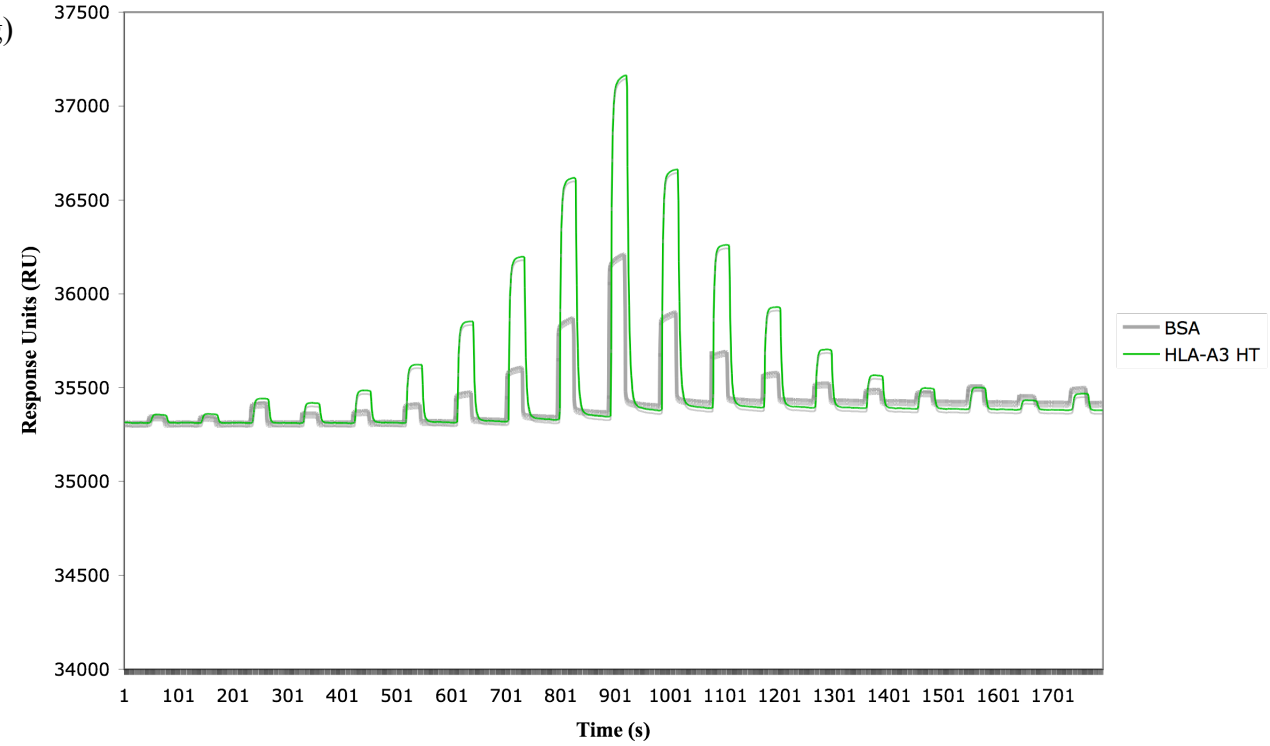
e)


Response Units
1000
800
600
400
200
0
0 20 40 60 80
LILRB2 Concentration (µM)

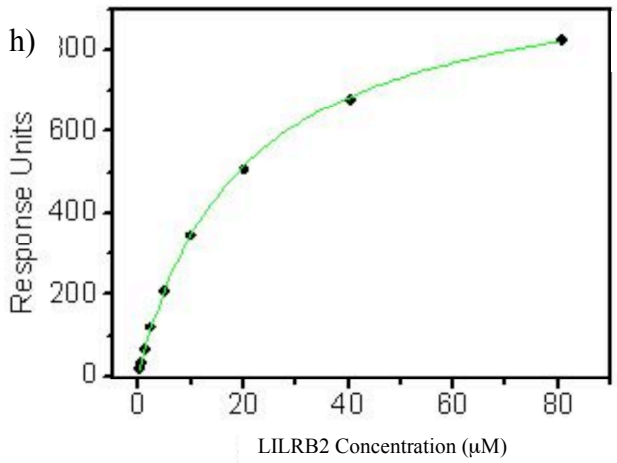
f)


Bound/Free
50.00
10.00
0.00
0 200 400 600 800 1000 1200
Bound (RU)
y = -0.042x + 56.966
KD = -1 / -0.042
KD = 23.8 µM

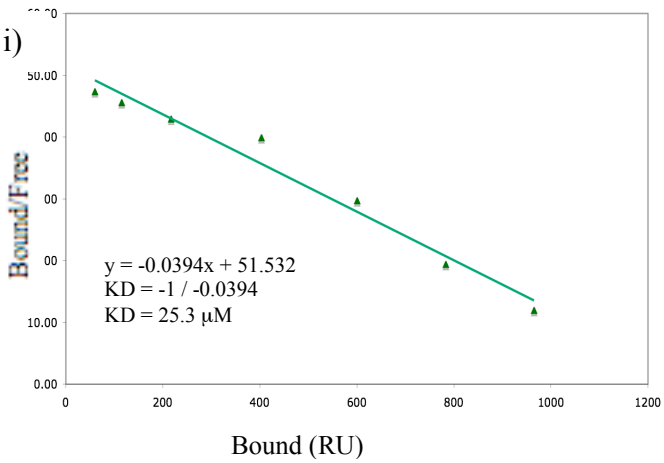
g)


37500
37000
36500
36000
35500
35000
34500
34000
Response Units (RU)
1 101 201 301 401 501 601 701 801 901 1001 1101 1201 1301 1401 1501 1601 1701
Time (s)
BSA
HLA-A3 HT

h)


800
600
400
200
0
Response Units
0 20 40 60 80
LILRB2 Concentration (µM)

i)


50.00
00
00
00
10.00
0.00
Bound/Free
y = -0.0394x + 51.532
KD = -1 / -0.0394
KD = 25.3 µM
0 200 400 600 800 1000 1200
Bound (RU)

K_D **values for binding to LILRB2 (μM):**	
HLA-B*2705 HT	**21.23 ± 3.63**
HLA-B*2709 HT	**21.60 ±2.60**
HLA-A3 HT	**21.10 ±2.10**

j) Table of K_D values for LILRB2 binding to B*2705 HT, B*2709 HT and HLA-A3 HT

Figure 4.5 Calculations of dissociation constants by SPR for LILRB2 binding to B*2705 HT, B*2709 HT and HLA-A3 respectively. *Figures a,d and g are the raw sensograms for LILRB2 equilibrium binding to B*2705 HT, B*2709 HT and HLA-A3 respectively. Figures b,e and h are hyperbolic-fit binding curves for LILRB2 binding to HLA complexes obtained using the Origin 7.5 program. The fits show that the binding to the hetetrotrimeric molecule increases until binding is saturated and equilibrium is reached. Figures c,f and i are Scatchard plots. The gradient of this line gives a* K_D *value for each interaction. Scatchard analysis shows that the* K_D *is a constant over a range of concentrations and that the binding is homogeneous. j is a summary table of mean* K_D *values obtained for HLA binding to LILRB2.*

4.5 Fluorescently labelled tetrameric complexes of B*2705 and B*2709 homodimers stain LILRB2-, KIR3DL1- and KIR3DL2- expressing Baf cells

B*2705 homodimers have been shown to bind LILRB2-, KIR3DL1- and KIR3DL2-expressing cells, but not to LILRB1- expressing cells. I have shown that both B*2705 and B*2709 fold to form homodimeric molecules *in vitro.* B27 homodimer proteins were purified, biotinylated and tetramerised using extravidin PE. Using FACS analysis, I investigated whether B*2709 homodimer tetrameric complexes bound with similar avidity to LILRB2, KIR3DL1 and KIR3DL2 expressing cells compared with B*2705 homodimer tetrameric complexes (fig. 4.6).

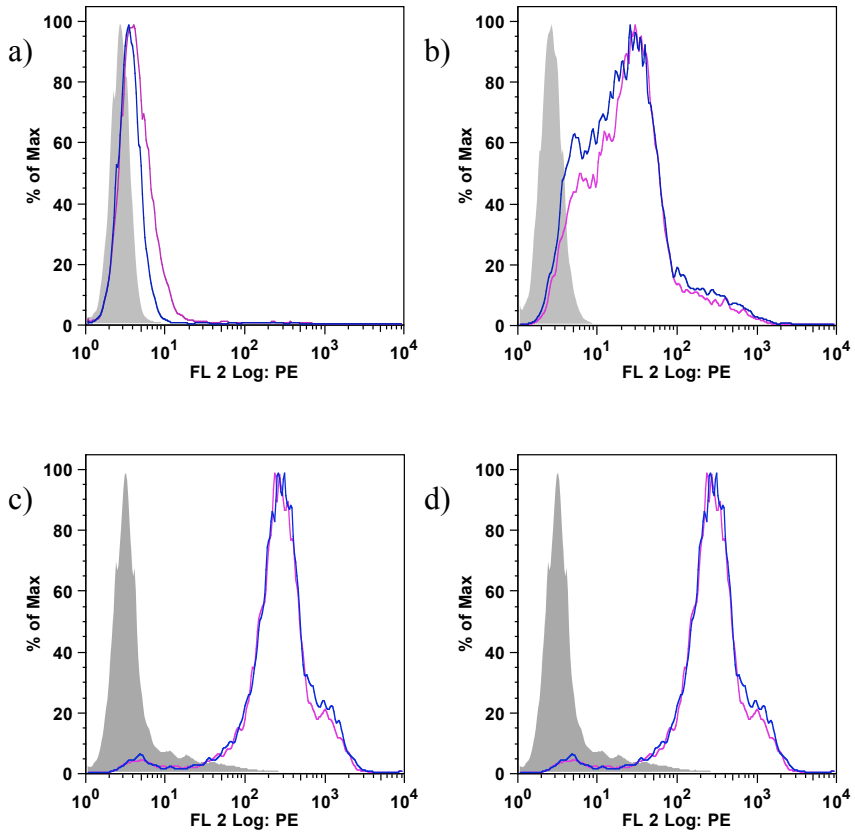
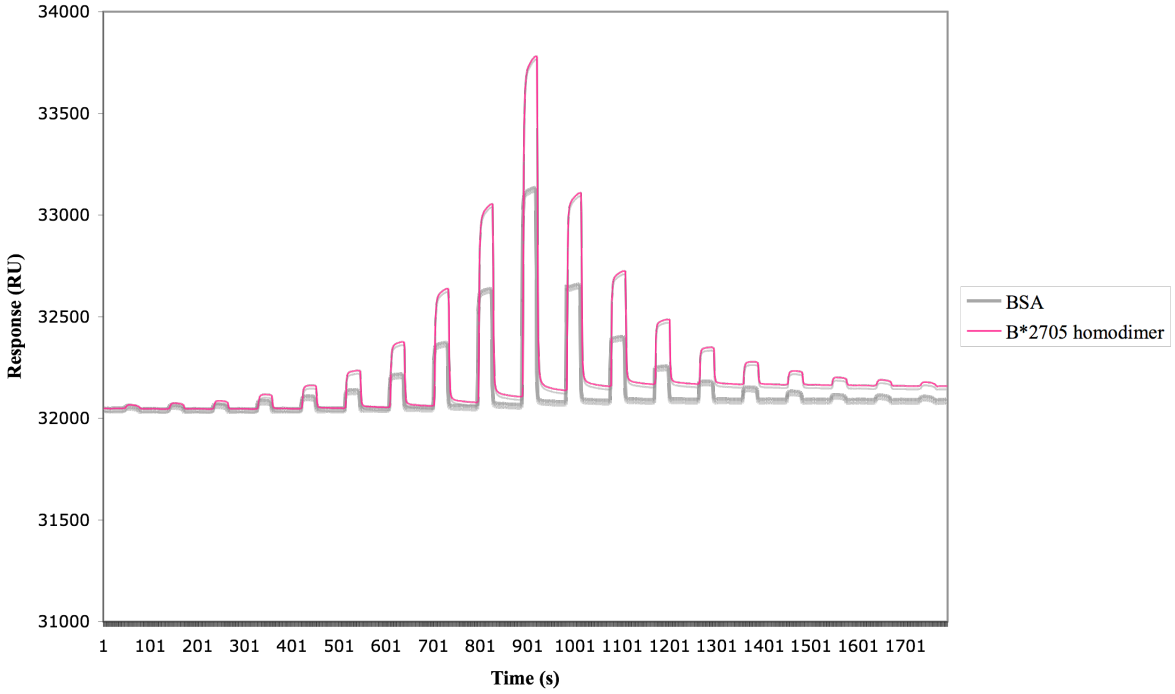


Figure 4.6 B*2705 (pink) and B*2709 (blue) homodimer tetramers stain a) LILRB1- b) LILRB2- c) KIR3DL1- and d) KIR3DL2- transfected cell lines. *FACS analysis shows similar staining of each of the cell lines by the B*2705 and B*2709 homodimer tetramers. Grey histograms show staining with Extravidin PE only.*

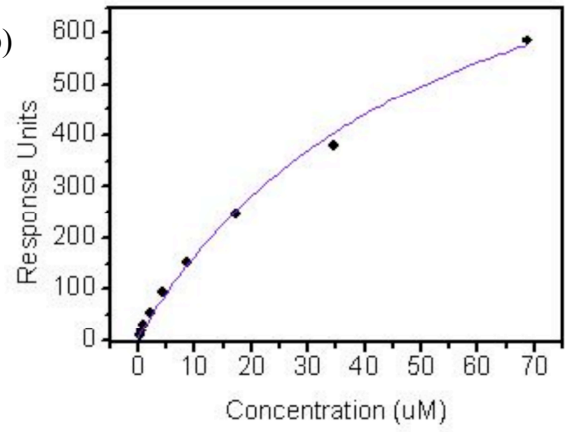
4.6 LILRB2 binds to B*2705 and B*2709 homodimers by SPR equilibrium binding analysis

The binding of LILRB2 to B*2705 and B*2709 homodimers was further investigated by equilibrium analysis using SPR. Biotinylated B27 homodimer complexes were immobilised on a streptavidin-coated gold chip and LILRB2 was flowed over in increasing then decreasing concentrations. In Figure 4.7, LILRB2 demonstrates the same binding responses to B*2705 and B*2709 homodimers over a range of concentrations. Results were analysed using Origin 7.5 and Scatchard analysis. As shown in Figures 4.7 b and e, binding of LILRB2 to the immobilised B*2705 and B*2709 homodimers did not saturate with the concentrations used. This binding does not obey conventional Michaels Menten Kinetics, and so reliable K_D values cannot be obtained. Figures 4.7 c and f are Scatchard plots of the data and demonstrate that the B27 homodimers do not demonstrate linear binding to the LILRB2 ligand. B*2705 and B*2709 both demonstrated non-linear binding to LILRB2 in equilibrium experiments and provide comparable responses to LILRB2 at different concentrations, suggesting comparable apparent dissociation constants. Results were repeated 8 times with consistent results.

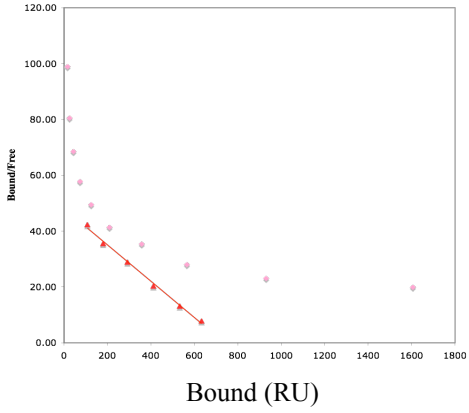
a)



b)



c)



B*2705 dimer
B*2705 HT

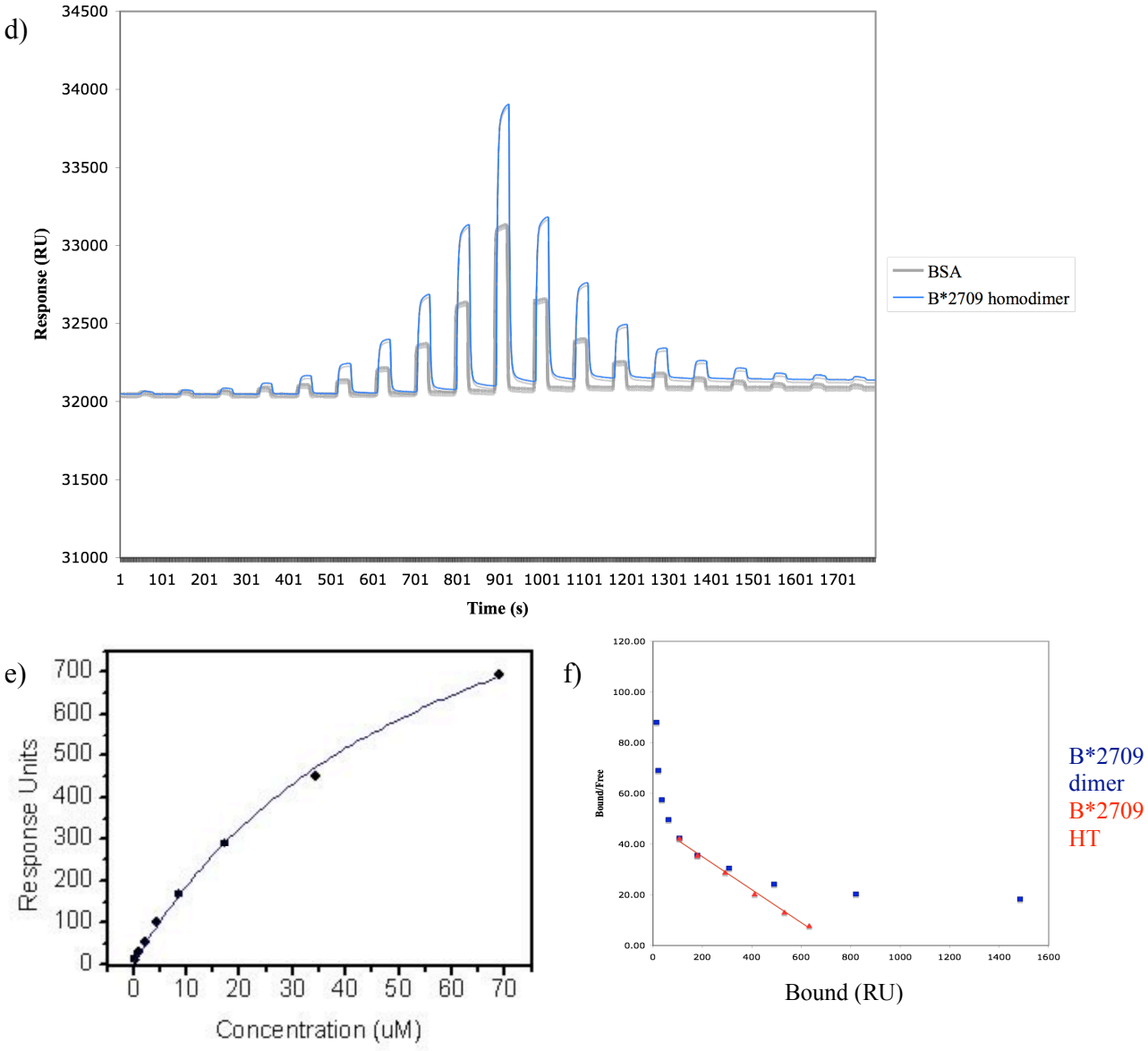


Figure 4.7 B*2705 and B*2709 homodimers demonstrate comparable binding responses to LILRB2 over a range of concentrations. *Figures a and d are raw sensograms of LILRB2 binding to B*2705 homodimers and B*2709 homodimers respectively. Figures b and e are hyperbolic-fit binding curves and figures c and f are Scatchard plots showing the binding mode is non-linear. The Scatchard plots also show a binding plot for the B*2709 heterotrimer for comparison.*

4.7 Discussion

The data presented in this chapter demonstrate that both B*2705 and B*2709 are able to form heavy-chain homodimeric molecules *in vitro,* and that the D116H substitution does not affect the binding capacity of B27 heterotrimers or homodimers to the LILR receptors, LILRB1 and LILRB2.

Using the refolding assays, I have shown that B*2705 yields more heavy chain homodimer than B*2709 *in vitro*. This is consistent for a range of selected peptide epitopes for B*2705/09. If these *in vitro* observations reflect the capacity of the subtypes to form homodimers in endosomes and at the cell surface, then this will have important implications on the theories of disease pathogenesis in AS. B*2709 transfected cell lines have been shown to express HC-10 reactive species at the cell surface (Bowness, unpublished data) and quantification of dimer expression levels in B*2705 transfectants compared to B*2709 transfectants is currently being studied. The work presented here strongly supports the homodimer theory as discussed in section 1.10, as the disease-associated subtype (B*2705) forms a higher yield of homodimers *in vitro* than the non-disease-associated subtype (B*2709), although it is important to note that the refolding assays had been previously developed for the B*2705 subtype and the conditions of refolding were not changed for the B*2709 subtype. It is striking how one amino acid difference in the peptide-binding groove significantly affects the folding of this heavy chain molecule under the chosen refolding conditions. The D116H substitution is located in the peptide binding groove, and so one

possible explanation for the observed results could be that the D116H substitution in B*2709 allows the molecule to bind to its cognate peptide more strongly than B*2705. The crystal structures of the two subtypes suggest that the subtle changes induced by the D116H substitution may well influence the properties of the B*2709 binding groove [116]. If the peptide binding properties are thus altered between the subtypes, it may mean that the B*2709 heterotrimer will form a stable complex at the cell surface, whereas in B*2705 the peptide may be prone to "fall out" of the groove, leading to disassembly of the B*2705 hetrotrimeric complex. Then, upon recycling of the heterotrimer *in vivo*, B27 free heavy chains may then be available for homodimer formation. Furthermore, the crystal structures of the two subtypes show that the K70 of the B*2709 is shifted compared to that in B*2705 [116]. This shifted K70 residue could also affect the reactivity of the nearby C67 and thus lead to either a more stable B*2709 heterotrimer or a less stable B*2709 homodimer. The difference between the *in vitro* homodimer yields would suggest that there might be an innate difference between the molecules in their flexibility and folding properties. Work by Ziegler's group [113] supports this suggestion by showing that the two alleles adopt different folding structures under thermal denaturation conditions.

During my project I have also cloned and expressed inclusion bodies containing the B*2702 protein; however, it proved technically difficult to perform three separate refolds in parallel. Preliminary refolding results suggest that B*2702 also yields more B27 homodimers than B*2709 (data not shown) and it will be interesting to further investigate this disease associated subtype (as well as others) in the future.

Once the B*2705 and B*2709 heterotrimers have formed *in vitro,* I have shown that the B27 interactions with the LILRB1 and LILRB2 molecules are almost identical. Using both FACS analysis and Biacore studies, I have shown that B*2705 and B*2709 heterotrimers bind to LILRB1 and LILRB2 receptors with comparable specificity and affinity. These binding interactions are also shown here to be comparable with the binding of HLA-A3 with K_D values in the 20-30μM range. These K_D values are also consistent with previous reports on the interactions between LILRB1/2 and the HLA-G and other class I heterotrimers [74].

In addition, B*2705 and B*2709 homodimer tetramers stain LILRB1-, LILRB2-, KIR3DL1- and KIR3DL2- transfected Baf cell lines with similar specificities by FACS analysis. SPR studies using B*2705 and B*2709 homodimer complexes reveal that both subtypes display non-linear binding to LILRB2 and neither subtype binds LILRB1 (data not shown). The SPR equilibrium studies of LILRB2 binding to B*2705 and B*2709 homodimers suggest that the D116H substitution does not affect the binding affinity or specificity of the interaction since measured responses for LILRB2 binding to B*2705 and B*2709 were comparable over a range of concentrations. The kinetic analysis ("stepwise") approach will confirm whether the LILRB2 binds to B*2709 homodimers, and would have been performed had time allowed.

In conclusion, although the amino acid difference between B*2705 and B*2709 may affect the folding properties of B27, it seems to have little or no effect on the ability of the folded B27 homodimers and heterotrimers to interact with LILRB1 and LILRB2. It will be important to extend these molecular interaction studies in order to further characterise the binding between

other disease-associated B27 subtype homodimers and heterotrimers with other ligands, including the KIRs. By understanding how the molecular interactions between B27 and its ligands are altered we will be able to develop our understanding of how cell signaling and cell function is perturbed *in vivo*.

Chapter 5 - Properties of the B*2705 homodimer and biophysical investigation of candidate B27 homodimer-specific monoclonal antibodies

5.1 Introduction……..127

5.2 B*2705 homodimers do not contain peptide……128

5.3 HD5, HD6 and HD8 bind B27 homodimer but not B27 heterotrimer……..132

5.4 HD6 binds to B*2705 homodimers, but not to HLA-G homodimers-…….....137

5.5 HD6 binds to B*2705 heavy chains, but not to HLA-A3 or HLA-G heavy chains…..…138

5.6 HD5/ HD6 / HD8 do not compete with LILRB2 for B*2705 homodimer binding but HC-10 partially competes for binding……..140

5.7 Epitope mapping of B*2705 dimer : HD6 interaction…….145

5.8 Discussion……147

5.1 Introduction

B27 homodimer expression and function is being investigated by a number of groups. Current antibodies used to study B27 expression include: **W6/32**, which recognises a conformation dependent epitope on HLA class I, also dependent on the presence of β_2m [117]. **HC-10**, which recognises unfolded HLA-B and HLA-C allele heavy chains, specifically mapped to amino acids 60-62 of the HLA molecules [118]. **ME1** recognises conformation specific β_2m -associated B27, B7 and Bw22 [119].

These antibodies are not of sufficient specificity for studies of B27 homodimer expression on human cell lines and tissues as they cross-react with other HLA molecules. Work in the field would be rapidly enhanced by the development of a B27-dimer-specific antibody. Specifically, it would be invaluable for the study of B27 homodimer expression on the surface of healthy B27-positive individuals and B27-positive patients with AS. Christoph Renner's group has developed candidate B27 dimer-specific antibodies by Phage Display technology. A non-immunised human Fab repertoire, comprising V_L and V_H genes derived from a synthetic library and a pool of 7 mixed autoimmune patients respectively, was used to generate a pCES vector phagemid library of 1.5 x 10^{10} clones. Phagemids express the heavy chain fragments fused to a spike protein, in combination with separate expression of the light chain. These phagemids were screened positively against B27 homodimers (expressed in bacteria) and then screened negatively against B27 HT as described in section 8.4 (appendix).

In this chapter, I further investigate the biochemical properties of the B27 homodimer, map its ligand interactions and measure the affinities between the candidate antibodies and the B27 homodimer. These data support that HD6 will be a useful tool in *in vivo* experiments.

5.2 B*2705 homodimers do not contain peptide

Mass Spectroscopy analysis

Early observations have suggested that cell surface B27 "empty" molecules are peptide-receptive [75]. But whether peptide is present in the peptide-binding grooves of the covalently bound B27 homodimer is still unanswered.

Recombinant B*2705 heterotrimers (refolded with GAG peptide) and B*2705 homodimers (refolded with GAG, EBV or Hsp70 peptides) were refolded, and purified by size exclusion chromatography as discussed in section 2.4. These protein complexes were then analysed by MALDI Mass spectroscopy analysis by Kati DiGleria. The Mass/Charge (m/z) range where peptide should be present (≈1200Da) was carefully analysed for each sample. Figure 5.1 shows that in four separate B27 homodimer samples, no peptide peak corresponding to the synthetic peptide is identifiable. For the B27 HT refold, the GAG peptide peak is present at 1208Da.

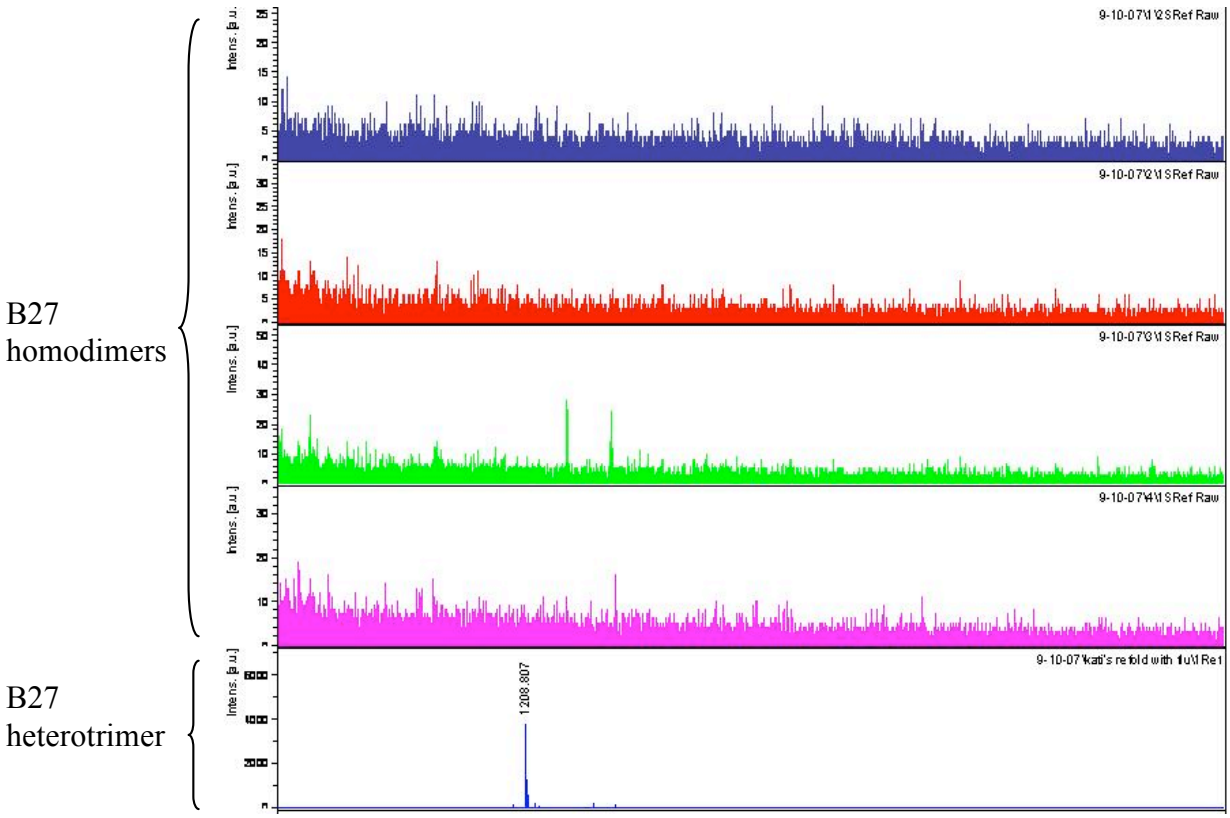


Figure 5.1 MALDI Mass Spectroscopy results for four B*2705 dimer refolds and one B*2705 heterotrimer refold. *B27 heterotrimer analysis reveals a peak of 40,000 a.u at an m/z of 1208Da, corresponding to the GAG peptide. B27 homodimers show no significant peak (above 15 a.u at this m/z value, note the difference in scales).*

*Refolding of B*2705 homodimers in the presence and absence of synthetic peptide*

B*2705 was expressed as inclusion bodies and then refolded in the presence or absence of synthetic GAG peptide (KRWIILGLNK). After refolding for 48hrs the solutions were concentrated on a pre-calibrated sd200 gel filtration column. The peak corresponding to homodimer was harvested and run on SDS-PAGE elecrophoresis gel to confirm its identity. This was repeated 3 times with consistent results. Figure 5.2 shows that B27 homodimers are able to form in the absence of synthetic peptide. It was observed that the B27 homodimers refolded in the absence of peptide were less stable than those refolded in the presence of peptide (data not shown).

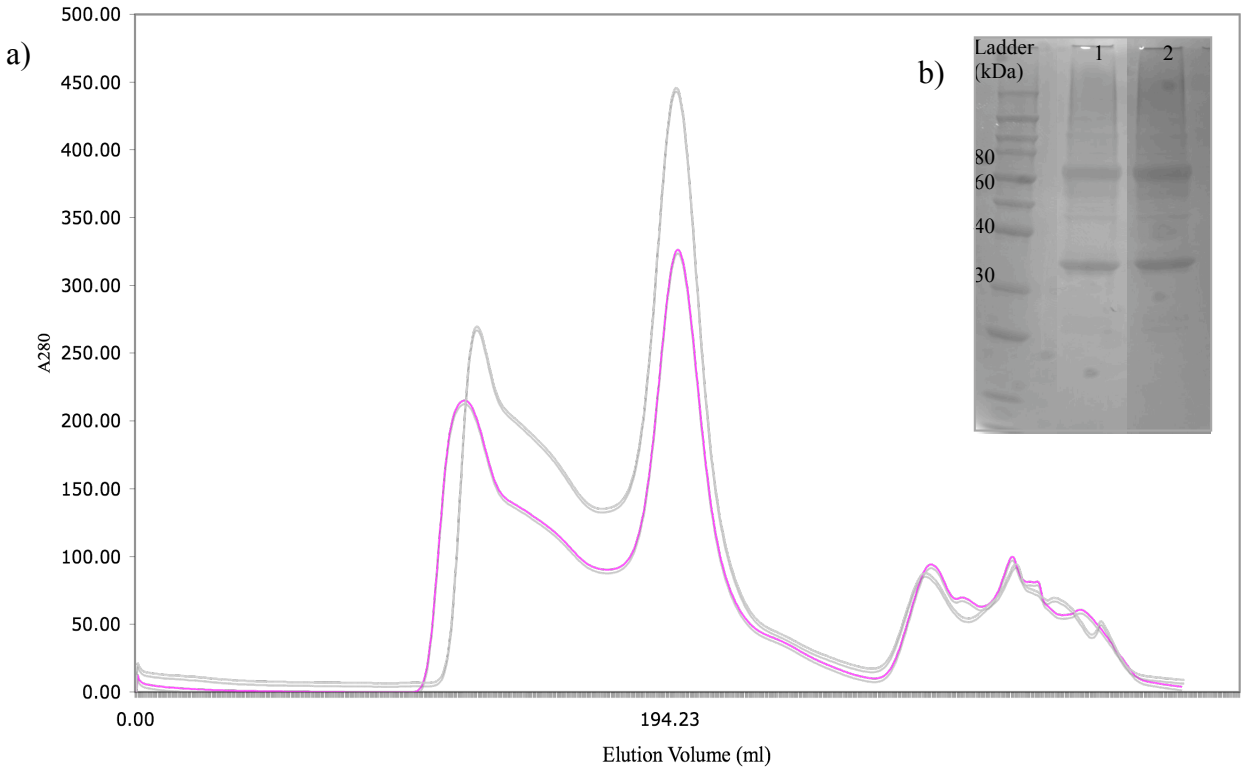


Figure 5.2 B*2705 homodimer formation in the absence of cognate peptide in an in vitro refold assay. *a) B*2705 forms homodimers in the presence of GAG peptide at an elution volume of ≈ 190ml (pink). B*2705 can form homodimers in the absence of peptide at an elution volume of ≈ 190ml (grey). b) SDS Non-Reducing gel of B*2705 homodimer with peptide (1) and without peptide (2).*

5.3 HD5, HD6 and HD8 bind to B27 homodimer, but not to B27 heterotrimer

HD5, HD6 and HD8 bind to B27 homodimer, but not B27 heterotrimer

In SPR experiments, HD5 (IgG), HD6 (IgG) and HD8 (Fab) were flowed over immobilised recombinant B*2705 homodimer and B*2705 heterotrimer in order to assess the specificity of binding. These were repeated 3-5 times for each antibody. Figure 5.3 shows that the antibodies all bind to immobilised B*2705 homodimer by SPR.

HD6, HD8 and HC-10 bind to B27 homodimer with high avidity and affinity

Measurements of the affinities between B*2705 (and B*2709) homodimer and antibodies were conducted by SPR. B27 homodimer was immobilised to a streptavidin-coated surface and increasing concentrations of antibody (for avidity measurements) or Fab (for affinity measurements) was flowed over the sensor surface. Between successive injections a regeneration step was incorporated in order to remove excess bound analyte from the ligand surface (fig. 5.4). Figure 5.5 shows that HD6 binds B*2705 and B*2709 homodimers with apparent K_Ds of 2.8nM and 1.3nM respectively. These values are comparable with ELISA studies performed using the HD6 antibody (S. Payeli, data not shown) and comparable to the avidity observed for HC-10 antibody binding to B27 homodimer (see figure 8.6, appendix). In order to measure the affinity for the 1:1 binding interaction, the Fab fragments of the antibodies were used as the analytes in SPR studies. Here it is shown that the K_D values for B27 dimer binding to HD6. HD8 and HC-10 are 280nM, 80nM and 220nM respectively (fig. 5.6).

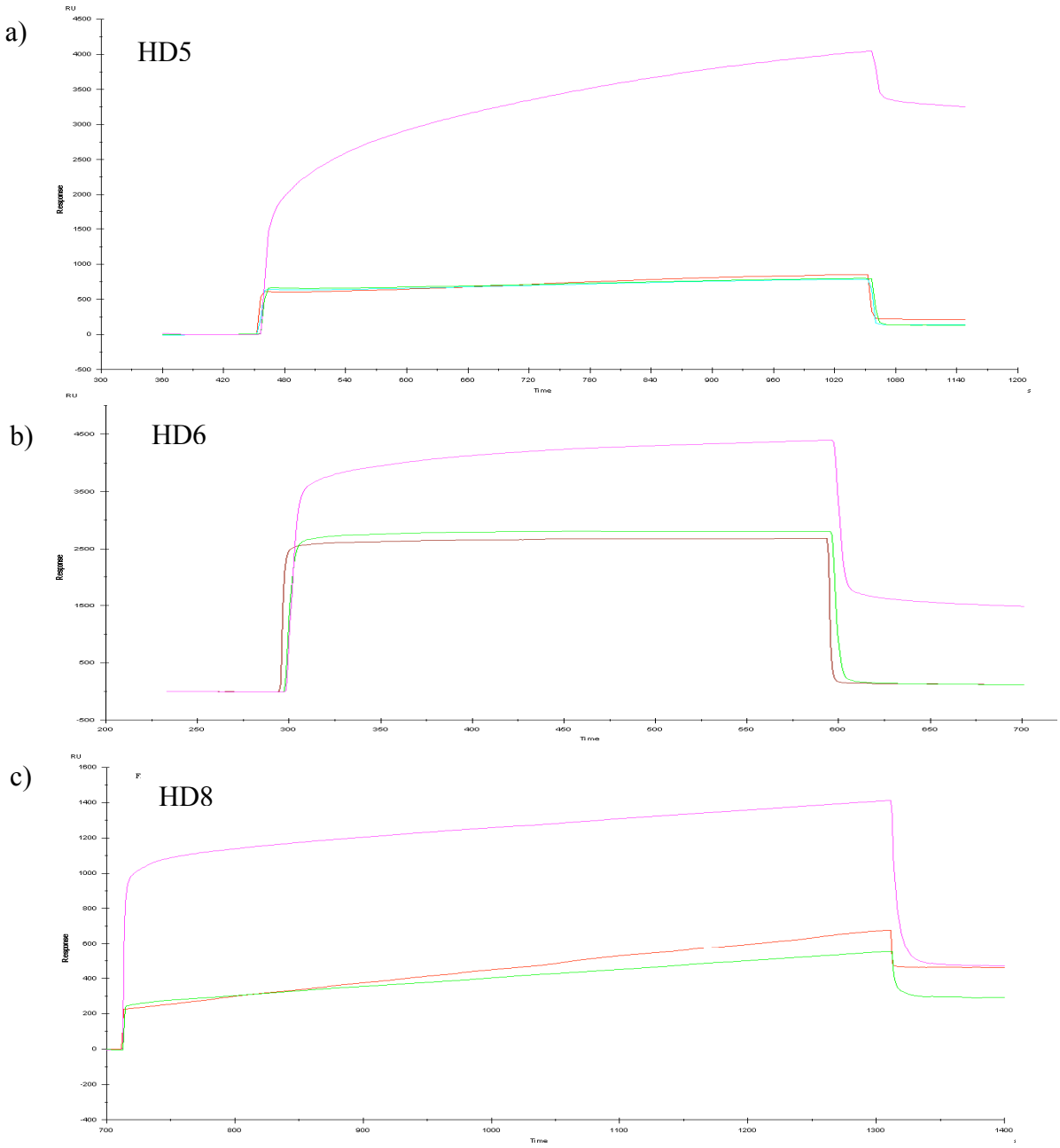


Figure 5.3 Candidate antibodies (IgGs) bind to B27 homodimers by SPR. *a) HD5 binding to B*2705 homodimer (pink), but not to B27 (GAG) heterotrimer (green) or empty flow cell (red) b) HD6 binding to B*2705 homodimer (pink), but not to B27 (GAG) heterotrimers (green) or empty flow cell (red) c) HD8 Fab binding to B*2705 homodimer (pink) but not B27 (GAG) heterotrimers (green) or empty flow cell (red).*

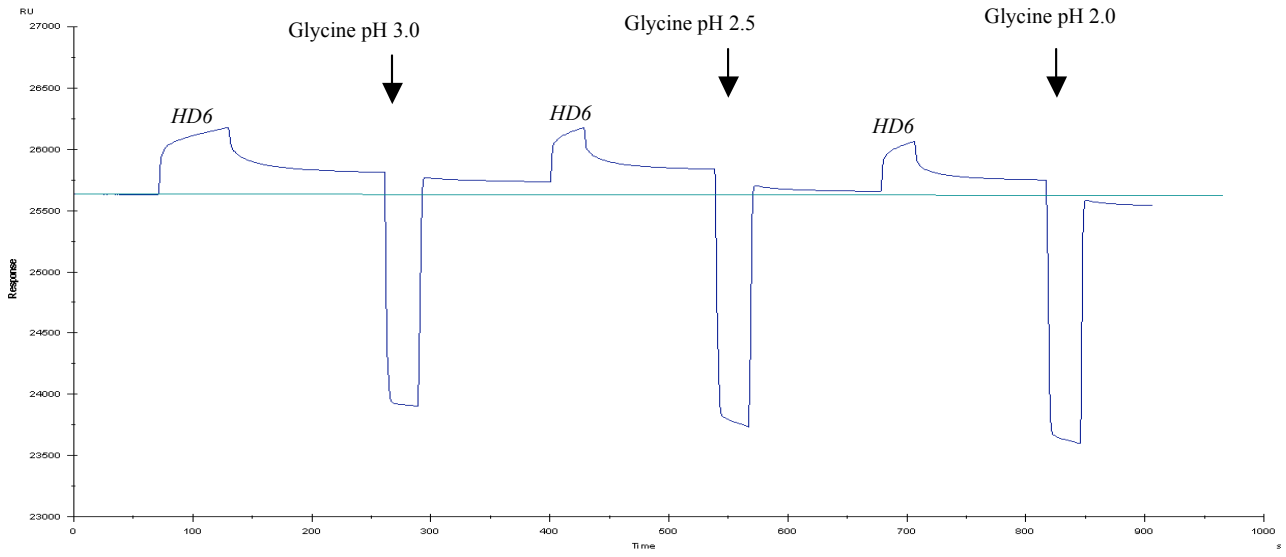


Figure 5.4 Glycine pH 2.5 was selected as a suitable pH for removing excess antibody from the immobilised B27 homodimer. *Glycine pH 2.5 removed excess HD6 antibody from the B*2705 homodimer complex without disturbing the baseline response for B*2705 homodimer immobilised on the chip. This suggests that the conformation and concentration of B*2705 immobilised onto the chip has not been compromised by the regeneration step.*

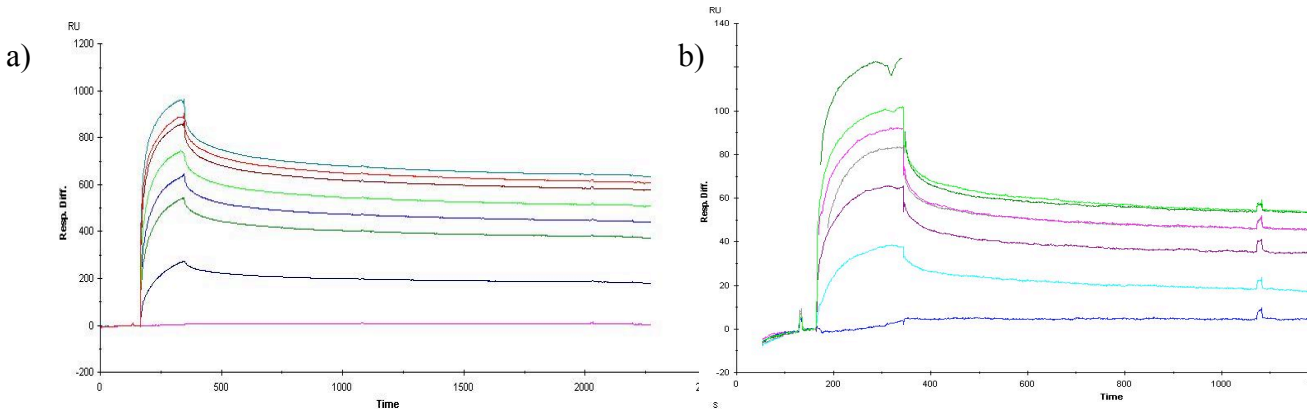


Figure 5.5 HD6 (IgG) binds to both B*2705 and B*2709 homodimers with high avidity. *HD6 antibody binds to a) B*2705 homodimer with a K_D value of 2.8nM. HD6 binds to b)B*2709 homodimer with a comparable K_D value of 1.3nM. Increasing concentrations of HD6 were flowed over the immobilised homodimer. The K_D values were calculated using the Langmuir fit on the Biaevaluate software as well as being plotted and analysed using Origin 7.5 (data not shown).*

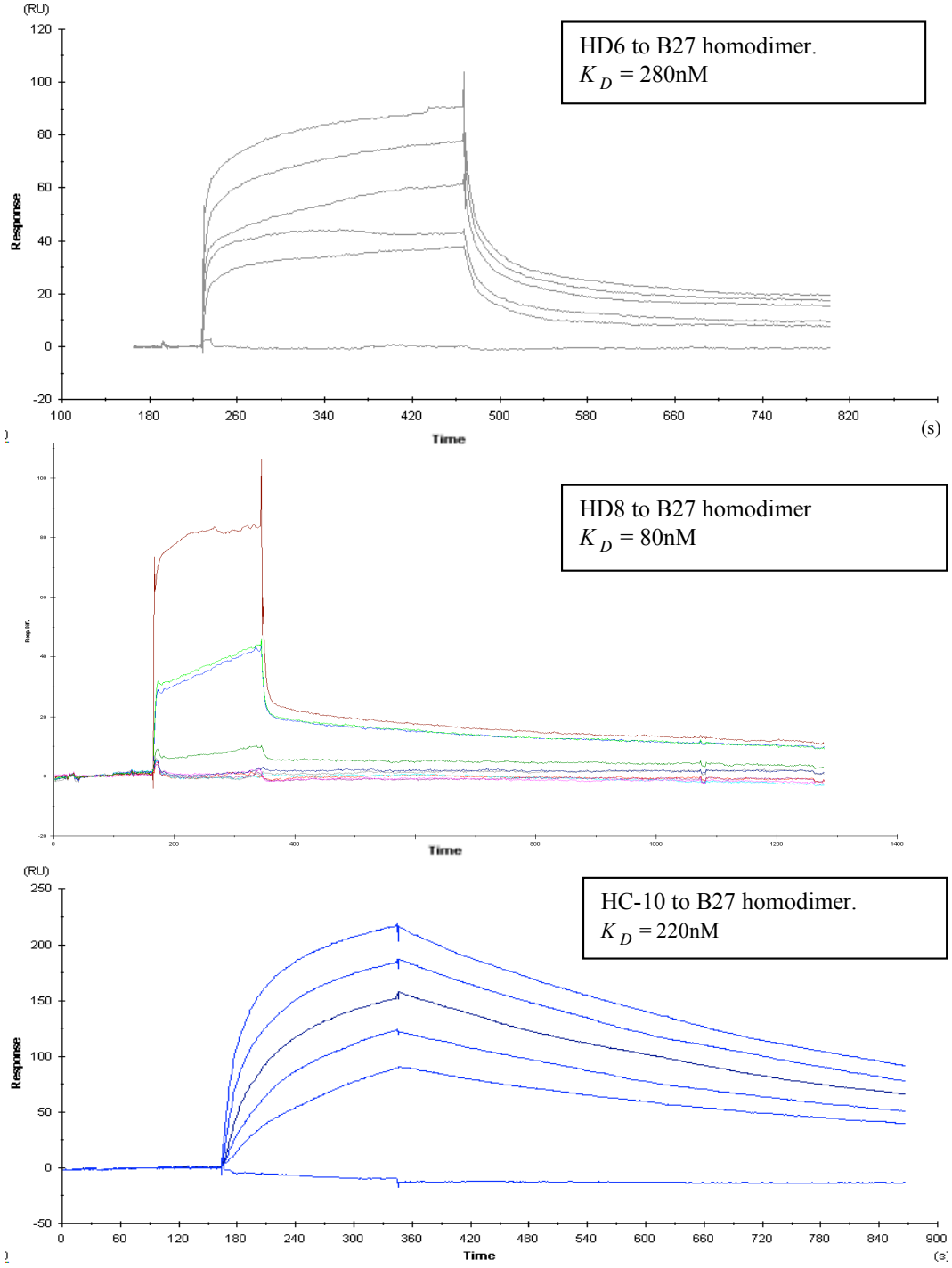


Figure 5.6 HD6, HD8 and HC-10 Fabs bind to B27 homodimer with high, and comparable affinities. *a) HD6 binds to B27 homodimer with K_D value of 280nM. b) HD8 binds to B27 homodimer with a K_D value of 80nM. c) HC-10 binds to B27 homodimer with K_D value of 220nM. Increasing concentrations of Fabs were flowed over the immobilised homodimer. The K_D values were calculated using the Langmuir fit on the Biaevaluate software as well as being plotted and analysed using Origin 7.5 (not shown).*

5.4 HD6 binds to B27 homodimers, but not to HLA-G homodimers

In order to assess whether the HD6 antibody was specific for B27 dimer, and not for other HLA dimer conformations, both biotinylated B*2705 homodimer, B*2709 homodimer and biotinylated HLA-G homodimer (made by Kimiko Kuroki and analysed by SDS PAGE) were immobilised to a streptavidin coated chip. HD6 was then flowed over and the response of binding was measured in real time. Figure 5.7 shows that HD6 binds to B*2705 and B*2709 homodimer, but does not bind to HLA-G homodimer.

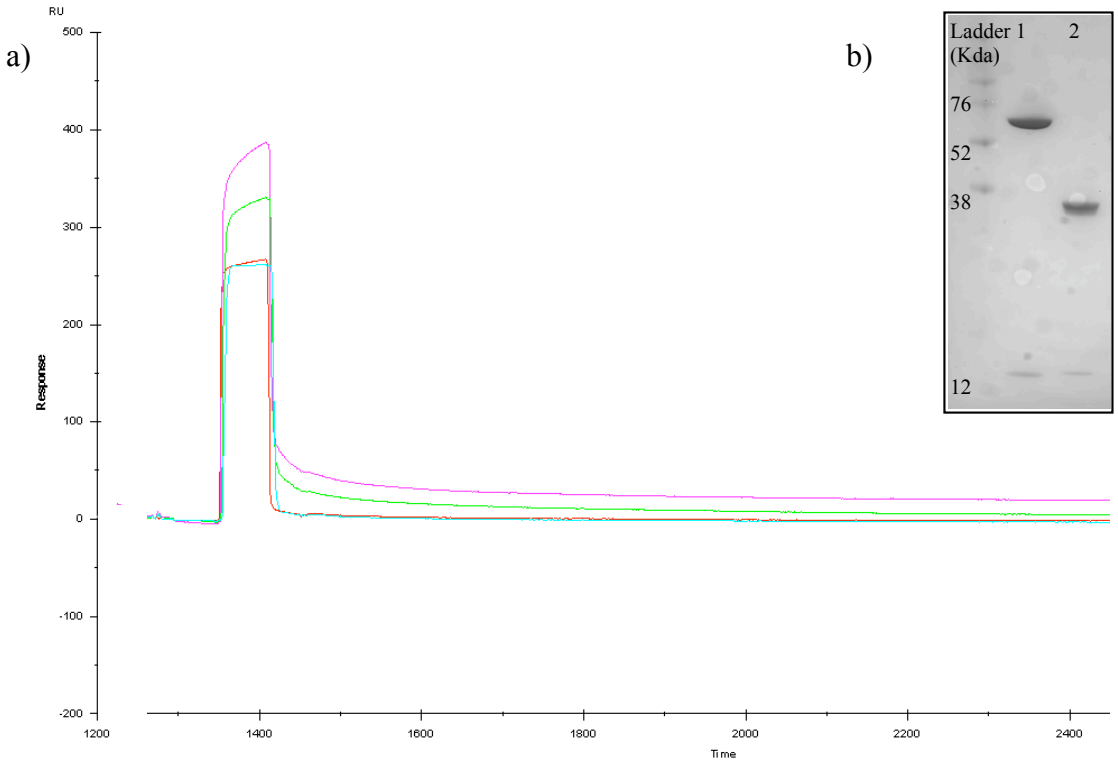


Figure 5.7 HD6 does not bind to HLA-G homodimers. *a) SPR experiment showing HD6 binding to B*2705 homodimer (pink), B*2709 homodimer (green) but not to HLA-G homodimer (blue) or empty flow cell (red) b) SDS gel showing HLA-G homodimer non reduced (1) and reduced (2).*

5.5 HD6 binds B*2705 free heavy chains, but not HLA-A3 nor HLA-G heavy chains

Having shown that HD6 could recognise B27 homodimers but not B*2705 heterotrimers, I extended these SPR studies to assess whether the antibody was recognising a specific conformation or sequence also present on the B27 free heavy chains. Biotinylated B*2705 HT and HLA-B27 homodimers were immobilised to a streptavidin- coated chip. Glycine pH 3.0 was flowed over the chip to remove peptide and β_2m. BBM-1 was next injected over the chip in order to confirm that all β_2m was removed from the chip. HD6 (IgG) was injected and binding between ligand and analyte was monitored in real time. Figure 5.8 shows the sensogram, showing that B*2705 free heavy chains bind to HD6. No binding is observed with HLA-A3 heavy chains, HLA-G free heavy chains and the negative control (empty flow cell). These experiments were also repeated in the presence of DTT to ensure that homodimer formation was not occurring prior to analyte injection.

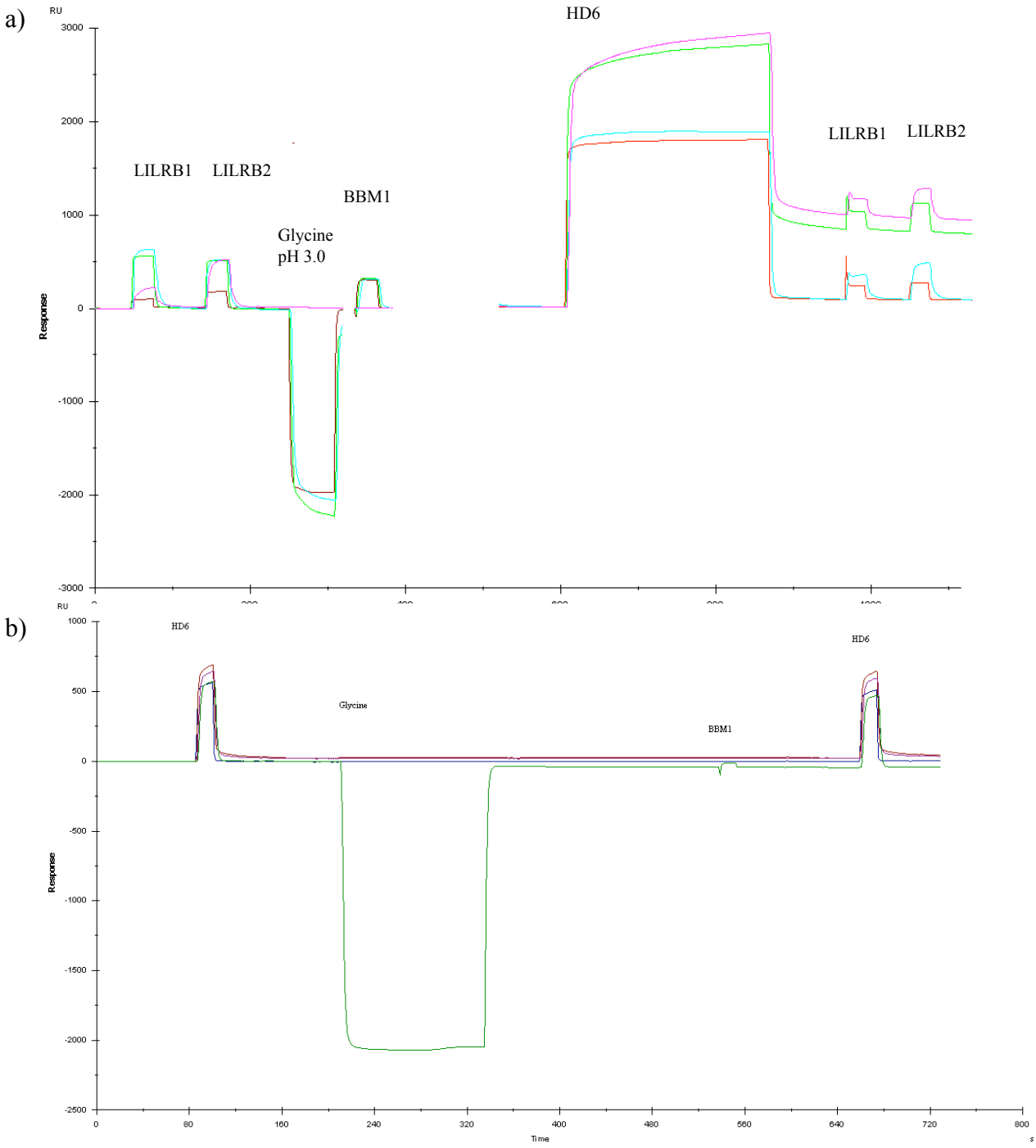


Figure 5.8 HD6 binds B*2705 homodimer and B*2705 heavy chains, but not HLA-G heavy chains or HLA-A3 heavy chains*. SPR experiments (as described in section 2.6.7) show that a) HD6 binds to B*2705 homodimers (pink) and B*2705 heavy chain (green) but not to HLA-A3 heavy chain (blue). b) HD6 binding to B*2705 homodimer (pink) but not to HLA-G heavy chains (green).*

5.6 HD6 does not compete with LILRB2 for B*2705 homodimer binding, but HC-10 partially competes

Antibody blocking experiments

The binding epitopes of the candidate antibodies were further investigated by observing their capacity to block the binding of the B*2705 homodimer to LILRB2 in SPR experiments. Immobilised onto separate flow cells of a streptavidin- coated chip were B*2705 homodimer and heterotrimer. LILRB1 and LILRB2 were injected and the binding responses measured. Next, the candidate antibody was injected until binding had saturated. This injection was followed by further injections of LILRB1 and LILRB2. The binding response for LILRB2 was compared before and after antibody binding. Figure 5.9a shows that the HD6 antibody does not block LILRB2 binding to B*2705. This observation was repeated 3 times, using different batches of HD6. This was also repeated for HD6 Fab (fig. 5.9b), HD5 antibody (fig. 5.10) and HD8 Fab (fig. 5.11).

The blocking ability of HC-10 was also investigated by SPR. Figure 5.12a shows that, in contrast to HD6, HC-10 diminishes the binding response between B*2705 homodimer and LILRB2 by half (1280RU compared to 2500RU). This experiment was also repeated 3 times with consistent results. To characterise the binding epitope of HC-10, the Fab fragment was used in order to eliminate the bivalent nature of binding of the HC-10 antibody and to reduce steric hindrance caused by use of the whole antibody molecule. Figure 5.12b shows that the binding of LILRB2 to the B*2705 homodimer is reduced by a quarter after HC-10 Fab injection (binding response before HC-10 Fab binding was 910RU where binding response after HC-10 binding was 660RU).

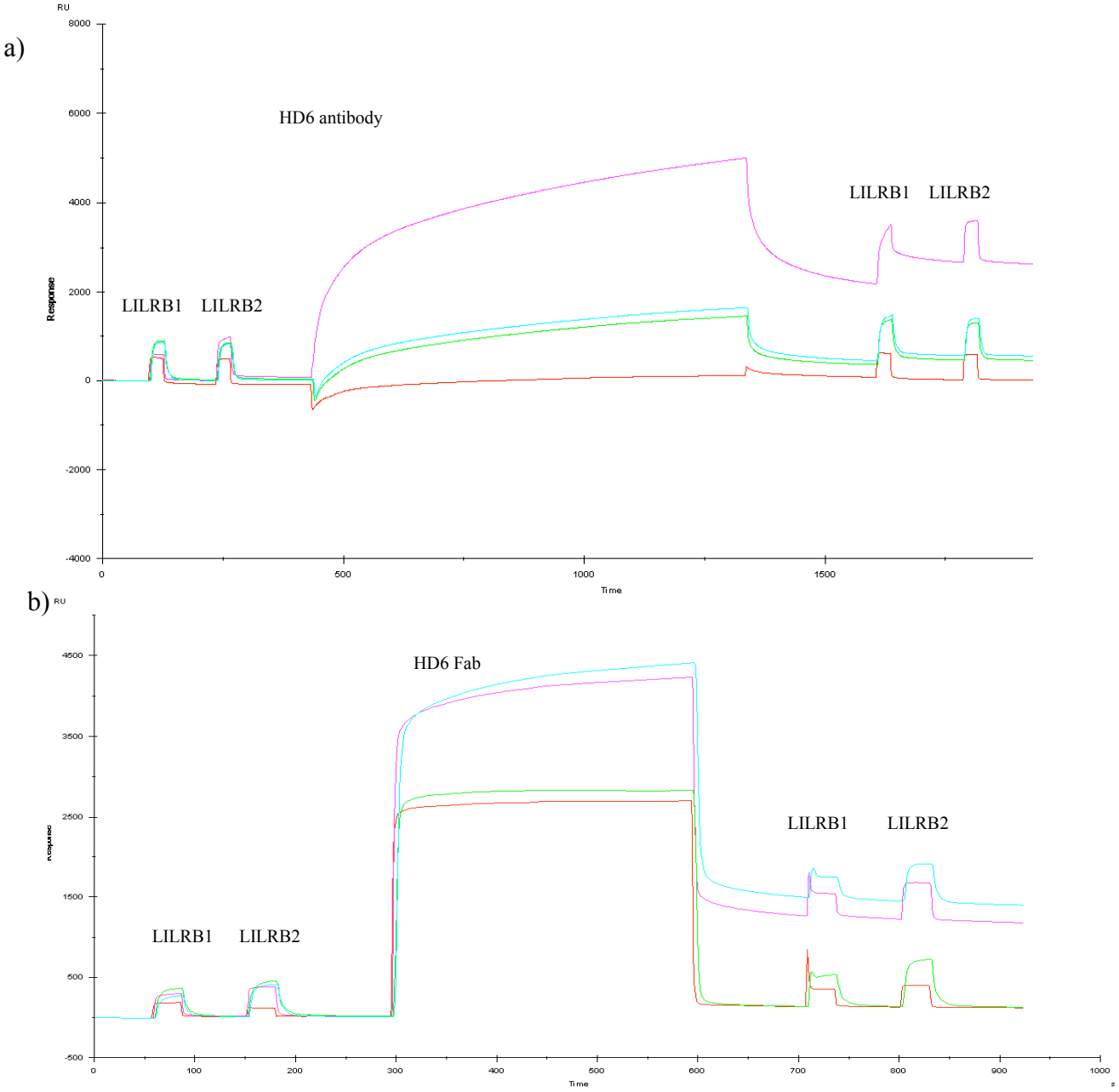


Figure 5.9 HD6 does not compete for LILRB2 binding to B*2705 homodimer. **a)** *SPR sensogram for LILRB1 and LILRB2 binding before and after HD6 binding. Sensograms shown are for B*2705 homodimer (pink), B*2705 heterotrimer (refolded with EBV peptide)(blue), B*2705 heterotrimer (refolded with GAG peptide)(green). b) SPR sensogram for LILRB1 and LILRB2 binding before and after HD6 binding. Sensograms correspond to HD6 Fab binding to B*2705 homodimer (pink) B*2709 homodimer (blue) and B*2705 heterotrimer (green). Red is empty flow cell for negative control.*

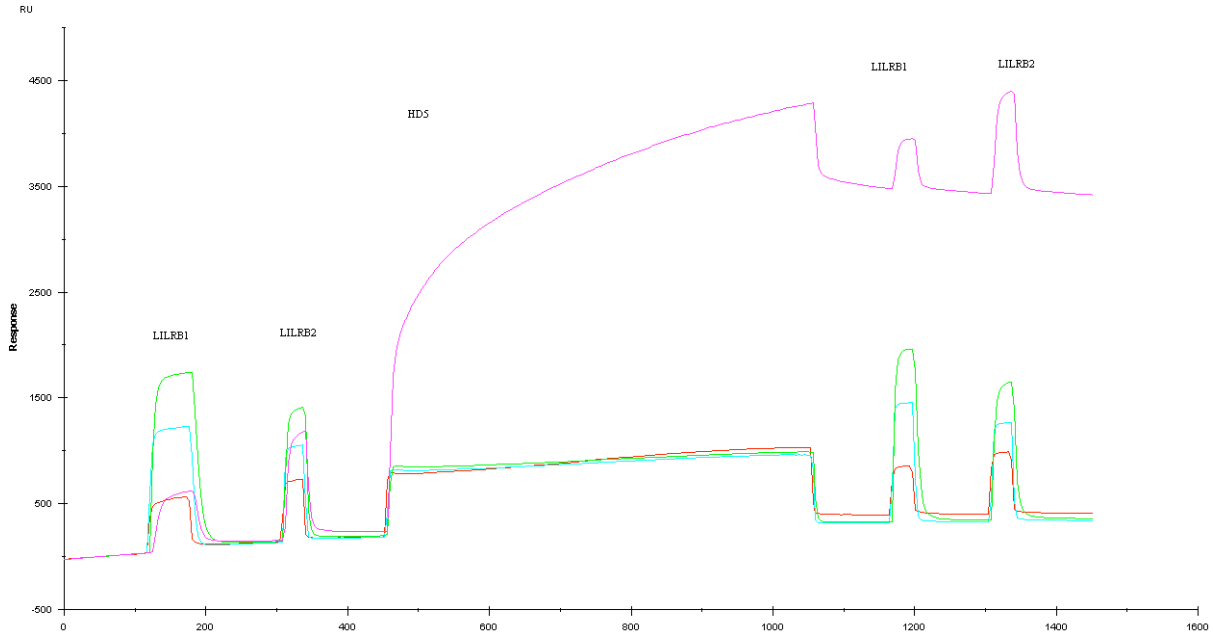


Figure 5.10 HD5 does not compete for LILRB2 binding to B*2705 homodimer. *SPR sensogram for HD5 binding to B*2705 homodimer (pink), B*2705 heterotrimer (refolded with GAG peptide)(blue) and HLA-A3 heterotrimer (green).*

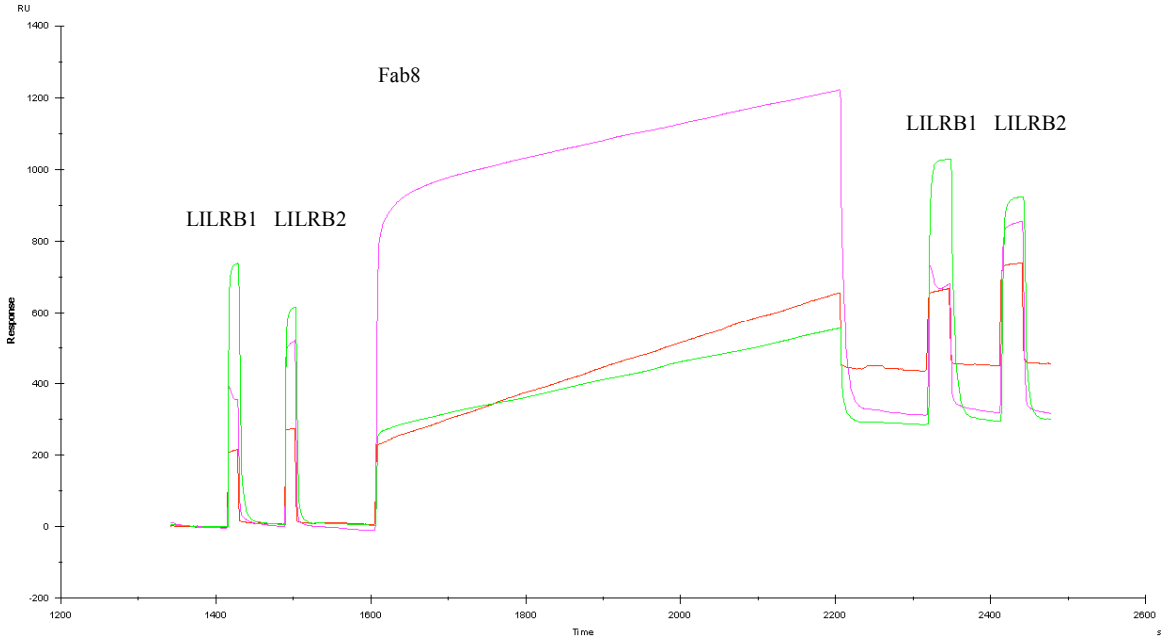


Figure 5.11 Fab of HD8 does not compete for LILRB2 binding to B*2705 homodimer. *SPR sensogram for Fab of HD8 binding to B*2705 homodimer (pink), B*2705 heterotrimer (refolded with EBV peptide)(green), empty flow cell (red).*

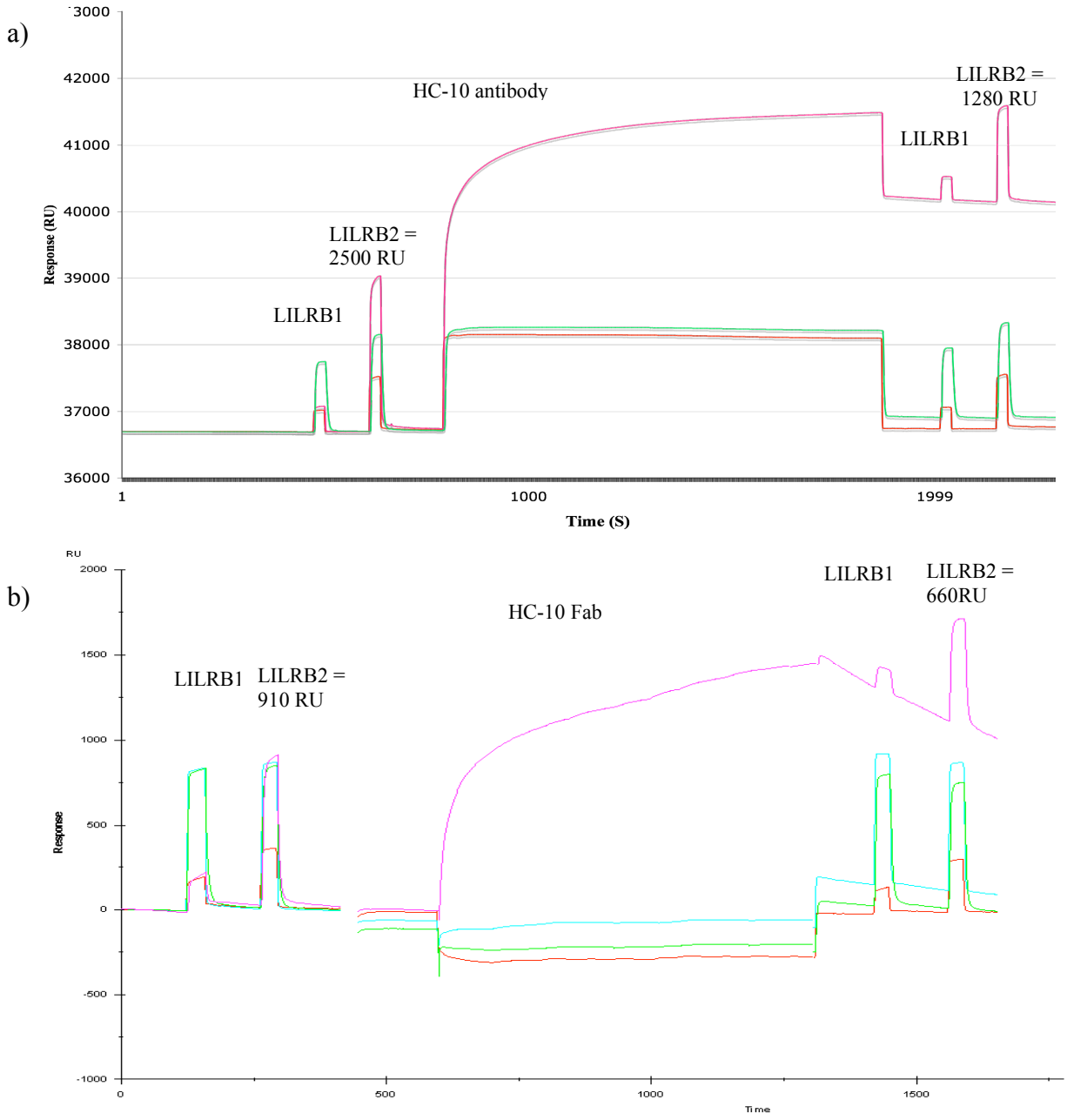
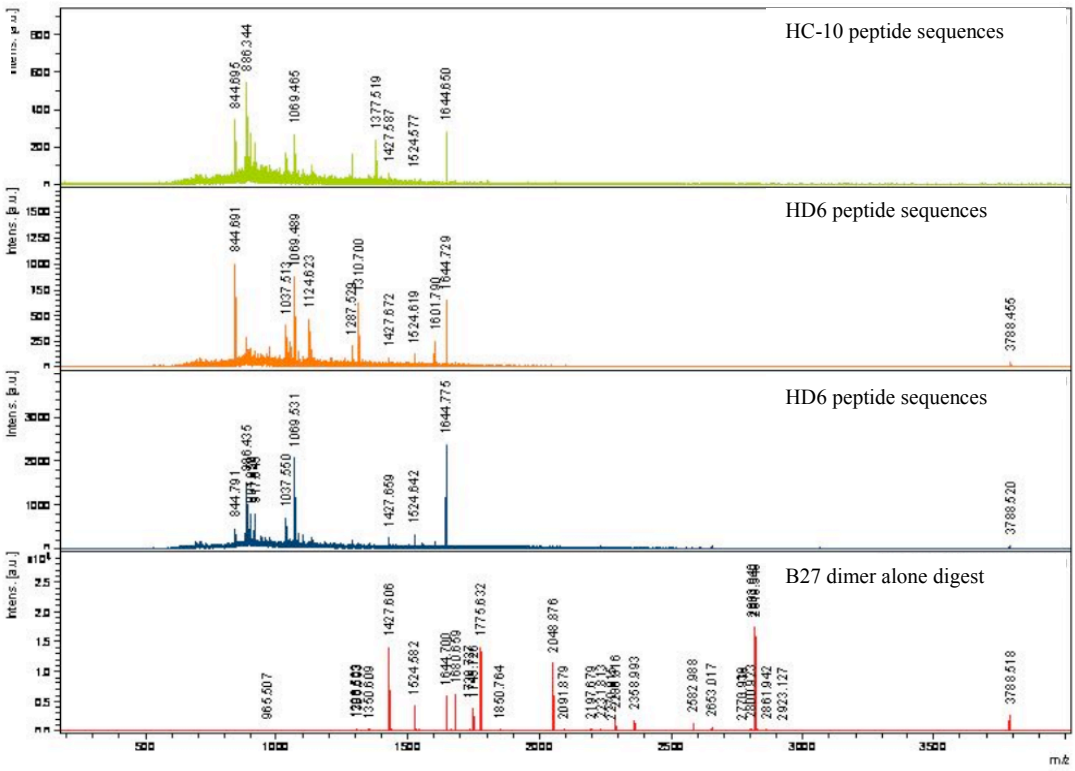


Figure 5.12 HC-10 Antibody binding diminishes the binding between B*2705 homodimer and LILRB2. *A) Sensogram showing the response of LILRB1 and LILRB2 binding before and after HC-10 antibody binding. b) Sensogram showing the response of LILRB1 and LILRB2 before and after HC-10 Fab binding.*

5.7 Epitope mapping of B*2705 dimer : HD6 interaction

I hypothesised that the epitope for HD6 could be an unfolded B27 sequence, only present in the β_2m- and peptide- free forms of B27. In order to investigate this, epitope mapping by Mass Spectroscopy was undertaken as described in section 2.7. Here, B*2705 homodimer was digested using Trypsin, and then incubated with HD6 or HC-10. Next the mixture was incubated with Protein A beads. The beads were then washed and then acid- treated to remove and isolate any bound peptide. The peptides were analysed by Mass Spectroscopy. The mass spectroscopy results from two (out of four) epitope mapping experiments show that a possible epitope of the HD6 antibody may be found within a 3,787Da peptide fragment. This 3,787Da peak is present in two experiments for HD6 mapping to the B27 dimer, but with no peak above background in HC-10 mapping experiment. The peaks visible before an m/z value of approximately 1100Da are due to matrix-associated peptides. All peptides, including the possible epitope, would be unfolded, due to the trypsin digestion and acid treatment undertaken in the procedure. The mass of 3,787Da was used in a Mascot search and was found to correspond to one B27 specific peptide located in the α2 domain of the B27 chain (fig. 5.13).

a)



b)

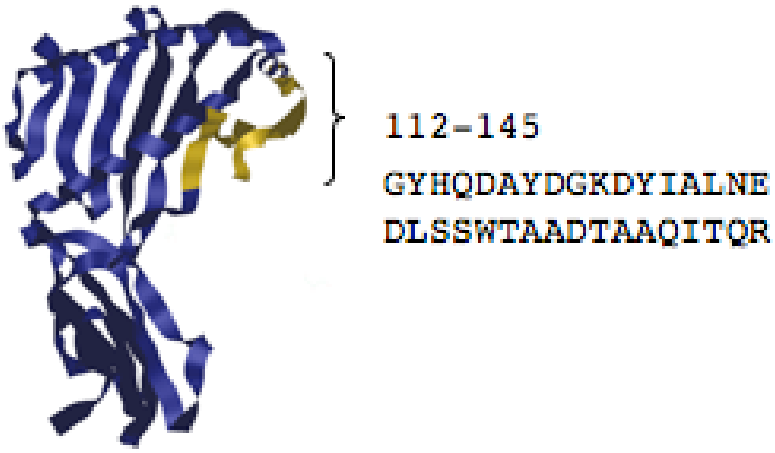


Figure 5.13 Epitope mapping of the HD6 interaction with B27 by Mass Spectroscopy. *a) the mass spectroscopy data showing peptides present after antibody-mediated isolation. The peptide of mass 3787Da is present in the B27 digest, and HD6 isolation experiment, but not in the HC-10 isolation experiment. b) Mascot search result show that the 3,787kDa corresponds to one B27 sequence (shown). The position of the identified peptide epitope is highlighted yellow in the B27 molecule.*

5.8 Discussion

In this chapter I investigate important structural characteristics of the B27 homodimer; specifically I show that there is no peptide present in the peptide-binding groove. In addition, I characterise the specificities and affinities of 3 new candidate B27- dimer-specific antibodies, and of the routinely used heavy-chain specific antibody, HC-10.

Data presented in section 5.1 show that there is no synthetic peptide present in the *in vitro* refolded and purified B27 homodimer preparations. This result is in accordance with previous hypotheses that antigenic peptide does not sit stably in the peptide-binding groove of B27, in comparison to other HLA class I molecules. The B27 homodimer theory postulates that a heterotrimeric complex at the cell surface "falls apart" due to an inadequately binding peptide, and this leads to B27 homodimer formation through endosomal recycling (section 1.10). Thus, without β_2m, it would be expected that the B27 homodimer would not bind its peptide very stably. This has never been shown before, and here I show that the peptide used in the refolding conditions is not present in the final purified complex by mass spectroscopy (fig. 5.1). This observation contradicts previous reports [21] suggesting that peptide could be eluted from the B27 homodimers. However, it is worth noting that this previous observation was made *in vivo* where there may have been other peptide contaminants. The absence of peptide noted here might explain the peptide-independence of binding reported by Kollnberger [58]. Finally, it was noted that the B27 homodimers refolded in the absence of peptide (fig. 5.2) appeared to be less stable than those refolded in the presence of synthetic peptide (data not shown). This observation suggests that the peptide has a role in the folding of the homodimer structure, where the peptide may assist in the folding of a more tightly

folded and a more stable tertiary structure. The absence of peptide in the peptide-binding groove may also allow the B27 homodimer to adopt a less rigid structure, allowing it to bind to innate receptors with more flexibility. This may then explain the observations in chapter 3, where the B27 homodimer binds to LILRB2 with a higher affinity than the B27 HT. The higher affinity interaction could be explained by flexibility of some of the B27 homodimer molecules allowing the formation of multiple binding contacts.

The candidate B27 dimer-specific antibodies investigated in this chapter have all been shown to bind to B27 homodimers with strong avidity and modest affinity by SPR (K_D between 280nM and 80nM). In addition, they have been shown not to recognise the correctly folded B27 heterotrimer complex (fig. 5.3). The affinities calculated for the candidate antibodies were comparable to the HC-10 monoclonal antibody (K_D = 220nM) and are also consistent with values for a highly selected mAb (as shown in previously published data [118]). Scatchard plots are not presented, as the antibody binding to the immobilized B27 was not an equilibrium reaction.

In order to further investigate the specificity of HD6, I have shown that HD6 can epitope B27 heavy chains, but not HLA-G homodimers or HLA-G heavy chains, and not HLA-A3 HT or heavy chains. From these specificity experiments, I believe that the HD6 antibody epitopees a β_2m-free epitope that is common to both the B27 homodimer and the B27 free heavy chains, but not to the correctly folded B27 heterotrimer. Such an epitope could correspond to a possible molten globule epitope of B27, which would be a partially unfolded epitope lacking a tightly packed structure, although further experiments such as Circular Dichroism of the B27 molecule would be needed to confirm this.

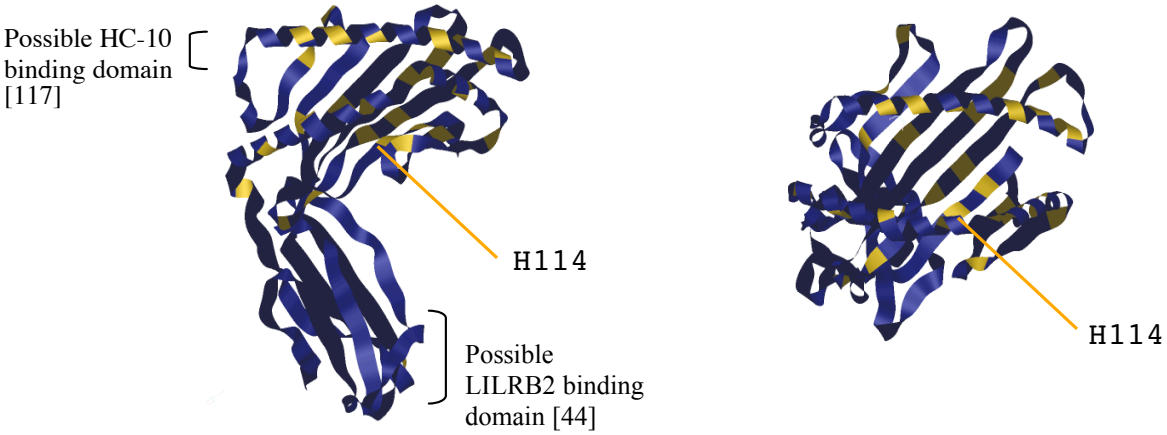
I then assessed the capacity of HD6 to compete for LILRB2 binding to the B27 homodimer. I observed that the HD6 binding did not interfere with LILRB2 binding by SPR, suggesting that the HD6 epitope is distinct and distal to the LILRB2 interaction. On the other hand, HC-10 was shown to partially compete with LILRB2 binding in six separate experiments, with the binding of LILRB2 to the B27 homodimer shown to be reduced by a quarter when saturated with HC-10 Fab (such an effect was also observed in FACS blocking experiments performed by Jackie Shaw (data not shown) and so is likely to be significant). This could be explained by the LILRB2 and HC-10 perhaps sharing an overlapping binding site; it may be possible that a second binding site is conformationally close to the HC-10 epitope leading to some competition when Fab is bound. Crystal structures have shown that the D2 domain of LILRB2 interacts with the β_2m moiety of the correctly folded HLA-G molecule. In the absence of β_2m, the D2 domain of LILRB2 may be able to form further contacts with the free heavy chain possibly in close proximity to (or overlapping) the HC-10 epitope on B27. This would explain why HC-10 diminishes the binding of LILRB2 to B27 homodimer, but does not abolish it.

The Mass Spectroscopy epitope mapping experiments have revealed a possible unfolded binding epitope for the HD6 interaction with B27 at positions 112-145. This result was observed in two separate experiments, but was found at a very low intensity compared to the starting material, and was not observed in two subsequent epitope mapping attempts. However, the peptide identified in this study is known to be a trypsin miscleavage product (where the digestion of the B27 by trypsin was not complete) and this would explain why the peptide was not observed in every experiment. Also, it is possible that the actual epitope has some partial folding properties, which would become completely denatured in this particular

epitope mapping process, and this would explain why the epitope was only observed at a low intensity.

In order to begin mapping the HD6 epitope, the sequence differences between HLA-B27 and HLA-G were aligned using BLAST (http://blast.ncbi.nlm.nih.gov/Blast.cgi) (fig. 5.14). Sequence alignment of several HLAs in the binding region (position 112-145) was performed and it revealed that the H114 in B27 is unusual (fig. 5.14). Interestingly, this residue is located in the β sheet region of the α2 domain, and so will be flat in its folded conformation (just as an unfolded peptide could be). This may well be a key residue for the HD6 and B27 interaction (fig. 5.15). In further support of position 114 in a possible HD6 epitope, the avidity of HD6 for binding B*2709 is shown to be twice as strong as that observed for B*2705 (fig. 5.5). This would suggest that the polymorphism at position 116 can also influence the binding of the HD6 antibody. Although the peptide identified is consistent with the discussed SPR based mapping experiments, the Epitope requires further characterisation. At present the peptide sequence of this region is being synthesised by Kati DiGleria and will be used to test for binding by the HD6 antibody (by ELISA), or competition with B27 for binding in cell based assays. From previous structural and mapping studies, I have developed a model for the binding of the B27 ligands. This attempts to explain why some of the molecules compete for interactions whereas others do not (fig. 5.15).

a)



b)

```
            112  116                                  145
HLA- A*0101 GYRQDAYDGKDYIALNEDLRSWTAADMAAQITKR
HLA- A*0301 ------------------------------------
HLA- B*2705 --H----------------S------T-----Q-
HLA- B*4001 -HN-Y--------------------T----SQ-
HLA- B*1401 --N-F--------------S------T-----Q-
HLA- B*5301 -HD-S--------------S------T-----Q-
HLA- C*0201 --D-S--------------------T-----Q-
```

Figure 5.14 Sequence differences between B27 and other HLAs. *a) This model of B27 shows the sequence similarities (blue) and the residue differences (yellow) between B27 and HLA-G. This figure shows a side view of the model and a top view of the peptide-binding groove, this is where most of the differences are found. b) Alignment of HLAs with HLA-A*0101 for the identified sequence reveals an unusual His present in B*2705 at position 114.*

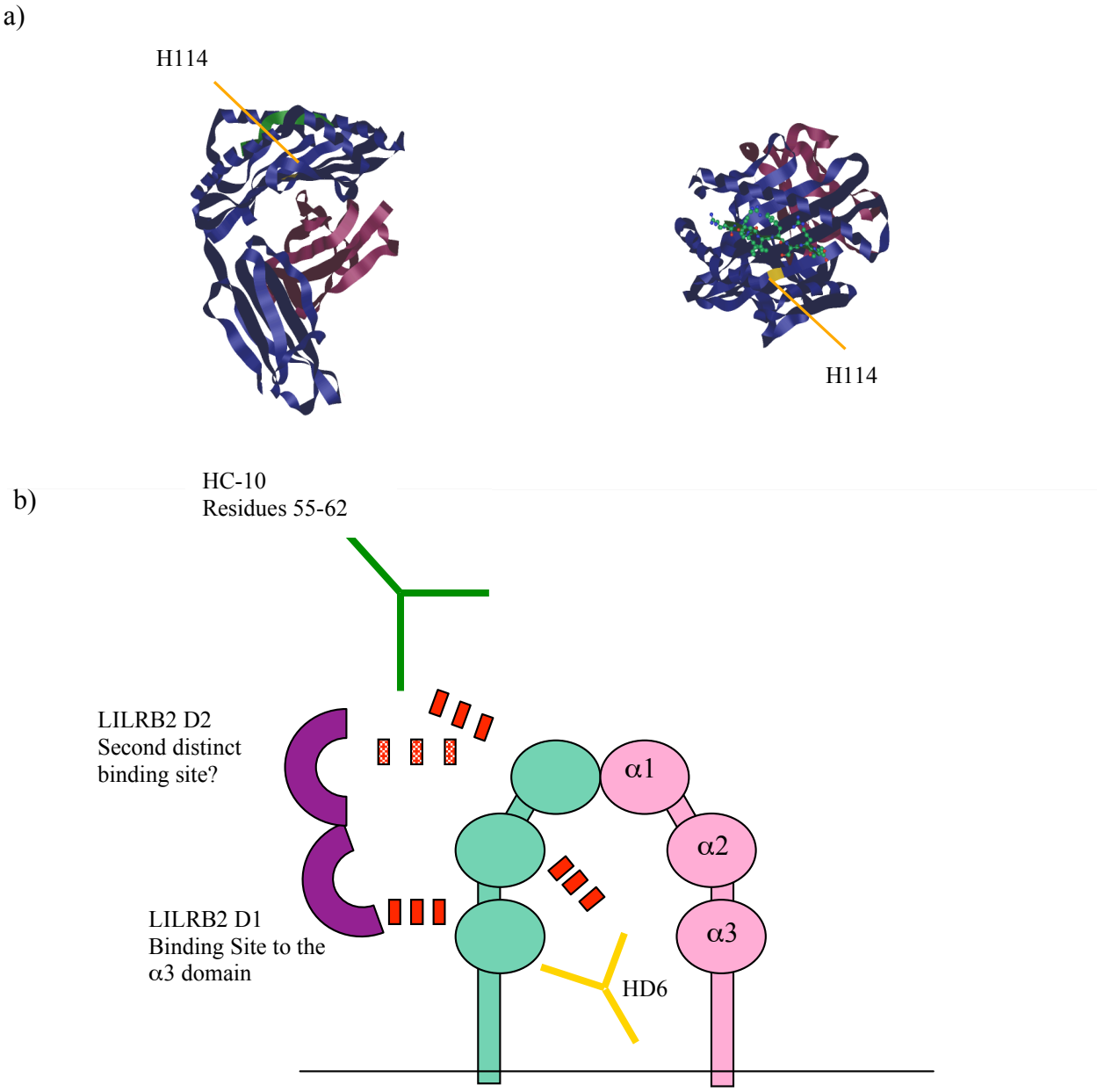


Figure 5.15 Model for ligand binding interactions with B27 homodimers. *a) Side view (left) and top view (right) of position 114 in HLA-B27. Epitope mapping studies show that position 114 may be important for HD6 binding. This position is hidden (by the peptide and* β_2*m) from HD6 when B27 is classically folded. HD6 could bind to this epitope either from the top or from the bottom when peptide and* β_2*m are absent. B) Cartoon showing ligands of B27. The heavy chains of B27 homodimer (pink and turquoise) are able to interact with LILRB2 domains D1 and D2 (purple), HC-10 antibody (green) and HD6 antibody (yellow).*

Chapter 6 – B27 homodimer expression and purification for Crystal trials

6.1 Introduction……..154

6.2 B27 homodimer purification ……...155

6.3 B27 homodimer : Fab of HD8 complex purification……...159

6.4 Crystal screening, optimisation and additive screen ……...161

6.5 Discussion …….……..167

6.1 Introduction

The crystal structure of the classically folded B27 heterotrimer has been solved in complex with a variety of peptides and some ligands [16, 49]. This structure has been invaluable to our understanding of the folding, recognition properties and stability of the molecule. In order to fully understand the function of the B27 homodimer at a molecular level, it will be important to obtain a crystal structure of the protein. Such a structure would reveal important details of its bonding nature, energetics and its ability to interact with different ligands.

In this chapter I explain how I have optimised the purification of the bacterial expressed recombinant B*2705 homodimer for crystallographic studies and prepared the groundwork for crystal trials by identifying initial crystal forming conditions. I have also developed a mammalian expression system for the B27 homodimer, should the bacterial expression system not yield protein of sufficient quality for crystal trials (see appendix section 8.6). B*2705 was selected in each of these systems because of better protein yields (compared to B*2709) as shown in chapter 4. Work described in this chapter will be used in future crystallography studies in order to elucidate the structure of the B27 homodimer.

6.2 B*2705 homodimer preparation

I first analysed the purity of refolded B*2705 homodimer protein (with a 6-histidine tag), as described for the previous biophysical experiments (section 2.4). These preparations did not yield protein of the high purity required for crystal screening (multiple bands in protein preparation some B27 heavy chains present). Figure 6.1 shows the purity of B27 homodimer obtained from the standard B27 homodimer refold and separation using an sd200 column. In order to maximise B27 homodimer refolding and purification, a refold was performed using a linked di-peptide (fig. 6.2a). The purpose of refolding using the linked di-peptide was to attempt to refold as much stable B27 homodimer as possible, and to bring the two free heavy chains to close proximity for bonding. Refolding using this linked di-peptide did yield stable homodimer, but did not appear to increase the purity or yield compared to the previous refolds. In addition SDS PAGE analysis revealed there was β_2m present in the harvested fractions (fig. 6.2). In a further attempt to obtain protein of high purity, inclusion body extracts were purified using a Nickel Affinity Column, and then refolded with HPLC-purified GAG peptide by limiting dilution and further purified by size exclusion Chromatography (fig. 6.3). These protein preparations were of high purity and sent to a collaborator's lab for crystal screening, where no crystal growth was observed.

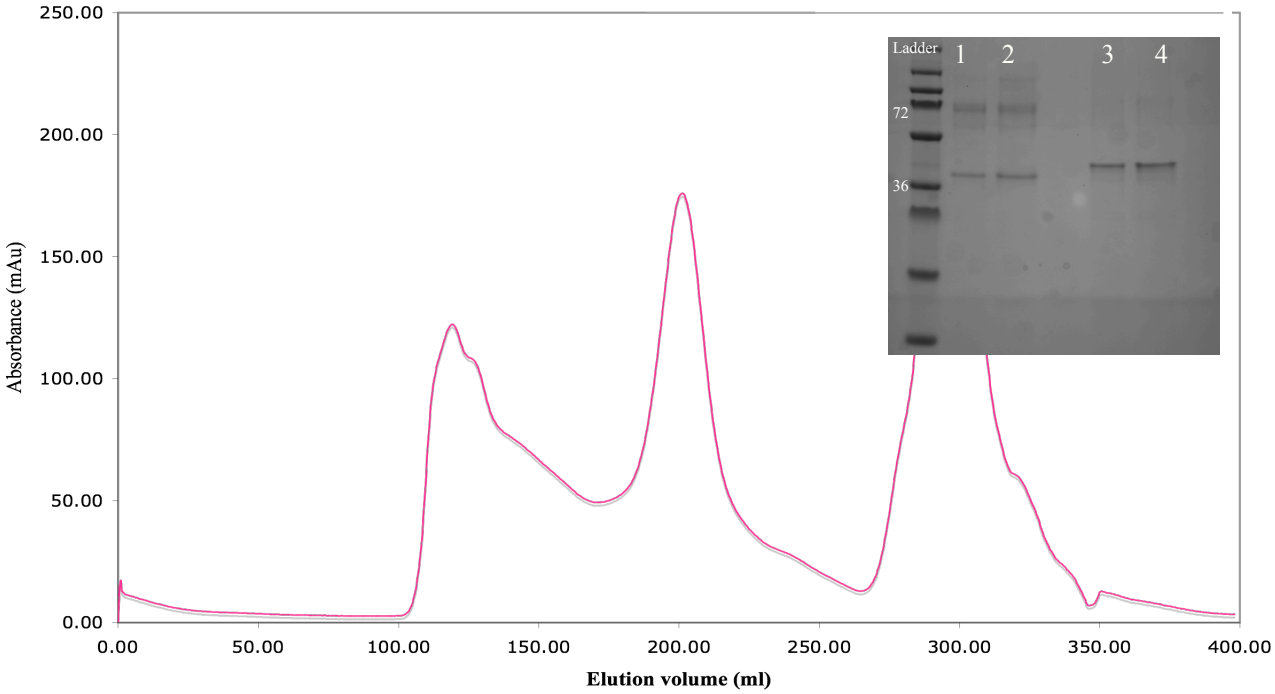


Figure 6.1 B*2705 homodimer refold and purification. *a) Size exclusion chromatography using the sd200 column. B27 homodimer elutes at 190ml. b) purity of non reduced B27 homodimer with (1) and without (2) iodoacetamide and reduced B27 homodimer with (3) and without (4) iodoacetamide.*

a) KRWIILGLNK - GGGGGG - K - GGGGGG - KRWIILGLNK
(resin)

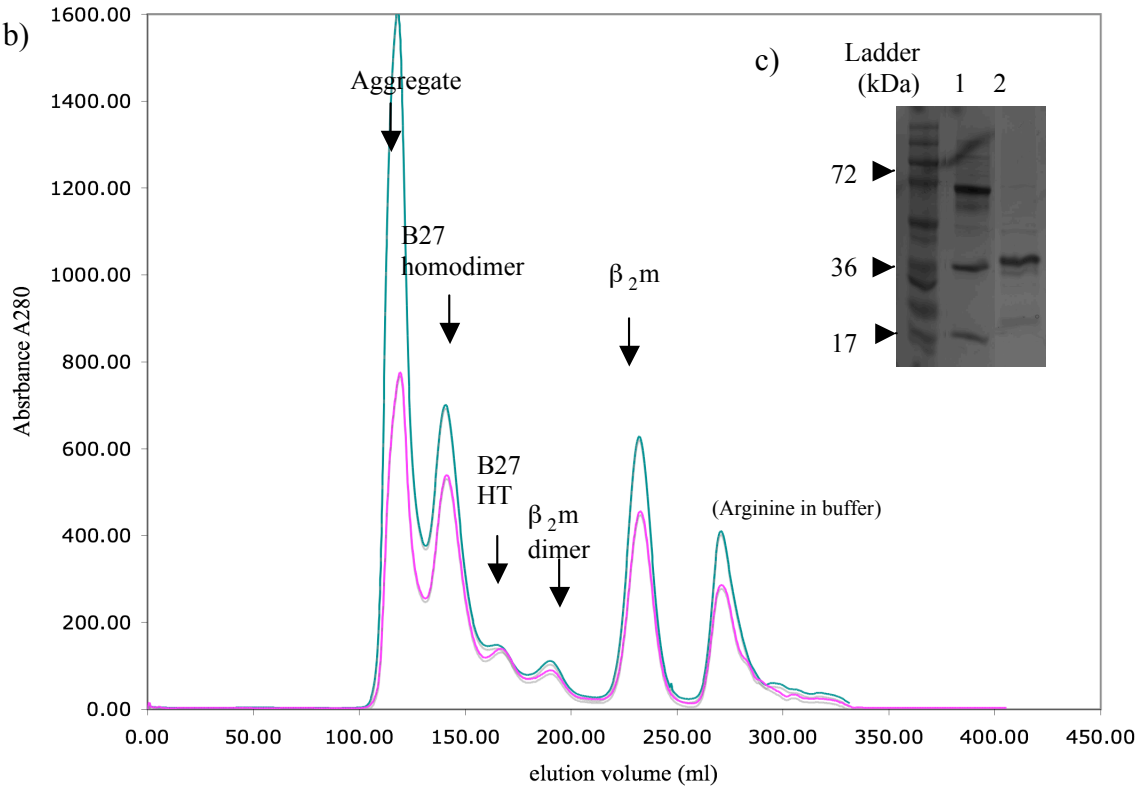


Figure 6.2 B*2705 refolding in the presence of the GAG linked di-peptide and β 2m (blue).

*a) Sequence of GAG linked di-peptide b) Size exclusion chromatography using Sd75 column. B27 homodimer elutes at 150m for refolds using both the di-peptide (blue) and the GAG peptide (pink) c) SDS PAGE gel of non-reduced (1) and reduced (2) B*2705 homodimer (when refolded with the dipeptide) peak shows that the B*2705 homodimer could be β 2m associated .*

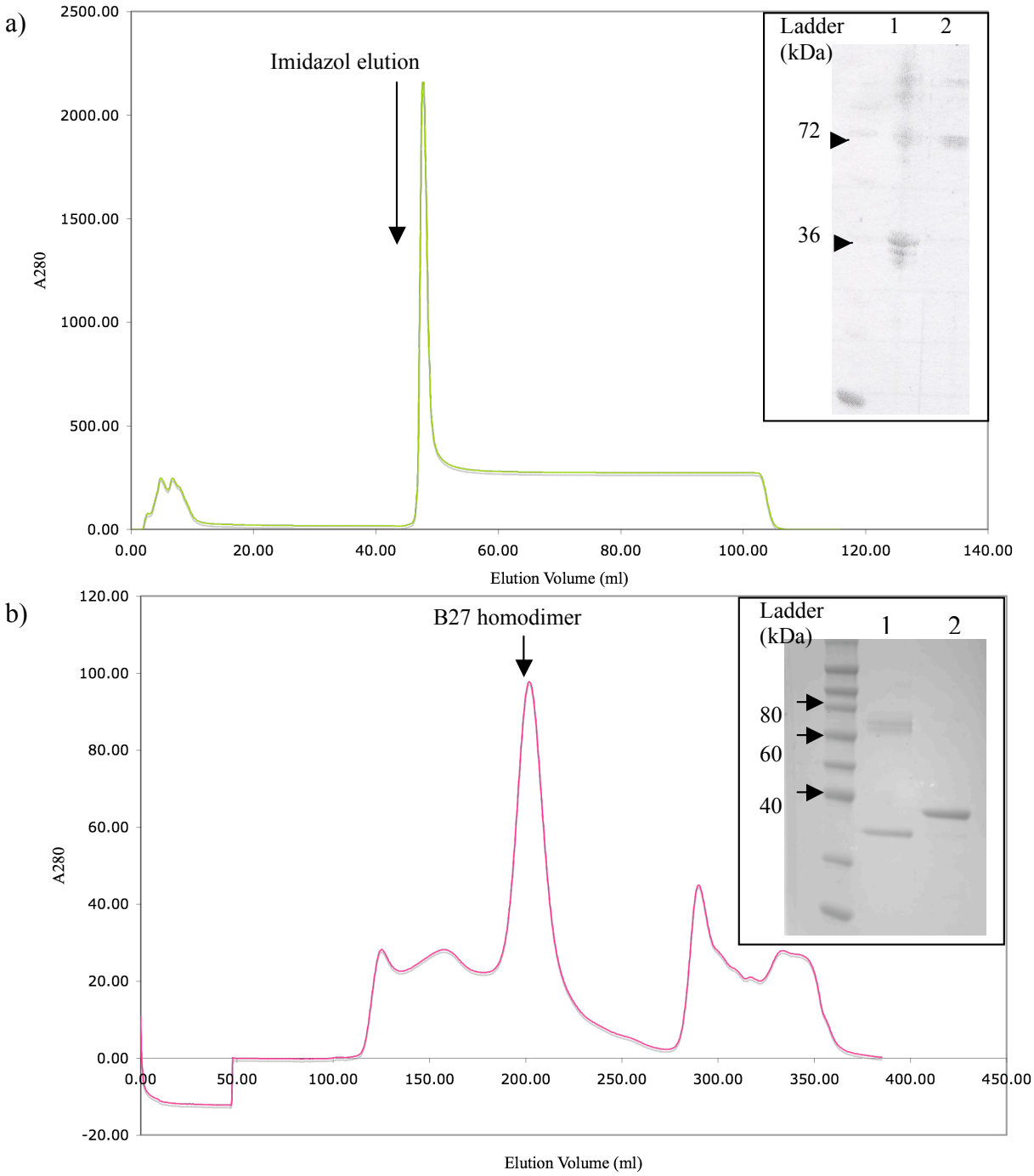


Figure 6.3 B*2705 homodimer refolding after extraction from Inclusion bodies and purification by Nickel affinity chromatography. *a) Representative elution profile of B27 inclusion bodies from Nickel Affinity Column. SDS Non Reduced gel showing purity of B27 before (1) and after (2) Ni purification b) Size exclusion Chromatography of refolded, Nickel purified B27 heavy chains with GAG (KRWIILGLNK) peptide. SDS Non-reduced (1) and Reduced (2) Gel for B27 dimer fraction.*

6.3 B*2705 homodimer : Fab of HD8 complex purification

Upon availability of a B27 dimer-specific candidate Fab, HD8 Fab, co-purification of B27 homodimer in complex with this Fab was conducted. The Fab fragment was used, as opposed to the whole antibody, in order to minimise distortion and flexibility within the complex, and thus promote crystal formation. Nickel-purified B27 heavy chains were refolded by limiting dilution in the presence of HPLC-purified GAG peptide. The resulting homodimer preparation was then incubated with pure Fab of HD8 (Fab8). This protein complex was then purified on a calibrated sd200 column (see appendix 8.1), concentrated and immediately used for crystal trial experiments. Prior to this, the B27 homodimer alone and the Fab8 alone were run on the calibrated sd200 column to determine their elution profiles (data not shown). In order to demonstrate that the peak harvested was a complex of two proteins, a sample was run on an SDS-PAGE gel to show that both B27 homodimer and Fab8 were present in the harvested peak (fig. 6.4).

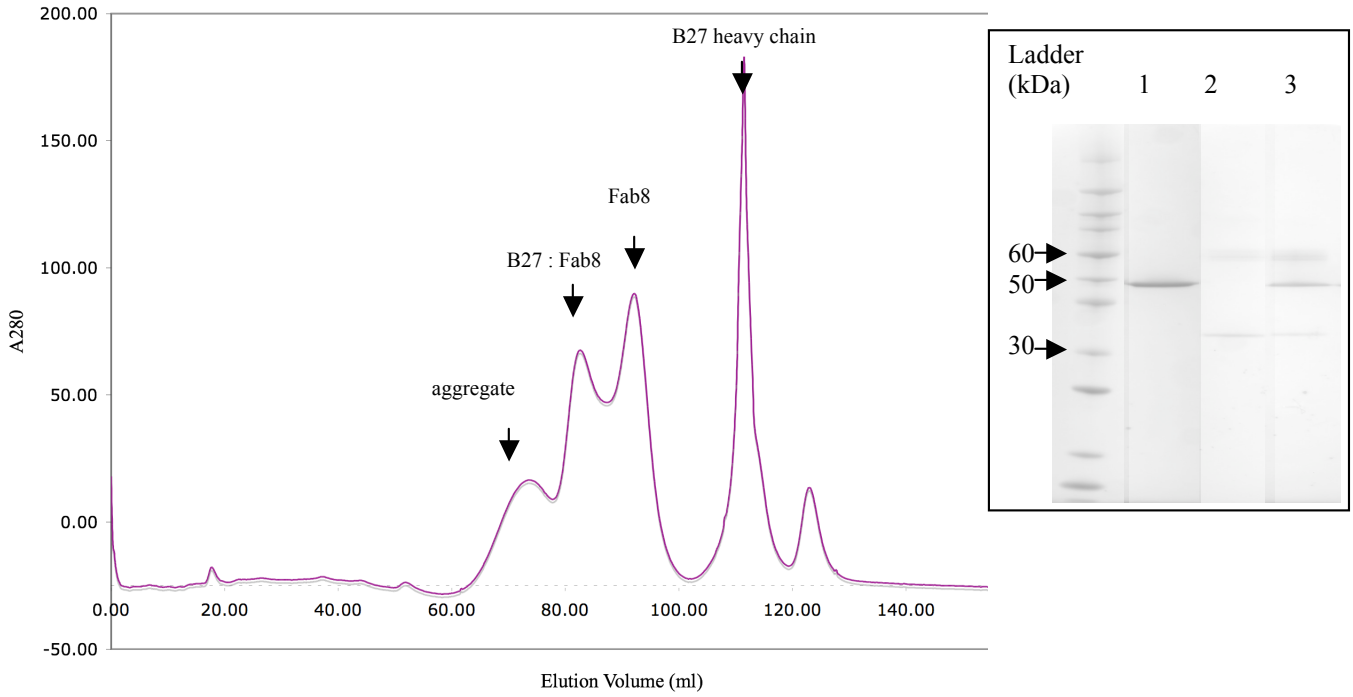


Figure 6.4 FPLC purification of the B27 homodimer ; Fab8 complex. *The B27 homodimer : Fab8 peak was harvested and used for crystal trial screening. SDS PAGE Non-Reducing Gel of (1) Fab 8 alone (50kDa), (2) B27 homodimer alone (66 kDa for homodimer and 33kDa for free heavy chain) and (3) B27 homodimer : Fab8 peak (shows presence of both 66kDa and 50kDa proteins).*

6.5 Crystal screening, optimisation and additive screen

The harvested B27 homodimer : Fab8 complex was concentrated to 2mg/ml and its tendency to precipitate out of solution was tested by performing a PCT test (section 2.9.1). The concentration was deemed to be suitable for crystal screening trials which were set up using the sitting drop method and 8 separate screening buffer blocks (section 2.9.2). Plates were incubated at 21°C for 2 months and later moved to 4°C. Plates were regularly imaged by an automated screening system and monitored for crystal formation. Precipitation of protein was observed for many crystallisation conditions; however, crystal formation was observed for two conditions. These are shown in figure 6.5.

Needle crystal formation was observed in two buffer conditions ((Ammonium Sulphate 2.4M, 0.1 M Bicine pH 9.0) and (Polyethylene Glycol (PEG) 30%, Sodium Acetate 0.2M and Sodium Cacodylate pH 6.5)). Following crystal screening, further protein complexes were prepared and the conditions for crystal growth were optimised as described in section 2.9.3. In the optimisation experiments, it was found that higher protein concentrations were more suitable for crystal formation and further needle crystals were grown using 5mg/ml of protein and the Ammonium Sulphate 2.4M, 0.1M Bicine pH 9.0 buffer at 4°C (fig. 6.6).

Following these crystal optimisation trials, an additive screen was conducted as described in section 2.9.4 using protein of 5mg/ml. An additive screen is a library of small molecules that can be added to a screening buffer in order to alter the solubility and crystallisation of biological molecules, by affecting the sample-solvent interactions. This screen yielded one additive (20mM Nickel Chloride) that gave excellent crystal growth at 4°C (fig. 6.7a) and

one condition that yielded microcrystal formation (fig. 6.7b). Upon identification of the helpful additive, 20mM Nickel Chloride was added to the previously mentioned optimisation trials in order to promote crystal growth; two additional crystals were then observed to grow of sufficient quality for use in X-Ray crystallography data collection (fig. 6.8). In order to clarify if crystals were biological (protein) or inorganic (salt), all crystals were analysed for birefringence by using polarised light microscopy. A biological crystal is weakly birefringent, whereas an inorganic crystal is strongly birefringent and so appear to sparkle under polarised light. All crystals were observed to be weakly birefringent (as shown in figures 6.5, 6.6 and 6.7).

a)



b)

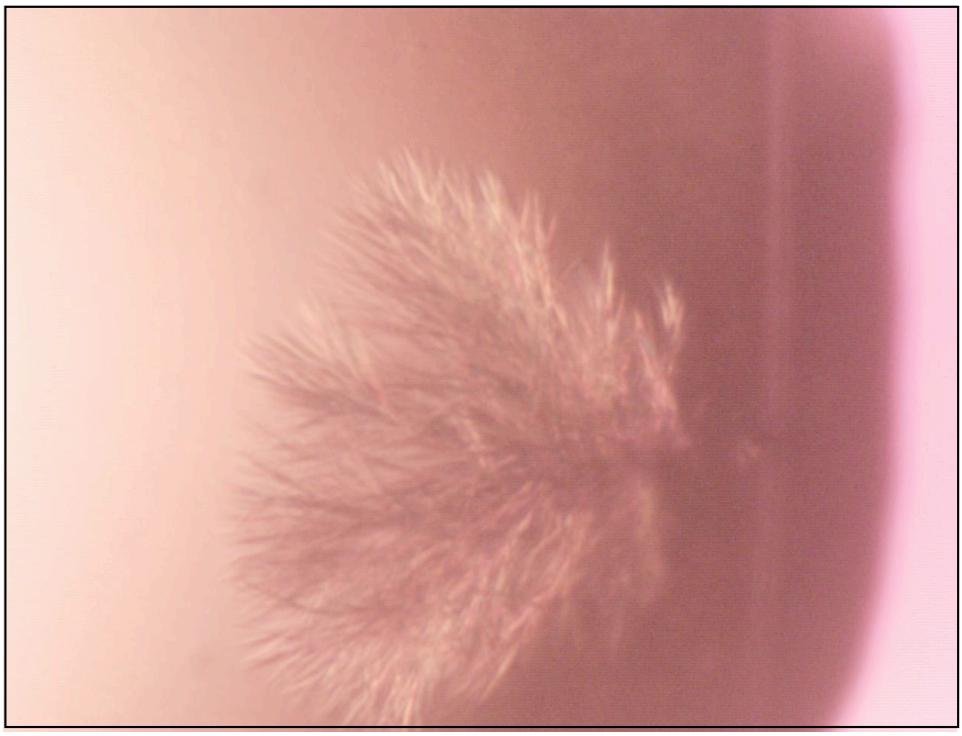
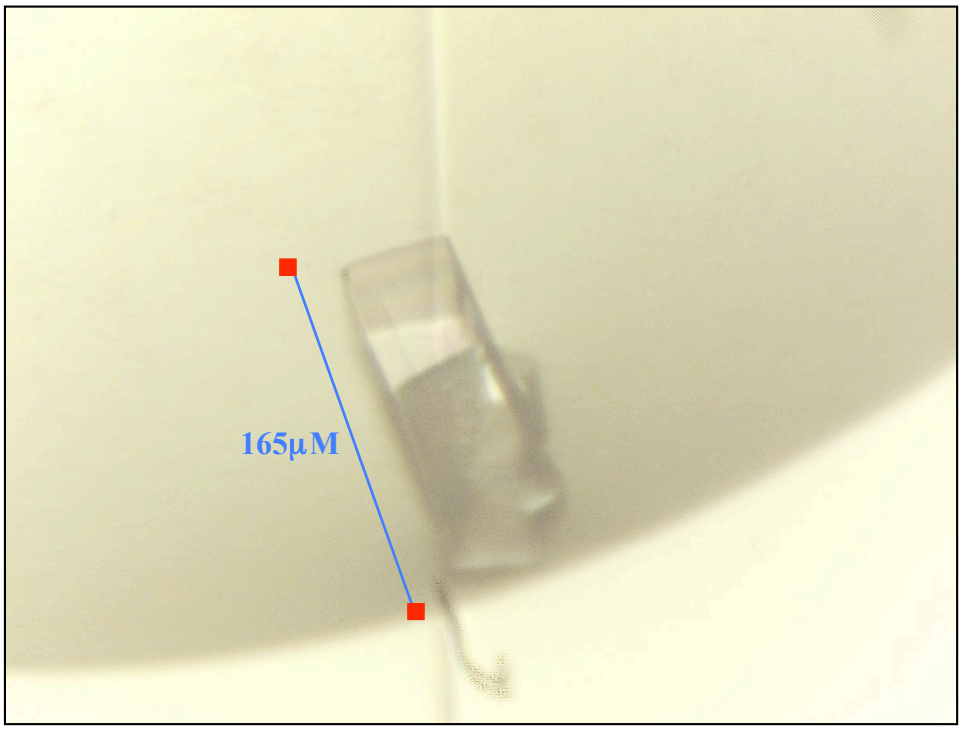


Figure 6.5 Needle Crystal formation of B27 homodimer : Fab8 complex. *a) Needle crystals in Ammonium Sulphate 2.4M, Bicine pH 9.0 buffer b) Needle formation from a single nucleation centre in PEG 30%, Sodium Acetate 0.2M and Sodium Cacodylate pH 6.5.*



Figure 6.6 Needle crystal formation of B27 homodimer : Fab8 complex. *Crystals grown in Ammonium Sulphate 2.4M, Bicine pH 9.0 with a protein to solute ratio of 2:1.*

a)



b)

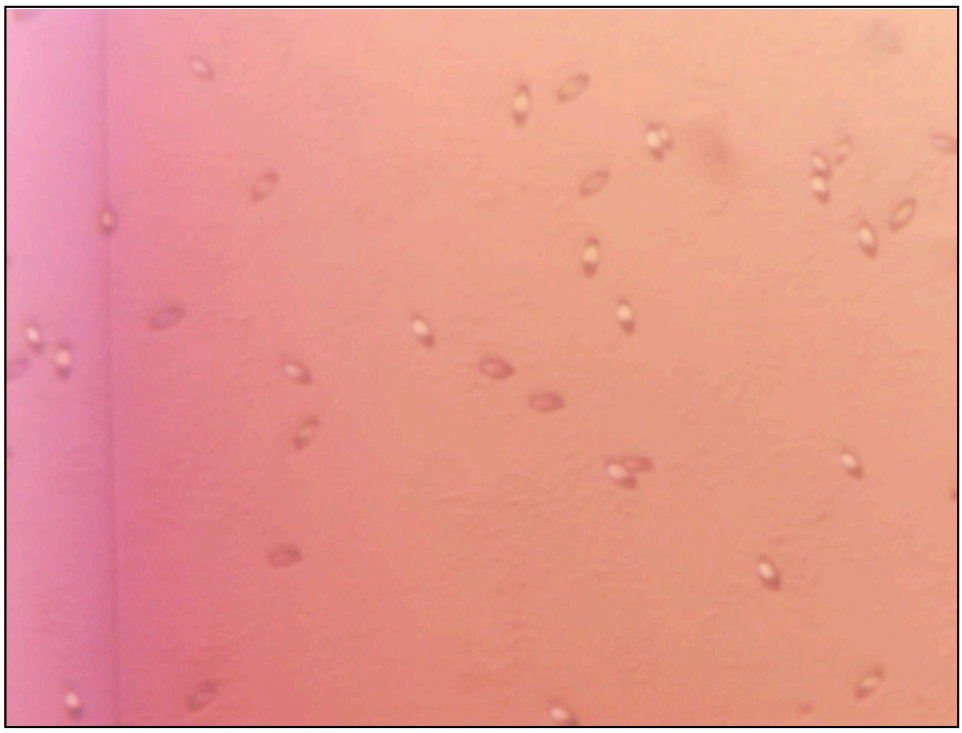


Figure 6.7 Crystal formation of B27 homodimer : Fab8 complex. *a) Crystal of B27 homodimer in complex with Fab of HD8, plus 20mM Nickel Chloride. B) Microcrystals grown in Ammonium Sulphate 2.4M, Bicine pH 9.0 in the presence of 0.1M Strontium Chloride hexahydrate.*

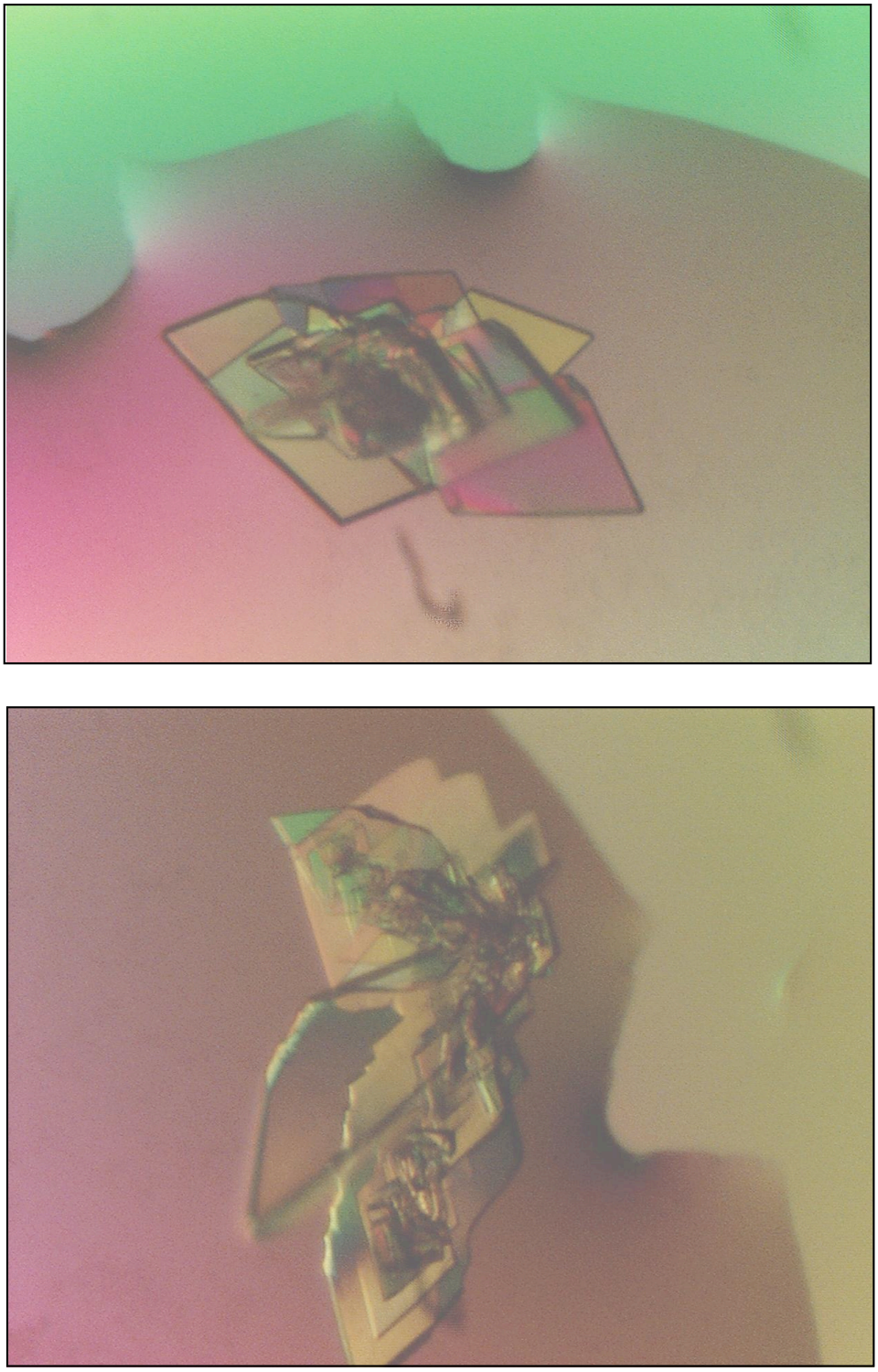


Figure 6.8 Crystal formation of B27 homodimer : Fab8 complex. *Birefringent crystals grown in the optimisation screen upon addition of Nickel Chloride to the crystallisation conditions.*

6.6 Discussion

The key experiments discussed in this chapter include the optimisation of the purification strategy for B27 homodimers and the development of a mammalian expression system for the soluble B27 homodimer. Expression and purification of the B27 homodimer has not been a trivial task, and many strategies have previously been attempted which did not yield B27 homodimer of sufficient purity for crystallisation experiments (not discussed here). The reason for the ambiguous purity observed for the homodimer is, more than likely, due to its unusual folding kinetics and unusual features as an MHC class I molecule [93]. As such, the expression and purification of the B27 homodimer has been a difficult undertaking.

In this Chapter, I have shown that the B27 homodimer can be isolated to a high purity, in complex with the Fab of HD8. I have also demonstrated that this complex is capable of forming protein crystals, sufficient for upcoming structural studies. Although we will not know exactly what is present in the crystal until crystallographic evidence is acquired using the synchotron, I am reasonably confident that it will be the B27 homodimer or B27 homodimer in complex with the Fab, rather than Fab alone, because the additive used was Nickel Chloride. It therefore seems logical that the Nickel Chloride additive would be aiding crystal growth of the B27 as the B27 protein used has a C terminal 6-histidine tag. The observation of protein crystal formation is of great importance, as it demonstrates that the B27 homodimer can be purified to a high quality for any further crystallisation trials, using the described purification and crystallisation strategy. Whether this recombinant B27 homodimer is representative of the B27 homodimer found at the cell surface is unclear at present, but with the further development of B27 homodimer specific antibodies, in the future

it will be possible to establish (by cell surface staining and intracellular staining) whether multiple species of homodimer exist both on the surface and within the ER.

Unfortunately, the crystal shown in figure 6.7a did not diffract in a recent diffraction study. Currently, the crystal trials are to be repeated using the purification strategy and crystallisation conditions outlined in this chapter.

Should the *E.coli*-expressed B27 homodimer crystals not provide structural data, it will also be possible to scale up the mammalian cell expression system that I have in place in order to isolate eukaryotic-expressed B27 (see appendix section 8.6). Such an undertaking may pose some technical difficulties, as mammalian expression systems tend to provide lower yields of protein. Mammalian systems also entail post-translational modifications of proteins, so the purification protocol may require a de-glycosylation step prior to crystal screening. These are the main reasons why this chapter has focused on the *E.coli* expression system and purification strategies used.

Chapter 7 – Discussion

7.1 Summary of results……..170

7.2 Discussion ……..……..170

7.3 Concluding remarks ……178

7.1 Summary of results

In this thesis I investigate the interactions of the NK cell receptors, LILRB1 and LILRB2, with different forms of HLA-B27. Specifically, I have characterised the affinities and specificities of LILRB1 and LILRB2 for the B27 homodimers and different subtypes of B27 heterotrimer molecules using the highly sensitive biophysical technique, Surface Plasmon Resonance. I have also analysed the abilities of two subtypes, B*2705 and B*2709 to form homodimeric molecules *in vitro,* and have shown that the disease-associated subtype (B*2705) has a higher propensity to form B27 homodimer molecules than the non-disease associated subtype (B*2709). I have also characterised candidate B27 dimer-specific antibodies by measuring their specificity and affinity for the B27 homodimer. This allows for the assessment of their usefulness as research tools in B27-associated disease. In addition, I have performed preliminary functional studies investigating the effect of the B27 homodimer on DC function. Finally I have made much progress in the crystallisation of the B27 homodimer in complex with the Fab portion of the candidate antibody, HD8. This will facilitate the future elucidation of the B27 homodimer structure.

7.2 Discussion

Understanding of the molecular interactions of B27 and its innate receptors will be key to the elucidation of the pathogenic role of B27 in B27-positive AS individuals. Data presented in this thesis have demonstrated, for the first time, that the interactions between LILRB1 and LILRB2 with B27 homodimer are significantly different from those with classical HLA class I molecules (summarised in table 7.1).

K_D values for paired interactions (μM)			
	LILRB1	LILRB2	CDαα
Expression:	*NK cells*	*Myelomonocytic cells*	*T cells in the small intestine*
HLA-B*2705 heterotrimer	5.10 ± 0.80	21.23 ± 3.63	131.0
HLA-B*2709 heterotrimer	5.46 ± 0.86	21.60 ± 2.60	Not Done
HLA-A3 heterotrimer	6.88 ± 1.30	21.10 ± 2.10	Not Done
HLA-B*2705 homodimer	Do not bind	2.50 ± 0.10	72.0
HLA-B*2705 Free Heavy Chains	Do not bind	2.60	Not Done

Table 7.1. Summary of biophysical measurements of B27 with its ligands measured in this thesis. *The B27 homodimer shows different binding properties compared to classically folded HLA class I molecules.*

Whether these interactions with the B27 homodimer are occurring in trans, in cis or with soluble LILRB2 molecules is still unknown at this stage, but is currently being studied by members of the Bowness lab. Nevertheless, the observed perturbation in interactions is highly likely to have a functional effect on cells expressing the LILRB1 and/or LILRB2 molecules. Whether such interactions would upset the balance of paired inhibitory and activatory interactions or influence DC maturation remains unclear. Perturbed HLA interactions with LILRB2 have been shown to alter DC maturation in studies by Huang et al [110]. The authors report that an increased affinity of LILRB2 for one subtype of HLA-B*35 (measured by SPR) correlated with an enhanced DC activation status, monitored by a change

in maturation marker expression on the DC surface. Although the expression of maturation markers (CD80, CD86, CD83) did not appear to be altered in my experiments, I did observe cell clumping of the DCs in the presence of B27 homodimer. This cell clumping could be a sign of enhanced DC activation and this will be studied in further cell-based experiments. It will be important to look at the cytokine profile in the supernatants of these cells in order to assess whether this cell clumping is indeed a sign of increased activation. Furthermore, it may be interesting to repeat these experiments using NK cells as opposed to DC cells to identify whether NK cell cultures are more activated in the presence of B27 homodimer or B27 heterotrimer tetramers (where activation could be analysed by measuring IFN-γ and TNF-α production).

To complement these data, I have also investigated the interactions of B27 with the CD8αα co-receptor in order to compare its affinity and ability to compete with LILRB2 for B27 homodimer binding. In preliminary experiments, I observed a higher affinity between B27 homodimer and LILRB2 than between B27 homodimer and the CD8αα co-receptor, suggesting that the B27 homodimer would preferentially bind to a LILRB2 receptor. This observation supports theories that the T cell receptor does not have a central role in B27 associated disease, where LILRB2 (and possibly other LILRs and KIRs) are able to compete with CD8αα for binding. This observation supports the idea that these innate receptors may have a prominent and important role in the pathogenesis of B27-associated disease.

Since LILRB2 has a higher affinity for B27 homodimer than the B27 heterotrimers, it is likely that other immune receptors will also display different and important binding properties. Other perturbed interactions may have a functional effect on NK cell licensing.

LILRB2 is not usually expressed on NK cells [72], as such, its influence on NK licensing is not likely to be significant; however, other immune receptors such as the KIRs and NKG2D may also display unusual binding to the B27 homodimer and hence influence licensing and thus enhance the activation of NK cells. Some attempts at the expression and purification of the KIR3DL2 protein were made during my project for SPR experiments; however, the expression of recombinant KIRs is difficult and the proteins expressed were not of sufficient purity or quantity for such biophysical experiments. These molecular interactions will be important to characterise in the future in order to fully understand how the balance of immune interactions is perturbed in B27 individuals.

In this thesis I also show that free heavy chains of B27 are able to interact with LILRB2 (but not LILRB1). My data thus suggest that free heavy chains may also have a role in perturbing immune cell interactions, but it is likely that any heavy chains present would have a tendency to form homodimers or multimers due to their di-sulphide bonding capacity. Whether the recombinant homodimers are single or multiple species is unclear, but having shown that the affinities with the HD6 antibody and LILRB2 ligands with both B27 homodimers and B27 free heavy chains are comparable, it is likely that they contain conserved conformations for ligand interactions. Additionally, I show that the B27 homodimers lacked any bound peptide (section 5.2), and this observation agrees with the idea that it is the B27 molecule interactions that are contributing to perturbed interactions at the cell surface. This finding explains an observation in a previous report that the interactions of B27 are independent of peptide [63]. Therefore, I suggest that homodimers and free heavy chains of B27 may both have a pathogenic role, but it will be the homodimers that would be more prevalent in a cell system due to their inherent tendency to form homodimers. Overall, these findings support the

hypothesis that the B27 homodimer has a functional role in B27 associated inflammation, involving NK cell receptors (fig. 7.1).

As an aside in chapter 3, I describe how an HIV escape mutation previously shown to exhibit different binding to LILRB2 when complexed to B*2705 [109] does not show an altered affinity by SPR (section 3.4). This finding argues against a role for the inhibitory LILRB2 receptor and B27 interaction in viral escape. These findings reported in this thesis are consistent with the crystal structure data for the LILRB2 molecules, which imply that the peptide-binding region of the LILR is not important for HLA class I recognition. It is therefore more likely that this HIV escape mutation influences the binding of another DC expressed inhibitory receptor, such as an inhibitory KIR (whose interactions have been shown to be peptide dependent). Alternatively, the viral escape mutation could be explained by the more obvious HLA interaction with the T-cell receptor. Since structural data have shown that the peptide-binding groove for B27 can accommodate some peptides in two conformations [16], it seems possible that the B27 may be able to bind to the GAG-M peptide in two conformations, one or both of which may escape T-cell recognition. These interactions will be important to characterise in order to understand this HIV escape mechanism.

Chapter 4 describes how two different subtypes of B27 differ in their ability to fold and form homodimers *in vitro*. I have shown that the disease-associated allele, B*2705 forms more homodimers than the non disease-associated molecule B*2709 in the presence of β_2m and a range of different peptide epitopes. The two subtypes studied in this thesis have previously been shown to have different peptide-binding repertoires. Thus, one explanation for the

observed results may be that the B*2709 allele is structurally more able to bind peptide epitopes in a stable conformation, whereas B*2705 may bind peptides more weakly. The weaker bound peptide in B*2705 heterotrimers may then be released with the β_2m at the cell surface, and this would allow for the formation of free heavy chain structures. This suggestion would agree with previous observations that B*2705 binds to a broader set of peptides than other subtypes [119-120]. Furthermore, reports have shown that position 116 of B27 may affect the association of HLAs with the TAP complex (via tapasin) and this may further affect peptide loading [120-122]. These studies suggest that B*2705 is relatively tapasin independent (meaning B27 would not require peptide optimisation before egression to the cell surface). B*2709, on the other hand, is believed to bind to tapasin more strongly with delayed egression from the ER [123]. Therefore, if these subtype-specific differences are a reflection of what is occurring at the cell surface, they may have serious and important implications for our ideas regarding the mechanism of pathogenesis in AS. It will be important to clarify whether my findings are a reflection of what is happening at a cellular level (work currently being undertaken in Bowness lab), and if this is so it will be interesting to uncover whether other B27 subtypes obey a similar trend (such as B*2702 and B*2706). In accordance with the B27 homodimer theory, my results offer an explanation as to why certain subtypes of B27 are associated with auto-inflammatory diseases, like AS, and other subtypes are either neutral or not-associated.

In addition to the biophysical properties of the B27 molecule, I have also tested three candidate monoclonal B27-dimer-specific antibodies. I have characterised the binding and mapping of the novel HD6 antibody, as this was the candidate antibody most readily available. The HD6 antibody has been used in FACS based experiments to stain B27-

transfected cell lines by members of the Bowness group (unpublished data). This observation suggests that the recombinant B27 homodimer used for the SPR studies is representative of the B27 homodimer present at the cell surface. However, as mentioned in the introduction, there may be several forms of the B27 homodimer due to the presence of multiple cysteines and its disulphide bonding capacity [93].

My data suggest that HD6 will be a useful tool in the study of the abberant folding of B27, as I have shown that it binds preferentially to B27 homodimers, but not B27 heterotrimers or HLA-G homodimers. Additionally, I have shown that it can bind to B27 homodimers with a high affinity, comparable to that of other commonly used monoclonal antibodies [118]. The HD6 antibody was also shown to bind to the free heavy chains of B27 (but not to HLA-A3 heavy chains or HLA-G heavy chains) by acid wash experiments using SPR. These results were also confirmed at the cell surface by Kirsty McHugh of the Bowness lab (unpublished data). This suggests that there may be some partially unfolded epitope of B27 that is exposed upon formation of B27 homdimers and free heavy chains. This suggestion agrees with the Mass Spectroscopy epitope-mapping experiment, identifying H114 as a possible important binding residue, which is located in a flat β sheet conformation of the peptide-binding groove. Therefore, the antibody may be binding to a region only exposed after loss of peptide and β_2m. As such, HD6 will be an invaluable tool for studying B27 positive (AS) patient samples by assessing whether their synovial fluid cells and PBMCs express the B27 homodimer. This will help to elucidate whether the homodimer plays a role in AS pathogenesis.

An exciting experiment that will be attempted in the near future will be the treatment of B27 transgenic animals with the HD6 antibody. Should the HD6 treatment ameliorate disease, it would provide convincing evidence that B27 homodimers (and/or free heavy chains) play a role in the pathogenesis of AS.

Using a combination of published structural and epitope mapping results for other HLA interactions, and SPR competition experiments discussed in this thesis, I have devised a molecular model describing the proposed binding sites for LILRB2, HC-10 and HD6 binding to B27 homodimers. The ideal way to show where the ligands are binding to the B27 homodimer would be by X-Ray crystallography of the complexes. However, since I have hypothesised that HD6 can bind to more than one species of the B27 structure, it may be extremely difficult, if not impossible, to isolate and purify either one of the B27 : HD6 complexes to a sufficient purity for crystal formation. Hence other experimental methods, such as ELISAs using the candidate peptide sequence, will be performed to confirm this binding site. The mapping of these interactions is important as it will further our understanding of how other B27 dimer interactions can be blocked in future experiments. It will also be essential, should the candidate antibodies be considered as therapeutic agents. It will be interesting and useful to further characterise the binding of HD8 to the B27 homodimer, once the antibody is more freely available.

Finally, I have prepared the groundwork for the future structural elucidation of the B27 homodimer in complex with the Fab portion of HD8. This is particularly exciting, as a crystal structure of the B27 homodimer would prove invaluable to future research and theories involving the role of B27 in disease. So far, I have optimised the purification of recombinant

B27 homodimer to a high enough purity to achieve crystallisation of the protein, and have grown some large protein crystals. These will be used in future X-Ray diffraction studies.

7.3 Concluding Remarks

Despite knowing of the association between HLA-B27 and inflammatory disease for over 30 years, the role of the molecule in disease remains elusive. The work presented in this thesis increases our understanding of the biophysical properties of the B27 homodimer at a molecular level. The data presented illustrate for the first time that the B27 homodimer has very distinct binding affinities and specificities from other HLA molecules and I believe that this plays some role in the pathogenesis of AS. There will, of course, be other contributing factors to this pathogenesis, but finding that B27 disrupts immune cell balance enhances our understanding of the inflammatory processes that occur in B27 positive SpA patients.

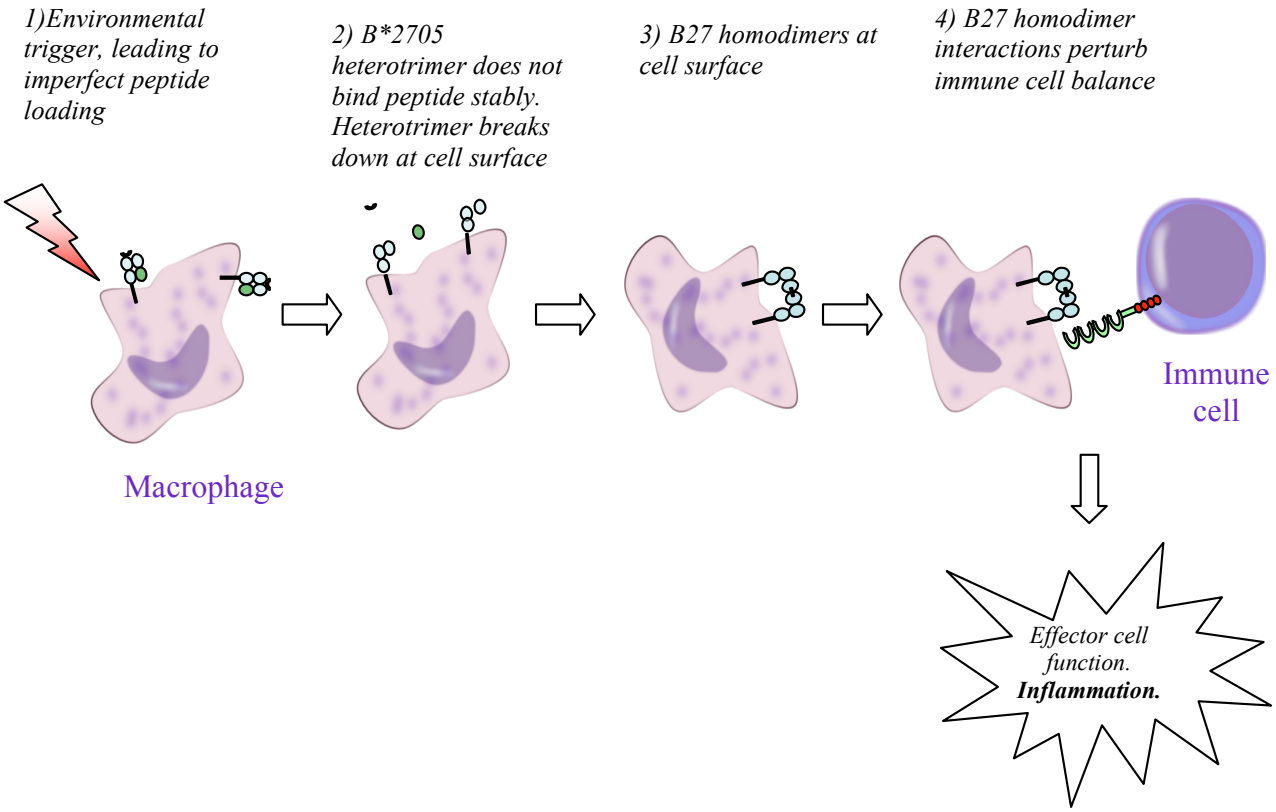


Figure 7.1 Cartoon showing the proposed involvement of B27 homodimer interactions in inflammatory processes of Ankylosing Spondylitis.

Chapter 8 - Appendix

8.1 Calibration of the Superdex 75 and Superdex 200 columns

In order to calibrate the superdex (Sd) column, standards of known molecular weights were run and their elution volumes were calculated to generate a standard curve. Details of how this was done are shown here:

A protein calibration kit was used (GE Healthcare) and the proteins Ovalbumin, Ribonuclease A and Aprotin were selected in accordance to manufacturer's guidelines.

Firstly the void volume (Vo) of the Sd 75 or Sd 200 column was determined by running a sample of Blue Dextran. The volume at which this protein elutes is denoted as the Vo.

Next, the Ovalbumin, Ribonuclease A and Aprotin mixture was applied to the column at the volume at which they began to elute was noted for each protein and denoted as individual elution volumes (Ve).

The column volume (Vc) of the Sd75 and Sd200 columns were given as 320ml.

In order to prepare a calibration curve, K_{av} values were determined using the equation below, and a standard calibration curve of K_{av} versus log molecular weight was then drawn for Sd75 (table 8.1 and figure 8.1) and Sd200 (table 8.2 and figure 8.2).

$$I Kav = \frac{I Ve - Vo}{Vc - Vo}$$

Protein	Elution Volume (ml)	Molecular weight (Da)	K_{av}
Blue Dextran (BD)	102	-	-
Ovalbumin (Ov)	131	43,000	0.13
Ribonuclease A (RbA)	183	13,700	0.36
Aprotin (Apr)	222	6,500	0.55

Table 8.1 Calibration of Sd75 column.

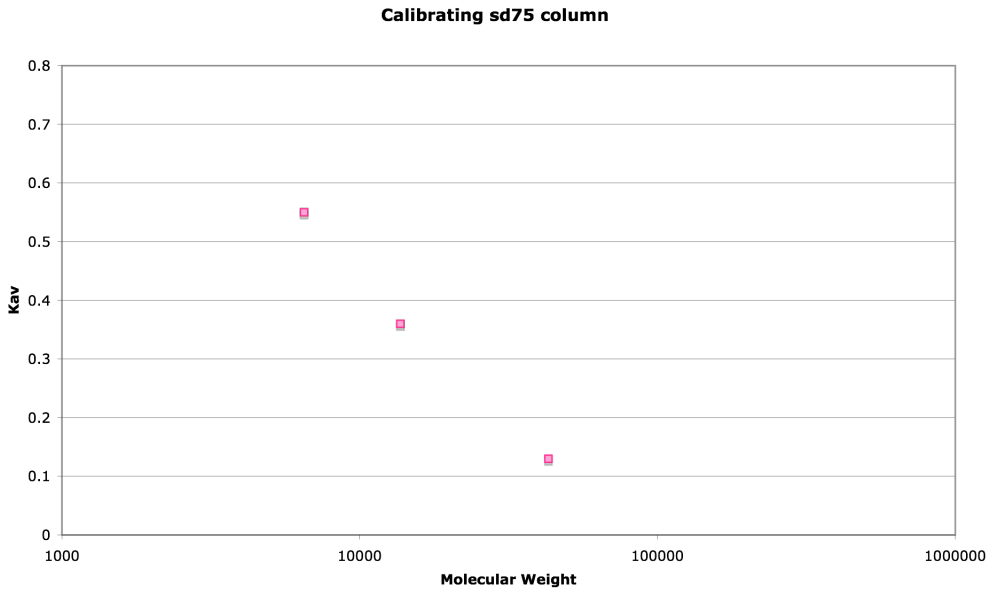


Figure 8.1. Calibration curve for Sd75 column.

Protein	Elution Volume (ml)	Molecular weight (Da)	K_{av}
Blue Dextran (BD)	44	-	-
Conalbumin (CA)	82	75,000	0.50
Fab	90	25,000	0.60
Ribonuclease A (RbA)	100	13,700	0.74

Table 8.2 Calibrating Sd200 column.

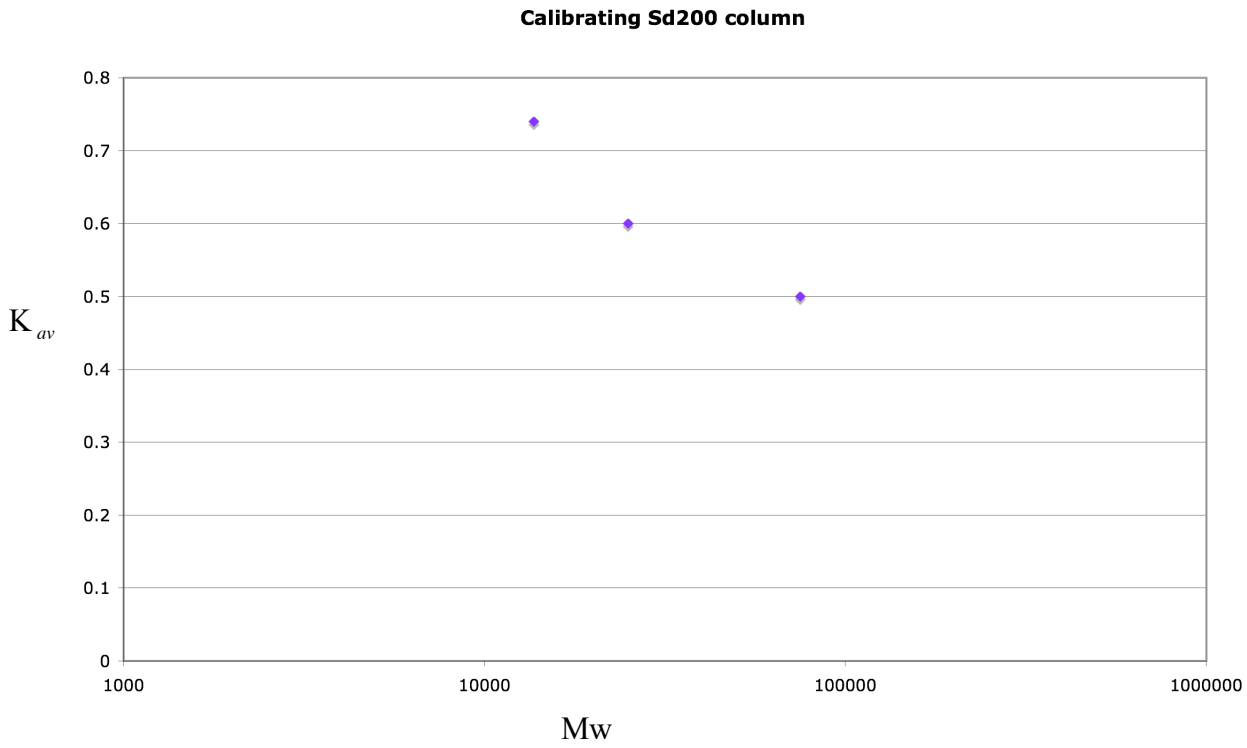


Figure 8.2 Calibration curve for Sd200 column.

8.2 Confirming the purity of analytes before SPR experiments

To confirm that the analyte used in each experiment was of high purity, a non-reducing SDS PAGE gel was run before each series of SPR experiments. Figure 8.3 shows a representative gel of the analytes LILRB1, LILRB2 and CD8αα.

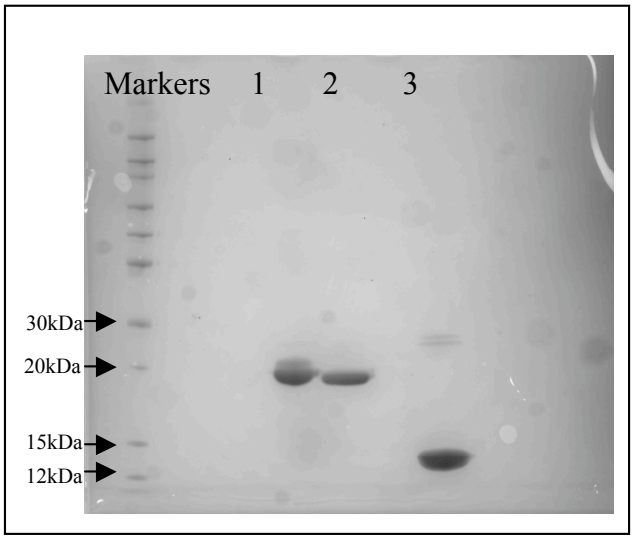


Figure 8.3 SDS PAGE non-reducing gels of LILRB1, LILRB2 and CD8αα analyte proteins. *Lane 1 is LILRB1, Lane 2 is LILRB2, Lane 3 is CD8αα.*

8.3 Doublet formation in Dendritic cell cultures

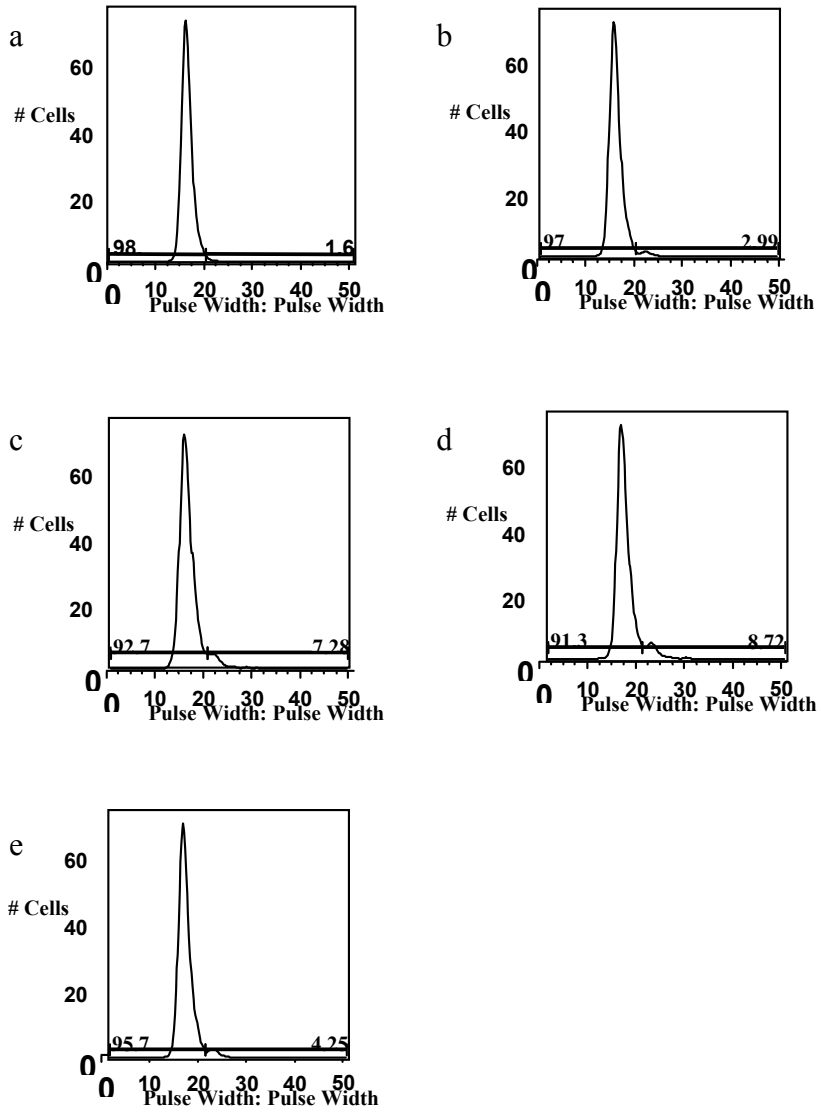


Figure 8.4 FACS analysis of the pulse width of cells illustrates the presence of a higher proportion of cell doublets in cells stimulated with B27 homodimer compared to B27 heterotrimer and cytokines only. *a) Immature cells have a high proportion of single cells b) 3% of cells form doublets when DCs are stimulated with cytokines only c) 7% of cells form doublets when DCs are stimulated with B27 homodimer only d) 9% of cells form doublets when DCs are stimulated with B27 homodimers and cytokines e) 4% of cells form doublets when DCs are stimulated with B27 heterotrimer and cytokines.*

8.4 Generation of candidate dimer specific antibodies by Phage Display Technology

B*2705 dimer specific antibodies were developed by Phage Display Technology (by the group of Christoph Renner, as described fully in [124]). A pCES phagemid library was used with a human Fab repertoire of ~$1.5x10^{10}$ clones. Biotinylated recombinant B*2705 dimer (expressed in bacteria, J.Giles) was used for a first round of positive selection. A negative selection round using biotinylated recombinant B*2705 heterotrimer (expressed in bacteria, J.Giles) was then performed. Twelve different antibodies were isolated and further characterised by colony PCR, fingerprinting and sequence analysis. Three Fabs were then converted to chimeric antibodies with a murine IgG1 Fc (fig. 8.5).

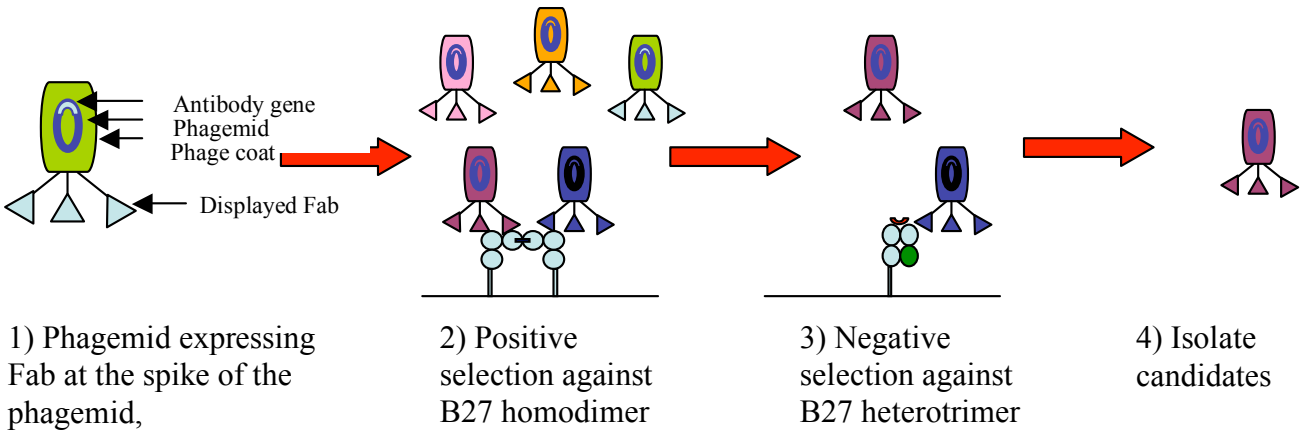


Figure 8.5 Generating B27 homodimer specific Fabs by Phage Display Technology.

8.5 HC-10 antibody avidity for B27 homodimer

Measurements of the affinities of HC-10 antibody for B*2705 homodimer was conducted by SPR. B27 homodimer was immobilised to a streptavidin coated surface and increasing concentrations of antibody (from 50nM to 17μM) was flowed over the sensor surface. Between successive injections a regeneration step was incorporated in order to remove excess bound analyte from the ligand surface (fig. 5.4). Figure 8.5 shows that HC-10 binds B*2705 and with an apparent K_D of 6.6nM.

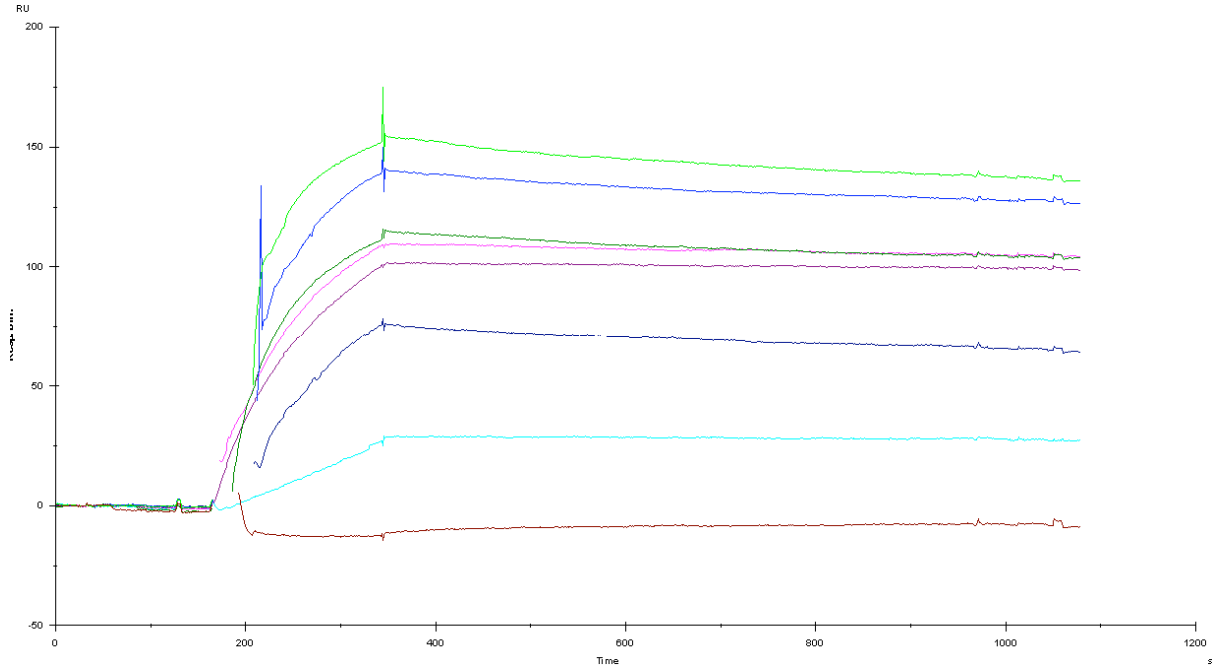


Figure 8.6 HC-10 binds to B*2705 homodimers with high avidity. *Increasing concentrations of HC-10 (IgG) was flowed over the B*2705 homodimer (range of colours). HC-10 antibody binds to B*2705 homodimer with a K_D value of 6.6nM. The K_D values were calculated using the Langmuir fit on the Biaevaluate software as well as being plotted and analysed using Origin 7.5 (data not shown).*

8.6 Mammalian Expression system

A mammalian expression system for B*2705 was developed in order to obtain soluble and refolded B27 protein that was refolded physiologically. In order to do this, a truncated B27 construct (transmembrane region removed), with a 6-histidine tag, was cloned into the pIRES expression vector. This vector allows the simultaneous expression of soluble B27, but also the co-expression of GFP as a marker of expression (fig. 8.7). This is due to the IRES site (Internal Ribosome Entry Site) which enables the ribosome to translate two open reading frames from a single mRNA transcript. The vector was used to make lentivirus, which was then used to transduce mammalian cell lines, including U937 cells. FACs analysis showed that GFP was being expressed (fig. 8.7) and Western Blot analysis (using anti-penta His antibody) showed expression of a protein corresponding to the B27 homodimer when non-reduced (NR) and the B27 monomer when reduced (R) (fig. 8.7).

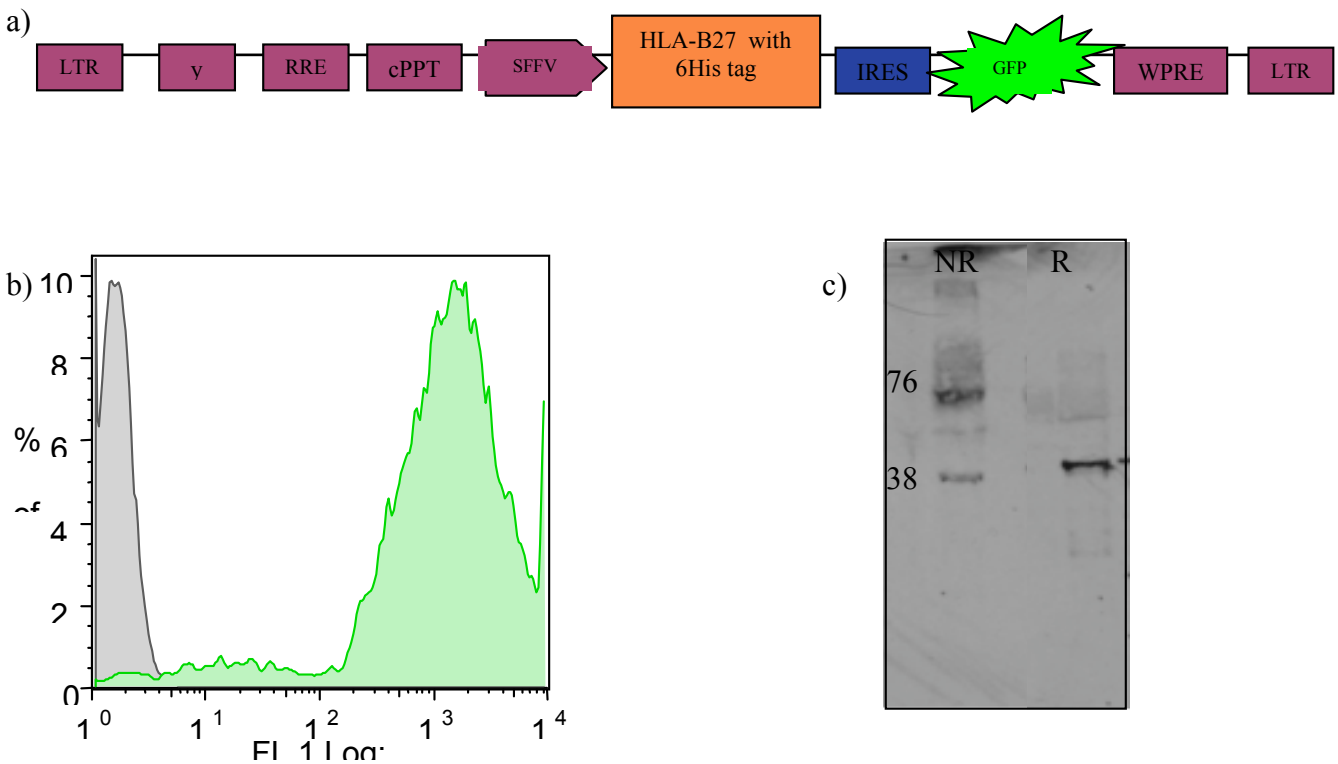


Figure 8.7 Mammalian Expression system for soluble B*2705. *a) A schematic representation of the pIRES expression vector. b) FACs plots for GFP expression of transduced U937 cells. c) Western Blot analysis of the transduced U937 lysate using an anti-penta-His antibody.*

References

1. Mansour, M., et al., *Ankylosing spondylitis: a contemporary perspective on diagnosis and treatment.* Semin Arthritis Rheum, 2007. **36**(4): p. 210-23.
2. Sieper, J., et al., *Ankylosing spondylitis: an overview.* Ann Rheum Dis, 2002. **61 Suppl 3**: p. iii8-18.
3. Braun, J., et al., *Prevalence of spondylarthropathies in HLA-B27 positive and negative blood donors.* Arthritis Rheum, 1998. **41**(1): p. 58-67.
4. Saraux, A., et al., *Prevalence of spondyloarthropathies in France: 2001.* Ann Rheum Dis, 2005. **64**(10): p. 1431-5.
5. Braun, J. and J. Sieper, *Ankylosing spondylitis.* Lancet, 2007. **369**(9570): p. 1379-90.
6. Ju, J.H., H.Y. Kim, and S.H. Park, *Clinical images: bamboo spine in a patient with ankylosing spondylitis.* Arthritis Rheum, 2007. **56**(9): p. 3043.
7. Brewerton, D.A., et al., *Ankylosing spondylitis and HL-A 27.* Lancet, 1973. **1**(7809): p. 904-7.
8. Brown, M.A., et al., *HLA class I associations of ankylosing spondylitis in the white population in the United Kingdom.* Ann Rheum Dis, 1996. **55**(4): p. 268-70.
9. Hammer, R.E., et al., *Spontaneous inflammatory disease in transgenic rats expressing HLA-B27 and human beta 2m: an animal model of HLA-B27-associated human disorders.* Cell, 1990. **63**(5): p. 1099-112.
10. Brown, M.A., et al., *Susceptibility to ankylosing spondylitis in twins: the role of genes, HLA, and the environment.* Arthritis Rheum, 1997. **40**(10): p. 1823-8.
11. Zhang, G., et al., *Genetic studies in familial ankylosing spondylitis susceptibility.* Arthritis Rheum, 2004. **50**(7): p. 2246-54.

12. Brown, M.A., *Breakthroughs in genetic studies of ankylosing spondylitis.* Rheumatology (Oxford), 2008. **47**(2): p. 132-7.

13. Timms, A.E., et al., *The interleukin 1 gene cluster contains a major susceptibility locus for ankylosing spondylitis.* Am J Hum Genet, 2004. **75**(4): p. 587-95.

14. Krensky, A.M., *The HLA system, antigen processing and presentation.* Kidney Int Suppl, 1997. **58**: p. S2-7.

15. Wearsch, P.A. and P. Cresswell, *The quality control of MHC class I peptide loading.* Curr Opin Cell Biol, 2008. **20**(6): p. 624-31.

16. Sadasivan, B., et al., *Roles for calreticulin and a novel glycoprotein, tapasin, in the interaction of MHC class I molecules with TAP.* Immunity, 1996. **5**(2): p. 103-14.

17. Antoniou, A.N. and S.J. Powis, *Characterization of the ERp57-Tapasin complex by rapid cellular acidification and thiol modification.* Antioxid Redox Signal, 2003. **5**(4): p. 375-9.

18. Cho, K., et al., *Redox-regulated peptide transfer from the transporter associated with antigen processing to MHC class I molecules by protein disulfide isomerase.* Antioxid Redox Signal. 2011 *(in press)*

19. Cresswell, P., et al., *Mechanisms of MHC class I-restricted antigen processing and cross-presentation.* Immunol Rev, 2005. **207**: p. 145-57.

20. Antoniou, A.N., S.J. Powis, and T. Elliott, *Assembly and export of MHC class I peptide ligands.* Curr Opin Immunol, 2003. **15**(1): p. 75-81.

21. Madden, D.R., et al., *The structure of HLA-B27 reveals nonamer self-peptides bound in an extended conformation.* Nature, 1991. **353**(6342): p. 321-5.

22. Jardetzky, T.S., et al., *Identification of self peptides bound to purified HLA-B27.* Nature, 1991. **353**(6342): p. 326-9.

23. Stodulkova, E., et al., *Peptides eluted from HLA-B27 of human splenocytes and blood cells reveal a similar but partially different profile compared to in vitro grown cell lines.* Immunol Lett, 2004. **94**(3): p. 261-5.

24. Bird, L.A., et al., *Lymphoblastoid cells express HLA-B27 homodimers both intracellularly and at the cell surface following endosomal recycling.* Eur J Immunol, 2003. **33**(3): p. 748-59.

25. Benjamin, R.J., J.A. Madrigal, and P. Parham, *Peptide binding to empty HLA-B27 molecules of viable human cells.* Nature, 1991. **351**(6321): p. 74-7.

26. Allen, R.L., et al., *Cutting edge: HLA-B27 can form a novel beta 2-microglobulin-free heavy chain homodimer structure.* J Immunol, 1999. **162**(9): p. 5045-8.

27. Kollnberger, S., et al., *Cell-surface expression and immune receptor recognition of HLA-B27 homodimers.* Arthritis Rheum, 2002. **46**(11): p. 2972-82.

28. Whelan, M.A. and J.R. Archer, *Chemical reactivity of an HLA-B27 thiol group.* Eur J Immunol, 1993. **23**(12): p. 3278-85.

29. Ishitani, A. and D.E. Geraghty, *Alternative splicing of HLA-G transcripts yields proteins with primary structures resembling both class I and class II antigens.* Proc Natl Acad Sci U S A, 1992. **89**(9): p. 3947-51.

30. Shiroishi, M., D. Kohda, and K. Maenaka, *Preparation and crystallization of the disulfide-linked HLA-G dimer.* Biochim Biophys Acta, 2006. **1764**(5): p. 985-8.

31. Khan, M.A., et al., *The pathogenetic role of HLA-B27 and its subtypes.* Autoimmun Rev, 2007. **6**(3): p. 183-9.

32. Khan, M.A., *Remarkable polymorphism of HLA-B27: an ongoing saga.* Curr Rheumatol Rep. **12**(5): p. 337-41.

33. Khan, M.A., *Update: the twenty subtypes of HLA-B27.* Curr Opin Rheumatol, 2000. **12**(4): p. 235-8.

34. Lopez-Larrea, C., S. Gonzalez-Roces, and V. Alvarez, *HLA-B27 structure, function, and disease association.* Curr Opin Rheumatol, 1996. **8**(4): p. 296-308.

35. Paladini, F., et al., *Distribution of HLA-B27 subtypes in Sardinia and continental Italy and their association with spondylarthropathies.* Arthritis Rheum, 2005. **52**(10): p. 3319-21.

36. D'Amato, M., et al., *Relevance of residue 116 of HLA-B27 in determining susceptibility to ankylosing spondylitis.* Eur J Immunol, 1995. **25**(11): p. 3199-201.

37. Khan, M.A., *HLA-B27 polymorphism and association with disease.* J Rheumatol, 2000. **27**(5): p. 1110-4.

38. Lanier, L.L., *NK cell receptors.* Annu Rev Immunol, 1998. **16**: p. 359-93.

39. Biron, C.A., *Natural killer cell regulation during viral infection.* Biochem Soc Trans, 1997. **25**(2): p. 687-90.

40. French, A.R. and W.M. Yokoyama, *Natural killer cells and autoimmunity.* Arthritis Res Ther, 2004. **6**(1): p. 8-14.

41. Scrivo, R., et al., *Evaluation of degranulation and cytokine production in natural killer cells from spondyloarthritis patients at single-cell level.* Cytometry B Clin Cytom. 2011 **80** (1) p: 22-7

42. Vivier E, e.a., *Innate or Adaptive immunity? The Example of Natural Killer Cells.* Science, 2011. **331**(44): p. 44-49.

43. Kim, S.e.a., *Licensing of natual killer cells by host MHC class I molecules.* Nature, 2005. **436**: p. 709-713.

44. Bix.M, *Rejection of class I MHC-deficient hemopoietic cells by irradiated MHC-matched mice.* Nature, 1991. **349**: p. 329-331.

45. Raulet, *Missing self recognition and self tolerance of natural killer (NK) cells.* Semin in Immunology, 2006. **18**: p. 145-150.

46. Moretta, A., et al., *Receptors for HLA class-I molecules in human natural killer cells.* Annu Rev Immunol, 1996. **14**: p. 619-48.

47. Lopez-Botet, M. and T. Bellon, *Natural killer cell activation and inhibition by receptors for MHC class I.* Curr Opin Immunol, 1999. **11**(3): p. 301-7.

48. Boyington, J.C., et al., *Crystal structure of an NK cell immunoglobulin-like receptor in complex with its class I MHC ligand.* Nature, 2000. **405**(6786): p. 537-43.

49. Thananchai, H., et al., *Cutting Edge: Allele-specific and peptide-dependent interactions between KIR3DL1 and HLA-A and HLA-B.* J Immunol, 2007. **178**(1): p. 33-7.

50. Shiroishi, M., et al., *Structural basis for recognition of the nonclassical MHC molecule HLA-G by the leukocyte Ig-like receptor B2 (LILRB2/LIR2/ILT4/CD85d).* Proc Natl Acad Sci U S A, 2006. **103**(44): p. 16412-7.

51. Brown, D., J. Trowsdale, and R. Allen, *The LILR family: modulators of innate and adaptive immune pathways in health and disease.* Tissue Antigens, 2004. **64**(3): p. 215-25.

52. Yokoyama, W.M. and B.F. Plougastel, *Immune functions encoded by the natural killer gene complex.* Nat Rev Immunol, 2003. **3**(4): p. 304-16.

53. Belkin, D., et al., *Killer cell Ig-like receptor and leukocyte Ig-like receptor transgenic mice exhibit tissue- and cell-specific transgene expression.* J Immunol, 2003. **171**(6): p. 3056-63.

54. Colonna, M., et al., *Human myelomonocytic cells express an inhibitory receptor for classical and nonclassical MHC class I molecules.* J Immunol, 1998. **160**(7): p. 3096-100.

55. Verbrugge, A., et al., *Leukocyte-associated Ig-like receptor-1 has SH2 domain-containing phosphatase-independent function and recruits C-terminal Src kinase.* Eur J Immunol, 2006. **36**(1): p. 190-8.

56. Middleton, D. and F. Gonzelez, *The extensive polymorphism of KIR genes.* Immunology. **129**(1): p. 8-19.

57. Dohring, C., J. Samaridis, and M. Colonna, *Alternatively spliced forms of human killer inhibitory receptors.* Immunogenetics, 1996. **44**(3): p. 227-30.

58. Marsh, S.G., et al., *Killer-cell immunoglobulin-like receptor (KIR) nomenclature report, 2002.* Tissue Antigens, 2003. **62**(1): p. 79-86.

59. Stewart-Jones, G.B., et al., *Crystal structures and KIR3DL1 recognition of three immunodominant viral peptides complexed to HLA-B*2705.* Eur J Immunol, 2005. **35**(2): p. 341-51.

60. Borrego, F., et al., *Structure and function of major histocompatibility complex (MHC) class I specific receptors expressed on human natural killer (NK) cells.* Mol Immunol, 2002. **38**(9): p. 637-60.

61. Gardiner, C.M., et al., *Different NK cell surface phenotypes defined by the DX9 antibody are due to KIR3DL1 gene polymorphism.* J Immunol, 2001. **166**(5): p. 2992-3001.

62. Hansasuta, P., et al., *Recognition of HLA-A3 and HLA-A11 by KIR3DL2 is peptide-specific.* Eur J Immunol, 2004. **34**(6): p. 1673-9.

63. Kollnberger, *Interaction of HLA-B27 homodimers with KIR3DL1 and KIR3DL2, unlike HLA-B27 heterotrimers, is independent of the sequence bound peptide.* European Journal of Immunology, 2007. **37**: p. 1313-1322.

64. Chan, A.T., et al., *Expansion and enhanced survival of natural killer cells expressing the killer immunoglobulin-like receptor KIR3DL2 in spondylarthritis.* Arthritis Rheum, 2005. **52**(11): p. 3586-95.

65. Wilson, M.J., et al., *Plasticity in the organization and sequences of human KIR/ILT gene families.* Proc Natl Acad Sci U S A, 2000. **97**(9): p. 4778-83.

66. Fanger, N.A., et al., *The MHC class I binding proteins LIR-1 and LIR-2 inhibit Fc receptor-mediated signaling in monocytes.* Eur J Immunol, 1998. **28**(11): p. 3423-34.

67. Chapman, T.L., A.P. Heikeman, and P.J. Bjorkman, *The inhibitory receptor LIR-1 uses a common binding interaction to recognize class I MHC molecules and the viral homolog UL18.* Immunity, 1999. **11**(5): p. 603-13.

68. Allan, D.S., et al., *Tetrameric complexes of human histocompatibility leukocyte antigen (HLA)-G bind to peripheral blood myelomonocytic cells.* J Exp Med, 1999. **189**(7): p. 1149-56.

69. Masuda, A., et al., *Cis binding between inhibitory receptors and MHC class I can regulate mast cell activation.* J Exp Med, 2007. **204**(4): p. 907-20.

70. Jones, D.C., et al., *Alternative mRNA splicing creates transcripts encoding soluble proteins from most LILR genes.* Eur J Immunol, 2009. **39**(11): p. 3195-206.

71. Willcox, B.E., L.M. Thomas, and P.J. Bjorkman, *Crystal structure of HLA-A2 bound to LIR-1, a host and viral major histocompatibility complex receptor.* Nat Immunol, 2003. **4**(9): p. 913-9.

72. Willcox, B.E., et al., *Crystal structure of LIR-2 (ILT4) at 1.8 A: differences from LIR-1 (ILT2) in regions implicated in the binding of the Human Cytomegalovirus class I MHC homolog UL18.* BMC Struct Biol, 2002. **2**: p. 6.

73. Saverino, D., et al., *The CD85/LIR-1/ILT2 inhibitory receptor is expressed by all human T lymphocytes and down-regulates their functions.* J Immunol, 2000. **165**(7): p. 3742-55.

74. Cosman, D., et al., *A novel immunoglobulin superfamily receptor for cellular and viral MHC class I molecules.* Immunity, 1997. **7**(2): p. 273-82.

75. Samaridis, J. and M. Colonna, *Cloning of novel immunoglobulin superfamily receptors expressed on human myeloid and lymphoid cells: structural evidence for new stimulatory and inhibitory pathways.* Eur J Immunol, 1997. **27**(3): p. 660-5.

76. Chapman, T.L., et al., *Crystal structure and ligand binding properties of the D1D2 region of the inhibitory receptor LIR-1 (ILT2).* Immunity, 2000. **13**(5): p. 727-36.

77. Allan, D.S., A.J. McMichael, and V.M. Braud, *The ILT family of leukocyte receptors.* Immunobiology, 2000. **202**(1): p. 34-41.

78. Allen, R.L., et al., *Leukocyte receptor complex-encoded immunomodulatory receptors show differing specificity for alternative HLA-B27 structures.* J Immunol, 2001. **167**(10): p. 5543-7.

79. Shiroishi, M., et al., *Efficient leukocyte Ig-like receptor signaling and crystal structure of disulfide-linked HLA-G dimer.* J Biol Chem, 2006. **281**(15): p. 10439-47.

80. Benjamin, R. and P. Parham, *Guilt by association: HLA-B27 and ankylosing spondylitis.* Immunol Today, 1990. **11**(4): p. 137-42.

81. Khare, S.D., H.S. Luthra, and C.S. David, *Spontaneous inflammatory arthritis in HLA-B27 transgenic mice lacking beta 2-microglobulin: a model of human spondyloarthropathies.* J Exp Med, 1995. **182**(4): p. 1153-8.

82. Khare, S.D., et al., *HLA-B27 heavy chains contribute to spontaneous inflammatory disease in B27/human beta2-microglobulin (beta2m) double transgenic mice with disrupted mouse beta2m.* J Clin Invest, 1996. **98**(12): p. 2746-55.

83. Taurog, J.D., *Spondyloarthritis in HLA-B27/Human b2 microgobulin-transgenic rats is not preented by the lack of CD8.* Arthritis & Rheum, 2009. **60**(7): p. 1977-1984.

84. Taurog, J.D., et al., *Susceptibility to inflammatory disease in HLA-B27 transgenic rat lines correlates with the level of B27 expression.* J Immunol, 1993. **150**(9): p. 4168-78.

85. Taurog, J.D., et al., *Inflammatory disease in HLA-B27 transgenic rats.* Immunol Rev, 1999. **169**: p. 209-23.

86. Kingsbury, D.J.e.a., *Development of spontaneous arthritis in beta-2-m deficient mice without expression of HLA-B27: Association with deficiency of endogenous major histocompatibility complex class I expression.* Arthritis & Rheum, 2000. **43**(10): p. 2290-2296.

87. Zochling, J., et al., *Infection and work stress are potential triggers of ankylosing spondylitis.* Clin Rheumatol, 2006. **25**(5): p. 660-6.

88. Allen, R.L., P. Bowness, and A. McMichael, *The role of HLA-B27 in spondyloarthritis.* Immunogenetics, 1999. **50**(3-4): p. 220-7.

89. Smith, J.A., E. Marker-Hermann, and R.A. Colbert, *Pathogenesis of ankylosing spondylitis: current concepts.* Best Pract Res Clin Rheumatol, 2006. **20**(3): p. 571-91.

90. Gaston, J.S., et al., *Synovial T lymphocyte recognition of organisms that trigger reactive arthritis.* Clin Exp Immunol, 1989. **76**(3): p. 348-53.

91. Toivanen, A., et al., *Do bacterial antigens persist in reactive arthritis?* Clin Exp Rheumatol, 1987. **5 Suppl 1**: p. S25-7.

92. Lahesmaa-Rantala, R., et al., *Yersinia specific immune complexes in the synovial fluid of patients with yersinia triggered reactive arthritis.* Ann Rheum Dis, 1987. **46**(7): p. 510-4.

93. Urban, R.G., et al., *A subset of HLA-B27 molecules contains peptides much longer than nonamers.* Proc Natl Acad Sci U S A, 1994. **91**(4): p. 1534-8.

94. Hermann, E., et al., *HLA-B27-restricted CD8 T cells derived from synovial fluids of patients with reactive arthritis and ankylosing spondylitis.* Lancet, 1993. **342**(8872): p. 646-50.

95. Atagunduz, P., et al., *HLA-B27-restricted CD8+ T cell response to cartilage-derived self peptides in ankylosing spondylitis.* Arthritis Rheum, 2005. **52**(3): p. 892-901.

96. Kuon, W. and J. Sieper, *Identification of HLA-B27-restricted peptides in reactive arthritis and other spondyloarthropathies: computer algorithms and fluorescent activated cell sorting analysis as tools for hunting of HLA-B27-restricted chlamydial and autologous crossreactive peptides involved in reactive arthritis and ankylosing spondylitis.* Rheum Dis Clin North Am, 2003. **29**(3): p. 595-611.

97. Breban, M., et al., *T cells, but not thymic exposure to HLA-B27, are required for the inflammatory disease of HLA-B27 transgenic rats.* J Immunol, 1996. **156**(2): p. 794-803.

98. Antoniou, A.N., et al., *Formation of HLA-B27 homodimers and their relationship to assembly kinetics.* J Biol Chem, 2004. **279**(10): p. 8895-902.

99. Colbert, R.A., et al., *Allele-specific B pocket transplant in class I major histocompatibility complex protein changes requirement for anchor residue at P2 of peptide.* Proc Natl Acad Sci U S A, 1993. **90**(14): p. 6879-83.

100. Mear, J.P., et al., *Misfolding of HLA-B27 as a result of its B pocket suggests a novel mechanism for its role in susceptibility to spondyloarthropathies.* J Immunol, 1999. **163**(12): p. 6665-70.

101. Dangoria, N.S., et al., *HLA-B27 misfolding is associated with aberrant intermolecular disulfide bond formation (dimerization) in the endoplasmic reticulum.* J Biol Chem, 2002. **277**(26): p. 23459-68.

102. Pahl, H.L. and P.A. Baeuerle, *The ER-overload response: activation of NF-kappa B.* Trends Biochem Sci, 1997. **22**(2): p. 63-7.

103. Dong, W., et al., *Upregulation of 78-kDa glucose-regulated protein in macrophages in peripheral joints of active ankylosing spondylitis.* Scand J Rheumatol, 2008. **37**(6): p. 427-34.

104. Turner, M.J., et al., *HLA-B27 misfolding in transgenic rats is associated with activation of the unfolded protein response.* J Immunol, 2005. **175**(4): p. 2438-48.

105. Tran, T.M., et al., *HLA-B27 in transgenic rats forms disulfide-linked heavy chain oligomers and multimers that bind to the chaperone BiP.* J Immunol, 2004. **172**(8): p. 5110-9.

106. Colbert, R.A., et al., *From HLA-B27 to spondyloarthritis: a journey through the ER.* Immunol Rev. **233**(1): p. 181-202.

107. Lanier, L.L., *Follow the leader: NK cell receptors for classical and nonclassical MHC class I.* Cell, 1998. **92**(6): p. 705-7.

108. Kollnberger, S., et al., *HLA-B27 heavy chain homodimers are expressed in HLA-B27 transgenic rodent models of spondyloarthritis and are ligands for paired Ig-like receptors.* J Immunol, 2004. **173**(3): p. 1699-710.

109. Lichterfield M., et al., *A viral CTL escape mutation leading to immunoglobulin-like transcript 4-mediated functional inhibition of myelomonocytic cells.* J Exp Med, 2007, 204 (12): p2813-2824

110. Huang, J et al., *HLA-B*35-Px- Mediated acceleration of HIV-1 infection by increased inhibitory immunoregulatory impulses.* J Exp Med, 2009, 206 (13): p2959-2966

111. Shiroishi, M et al, *Human inhibitory receptors Ig-like transcript 2 (ILT2) and ILT4 compete with CD8 for MHC class I binding and bind preferentially to HLA-G* Prot Natl Acad Sci, 2003, 100 (15): p8856-61

112. Latthe, M., et al. *High frequenct of CD8 alpha alpha homodimer-bearing T cells in human fetal intestine.* Eur J Immunol. 1994 **24,** (7): p1703-5

113. Hulsmeyer, M., et al. *HLA-B27 subtypes differentially associated with disease exhibit subtle structural alterations.* J Biol Chem, 2002, 6, (227): p47844-53

114. Ziegler, A., et al., *Implications of structural and thermodynamic studies of HLA-B27 subtypes exhibiting differential association with ankylosing spondylitis.* Adv Exp Med Biol, 2009. **649**: p. 177-95.

115. Barnstable C.et al . *Production of monoclonal antibodies to group A erythrocytes, HLA and other human cell surface antigens-new tools for genetic analysis,* Cell, 1978, (**14**) p. 9–20

116. Stam N. J., et al. *Monoclonal antibodies raised against denatured HLA-B locus heavy chains permit biochemical characterization of certain HLA-C locus products* J. Immunol. 1986 **137** p:2299–2306.

117. Ellis S. A., et al *Recognition of HLA-B27 and related antigen by a monoclonal antibody* Hum. Immunol. 1982 **5** p:49–59.

118. Zhou H., et al., *Generation of Monoclonal Antibodies against highly Conserved Antigens* PLoS one, 2009, **4** (6), p6086

119. Ramos, M, et al *HLA-B27-bound peptide repertoires: their nature, origin and pathogenetic relevance,* Adv Exp Med Biol. 2009, **(649),** p: 196-209

120. Turnquist, H.R., et al., *Differential association of HLA-B*2705 and HLA-B*2709 to ankylosing spondylitis correlates with limited peptide subsets but not with altered cell surface stability.* J Biol Chem, 2002. **277**(32): p. 28749-56.

121. Neisig, A., et al., *Allele-specific differences in the interaction of MHC class I molecules with transporters associated with antigen processing.* J Immunol, 1996. **156**(9): p. 3196-206.

122. Thammavongsa, V., et al., *HLA-B44 polymorphisms at position 116 of the heavy chain influence TAP complex binding via an effect on peptide occupancy.* J Immunol, 2006. **177**(5): p. 3150-61.

123. Williams, A.P., et al., *Optimization of the MHC class I peptide cargo is dependent on tapasin.* Immunity, 2002. **16**(4): p. 509-20.

124. De Haard, H.J., et al., *A large non-immunized human Fab fragment phage library that permits the rapid isolation and kinetic analysis of high affinity antibodies.* J Biol Chem, 1999, **274** (26): p18218-30.